

A Novel Hollow Cylinder Apparatus to Investigate Shearing Characteristic of Asphalt

by

Katarzyna Tekieli

Thesis submitted to the University of Nottingham
for the degree of Doctor of Philosophy

June 2019

DEPARTMENT OF CIVIL ENGINEERING

ABSTRACT

The design and testing of asphalt to minimise wheel track rutting in highways and the prediction of its development with time remain areas requiring improved technology. Simple tests such as wheel tracking and repeated load compression are, at best, approximate and rely on empirical calibration against field performance. In the US, the Superpave Shear Test (SST) was developed during the Strategic Highway Research Program (SHRP) but, while this has proved useful, question marks remain about its reliability for fundamental research.

Permanent deformation (rutting) is one form of bituminous pavement distress that affects a road performance significantly and it may lead to premature pavement failure. Research shows that rutting is generally associated with a shear deformation in the upper asphalt layers of pavement structures and better characterisation of the shear deformation of asphalt mixtures is required in order to improve rutting predictions. In order to investigate this phenomenon, a large, innovative hollow cylinder apparatus has been designed and commissioned at the University of Nottingham and this thesis describes the development process. The equipment used a hollow cylinder as the test specimen and applied repeated torsion and axial stress together with a confining stress, if required. The test philosophy is that an

element of the cylinder wall can be subjected to the combination of shear and normal stresses that arise in the pavement under a moving wheel load.

The results of the literature review stressed the importance of specimen geometry and end boundary conditions. It was demonstrated that a specimen that reflects the asphalt mixture in the top 50mm to 100mm of a pavement should be used. Therefore, the large size specimen was adopted in order to test asphalt with realistic sized aggregate (10mm maximum).

The new HCA proved to be a versatile shear testing device, that can follow stress paths involving stress invariants which are functions of the principal stresses but allow the stress conditions and corresponding strains to be expressed in a way which is independent of direction. The flexibility of stress path application afforded by the HCA is such that a wide range of possibilities arise for future research.

The test programme allowed initial exploration of the relative effects of stress ratio (shear/normal stress) and shear stress level. The results indicated that permanent deformation is affected by load magnitude. It was found that for a high stress ratio, the results appear to be unreliable. At this state of stress, the mixture became unstable and the load magnitude does not appear to influence the permanent strain in a similar trend. The HCA results provided considerable evidence for the dilation phenomenon.

Comparison of data from the HCA, Repeated Load Axial Test (RLAT) and SST, revealed discrepancies between the RLAT, SST and HCA tests and it showed

the HCA test is a more reliable tool to investigate asphalt permanent deformation performance than the RLAT and SST but it is too complex for routine use.

From the results presented, it can be seen that the new HCA equipment behaved in a consistent manner and the results obtained during this research appeared to be generally acceptable. The device showed the potential to correctly reproduce the insitu stress regime and, hence, allow more appropriate relationships to be developed between the applied stresses and the resulting deformations.

The resulting high quality data on shear and volumetric strains, particularly permanent strains, will assist with the development of theoretical methods for pavement analysis of rut development in future research and act as an accurate reference to assess the performance of simpler test equipment.

Key words: asphalt, shear testing, permanent deformation, laboratory testing

DECLARATION

The research described in this thesis was conducted at the University of Nottingham, School of Civil Engineering between September 2008 and November 2016. I declare that this dissertation is the result of my own original work and no part of the work has been, or is currently being submitted for any degree, diploma or other qualifications.

Katarzyna Tekieli

University of Nottingham

June 2019

To my Mother

Mamuś dedykuję Ci tą pracę.

Wszystko, co mam zawdzięczam Tobie.

Dziękuję za bezgraniczną miłość i wsparcie.

ACKNOWLEDGMENTS

This research was principally financed by a research grant from the UK Engineering and Physical Sciences Research Council. Other support in cash and kind was received from the Highways Agency, Aggregate Industries, URS Scott Wilson and the University of California at Berkeley and at Davis.

The Author would like to express her thanks to the following people who have provided the assistance, advice, encouragement and funding without which this research would not have been possible:

- Professor S F Brown, Professor G D Airey, Professor A C Collop for their supervision and invaluable support and guidance throughout this research;
- Mr B V Brodrick and Mr E Hornby who put a lot of time and effort to design, build and develop the HCA;
- Professor Monismith and Professor Harvey for making available the facilities of the University of California at Berkeley and at Davis;
- Mr R Elliott and Mr I Artamendi for their help and advice during this research;
- And to all colleagues from NTEC, University of California and Arup for their friendship and encouragement;
- Finally, all my gratitude goes to my boyfriend and my family for their constant encouragement while I was preparing this thesis.

TABLE OF CONTENTS

ABSTRACT ..... **i**

DECLARATION ..... **iv**

ACKNOWLEDGMENTS ..... **vi**

TABLE OF CONTENTS ..... **vii**

LIST OF FIGURES ..... **xi**

LIST OF TABLES ..... **xvi**

LIST OF SYMBOLS ..... **xvii**

LIST OF ABBREVIATIONS ..... **xviii**

1 **1**

INTRODUCTION **1**

1.1. Background 1

1.2. Problem Definition 4

1.3. The Hollow Cylinder Apparatus (HCA) 10

1.4. Objectives and Scope of This Research 16

1.5. Outline of the Thesis 18

2 **19**

LITERATURE REVIEW **19**

2.1. Introduction 19

2.2. General Background 20

2.3. Pavement Failure 22

2.4. Pavement Design 27

2.4.1. Mix design 27

2.4.2. Structural design 30

2.5. Behaviour of Asphalt Mixtures 35

2.6. Factors Affecting Permanent Deformation 40

2.6.1. Aggregate 40

2.6.2. Binder 44
2.6.3. Types of Hot Asphalt Mixtures 48
2.6.4. Traffic 55
2.6.5. Environment 59
2.6.6. Compaction 63
2.7. Laboratory Testing 67
2.7.1. Uniaxial and Triaxial Creep Test 70
2.7.2. Repeated Load Triaxial Test 74
2.7.3. Superpave Shear Test (SST) 77
2.7.4. Wheel Tracking Test 80
2.8. The Hollow Cylinder Apparatus (HCA) 84
2.8.1. Research on Granular Material 84
2.8.2. Application to asphalt 90
2.9. Asphalt Layer Rutting Performance Prediction Models 94
2.9.1. Layer-strain Method 95
2.9.2. Viscoelastic Method 98
2.10. Conclusions 101

3 103

DEVELOPMENT OF THE HOLLOW CYLINDER APPARATUS (HCA) .103

3.1. Introduction 103
3.2. Large Torsional Hollow Cylinder Apparatus (HCA) 104
3.2.1. Linear Elastic Analyses 105
3.2.2. HCA Specification 118
3.2.3. Loading System 121
3.2.4. Specimen Geometry 135
3.2.5. Deformation Measurement 137
3.2.6. Calibration of the HCA stress and strain measuring system .. 143
3.2.7. System Control and Data Acquisition 147
3.3. Data Analysis of Stress and Strain in HCA 153
3.3.1. Hollow Cylinder Apparatus Software (HCAS) 153
3.3.2. Analysis of stress and strain 155
3.3.3. Principal stress and strain components 156

4 161

SPECIMEN PREPARATION AND TESTING SET-UP 161

4.1. Specimen Preparation 161

4.1.1. Trench Excavation 163

4.1.2. Trial Slab Construction 165

4.1.3. Coring 169

4.1.4. Sawing 171

4.2. Test Set-UP 175

4.2.1. Determination of Air Void Content 175

4.2.2. Glueing 177

4.2.3. Conditioning 182

5 187

TEST PROGRAMME FOR THE HCA TESTS 187

5.1. Aim of the Investigation 187

5.2. Commissioning Tests 188

5.1.1. Introduction 188

5.1.2. Specimens 188

5.1.3. Test Details 189

5.1.4. Equipment Assessment 195

5.1.5. Concluding Remarks 202

5.3. Main HCA Tests 205

5.4. Test Programme 206

5.5. Test Materials 208

5.6. Results of HCA Tests 211

5.7. Summary and Conclusions 221

6 224

SUPERPAVE SHEAR TEST AND REPEATED LOAD AXIAL TEST 224

6.1. Introduction 224

6.2. Repeated Load Axial Tests (RLAT) 225

6.2.1. Testing Apparatus 226

6.2.2. Specimen Preparation 226

6.2.3. Test Conditions 228

6.2.4. Test Procedure 230
6.2.5. Data Anaysis 230
6.2.6. Results of RLAT 232
6.3. Superpave Shear Test (SST) 234
6.3.1. Testing Device 235
6.3.2. Specimen Preparation 237
6.3.3. Test Conditions 242
6.3.4. RSCSR Tests 243
6.3.5. Data Anaysis 230
6.3.6. Results of SST RSCSR 247
6.4. Summary 259
7 262
DISCUSSION AND COMPARISON OF THE HCA 262
7.1. Introduction 262
7.2. Permanent Shear Strain 263
7.3. Permanent Axial Strain 271
7.4. Volume Change Characteristics 271
7.5. Summary 275
8 278
CONCLUSIONS AND RECOMMENDATION FOR FURTHER INVESTIGATION 278
8.1. Introduction 278
8.1.1. HCA development and commissioning 280
8.1.2. Specimen preparation 283
8.1.3. Experimental work 283
8.2. Conclusions 284
8.3. Recommendations for Future Research 288
REFERENCES 292
APPENDIX A 304
APPENDIX B 305

LIST OF FIGURES

Page

Figure 1.1. Forecast Traffic and Congestion Growth by 2050 2
Figure 1.2. An asphalt response to: (a) a single wheel load pulse; (b) a repeated wheel loading 5
Figure 1.3. Age of pavements rehabilitated for permanent deformation 9
Figure 1.4. Percentage contribution of defects to defects index in 2006, England and Wales 9
Figure 1.5. Stress regime on a pavement element caused by moving wheel loading 12

Table 2.1. Summary of mixture design requirements (AI, 1983) 28
Table 5.1. Test conditions for initial experiments 191
Figure 2.21. Effect of test temperature: 100Pen 20mm DBM Basecourse ... 62
Figure 2.22. Different stresses acting on an element in the pavement 68
Figure 2.23. Diagram layout of uniaxial creep equipment 71
Figure 2.24. A typical creep strain response 72
Figure 2.25. Repeated Loading Triaxial Test 76
Figure 2.26. Stress regimes under a moving wheel in a triaxial compression test 76
Figure 2.27. The Superpave Shear Test (SST) device 79
Figure 2.28. The Laboratoire Central des Ponts et Chaussées (LCPC) wheel tracker, also known as French Rutting Tester (FRT) 82
Figure 2.29. Hamburg Wheel Tracking Device (HWTD) 82
Figure 2.30. The Nottingham Slab Testing Facility 83
Figure 2.31. TRL Wheel Tracker 83
Figure 2.32. Simple shear and pure shear 86
Figure 2.33. Stress regime on an element of the wall of the HCA 87
Figure 2.34. The Nottingham Hollow Cylinder Apparatus – Basic Arrangement 88
Figure 3.1. Locations of calculated stresses at predefined points using BISAR 108
Figure 3.2. Pavement structures analysed 109
Figure 3.3. Normal and Shear Stresses on centre line of load 113
Figure 3.4. Mean Normal and Deviator Stresses on centre line of load 114
Figure 3.5. Normal and Shear Stresses under edge of load 115

Figure 3.6. Mean Normal and Deviator Stresses on under edge of load 116
Figure 3.7. Stress Paths on centre line of load 117
Figure 3.8. Stress Paths under edge of load 118
Figure 3.9. Resulting strain evolution at the bottom of an asphalt base course at 34cm depth, taking into account different loading frequencies for duration of one month..... 120
Figure 3.10. Closed loop servo control diagram..... 123
Figure 3.11. Servo hydraulic loading arrangement 124
Figure 3.12. Cross section of new Hollow Cylinder Apparatus showing principal components 126
Figure 3.13. HCA with test specimen in position and pressure chamber open.. 127
Figure 3.14. Details of vertical load application system 129
Figure 3.15. Torque application mechanism..... 131
Figure 3.16. Torque drive mechanism and load cells..... 132
Figure 3.17. HCA with test specimen in position and pressure chamber closed 134
Figure 3.18. Arrangement of deformation measuring instrumentation..... 138
Figure 3.19. Hinged strain collar 140
Figure 3.20. Vertical and 45° LVDTs..... 140
Figure 3.21. Radial LVDTs 141
Figure 3.22. Internal radial LVDTs..... 141
Figure 3.23. Thermocouple attached to the HC specimen 142
Figure 3.24. LVDT calibration 144
Figure 3.25. Strain collar calibration 144
Figure 3.26. HCA on-specimen LVDTs calibration (18/08/2010) 145
Figure 3.27. Calibration Wizard Window from control software..... 146
Figure 3.28. Schematic diagram of HCA digital servo control system 148
Figure 3.29. HCA digital servo control system..... 149
Figure 3.30. The loading waveforms produced by SmartWAVE for HCA testing 151
Figure 3.31. Welcome screen of webserver 152
Figure 3.32. The system used to direct a heated flow of air into the pressure chamber 152
Figure 3.33. Amplitude and offset calculation for one cycle..... 154
Figure 3.34. Principal stresses on the θ-z plane 159
Figure 3.35. Principal strains on the θ-z plane 160
Figure 4.1. Coring rig dimensions: (a) lateral view; (b) longitudinal view 163
Figure 4.2. Slab dimensions and specimen locations..... 164
Figure 4.3. The Aggregate Industries Hulland Ward site – trench excavation 164
Figure 4.4. Prepared trench after rain..... 165

Figure 4.5. Installing a layer of crushed stone 166
Figure 4.6. Installing an AC sub-base 168
Figure 4.7. Sand capping 168
Figure 4.8. Tack coat..... 169
Figure 4.9. The drilling rig 170
Figure 4.10. Coring barrels..... 170
Figure 4.11. Cutting of test specimens from slab..... 170
Figure 4.12. Hand rotated trimming jig for HCA specimens..... 172
Figure 4.13. HC specimen with inner and outer steel tube 173
4.14. HC specimen clamped and aligned with a diamond saw blade..... 173
Figure 4.15. Specimen after first saw cut 174
Figure 4.16. Jig set up for second cut 174
Figure 4.17. Failed hollow cylinder (an adhesion test on the glue) 178
Figure 4.18. The HCA specimen fitting arrangement 179
Figure 4.19. HC specimen glueing 181
Figure 4.20. Inner and outer membranes..... 182
Figure 4.21. HC specimen ready to be tested 184
Figure 4.22. Clamps holding the pedestal to the bottom of the pressure chamber 185
Figure 4.23. Insulation installed around the chamber 185
Figure 4.24. Specimen preparation and set-up flow chart..... 186
Figure 5.1. Polyurethane cylindrical test specimen 190
Figure 5.2. Typical applied stress regime 192
Figure 5.3. Failure of specimen no. 5 through the top interface..... 193
Figure 5.4. Specimen no. 6 at the end of the test..... 193
Figure 5.5. Specimen no. 7 at the end of the test..... 194
Figure 5.6. Specimen no. 8 at the end of the test..... 194
Figure 5.7. Initial top strain collar components 196
Figure 5.8. Support brackets under the strain collars and the extended plate above the vertical LVDT 197
Figure 5.9. Guide plates to keep the open end of the collars aligned..... 197
Figure 5.10. HCA haversine testing - improvement in stress ratio control. 199
Figure 5.11. Vertical load cell coupling before and after modification 200
Figure 5.12. Vertical load cell coupling before modification 201
Figure 5.13. Modified vertical load cell coupling 201
Figure 5.14. Typical output from LVDTs for Specimen no. 6..... 203
Figure 5.15. Material specification 208
Figure 5.16. Mean and Standard Deviation of air void content profiles through test specimens 210
Figure 5.17. Mean and Standard Deviation of air void content profiles through test specimens 210
Figure 5.18. Typical wave load for cycles 209 to 211: Test No. 3 211

Figure 5.19. Typical response of LVDT's under the load (cycles 209 to 211): Test No. 3 212
Figure 5.20. The deviator stress vs. mean normal stress 213
Figure 5.21. Variation of permanent shear strain with number of load cycles for different stress ratios 217
Figure 5.22. Variation of permanent shear strain with number of load cycles for different shear stress levels 218
Figure 5.23. Variation of volumetric strain with number of load cycles for different stress ratios 219
Figure 5.24. HCA Mohr's Circles for shear stress of 70kPa and stress ratio values of SR=1, SR=2 & SR=3 220
Figure 6.1. Nottingham Asphalt Tester 227
Figure. 6.2. RLAT loading pulse 229
Figure. 6.3. Principal stresses on the θ-z plane in the RLAT 231
Figure 6.4. Summary of RLAT Tests 233
Figure 6.5. SST specimen with LVDTs attached 236
Figure 6.6. General view of the SST in the UC Berkeley Laboratory 236
Figure 6.7. SST with test specimen in position 237
Figure 6.8. SST specimens 239
Figure 6.9. SST specimen with platens glued to top and bottom 239
Figure 6.10. SST specimen ready for testing showing LVDTs setup 240
Figure 6.11. Principal stresses on the θ-z plane in the SST 246
Figure 6.12. SST-RSCSR Tests: Stress Ratio 4.1 / 45ºC (Phase 1) 248
Figure 6.13. SST-RSCSR Tests: Stress Ratio 2.5 / 55ºC (Phase 1) 248
Figure 6.14. Cracks formed in the SST specimen tested at 130kPa shear stress at 55°C 249
Figure 6.15. The effect of SR on permanent deformation for τ=70kPa 253
Figure 6.16. The effect of SR on permanent deformation for τ=100kPa 253
Figure 6.17. The effect of SR on permanent deformation for τ=130kPa 254
Figure 6.18. The effect of τ on permanent deformation for SR=1 254
Figure 6.19. The effect of τ on permanent deformation for SR=2 255
Figure 6.20. The effect of τ on permanent deformation for SR=3 255
Figure 6.21. The effect of τ on permanent deformation for SR=1 257
Figure 6.22. The effect of τ on permanent deformation for SR=2 257
Figure 6.23. The effect of SR on permanent deformation for τ=100kPa 258
Figure 7.1. Variation in void content and performance: SST SR=2 267
Figure 7.2. Variation in void content and performance: HCA SR=1 267
Figure 7.3. SST at SR=1 vs RLAT Mohr's Circle 268
Figure 7.4. Variation of permanent axial strain with load repetition in the HCA 272
Figure 7.5. Variation of permanent axial strain with load repetition in the SST 273

Figure 7.6. Variation of permanent axial strain with load repetition – RLAT vs SST..... 273

LIST OF TABLES

Page

Table 2.1. Summary of mixture design requirements..... 28
Table 2.2. Compaction methods in the UK..... 66
Table 3.1. Summary of all the factors defined for HCA testing 121
Table 5.1. Test conditions for initial experiments..... 191
Table 5.2. Initial test programme..... 207
Table 6.1. Air void contents of RLAT specimens 228
Table 6.2. RLAT test conditions..... 229
Table 6.3. Summary of SST specimens air void content 241
Table 6.4. RSCSR test conditions 244

LIST OF SYMBOLS

W	Axial force
M	Torque
p_i, p_o	Inner and outer cell pressures
$\sigma_{1,2,3}$	Major, intermediate and minor principal stresses
H	Specimen height
R_o, R_i	External and internal radius of the hollow cylindrical specimen
α	Major principal stress direction
σ_z, σ_r, σ_θ	Vertical, radial and circumferential stress
$\tau_{\theta z}$	Shear stress in the θ-z plane
δl, u_i, u_o, δt	Changes in height, outer and inner radii and thickness of the specimen wall
ε_z, ε_θ, ε_r	Vertical, circumferential and radial normal strain
$\gamma_{z\theta}$	Shear strain in z - θ plane (= 2*εzθ)
$\varepsilon_{1,2,3}$	Major, intermediate and minor principal strains
ε_s	Invariant shear strain
ε_v	Volumetric strain
η	Stress ratio (q/p)
q	Invariant shear stress
p	Mean normal stress
τ_{oct}	Octahedral shear stress
γ_{max}	Maximum shear strain in the the z-θ plane

LIST OF ABBREVIATIONS

HCA	Hollow Cylinder Apparatus
UCB	University of California at Berkeley
SHRP	US Strategic Highway Research Program
HMA	Hot mix asphalt
AC	Asphalt Concrete
A/D	Analogue to digital convertor
I/O	Input/output card
SST	Superpave Shear Test
RSCSR	Repeated Shear at Constant Stress Ratio
RSCH	Repeated Shear at Constant Height
FS	Frequency Sweep
NAT	Nottingham Asphalt Tester
LVDT	Linear Variable Differential Transformer
RLAT	Repeated Load Axial Test
LGV	Large Goods Vehicle
HGV	Heavy Goods Vehicle

1

INTRODUCTION

1.1. Background

Transport plays a critical role in the economy. An efficient transport network is vital to a strong economy - locally, regionally and nationally, particularly, the road transport sector, which is both the lifeblood and a major contributor to the globalisation of business and economic activity. Over the last decade, the majority of the freight in the UK has been carried by roads and will continue to do so for the foreseeable future. Traffic in England and Wales is forecast to increase across all scenarios, from 2015 traffic is forecast to grow by between 17% and 51% by 2050, as shown in Figure 1.1. Over the period from 2015 to 2050, Light Goods Vehicle (LGV) traffic is forecast to increase most rapidly and has potential to double with expected growth from 23% of 108% and the Heavy Goods Vehicle (HGV) Traffic is forecast to grow from 5% to 12%. The traffic demand will affect congestion, with the forecast of proportion of traffic in congested conditions in 2050 to range from 8% to 16%. This is compared to 7% of traffic in congested conditions in 2015 (DfT, 2018).

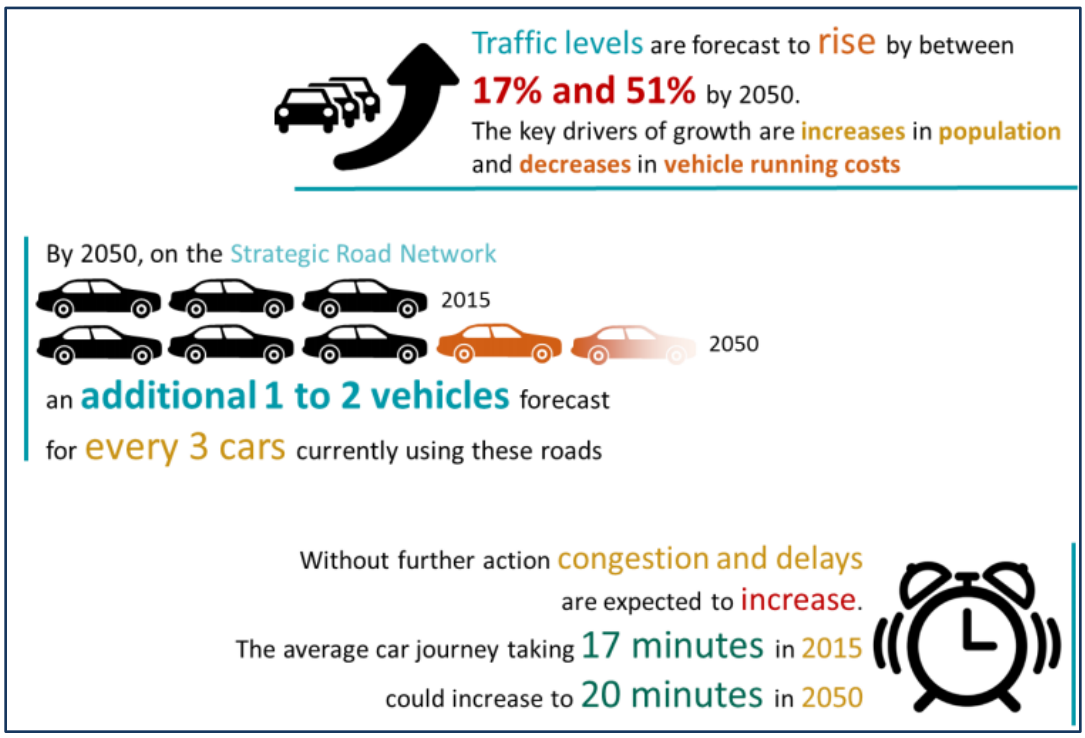


Figure 1.1. Forecast Traffic and Congestion Growth by 2050 (DfT, 2018)

Roads are like vines and arteries of the economy. Therefore, a constant increase in traffic volumes demands a quality road infrastructure, up to the standard that a modern economy needs.

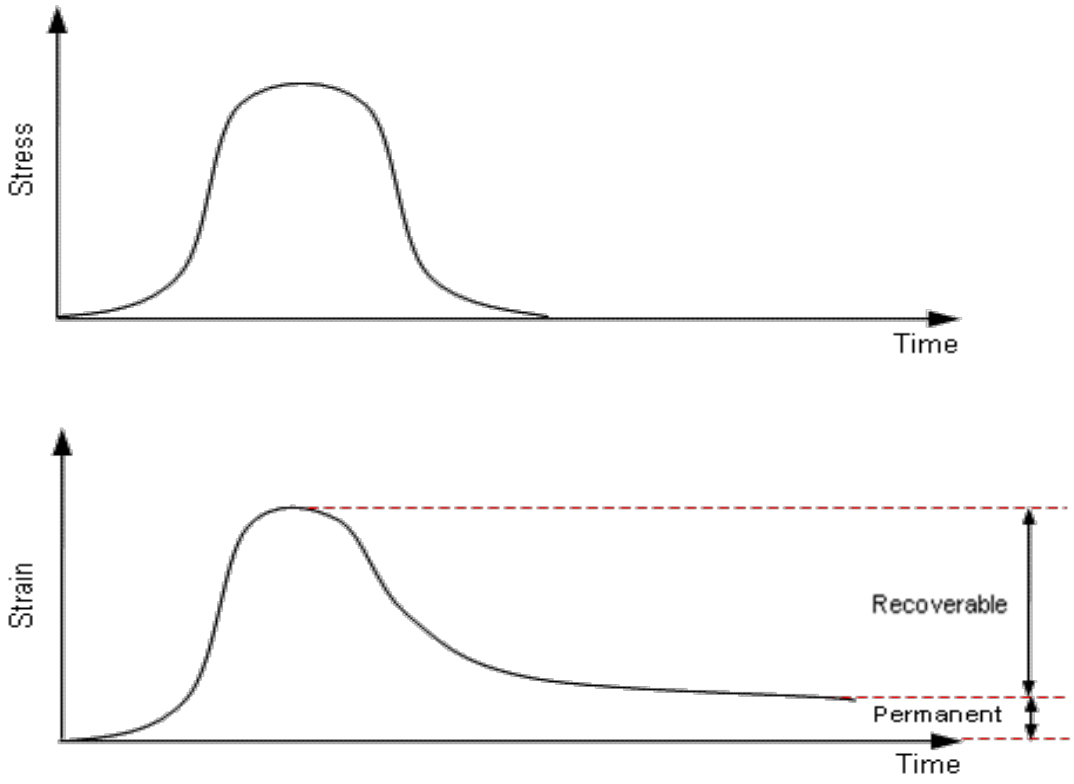
As of today, 95% of pavements in Europe are asphalt pavements; a huge emphasis is placed on the asphalt industry to construct high performance, long lasting, safe and environmentally friendly roads that will be serviceable over a wide range of climatic conditions. To this end, many studies have been conducted and many advances in material technology, design and functionality have been introduced in recent decades. However, to extend current pavement design life hand-in-hand with lowering life-cycle costs it is important to minimise the development of common pavement distress

mechanisms, such as cracking and rutting. Although fatigue and thermal cracking may affect permanent deformation due to water ingress, such mechanisms will not be considered in this research as they are considered of secondary importance.

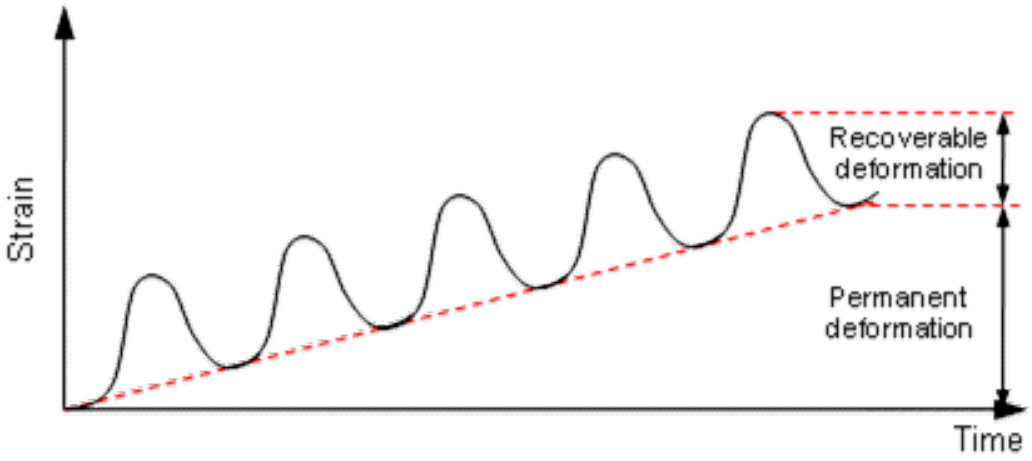
1.2. Problem Definition

Rutting is one of the major distresses of asphalt pavements which occur as a result of an accumulation of irrecoverable deformation with load repetitions (Figure 1.2). Its mechanism is very complicated and depends on a large number of variables, which comprise mixture properties (aggregate gradation, aggregate texture, binder stiffness, and binder content), traffic (wheel load, tyre pressure, and vehicle speed), environment (moisture, temperature), and construction procedures (compaction).

The development of this longitudinal deformation in the vehicle wheel paths relative to the lane centre and edge has been and remains one of the key performance problems for asphalt roads, notably where combinations of heavy traffic and high temperatures arise, a situation that is likely to get worse as a result of constant increase in traffic volumes and global warming. Research has found that majority of surface rutting occurs on few days of the year, when the temperature of road surfacing exceeds 45ºC. There is also evidence that above a certain level of aggressiveness (combination of temperature and wheel load) asphalt materials can become relatively unstable (Willway et al. 2008). This is a serious mode of distress alongside fatigue in bituminous pavement which may lead to an early and costly rehabilitation as a result of premature pavement failure.



(a)



(b)

Figure 1.2. An asphalt response to: (a) a single wheel load pulse; (b) a repeated wheel loading (Brown et al., 1995)

Yet, above all, rutting presents a serious hazard to road users, particularly in wet conditions. Water filled ruts create the danger of aquaplaning and a deformed road makes steering more difficult, thereby increasing the potential for accidents. In addition, there is a hazard to cyclists and motorcyclists.

Rutting can be subdivided into two main categories. Where the rutting emanates from the subgrade or pavement foundation and the entire pavement structure is deformed, this is referred to as **structural deformation**, which manifests itself as a wide rut with mild slopes. A commonly made assumption is that this mechanism can be controlled by adequate design of pavement thickness and selection of good quality materials. Therefore, the permanent deformation resistance of the granular and unbound layers often does not constitute a major problem. Consequently, the aim of this research project is to investigate only permanent deformation confined to hot mix asphalt (HMA) layers.

Rutting that is confined to the asphalt surfacing is termed **non-structural** and is associated with near surface deformation, which can be characterised by shoulders formed on either side of the wheel path. Hofstra and Klomp, (1972) found that non-structural asphalt pavement deformation was greatest near the loaded surface and gradually decreased at lower level. Evidence from previous studies demonstrated that as a result of the repeated application of shear stress from vehicle wheel loading, rut development arises from permanent shear strains within 50 to 100mm from the surface, approximately

beneath the edge of the load (Lytton et al., 1993, Monismith et al., 1994, White, 2002).

Test-track studies reported by Hofstra and Klomp, (1972) indicated that shear deformation rather than densification was the primary rutting mechanism. They emphasised the importance of placing materials at high densities in order to minimise shear deformation. Sousa et al., (1991) illustrated that repetitive loading in shear is required in order to accurately measure, in the laboratory, the influence of mixture composition on resistance to permanent deformation.

Some contributions to rutting in the asphalt layers can also come from additional compaction (decrease in mixture volume) under traffic but, for a well-constructed pavement, this will be less significant than the shearing effect. Eisenmann and Hilmer, (1987) also concluded that once the compaction under traffic is completed for the most part, the further rutting is caused essentially by displacement with constancy of volume. This phase is considered to be representative of the deformation behaviour for the greater part of the life of a pavement.

The relative contributions to rutting from shear and volumetric strains for materials at different states of compaction are however, one of the issues to be studied since high levels of compaction are still not universally achieved in construction practice. Rutting of asphalt mixtures is strongly controlled by the viscous component due to the mechanical properties of the binder. This causes

permanent deformation changes either in shear or in volume to occur mostly at high temperatures or under heavy loads (Sousa et al., 1994). Therefore, laboratory testing should be conducted at temperatures and with loading conditions simulating the highest levels expected in the paving mixture in service.

While permanent deformation of asphalt roads does not necessarily constitute a structural failure, it does shorten the service life of the pavement and increases maintenance cost. Based on the survey data collected in the US in 1997, the average age of pavements experiencing permanent deformation is 11 years. However, many rutted pavements (42%), fail at ages between 6 and 10 years as shown in Figure 1.3 (Huber, 1999). Figure 1.4 indicates that in England and Wales in 2006, rutting contributed almost 40% to the defects index on non built-up principal and classified roads and below 20% on built-up principal and classified roads (DfT, 2006).

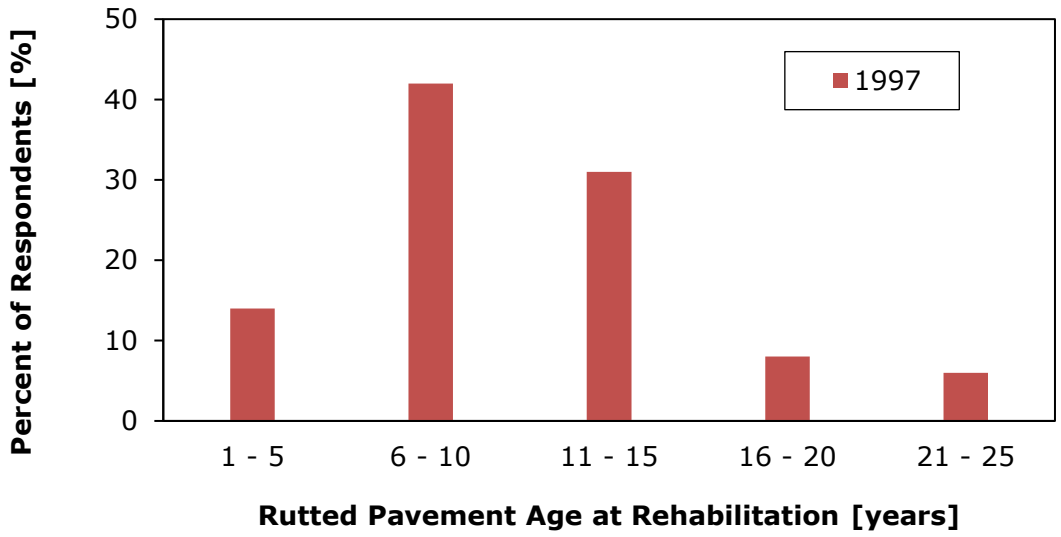


Figure 1.3. Age of pavements rehabilitated for permanent deformation (Huber, 1999)

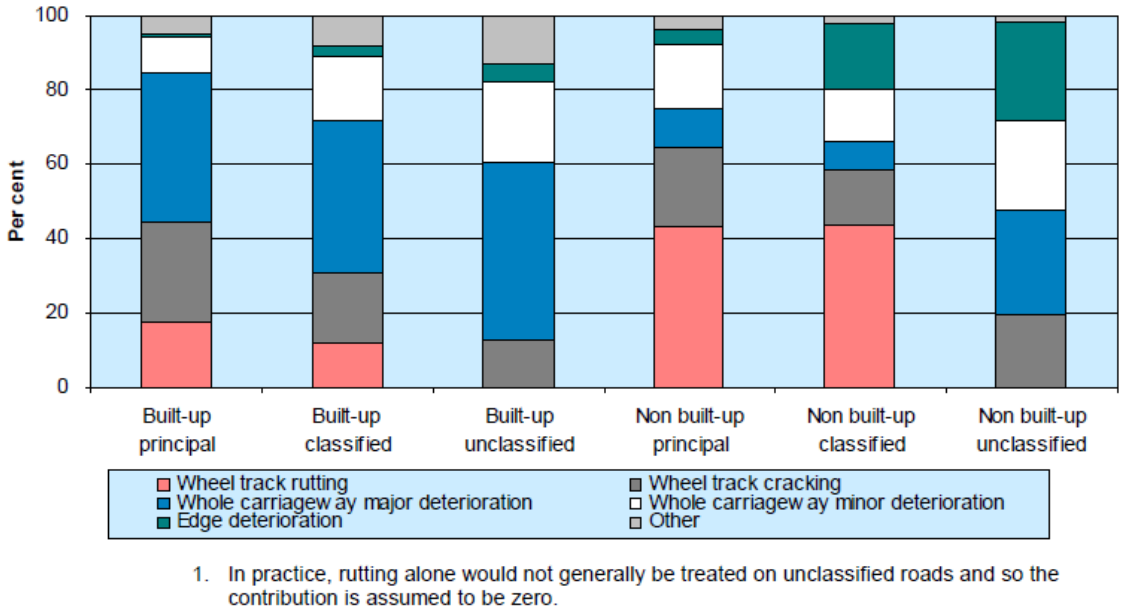


Figure 1.4. Percentage contribution of defects to defects index in 2006, England and Wales (DfT, 2006)

1.3. The Hollow Cylinder Apparatus (HCA)

Since asphalt was introduced to the road construction industry, many studies have been conducted to address performance issues and to create pavements that are rut-resistant but at the same time remain durable (resistant to environmental effects). Although, the last 20 years of development has led to significant changes and modifications in mix design technology and testing techniques, a good understanding of the fundamental behaviour is still lacking and the tests used in practice are often empirical and not well validated (Brown and Gibb, 1996). The "Desired Laboratory Performance Test" should accurately measure a mixture response over a wide range of conditions (i.e. stress condition, loading time, temperature, etc.) and reproduce the field loading regime as closely as possible. This characterisation of material properties under realistic stress conditions is an essential part of the structural design approach. It also contributes to the longer term objective of developing theoretical models for materials which can predict insitu performance from the results of a series of relatively straightforward standard tests in which the stress conditions do not necessarily bear any relation to the insitu condition.

The stress paths to which an element of material in a pavement is subjected have long been recognised as complex. Loads generated by traffic induce radial, axial and shear stresses and as the wheel passes over the element, these stresses change with time as shown in Figure 1.5 (Chan and Brown, 1994). Pell and Brown, (1972) discussed the need to design laboratory materials testing apparatus that could reproduce the complicated stress

conditions experienced in a pavement structure under traffic loading. Their ideas were stimulated by the need to understand and to quantify the key mechanical properties required for developing an analytically-based pavement design method. The nearest practical test to capture this regime is the axi-symmetric repeated load triaxial test, which had been effectively applied for soils and granular materials since the early 1960's (Hicks and Monismith, 1971, Seed et al., 1962). However, this apparatus suffers from the disadvantage of only being able to directly apply principal stresses and cannot reproduce the shear reversal effect (Figure 1.5). Pell and Brown, (1972) concluded that research up to that date had properly focussed on apparatus that captured the most important stress parameter related to the failure mode of interest. Hence, for asphalt, tensile or flexure testing was used to study fatigue cracking and triaxial testing for permanent deformation. This configuration was also used extensively to study the resilient characteristics of soils, granular materials and asphalt as the secondary effects of shear stress reversal were not considered to be of such importance where small strains were involved. This was later confirmed by Chan and Brown, (1994).

Since shear strains were recognised as being of critical importance for rutting, the University of California contribution to the US SHRP study led to the development of the Superpave Shear Test (SST). The SST was introduced to complement the Superpave volumetric mixture design method and it was envisioned that this simple performance test would play a key role in the quality control and acceptance of HMA mixtures (Monismith et al., 1994). The

equipment is capable of applying direct shear to laboratory specimens and the data can be correlated with field performance (Harvey et al., 2002). Since then the SST has become quite widely used in US research laboratories; however, it is regarded as too complex and expensive to use for routine design.

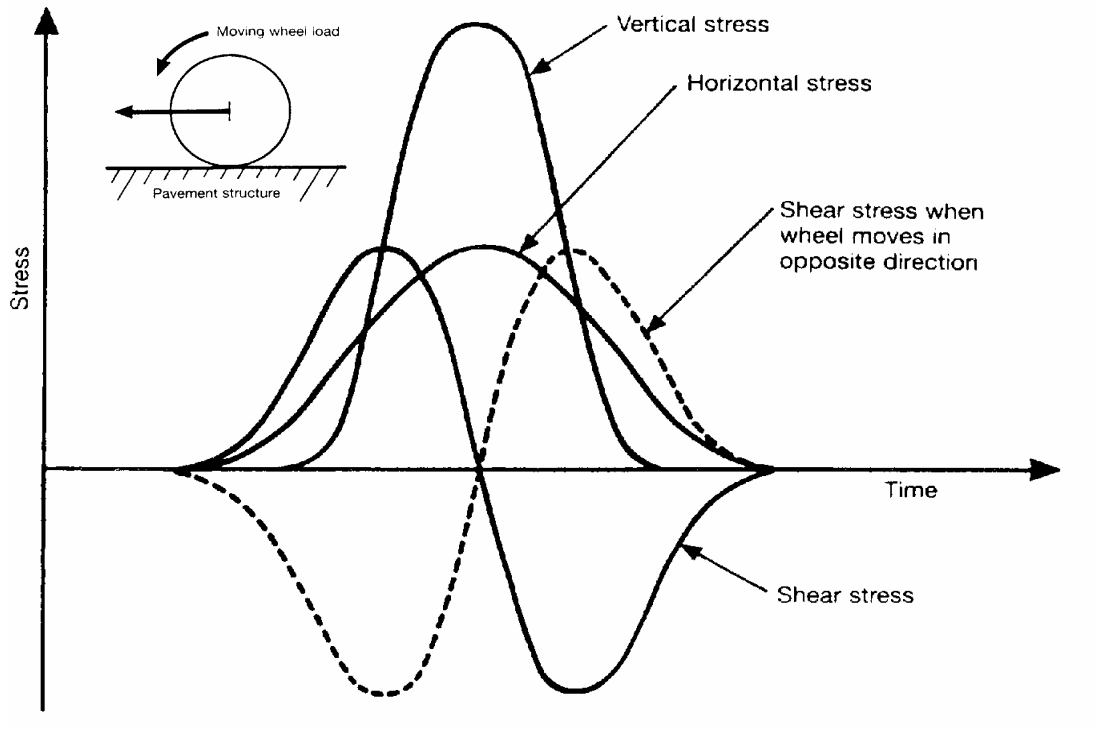


Figure 1.5. Stress regime on a pavement element caused by moving wheel loading

Pell and Brown, (1972) stated that the time had come to develop apparatus that could directly apply shear stresses to test specimens as well as normal stresses. The Nottingham pavement research team pursued this philosophy over subsequent years but with an emphasis on unbound materials.

The approach for asphalt involved the evolution, from soil mechanics research, of an improved theoretical philosophy for planning tests with the repeated load triaxial apparatus (Brown, 1975) in order to get as much from this configuration as was physically possible. This involved application of cyclic confining stress and the use of triaxial extension tests, in which a negative deviator stress was applied, as well as conventional compression tests. Brown and Bell, (1977) illustrated this approach and applied it to the prediction of rutting for a series of wheel tracking tests carried out in the pilot-scale Nottingham Pavement Test Facility. The approach involved use of invariants which are functions of the principal stresses but allow the stress conditions and corresponding strains to be expressed in a way which is independent of direction. While this approach was useful, it did not entirely overcome the inherent limitations of the triaxial configuration. Only two stress components can be varied independently out of maximum six for general conditions. To control three or more components of stress is more complicated (Thom, 1988).

Consequently, research effort in more recent years has focussed on use of the torsional Hollow Cylinder Apparatus (HCA) for fundamental work on granular materials. This configuration allows the field stress paths to be more accurately reproduced and controlled on elements of the cylinder wall. In addition to confining stress and axial deviator stress that can be applied the same way as in a triaxial device, it is also possible both to apply a torque to the cylindrical shape and also vary the pressure in the centre of the cylinder

from the external confining stress. The axial load generates a vertical stress; the torque develops complementary shear stress on horizontal and vertical planes in the wall of the cylinder, whereas variation of internal pressure imposes variation in circumferential stress much greater than variation in radial stress perpendicular to the wall (Thom, 1988). If the considered element is free from end effects then there are no shear stresses in the radial circumferential plane. The radial stress is a principal stress and the other three stress components define the remaining two principal stresses. As the loads can be applied independently, it is possible to control the magnitudes of the three principal stresses and the inclination of the major principal stress. HCA is particularly advantageous when predicting deformation away from the axis of symmetry of loading. Moreover, the instrumentation can be directly attached to the specimen, enabling accurate strain measurement.

It is desirable to have uniformities in the stress and strain distributions within the specimen. This and the capability of reliable determinations of loads and displacements are vital for any device as only then the resulting stress and strain states within the specimen can be accurately defined. A HCA disadvantage is that some stress non-uniformity is inevitable, particularly when there is a difference between internal and external confining stress. However, Hight at al. (1983) reported that as long as the ratio of diameter to wall thickness and height to diameter were sufficiently large, such uniformities could be ignored.

In 1985, a repeated load HCA was developed at the University of Nottingham for granular materials testing and since then was used by number of researchers (Thom, 1988 and Richardson, 1999). The apparatus was specifically designed to apply cyclic loads, simulative of the stress condition in the pavement under moving wheel loads. The torsional hollow cylinder apparatus (HCA) had proved much more effective than any type of shear box, so the same configuration was used to develop a realistically sized HCA for the testing of asphaltic concrete. This type of apparatus was first introduced for asphalt by Sousa, (1986) at the University of California at Berkeley (UCB) and, subsequently, used by Alavi and Monismith, (1994) to study dynamic properties of asphalt under axial and torsional loads. Most recently, Rueda et al. (2017) developed a hollow cylinder apparatus (HCT-AM) at Los Andes University (Colombia) to study effect of climatic conditions on the dynamic response of asphalt mixtures. Neither of these projects investigated permanent deformation characteristics in any detail.

Because of the success of previous research, this new study focused on the application of a thick-walled hollow cylinder device to asphaltic materials in order to assess their resistance to rutting.

1.4. Objectives and Scope of This Research

With the foregoing in mind, this project has been concerned with developing a research level HCA apparatus for quantifying the permanent deformation characteristics of asphalt with respect both to shear and volume change characteristics. This should be done under appropriate laboratory test conditions to provide better insight into rut development. This will allow simpler, more practical methods, such as the SST and the various other methods in common use, including the uniaxial or triaxial test to be assessed and calibrated. It will also improve understanding of asphalt mechanics and so assist with developments in computational modelling of pavement rutting through better definition of the required constitutive equations.

This research project was funded by both the government and industry and the principal objectives of this study were to:

(1) Design, build and commission a new Hollow Cylinder Apparatus (HCA) for testing realistic asphalt mixtures under appropriate stress paths to investigate permanent deformation (Chapters 3 to 5);
(2) Generate data on stress/permanent strain relationships to assist in the development of realistic models for the prediction of pavement rutting (Chapters 5 and 7);
(3) Compare the results with the US SST and the simpler permanent deformation tests used for practical materials design to verify accuracy and reliability (Chapters 6 and 7).

In the EU, test methods for asphalt have been agreed by the relevant standardisation committee and are implemented into practice now. This research is intended to assist in generating background knowledge, which will allow future revisions of the EU standard to be improved and to provide a realistic basis for the determination of material properties to assist with the evolution of theoretical prediction methods for rutting. Such methods will increasingly be required by companies responsible for the long term management of highway networks to plan future maintenance requirements within a whole life cost approach.

In order to accomplish these objectives, the following tasks were set out:

I. Development of a new HCA which could simulate the stress paths experienced under moving wheel loads;
II. Development of a reliable method of asphalt test specimen preparation;
III. Collaboration with the University of California at Berkeley and Davis in order to compare data on identical materials in their SST device;
IV. Completion of the general HCA test programme;
V. Assessment of simple repeated load compression tests for use by industry for assessing the rutting resistance of asphalt layers in roads.

1.5. Outline of the Thesis

This thesis is organised into eight chapters, including this introduction (Chapter 1). Chapter 2 presents the literature review concerning the permanent deformation behaviour of hot asphalt mixtures. It also includes a brief description of pavement design and a summary of the test methods used for measuring the rutting performance of asphalt. Chapter 3 describes development of the new HCA. Specimen preparation and testing set-up is presented in Chapter 4. Chapters 5 and 6 present the experimental work undertaken in this study, detail the testing procedure for each test method and present results. Chapter 7 summarizes the results and presents discussion. Chapter 8 includes conclusions and presents a framework for future work.

2

LITERATURE REVIEW

2.1. Introduction

This chapter consists of the literature review conducted on permanent deformation of flexible pavements, which provides the reader with the background knowledge necessary for this study. The following topics are considered:

1) General Background
2) Pavement Failure
3) Pavement Design
4) Behaviour of Asphalt Mixtures
5) Factors Affecting Permanent Deformation
6) Laboratory Testing
7) The Hollow Cylinder Apparatus
8) Asphalt Layer Rutting Performance Prediction Models

2.2. General Background

The road pavement is the structure built to protect the subgrade soil from the destructive effect of wheel loading and constantly changing environmental conditions. There are two main types of pavements commonly used for highways construction: flexible (bituminous) and rigid (concrete). The primary aim of this research is to investigate the shearing characteristics of asphalt therefore consideration will not be given to rigid pavements.

A flexible pavement structure normally consists of several layers of different materials bonded together placed over the top of the subgrade. Figure 2.1 shows a typical cross section of a bituminous pavement. The surfacing should be abrasion, deformation and skid resistant and must provide a good riding quality and acceptable low levels of noise generation. It may be sub-divided into the surfacing course and the binder course. The road base provides the main structural support to the pavement and it may be laid in two or more sublayers. The subbase course provides a working platform to the construction traffic and paving operations and enables adequate drainage and frost protection. It may be sub-divided into the subbase and the capping layer. Figure 2.2 illustrates the "Ideal Pavement" and highlights the key characteristics of each layer (Brown, 2000). Although, each of the pavement layers has a specific role and specific function to fulfil, the ultimate aim is to ensure that the repeated rolling loads are distributed to the soil in such a way that stresses are low enough to avoid excessive deformation.

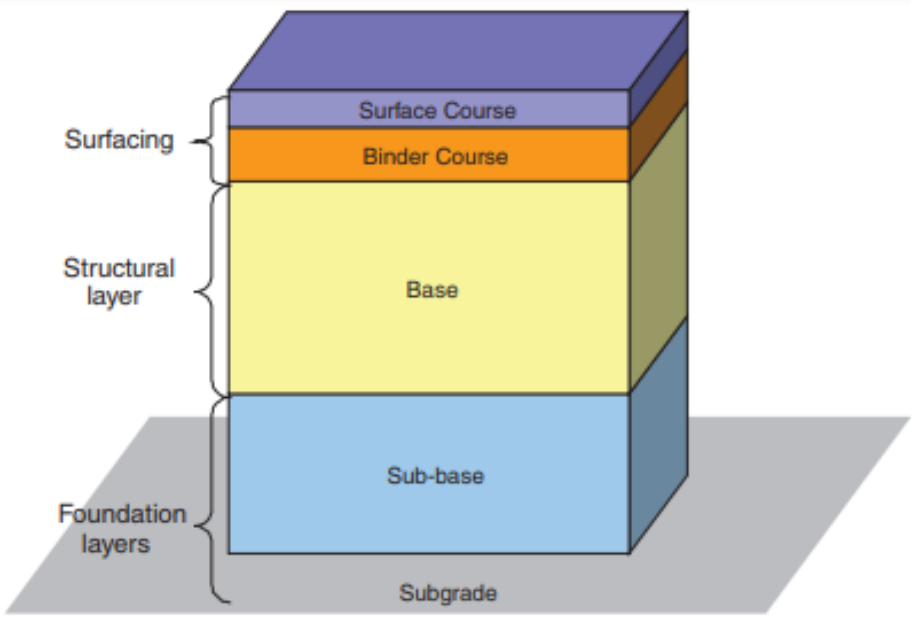


Figure 2.1. Cross section of a typical UK flexible pavement (Merrill, 2005)

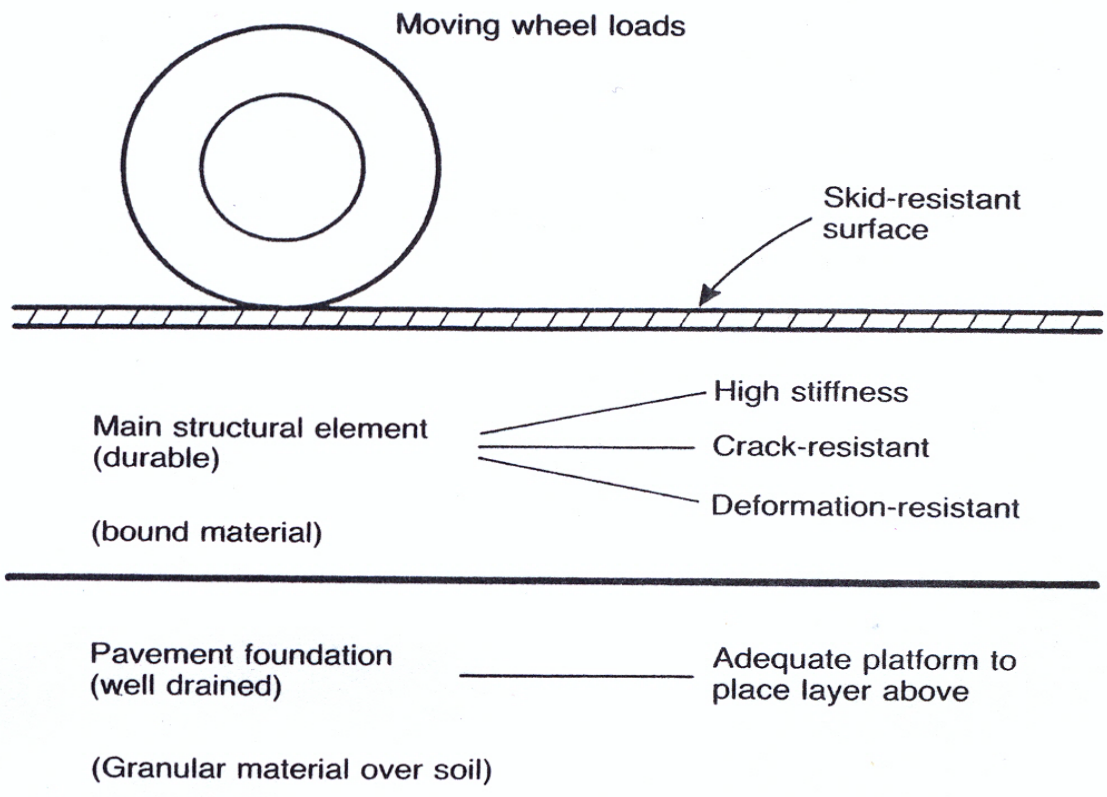


Figure 2.2. The ideal pavement (Brown, 2000)

2.3. Pavement Failure

As soon as the road is open to traffic, the pavement starts to deteriorate. Under the impact of traffic loading and environmental effects, the service life of asphalt slowly decreases year after year, ultimately leading to failure. In order to predict a realistic performance of the pavement, which is necessary for keeping a road network at an acceptable level of service while minimising the cost of maintenance, highway engineers should have a good understanding of the nature of flexible pavement failures.

Figures 2.3-2.4 illustrate two most common distresses occurring on bituminous roads, cracking and rutting. These are two main components taken into consideration during the design process.

Under the impact of wheel loads pavement tends to deform/flex, inducing compressive, tensile and shear stresses in the bituminous pavement structure (Figure 2.5). Most of this deformation is recovered, when the load is removed. However, there is a small amount which remains irrecoverable. Repeated traffic loads cause the irrecoverable part to accumulate leading to rutting. The design criteria applied in current (analytical) design methods are intended to guard against serious permanent deformation originating within the subgrade. This is currently attributed to the excessive compressive stresses which are developed at the top of the subgrade layer (Akbulut and Aslantas, 2005). Such procedures assume that permanent deformation is

mainly due to the subgrade deformation and they do not consider rutting within the asphalt layer.

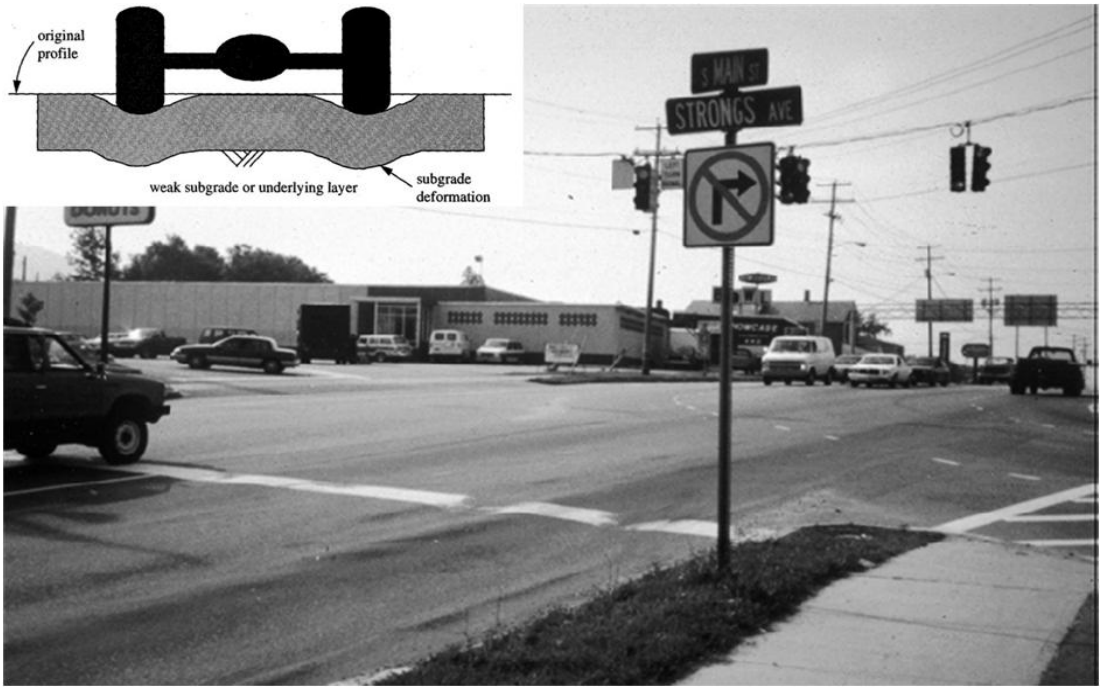


Figure 2.3a. Subgrade deformation (Drakos, 2012)

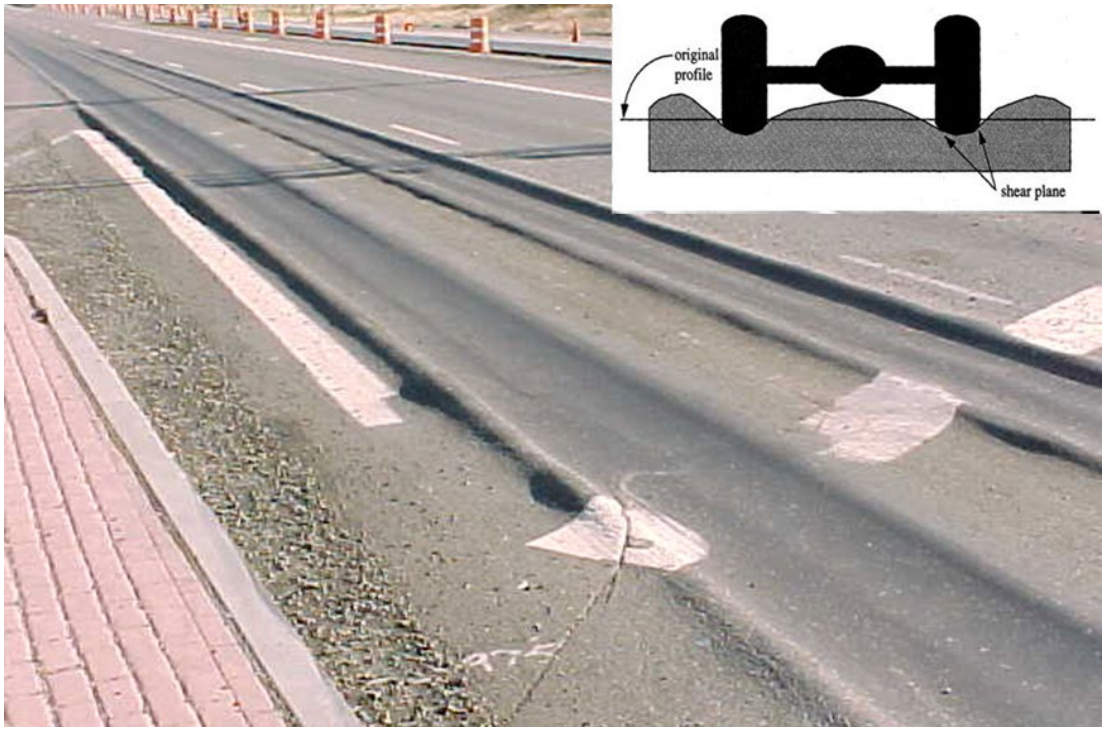


Figure 2.3b. Mix instability rutting (Web, 2012)



Figure 2.4. Cracking (Web, 2011)

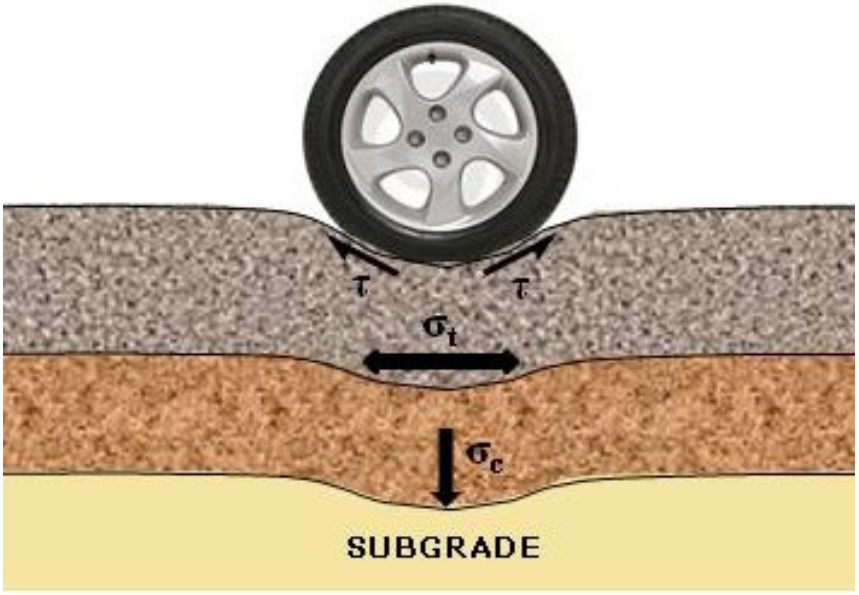


Figure 2.5. Stresses induced in the flexible pavement under the wheel loading

Fatigue cracking can be caused by a number of factors. However, bituminous pavements usually crack as a result of overloading. Fatigue failure relates to the tension developed at the bottom of a stiff asphalt layer. Therefore, pavement design models predicting pavement performance with respect to cracking control the maximum permissible horizontal strain at the bottom of the bituminous material (Brown and Brunton, 1985). More recent studies, however, suggest that cracking can also initiate at the surface, generally in thick pavements (Leech and Nunn, 1997). The fatigue behaviour of asphalt mixtures is outside the bounds of this research; thus, it will not be discussed in detail hereinafter.

Failure is usually defined in terms of the amount of cracking or the rut depth. In the UK, a pavement is considered failed if maximum deformation of 20mm has been encountered or if 20% of the surface has cracked (Read and Whiteoak, 2003).

The magnitudes of critical stresses developed in the structure are controlled by the relative stiffness of individual layers. Figure 2.6 illustrates the load-spreading principle in pavement engineering (Brown, 2000). Since on the one hand, the increase of the elastic stiffness of a pavement improves its load spreading ability, on the other hand, it creates a potential risk of fatigue failure at the bottom of the asphalt layer (Figure 2.7), pavement design predominantly involves determining the most adequate combination of the

thickness and mechanical properties of the individual layers in order to obtain a long lasting and distress free road.

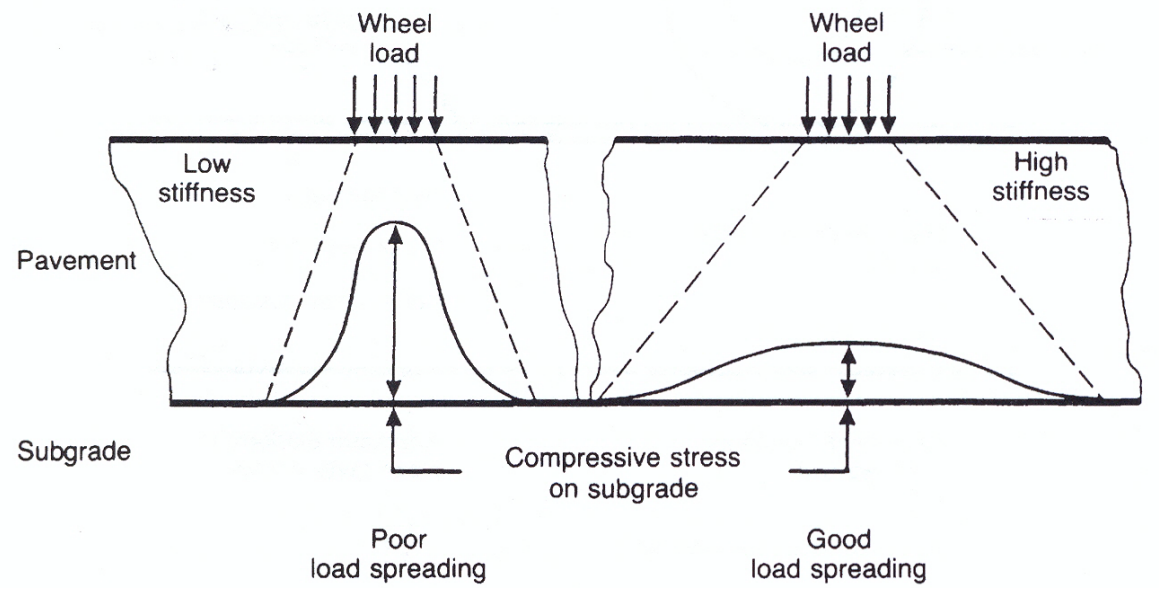


Figure 2.6. Spread of loading in road pavement (Brown, 2000)

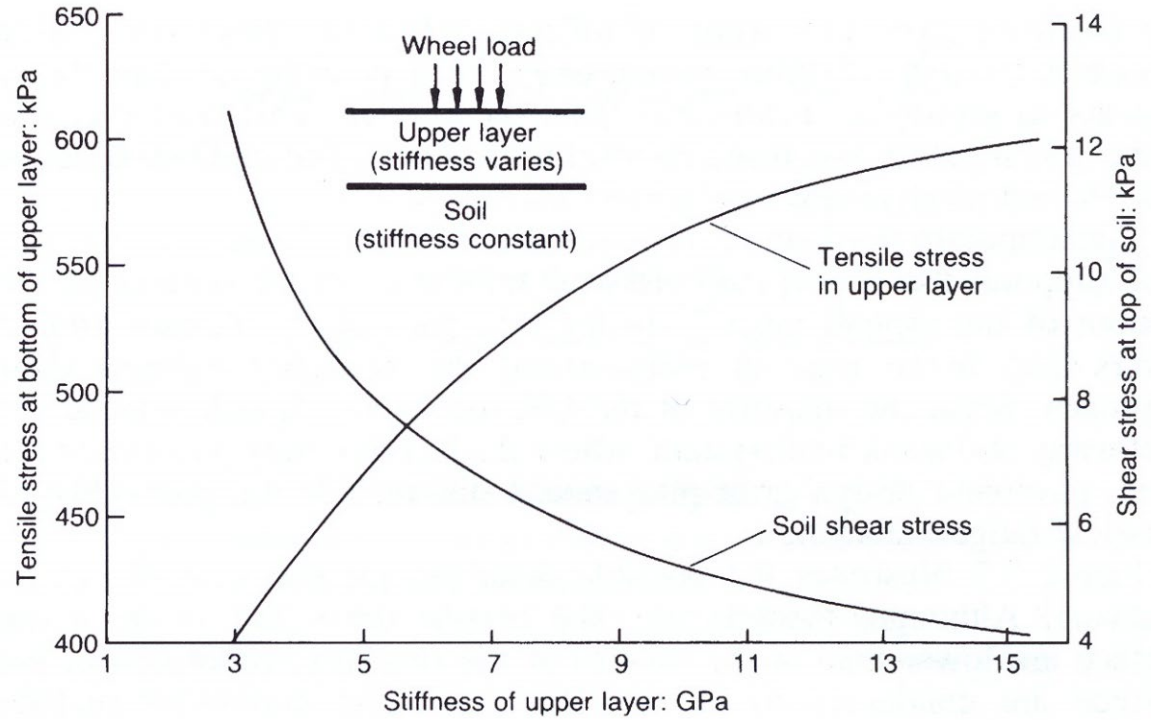


Figure 2.7. Variation of critical stresses in a road pavement (Brown, 2000)

2.4. Pavement Design

Flexible pavements are typically constructed from layers of compacted asphalt materials. Hot mix asphalts (HMA) consists of combination of mineral aggregate with bituminous binder and any other additive. The process of selecting the optimum proportion of these components is called mix design and the process of determining the number and thickness of different layers within a pavement structure is called structural design. Mix and structural design are the two key components of pavement design and are totally dependent on each other. The primary purpose of a good pavement design is that pavement can withstand environmental and traffic conditions encountered over the design life.

2.4.1. Mix design

Mix design typically involves an iterative search for an economical combination of ingredients which meets performance requirements while, at the same time, minimising the risk of premature failure.

Table 2.1 summarises essential requirements that a material needs to acquire and gives a general indication of the levels of binder content, aggregate gradation, and air voids needed to achieve each of these demands.

Table 2.1. Summary of mixture design requirements (AI, 1983)

Mixture Property	Bitumen Content		Aggregate Gradation		Air Voids	
	Low	High	Dense	Open	Low	High
Stability	●		●		●	
Durability		●	●	●	●	
Flexibility		●		●		●
Fatigue resistance		●	●		●	
Skid resistance	●			●		●
Imperviousness		●	●		●	
Fracture strength		●	●		●	

Two general methods of mix design are adopted, recipe approach and engineering design. Currently in the UK, bituminous mixture specifications are given in the relevant parts of British Standard BS EN 13108 with guidance on the requirements to be selected in the UK in BSI PD6691 (BSI, 2016e). The British Standard is based on a common format and common principles. The overall principle is to provide a way for the target composition of a mixture to be declared in a standard way and demonstrate that, at that target composition, it has certain defined properties. Each mixture formulation needs a declaration of the properties which are being claimed, demonstrated through a product-type testing procedure. In the simplest case it can be just grading and binder content. In more complex situations it can include performance-related properties, such as stiffness, deformation resistance and fatigue resistance. The demonstration of performance and conformity of the mixture on an ongoing basis requires the producer to undertake factory production control. This is a quality management procedure involving defined inspection and test regimes, and conformity

criteria to prove that the mixture conforms to the declared target composition within defined tolerances.

Recipe Approach. A recipe specification for selecting the types and proportions of the materials comprising an asphalt mixture is entirely based on experience of traditional mixtures of known composition that have performed well in practice. Nevertheless, the success of the mix is not only dependant on its composition but also on workmanship in construction.

This experience based approach has a number of severe limitations. The conditions to which an in-service mixture is subjected (e.g., traffic, climate, etc.) will almost certainly not be the same as those existing when the specifications were developed. Additionally, recipe specifications are based on the aggregate grading curves and as these curves cannot take into account aggregate properties and packing characteristics, they are not very reliable, particularly when different source aggregates are used in the mixture (Read and Whiteoak, 2003). Moreover, specification by recipe may not be suitable for innovative asphalt mixtures that are beyond previous experience.

For recipe mixtures BS EN 13108 adopts the principle of a declared target composition selected from a permitted range. This UK guidance gives recommendations for an approach to using BS EN 13108 to arrive at mixtures similar to those which have been traditionally used over many years.

Engineering Design. This approach involves selection of an aggregate grading and determination of appropriate binder content based on performance testing so that the material after compaction possesses sufficient stiffness, deformation resistance and air voids. There are several different mixture design methods used, of which the Hveem, Marshall and Superpave methods are the most common. References (AI, 1988, AI, 2001) provide details of these procedures.

Regardless of what specific method is used, the basic mix design procedure remains the same. All mix design processes involve three basic steps: aggregate selection, binder selection and optimum asphalt binder content determination, as shown in Figure 2.8.

2.4.2. Structural design

The objective of pavement thickness design is to produce an engineering structure that will distribute traffic loads efficiently ensuring long-life performance, whilst minimising the whole-life cost of the pavement. There are two approaches to structural design, empirically-based and analytically-based, also referred to as mechanistic-empirical (Monismith and Brown, 1999).

Empirical design methods were introduced to the UK more than 50 years ago. They were established by studying the performance of experimental

road pavements constructed of various surfacing, road base, and subbase materials placed in a range of thicknesses.

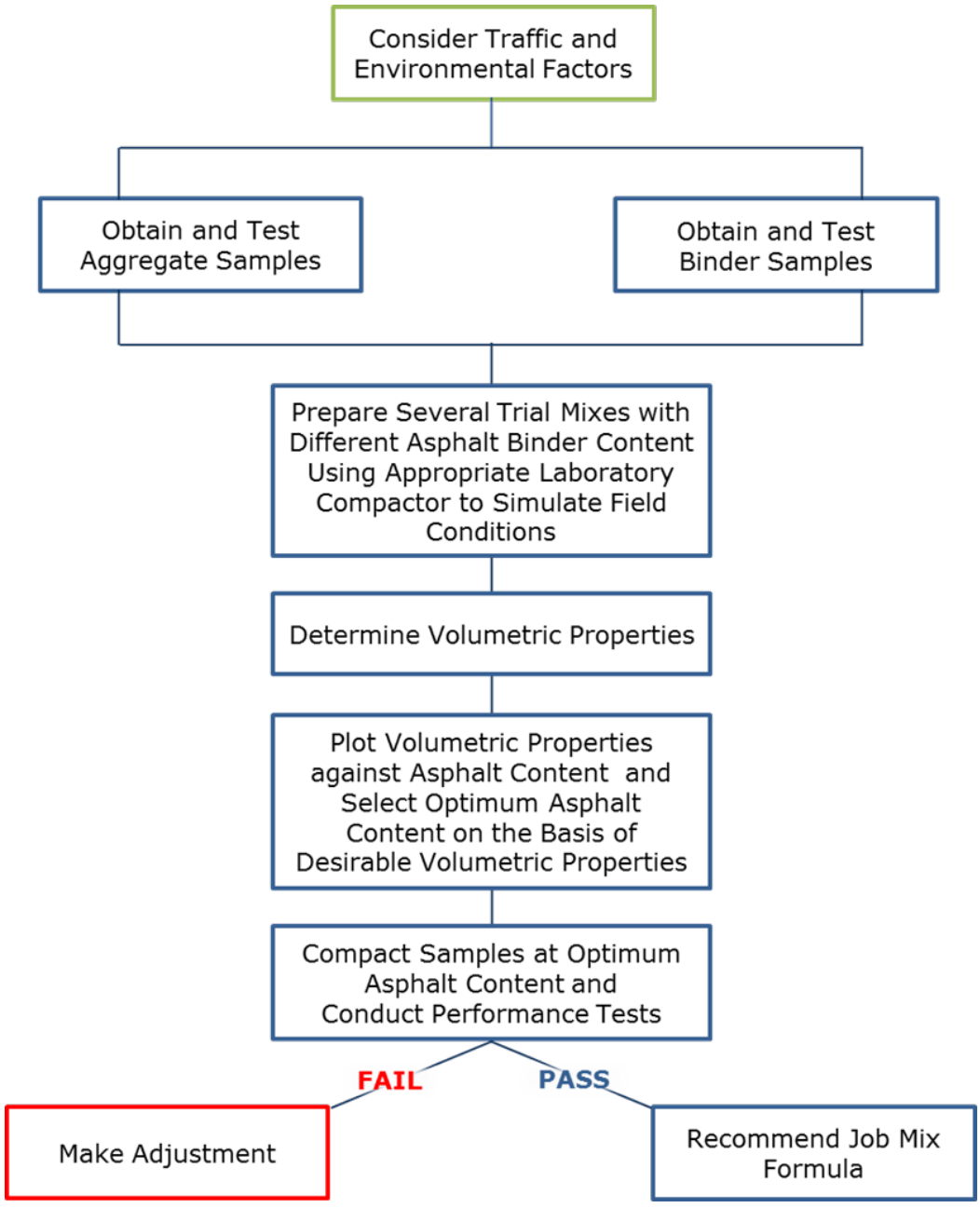


Figure 2.8. The Mixture Design Process (AI, 1988, AI, 2001)

The empirical approaches do not demand detailed knowledge of engineering principles and cannot cope with circumstances beyond those included in the experience on which the method is based (Read and Whiteoak, 2003).

In contrast, an analytically-based design approach uses theoretical analysis of stresses and strains induced in various layers and the mechanical properties of materials, and should in principle, be capable of dealing with any design situation. It also provides the opportunity for new materials to be incorporated in the design.

The calculations are made under the full range of the load and climatic conditions and fatigue and deformation data are used to determine potential mode of failure and the potential life. Figure 2.9 summarizes these procedures (Monismith, 2004). The design process consists of three stages: evaluation (the data input stage), analysis (the complex distress prediction stage), and strategy selection (the design decision stage). The main purpose of this method is to adequately predict stress and strain response of the pavement over a particular design life to the transient loads generated by traffic that can be used in the development of models for any load associated deterioration mechanism. In order to do that, numerical analysis using both multilayered elastic theory and finite element (FE) technique has been used.

In terms of current theoretical pavement design procedures, linear elastic theory is most often used for defining pavement response. Finite-element

(FE) analysis was developed to model non-linear behaviour of soils and granular materials in the late 1960s; however due to its complexity, computational time constrains, and cost, use of this methodology has had limited application to date (Duncan et al., 1968, Monismith, 2004).

A multilayered elastic system was developed by extending Burmister's two-layer analytical solution (Burmister et al., 1944, Papagiannakis and Masad, 2008). The pavement system consists of multiple layers of a finite thickness and infinite dimensions in all horizontal directions, resting on a subgrade of infinite thickness. The theory assumes that all layers are homogenous, isotropic, and can be described by their elastic Young's modulus E and their Poisson's ratio μ (Hooke's Law). The tyre loads are modelled as either point loads or circular loads of uniform pressure. Pavement response is calculated using linear elastic theory. Therefore, it is not possible to analyse layered systems consisting of non-linear subbases or subgrade materials. The study by Monismith et al., (1994) indicates that this theory is not able to accurately model pavement performance. Regardless of these results, the multilayer elastic models are considered to be satisfactory for predicting flexible roads response under external wheel loads and have been implemented into numerous computer codes. Several computer programs are available for the pavement structural analysis such as: BISAR: Multi-layer Linear Elastic Half-space Analysis (Shell, 1998), VEROAD: Viscoelastic Multilayer Program (Hopman, 1996), EVERSTRESS: Multi-layer Nonlinear Elastic Half-space Analysis (EUG, 2005), and ABAQUs: Finite Element Analysis (DSS, 2009).

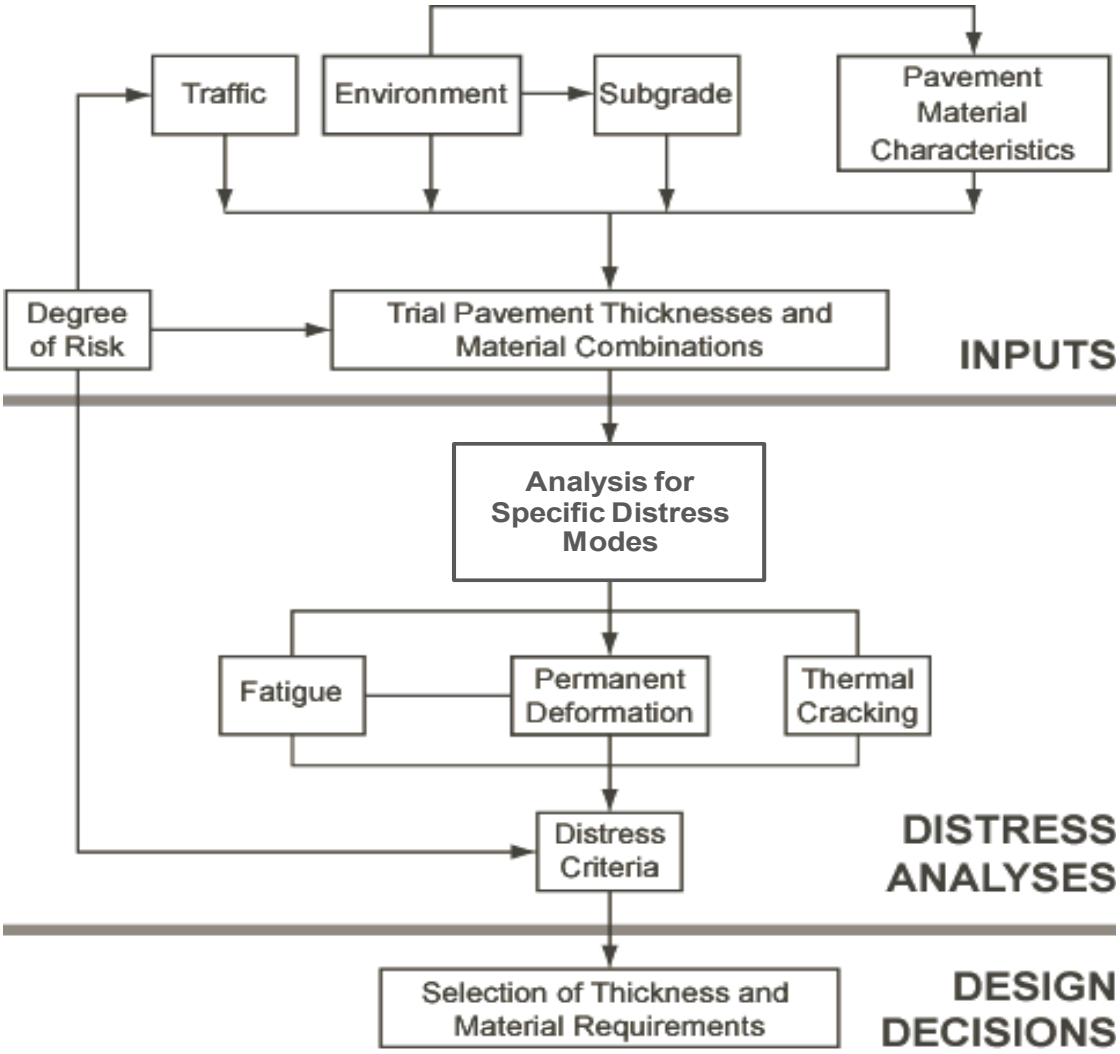


Figure 2.9. Analytical Pavement Design (Monismith, 2004)

2.5. Behaviour of Asphalt Mixtures

The behaviour of asphalt is very complex as its mechanical properties are strongly susceptible to loading time and the temperature. The material response to wheel loads can be expressed by elasticity, plasticity, and viscoelasticity. The deformation of asphalt layers of the pavement is controlled by plastic and viscous components. In order to adequately evaluate and predict changes that occur within the asphalt over the life of the road, a fundamental understanding of mechanical characteristics of bituminous materials is required.

Asphalt behaves like an elastic solid at low temperatures and rapid loading. Under these conditions, the pavement is able to return to its original shape after a load is removed (all deformation is recoverable). Therefore, during the winter, when the mixture is very stiff rutting does not occur. At high temperatures and slow loading, asphalt acts more like a viscous liquid. This behaviour is in contrast with that of elasticity, the stiffness of pavement decreases, and strains induced by traffic increase. A portion of strain within the viscous component is not recovered and permanent deformation occurs. At the intermediate conditions found in most pavement systems, asphalt material displays partly elastic and partly viscous behaviour.

The response of loading time and temperature-dependent asphalt materials to stress can be described by rheological models, e.g. Burger’s Model.

The principal requirement of a suitable model is its ability to simulate the deformation response of an asphalt material (Wa and Muthen, 1997). Burger's model (see Figure 2.10) consists of Maxwell's model (spring, E1, and dashpot, η1, in series) and Kelvin's model (spring, E2, and dashpot, η2, in parallel). The spring acts to model elastic properties of material, while the dashpot acts to model viscous properties of material. Figure 2.11 illustrates the viscoelastic response of asphalt by Burger's model.

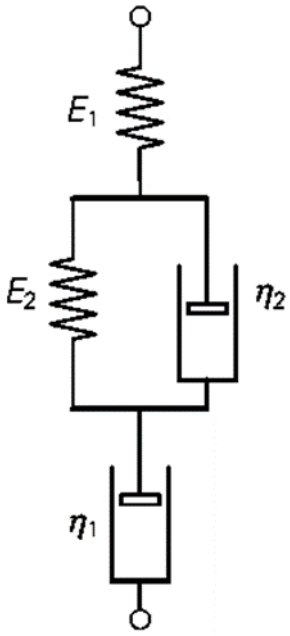


Figure 2.10. Burger's Model (Thom, 2008)

The elastic and delayed elastic strain is totally recoverable once the load and applied stress are released. However, the viscous strain represents the non-recoverable deformation.

As the rheological properties of bitumen are functions of time and temperature, both the magnitude and the shape of the creep curve will change with loading time and temperature. The elastic response of the bitumen dominates at short loading times and/or low temperatures, while the viscous response dominates at long loading times and/or high temperatures (Airey, 1997). Consequently, at normal pavement temperatures the bitumen exhibits viscoelastic behaviour, hence delayed elastic response dominates.

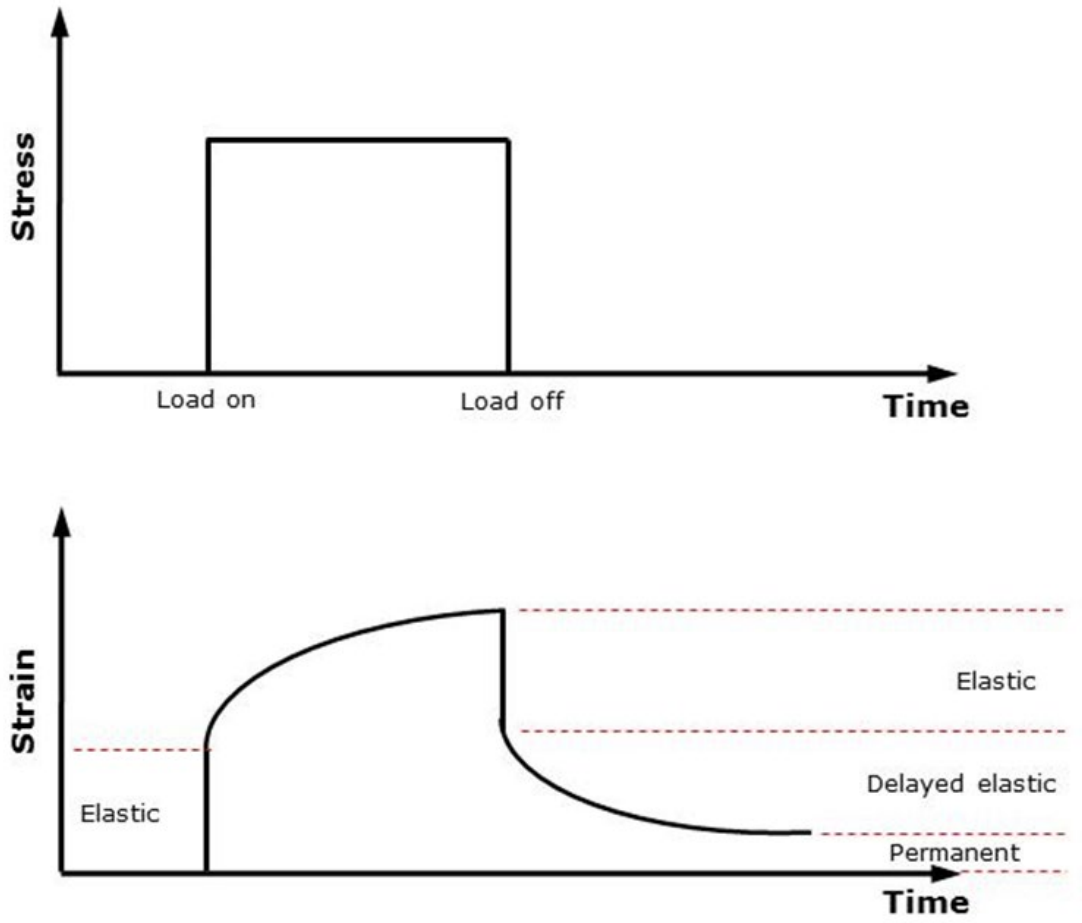


Figure 2.11. Visco-elastic response of asphalt - Burger's model (Read and Whiteoak, 2003)

Furthermore, since the viscosity is temperature and loading time dependant, a series of such curves is required to describe an asphalt material (Bouldin and Collins, 1992).

The non-linear response of asphalt material is difficult to model or to characterise in the laboratory tests (Airey, 1997). It is necessary to supplement the mechanical models with damage models which degrade or

change the mix properties as a function of the temperature and load cycles (Monismith et al., 1994).

In order to define viscoelastic properties of asphalt mixtures, Van der Poel introduced the concept of stiffness modulus in 1954 (Read and Whiteoak, 2003). Traditionally the stiffness modulus was assumed to be dominated by elastic behaviour but this is not the case for asphalt material. Stiffness modulus of bitumen is a function of temperature and the duration of load. Under the impact of these two factors there is a transition from elastic to the viscous situation. Stiffness modulus is defined as the ratio between the applied stress and the resulting strain at the loading time.

The two most popular methods which enable determination of stiffness modulus include a creep test (static measurement, constant stress) and an oscillatory-type testing (dynamic measurement, sinusoidal strain).

From the dynamic test, the complex shear modulus (G*) as well as its elastic and viscous components can be calculated. Figure 2.12 shows the response of the material under sinusoidal dynamic stress loading. Generally testing is conducted within the region of linear viscoelastic response. The phase angle, δ, is a measure of the degree of viscosity of the asphalt mixture.

An increase in phase angle indicates an increase in the viscous properties of the material. Asphalt exhibits purely elastic behaviour when load and

deformation are in phase (the phase angle is equal to zero). In contrast, phase angle of 90 degrees between load and deformation represents purely viscous behaviour. Consequently, viscoelastic materials have a phase angle between zero and 90 degrees.

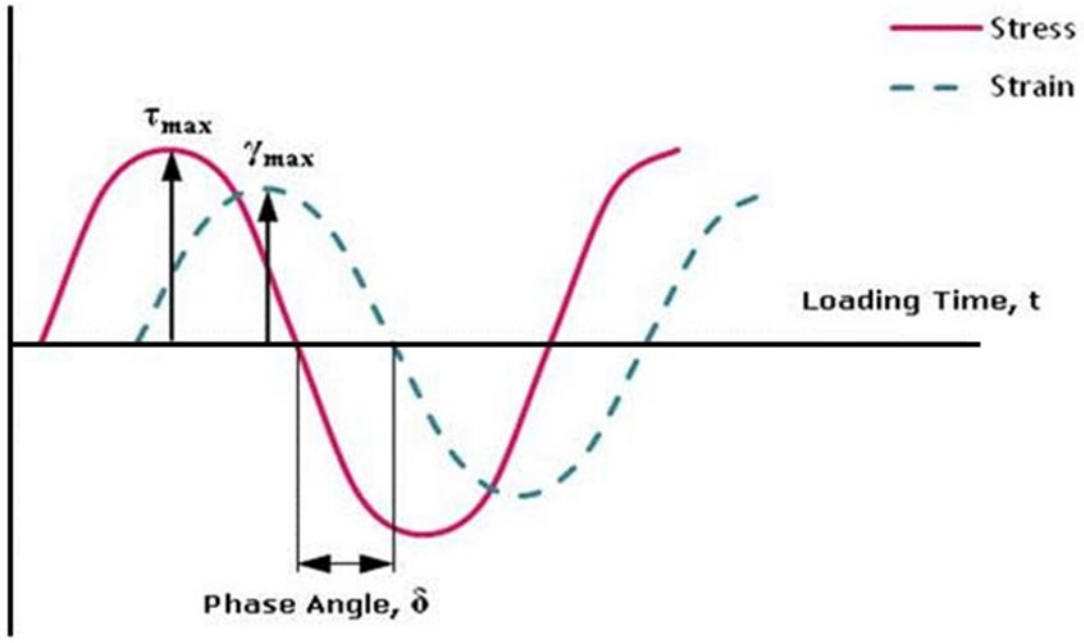


Figure 2.12. A dynamic test in shear (Read and Whiteoak, 2003)

2.6. Factors Affecting Permanent Deformation

Hot Mix Asphalt (HMA) consists by volume, 70 to 85 per cent of aggregate and 10 to 15 per cent of binder. It is self-evident that the response of asphalt pavement to loads is significantly affected by the mechanical properties of these two components. Over the years many studies have been conducted in an effort to investigate rut resistance of asphalt mixtures and it has been concluded that permanent deformation of HMA depends not only on the aggregate and asphalt binder properties and how they interact with each other but also on the environmental conditions to which the mix is subjected. Based on the review of others' work, the factors that influence the deformation damage of asphalt concrete the most are: mixture characteristics (aggregate properties, binder properties, and air void content), traffic (wheel load, tyre pressure, and vehicle speed), environment (temperature, moisture), and construction practice (compaction). The effect of each of these factors is discussed in the following sections.

2.6.1. Aggregate

Typically, a road is constructed by combining aggregate particles and asphalt binder to serve as a flexible structure over a wide range of environmental conditions. The aggregate skeleton is the primary component of the mixture, hence it is clear that it plays an important role in controlling the behaviour of asphalt and rut resistance relies predominantly on particle properties (Flowers et al., 1989, Brown and Bassett, 1990, Mahboub and Allen, 1990).

Aggregate gradation refers to the amount of each size particles used in the mix. Aggregate size distributions are classified as: continuously graded – asphalt mix in which there are proportions of various sizes of aggregate resulting in a smooth grading envelope, gap graded – asphalt mix from which intermediate aggregate sizes are omitted to follow a stepped grading envelope, or open graded – asphalt mix which consists of single sized crushed aggregate, with no fine particles (see Figure 2.13).

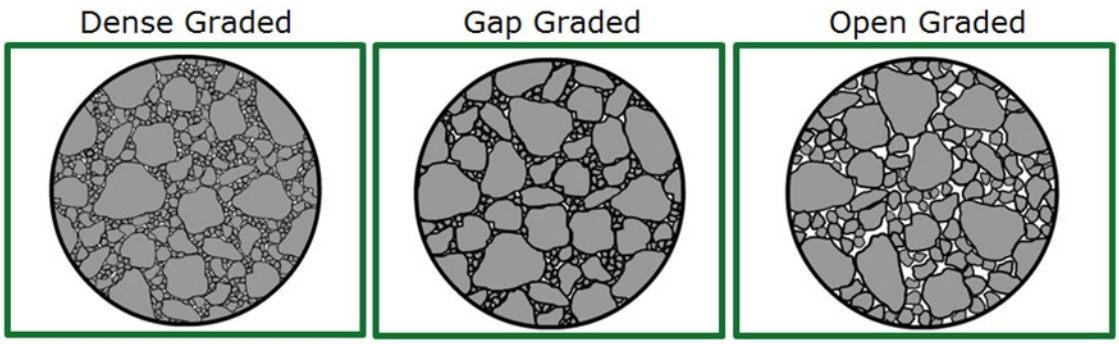


Figure 2.13. Aggregate size distribution

Many researchers have shown that gradation is one of the most important factors responsible for permanent deformation (Huber, 1999, Hensley and Leahy, 1989). Maccarrone and Holleran, (1990) studied rut resistant mixes for Australian conditions and found that improper gradation as well as excessive binder are the main factors causing rutting in the field.

Available evidence indicates that mechanical properties of the asphalt result more from the internal friction of aggregate interlock. The aggregate interlock phenomenon has a significant contribution to shear strength. These

observations were confirmed by Brown and Pell, (1974), who showed that a continuously graded mixture can resist permanent deformation more than a gap graded mixture due to stone-on-stone contact. Because of that, they proved as well that gap graded mixtures will be more prone to rutting at higher temperatures.

Geometry of the particles plays an extremely important role in developing asphalt mixtures that will be able to withstand heavy vehicle loads. A few previous researchers have shown that an increase in aggregate angularity and texture increase the strength and stability of the asphalt mixture (Krutz and Sebaaly, 1993, Masad et al., 2005, Uge and Van de Loo, 1974). Kim et al., (1992) revealed that mixtures comprised of aggregates with rough surface texture and an angular shape, have better permanent deformation properties. Oduroh et al., (2000) showed that as the percentage of crushed coarse particles decreased, the rutting potential of HMA increased. Chen et al., (2005) found that cubical particles possessed the best rutting resistance over other shapes. Flaky or elongated aggregates were shown to have lower compatibility hence poorer mechanical stability.

In general, to maximise aggregate interlock it is desirable to use angular particles rather than rounded or flat and elongated. Rounded aggregate particles have a tendency to slide by each other under the impact of traffic. Flat and elongated particles have a tendency to break during the compaction

process, changing the mixture gradation, hence the overall mixture performance.

Most of the permanent deformation in surface layers results from an asphalt mixture that does not have enough shear strength to resist repeated loads (Monismith et al., 1994, White, 2002). In order to overcome this problem and to enhance shear resistance of the mixture it is desirable to have particles with a rough surface texture. Fletcher et al., (2002) identified aggregate texture to be the shape property that has the most significant influence on the asphalt mix performance.

Fine aggregate angularity is one of the most important factors affecting the rutting performance of asphalt concrete pavements. Similarly, as in the case of coarse aggregates, angular shape and rough surface texture of the crushed fine aggregate provides better stability of the mixture and consequently lesser susceptibility to rutting (Wedding and Gaynor, 1961). Smooth rounded particles of natural sand tend to slip easily producing a weak aggregate skeleton. This statement was confirmed by Sigurjonsson and Ruth, (1990) who reported that natural sand contributes to the poor resistance to permanent deformation. Several researchers concluded that replacing natural sand with crushed fines not only improves rutting resistance but also significantly increases water damage resistance and reduces bitumen susceptibility to the effects of temperature (Lee et al., 1999). Lee et al., (1999) studied the effects of fine aggregate angularity on

asphalt mixture performance and found that fine aggregate angularity has correlation with the performance of the mixture, however the asphalt performance depends on many other factors. Different mixtures with the same fine aggregate can either perform well or poorly.

2.6.2. Binder

Despite the fact that that binder constitutes only 10 to 15 percent of the asphalt mixture by volume, it still has an important bearing on the pavement performance (Gibb, 1996). The influence is highly dependent on the condition to which the road is subjected. This was recognised by Leahy et al., (1995) reporting that the effect of asphalt was significant, but that its influence was small compared to the influence of aggregate and air voids, especially when mix was subjected to states of stress which amplified the aggregate influence. However, in cases where mix characteristics are such that interparticle friction is low and the mix is subjected to harsh environmental and loading conditions, the influence of the binder becomes more readily apparent.

The binder content should be sufficient to provide thick enough binder films on the aggregate to provide durability and good workability. If the relative volume of the bitumen exceeds the optimum level, there is a loss of internal friction at aggregate contacts and the mixture will become unstable

(Hunter, 1994). Use of excessive asphalt binder is a common cause of rutting (Maccarrone and Holleran, 1990).

Viscosity determines how bitumen material will behave over a temperature range. Generally higher viscosity means better stiffness of the mixture. Thus, the higher viscosity, the better resistance to rutting at higher temperatures (Monismith et al., 1985, Stuart and Izzo, 1995).

It is well known that not all asphalts will meet all of the performance criteria required, thus bitumen modifiers can be added to asphalt binders to improve viscoelastic behaviour of the material. The mixture stiffness should increase, enhancing rut resistance of the pavement at high temperatures without affecting the properties of the asphalt at low temperatures.

These bitumen modifying materials and additives include a wide range of polymers, crumb rubber, chemical agents (e.g. sulphur), adhesion improvers, natural asphalts, fillers and fibres, among other materials. According to Airey, (1997), ethylene vinyl acetate (EVA) and styrene butadiene styrene (SBS) copolymers were two of the most widely used polymers in bitumen modification.

Over the past 50 years there have been numerous studies conducted in order to compare mechanical properties of modified and unmodified asphalt binders (King et al., 1999, Monismith, 1988, Qi et al., 1995). For example,

Williamson and Gaughan, (1992) investigated pavement performance related to rutting and cracking in asphalt with modified binders. 100 meters long trial sections were built on a road carrying 44,500 vehicles per day, just at approaches to traffic lights. Different types of modified and unmodified asphalt were used in the experiment. The results indicated that modified binders performed better than the unmodified and lasted twice longer. Other research proved that one of the primary benefits of many polymer modified binders is a reduced susceptibility to temperature (King et al., 1999). Furthermore, modified asphalt binders improve pavement durability and hence reduce life cycle cost.

Measurement of the physical properties of bitumen is traditionally carried out using tests such as: penetration, softening point, Fraass breaking point and viscosity. These conventional tests are used to determine the consistency of bitumen and prediction of asphalt mixture performance has been historically based on the parameters calculated from these tests. Because binder properties cannot be tested over a wide range of temperatures and loading times, this empirical approach does not allow for complete and accurate prediction of the viscoelastic behaviour of bitumen.

Furthermore, the conventional bitumen test procedures are not able to adequately characterise rheological properties of polymer modified binders (PMB). King et. al. (1992) reported that the present trend of using softening point as a parameter to predict resistance to permanent deformation should

be changed. The results from wheel tracking test indicated the correlation between softening points and permanent deformation can reasonably be used at fairly low level of polymer modifier concentration. They showed that at higher level of polymer content, this correlation should not be used as soft bitumen with high polymer content can achieve high softening point while these do not necessarily have a good rut resistance. However, the addition of polymer at a proportional amount can be used effectively to improve high temperature performance. The wheel tracking test results indicated that once a binder reached a certain stiffness level, the addition of polymer had only a marginal effect on resistance to permanent deformation. Conclusions drawn from this experiment was that conventional bitumen tests such as penetration, absolute viscosity, kinematic viscosity, and ring and ball softening point did not correlate well with the predicted rutting result from laboratory simulator when PMB were used.

In order to provide a suitable method of quantifying the rheological behaviour of binders over a wide range of temperatures and loading times as well as to address the long-term performance of binders, the US SHRP developed specifications which grade bitumen on the basis of its rheological properties. A number of new tests have been developed and implemented to measure physical properties over the complete range of the binder service life. Binder specification criteria relate to insitu performance and the test procedures evaluate binder resistance to rutting, fatigue cracking and low temperature cracking.

The rutting performance of the binder is determined by measuring the shear stiffness and viscoelastic balance of the bitumen using a Dynamic Shear Rheometer (DSR) (Airey, 1997).

As there was a need in the UK, to correlate binder physical properties with pavement performance, SHRP findings were used to develop a new performance-based specification. The specification enables the selection of an appropriate asphalt mixture, including mixes containing PMBs that will have long-field performance.

2.6.3. Hot Asphalt Mixtures

Asphalt is one of the oldest engineering materials. The first asphalt mixture was used in Paris in 1858 for surfacing the Rue Begere. The UK laid their first asphalt pavement in London's Threadneedle Street in 1870 (Croney and Croney, 1991). Asphalt is also one of the most often used materials in road paving. More than 100 million tons of asphalt is used annually worldwide, from which 90 percent is used in highways construction (SGEP, 2010).

Asphalt is a mixture of mineral aggregates, bitumen binder and air. **Air void content** is defined as "the total volume of the small pockets of air between the coated aggregate particles throughout a compacted paving mixture, expressed as percent of the bulk volume of the compacted paving" (AI,

2001). Results from many studies indicate that the performance of asphalt is strongly dependent on density of a mixture. According to Brown, (1990) a 1 percent increase in air voids (applied to air voids above 7 percent) may lead to a decrease of pavement life by 10 percent. Figures 2.14 and 2.15 show that specimens with high void contents (9-12 percent) exhibit higher deformation than denser material compacted by the same method.

Under the impact of wheel loads the air void content in an asphalt mixture can change, mainly in early life of the pavement, therefore to ensure that the voids stay within an acceptable range the density must be closely controlled. Ideally, the initial air voids content must be below approximately 8 percent and should never fall below 3 percent during the life of the pavement. Brown, (1990) indicated that once air voids reaches 3 percent the stability of a mixture decreases and severe rutting is likely to occur. Hunter, (2000) studied the effect of different states of compaction on properties of Hot Rolled Asphalt and Asphaltic Concrete and found that the deformation in AC increased when air voids content fell below 3 percent; however, in HRA this was not the case. It needs to be noted that he did not consider air voids content of 2.5 percent or below. Huber and Heiman, (1987) concluded that a major cause of rutting is low volume of air voids in asphalt mixtures (below 3 percent). The results of research done by Brown, (1990) showed that asphalt mixtures with an initial air void content below 8 percent have very low permeability of water and air, preventing rapid oxidation.

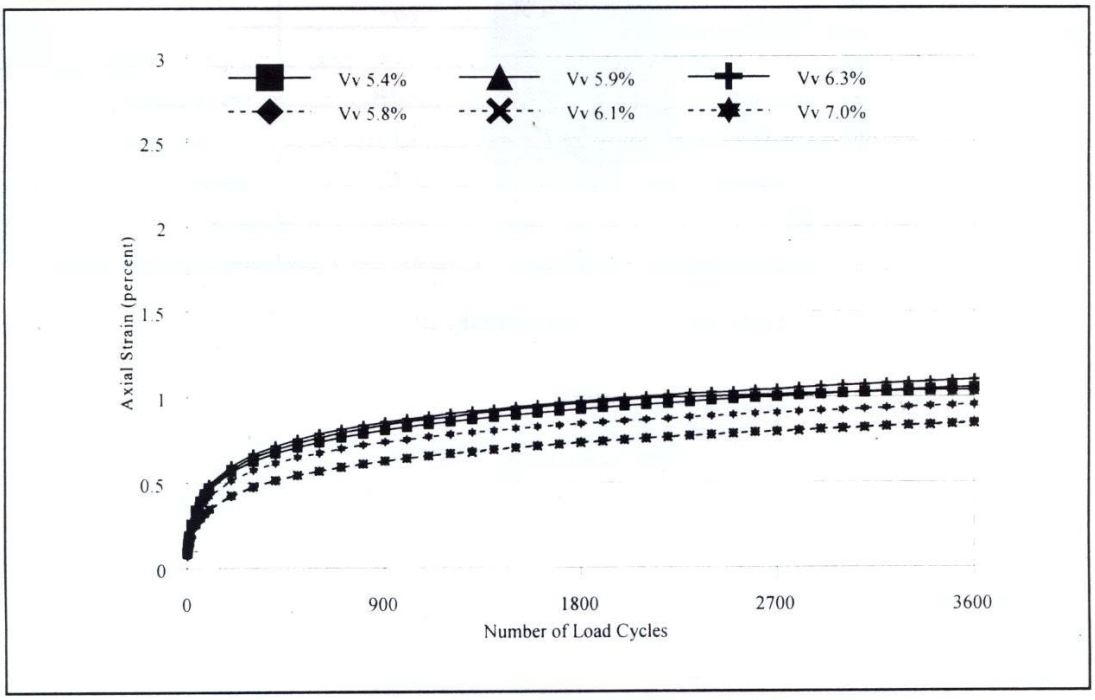


Figure 2.14. Asphaltic Concrete: Roller compaction, Low voids (Brown et al., 1995)

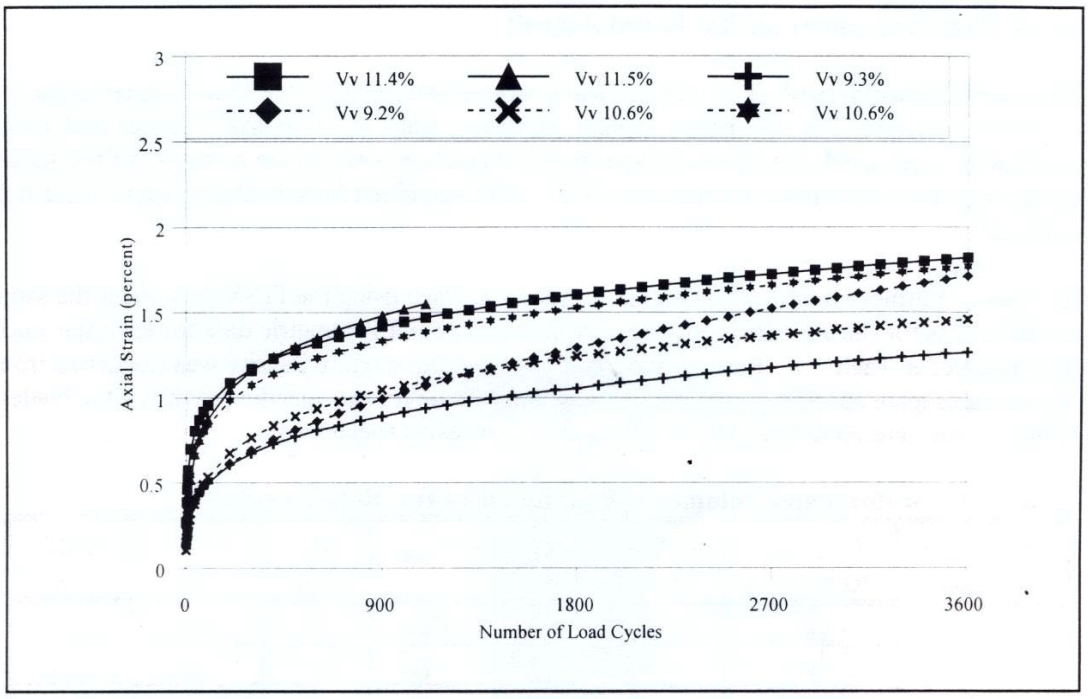


Figure 2.15. Asphaltic Concrete: Roller compaction, High voids (Brown et al., 1995)

Depending on the required fundamental properties and the function of the pavement, the European asphalt industry offers a wide variety of bituminous materials. Historically, there were two main types of asphalt mixture used in highway engineering, continuously-graded mixes (Asphalt Concrete) and gap-graded mixes (Hot Rolled Asphalt). However, constantly growing demands for improvement in the performance of roads has led to development of new stiffer and deformation resistant mixtures such as, Enrobé á Module Élevé (EME) or Stone Mastic Asphalt (SMA). The following sections describe three materials that appeared to be of possible interest and relevance for this study.

Asphalt Concrete is the most commonly used pavement material and accounts for approximately 80 percent of asphalt consumed in highway engineering. It consists of continuously graded aggregate particles held together by the bitumen binder, as specified in the European Standard BS EN 13108-1:2016 (BSI, 2016a). An example of the grading for this material (14mm close graded) is presented in the Figure 2.16. The material has a distribution of aggregate particle sizes often designed to follow closely the Fuller curve to give the maximum density after compaction.

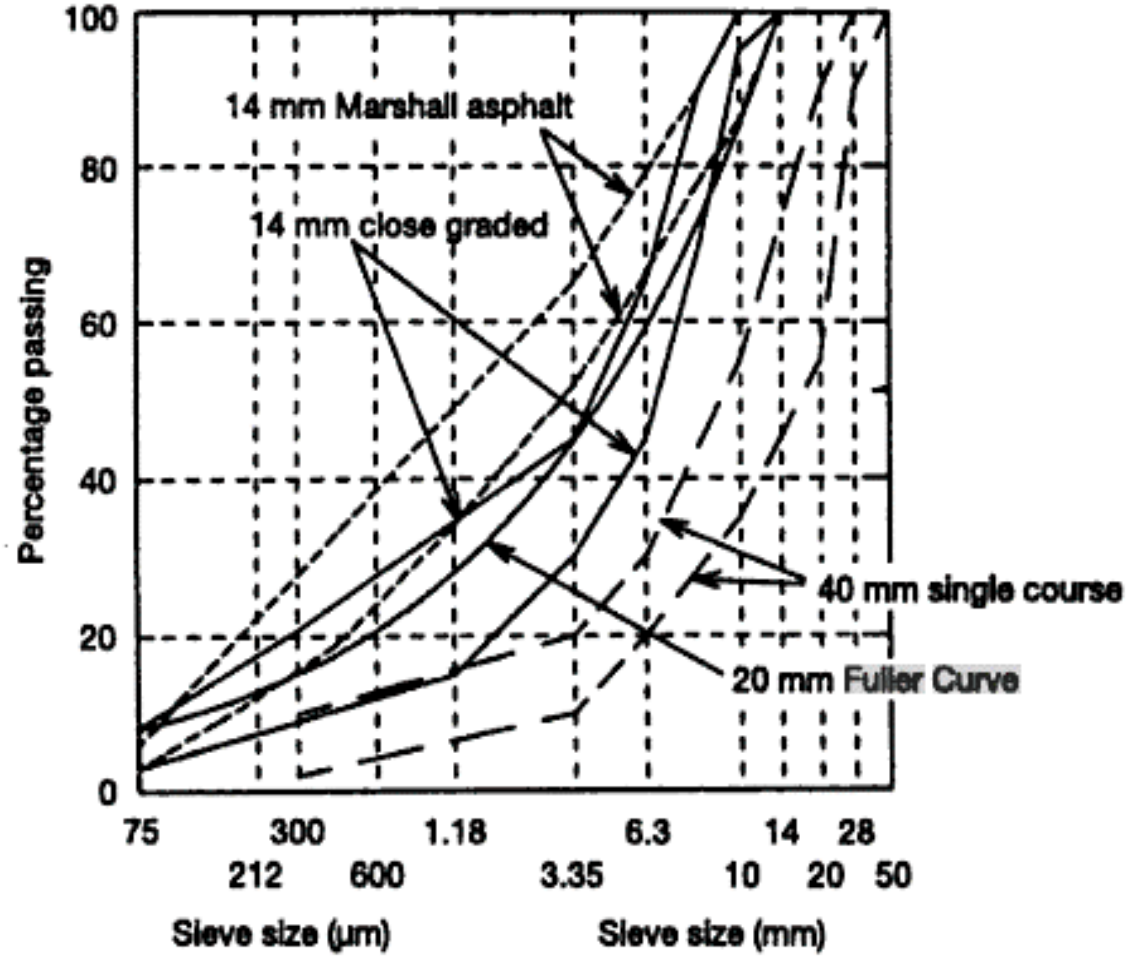


Figure 2.16. Comparison of grading curves (Nicholls, 1998a)

Stone Mastic Asphalt (SMA) is a surface course material originally developed in Germany in the late 1960s to resist wear from studded tyres (Huber, 1999). The mixture has proved to be highly deformation resistant and nowadays is widely used in many different countries such as: Scandinavia, France, Austria, Japan, the United States and the United Kingdom.

SMA is composed of a gap-graded coarse aggregate skeleton with voids filled with a fine aggregate/filler/bitumen mortar. Although, the stone-to-stone skeleton carries all the traffic loads providing mixture with excellent rut resistant properties, the adequate composition of the mortar is equally important to ensure durability and laying characteristics (Nicholls, 1998b). Fibres are used, primarily to prevent drainage of the bitumen during transport, however wheel tracking tests carried out in Germany, Austria and Japan found that fibres also act as a micro-reinforcement of the mastic. Thus, by dint of improved stability of the mix, the deformation capacity of SMA is enhanced (Nicholls, 1998b). Composition of the mixture is specified according to the European Standard BS EN 13108-5:2016 based only on empirical requirements (BSI, 2016c).

The process of designing a SMA mixture involves adjusting the grading to accommodate the required binder and void content rather than the more familiar process of adjusting the binder content to suit the aggregate grading (Nicholls, 1998b).

The SMA aggregate gradings in the UK are illustrated in Figure 2.17 and compared with an idealised Fuller curve, representing the grading with the most optimum density (Nicholls, 1998b). SMA gradation contains only a small percentage of aggregate particles in the mid-size range. The curve is flat in the mid-size range. Gap graded mixes can be prone to segregation during placement.

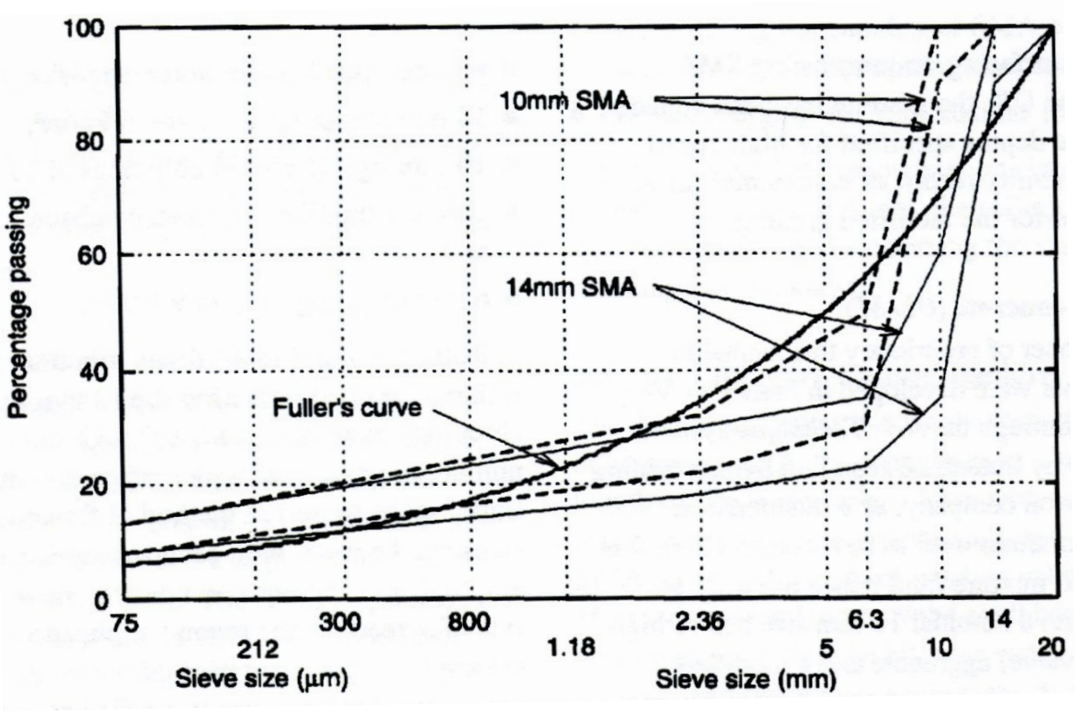


Figure 2.17. Stone Mastic Asphalt gradings (Nicholls, 1998b)

Enrobé á Module Élevé (EME) is a very high modulus binder course/road base material which was introduced in France in the early 1980s as a result of economic concerns following the oil crisis (Nunn, 1994). The high stiffness of EME enabled the thickness of the road base to be reduced by up to 40 percent compared to the traditional French road material, grave bitume.

There are two types of EME defined in the French standard, EME Class 1 with binder content around 4.8 percent and EME Class 2 with slightly higher binder content around 6 percent (Nunn and Smith, 1994).

Transport Research Laboratory studies have shown that EME fulfils the requirements of modern highly trafficked and long lasting flexible pavements (Sanders and Nunn, 2005). High elastic stiffness provides material with excellent load-spreading properties and deformation resistance and its higher binder content helps ensure good durability, workability and sufficient moisture proofing.

The design of EME should be in line with the criteria of the French standard NF EN 13108-1 (NF, 2007).

2.6.4. Traffic

Tyre Pressure and Wheel Load. It is well recognised that pavement deterioration caused by traffic is mainly associated with vehicles with high axle loading. Trucks have much higher tyre inflation pressures than passenger cars, which result in higher contact pressures at the surface of the pavement and, therefore, increase the risk of potential pavement damage in the form of rutting. Over the last decade, the majority of the freight in the UK (about 82 percent of the annual freight, by tonnes lifted), has been carried by road, and Heavy Goods Vehicles have accounted for about 6 percent of traffic each year (DfT, 2008).

Due to ongoing increase in traffic volumes, axle loads, and tyre pressures, premature permanent deformation has become a major concern of the

highway engineer. In recent years, many studies were carried out to investigate the effect of those changing traffic loading factors on pavement damage (Bonaquist et al., 1988, Hudson and Seeds, 1988, Sousa et al., 1988). For example, Smith, (1991) studied the vehicle-tyre-pavement interaction related to Asphalt Concrete (AC) pavement performance, particularly premature wheel path rutting, and concluded that it is essential to establish realistic maximum limits for tyre-pavement contact pressures for which AC pavements can be designed and built using readily available materials and generally accepted construction technology, not only to minimize pavement deterioration now but also to provide the critical link to vehicle-tyre-pavement optimisation in the future.

Speed. The effect of speed reflects the viscoelastic behaviour of HMA. In general, maximum strains (greater deformation) occur under longer loading times (slower speeds). Work done by Garg and Hayhoe, (2001) clearly demonstrated the effect of the vehicle speed on the induced strains in asphalt concrete layers. Increasing the speed from 0.08 m/sec to 2.2 m/sec, caused a reduction in the longitudinal strain by 50 - 55 percent and a reduction in the transverse strain by 40 - 50 percent (for a given load level). This observation was confirmed by Chatti et al., (1996), who showed that increasing the truck speed from 32 km/hr to 64 km/hr, reduces the longitudinal strain by 30 - 40 percent. However, it should be noted that the effect decreases with decreasing tyre pressure and at the lowest tyre pressure, the longitudinal strains were reduced only by 4 - 13 percent. Figure

2.18 presents the mean reduction in longitudinal strains with increasing speed in three different cores and at three different tyre pressures. Figure 2.19 presents the mean reduction in transverse strains with increasing speed in three different cores and at three different tyre pressures. Blocks 1, 2, and 3 represents midmorning and afternoon of September 28 and midmorning of September 29, respectively. The study has indicated that there is less reduction in transverse strain than in the longitudinal strain.

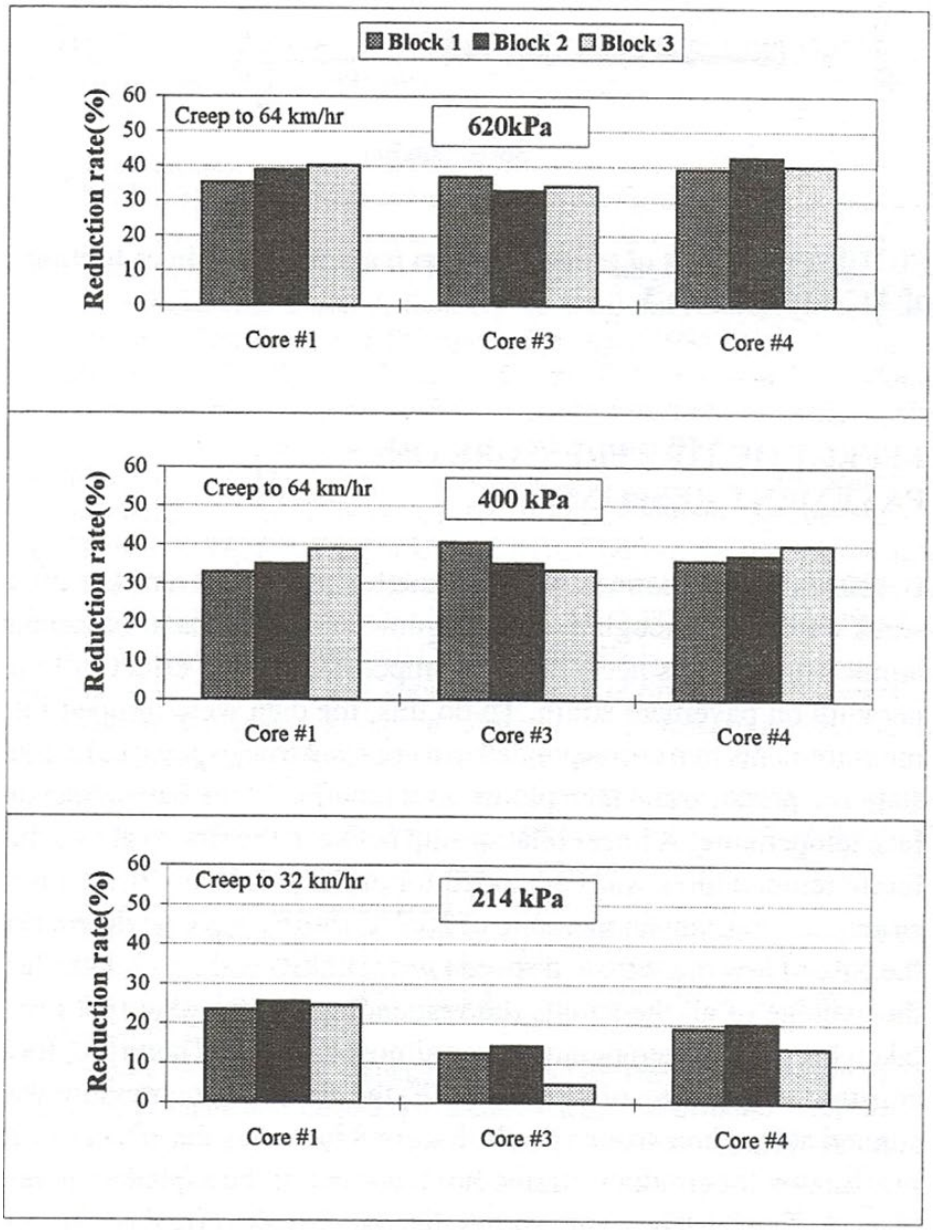


Figure 2.18. Reduction in the longitudinal strain at the bottom of the AC layer with increasing speed (Chatti et al., 1996)

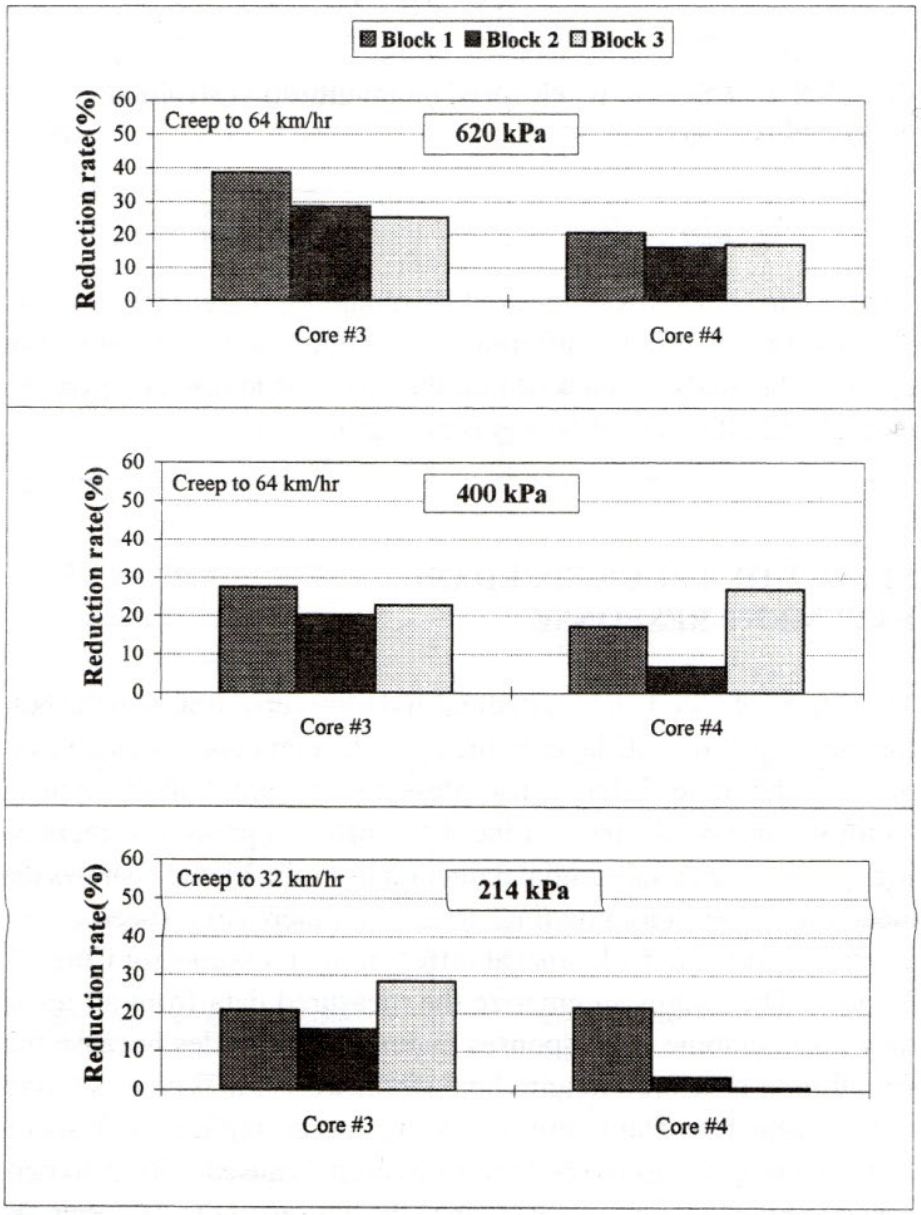


Figure 2.19. Reduction in the transverse strain at the bottom of the AC layer with increasing speed (Chatti et al., 1996)

2.6.5. Environment

The effects of environmental factors such as, temperature and moisture, on the structural behaviour of the pavement have long been recognised as

important. It is therefore quite obvious that in order to predict realistic pavement performance, weather and climatic information needs to be characterised and taken into account.

Temperature is probably the most important factor from all the variables related to asphalt rutting discussed in this chapter. Due to the viscoelastic properties of bitumen binder, pavements are strongly temperature susceptible (Figures 2.20 and 2.21). As the temperature increases, the stiffness of material decreases and therefore its permanent deformation propensity increases.

Hofstra and Klomp, (1972) observed during the laboratory test track studies that the increase of temperature from 20°C to 60°C significantly increases rutting. It is well known that most of the rutting occurs during the summer time and in order to properly evaluate the phenomenon of rutting in the laboratory it is essential to test specimens within the high temperature range of those encountered in the field (Bonnot, 1986, Mahboub and Little, 1988).

According to Goodrich, (1991), who used dynamic mechanical analysis to study rheological behaviour of asphalt mixtures, at low temperature the asphalt properties are strongly influenced by binder and the deformation is that of the binder, while at high temperature plastic behaviour of the mix is mainly controlled by the aggregate skeleton. He also indicated that at

temperatures between 10°C and 50°C permanent deformation is related to both the binder and the aggregate.

On the other hand, Bouldin and Collins, (1992) carried out wheel tracking tests to investigate the effect of binder rheological properties on permanent deformation of polymer modified and unmodified HMA and concluded the at elevated temperature (60°C) the mechanical properties of the binder have a significant impact on the deformation resistance of the asphalt mixture. Consequently, the insertion of the polymer modifier into the binders will result in less temperature susceptibility, thereby leading to improved rut resistance.

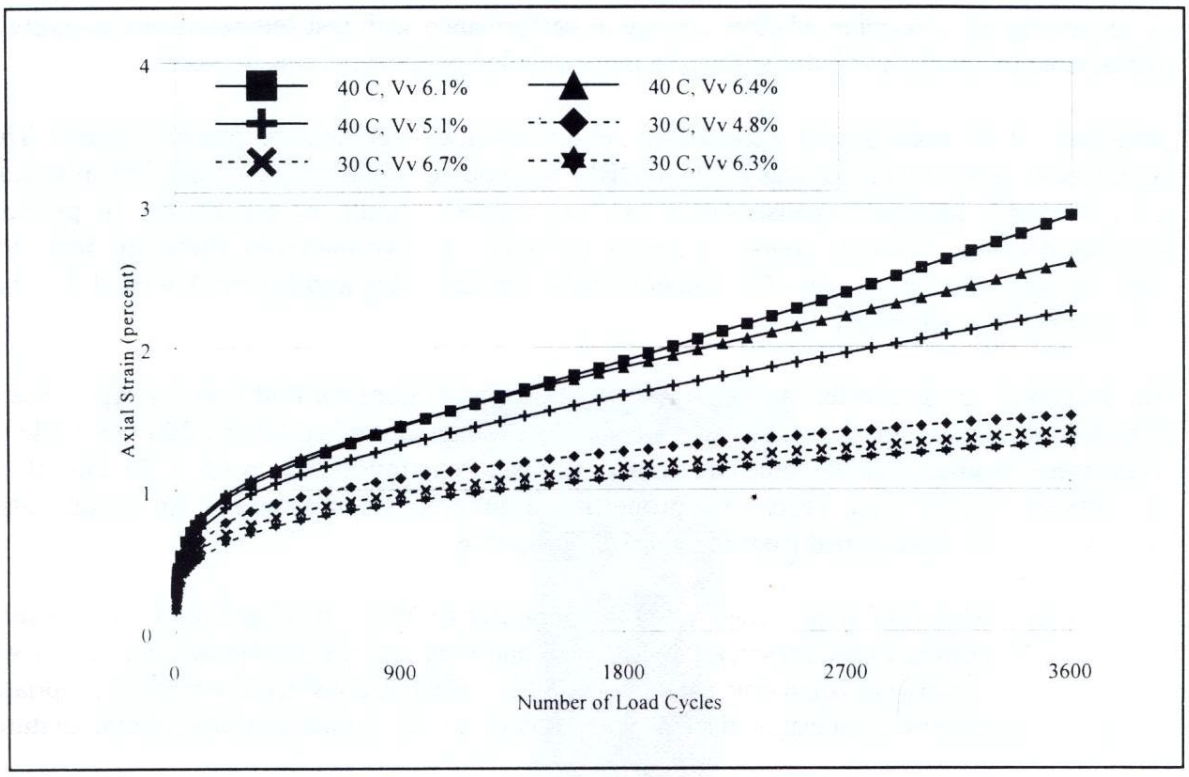


Figure 2.20. Effect of test temperature: 200Pen 20mm DBM Basecourse (Brown et al., 1995)

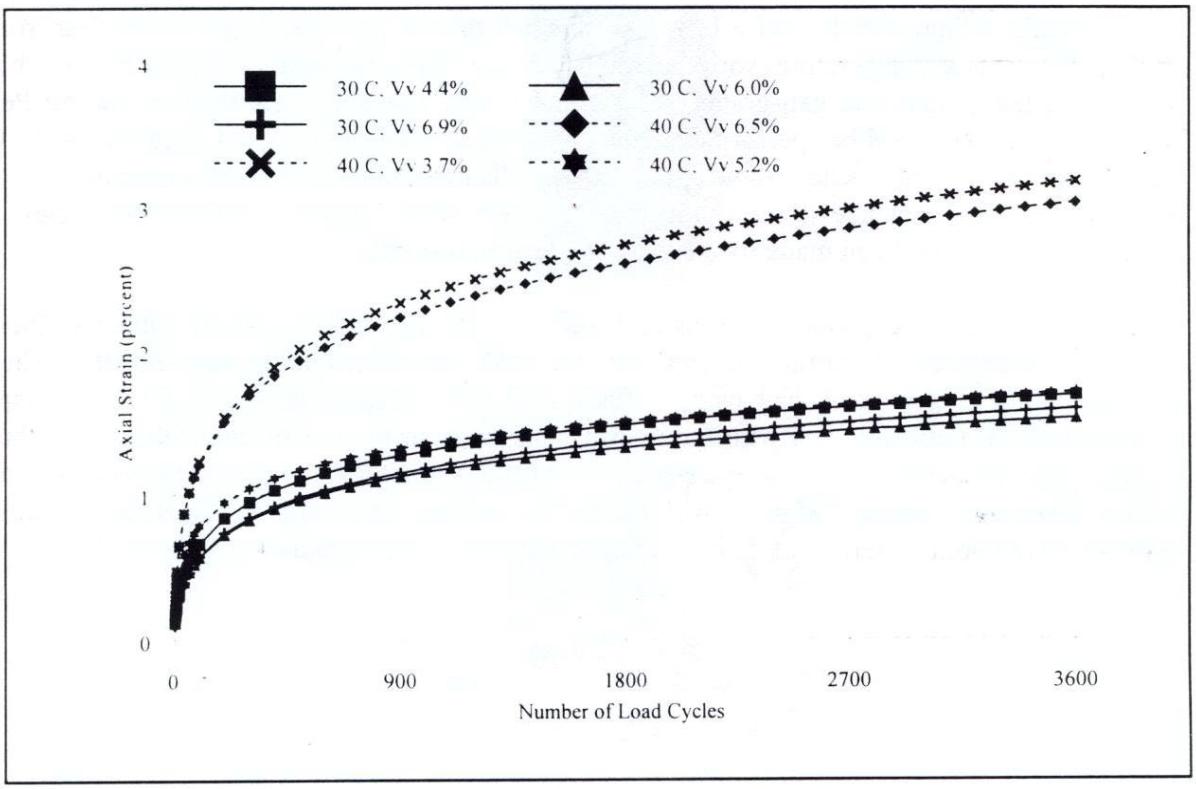


Figure 2.21. Effect of test temperature: 100Pen 20mm DBM Basecourse (Brown et al., 1995)

Moisture (Water) damage refers to loss of the adhesive bond between the asphalt and aggregate due to ingress of water. It decreases the stiffness and strength of the asphalt concrete and gradually, under the action of traffic, can contribute to the development of lateral flow of the material. According to Hicks, (1991) many asphalt pavements experience stripping failure within the mixture without structural failure of the pavement. However, excessive stripping in the asphalt may lead to severe pavement deformation and failure may occur as a result of repeated loading. Kennedy et al., (1983) also suggest that damage will be minimal if stripping is restricted to coarser

aggregates but if stripping occurs to finer particles then the impact will be severe because it constitutes the basic matrix of the mixture.

Wong et al., (2004) studied the effect of water on permanent deformation potential of asphalt concrete mixtures by using the Asphalt Pavement Analyzer (APA) and concluded that water influences the rut depths. They found that depths of wet rut are greater than those of dry in most preconditioning states except for the one with saturation at 25% (St.25%).

2.6.6. Compaction

Compaction is a densification process during which the volume of air voids is reduced by applying a force which allows aggregate particles to move closer to each other. Compaction plays a major role in the performance of flexible pavements. The strength and durability of an asphalt mixture is strongly dependant on the degree and method of compaction (Khan et al., 1998, Muniandy et al., 2007, Van de Loo, 1978). Poor compaction results in excessive air voids content (density), which in turn may lead to premature failure of asphalt layers. Several experimental studies have shown that in order to design an asphalt mixture which will be stable, durable, and rut resistant the initial air voids content must be between 3 and 8 percent (Roberts et al., 1996).

Past studies have shown that if the field conditions for which mixtures are being designed are different from those for which the design method was developed, the mixture may not be adequate for service even though it is designed according to the method. Therefore, it is important that the laboratory compaction procedure of asphalt mixtures should be able to achieve materials and engineering properties such as density, air voids and resilient modulus as close as possible to those of the materials placed in the field using standard compaction practices (Muniandy et al., 2007).

Over the years, many different methods of compaction have been used such as, impact compactor, gyratory compactor, vibratory compactor, roller compactor, kneading compactor and Marshall hammer. A number of research studies have been undertaken in order to evaluate their ability to simulate field conditions and the extent to which they affect engineering properties of asphalt mixes.

Sousa et al., (1991) focused their research on the extent to which compaction methodology affects fundamental mixture properties related to the performance of pavements in service. Evaluated compaction methods included Texas gyratory compaction, kneading compaction, and rolling-wheel compaction. The results indicated that rolling-wheel compaction can produce the stiffest mixture and can more closely simulate the field properties than some other compactors. Kneading compaction produces the most rut resistant specimens. They also indicated that kneaded specimens are more

sensitive to aggregate characteristics while gyratory and rolling-wheel specimens have greater sensitivity to bitumen type. Because the response of rolling-wheel specimens to test loads was typically between the gyratory and kneaded specimens, rolling-wheel compaction has proven to be best suited for preparing laboratory specimens. Among the methods investigated, it appears to simulate insitu compaction quite well and also has an advantage that the large-size aggregate mixes can be compacted without difficulty (Monismith et al., 1994).

Cooley and Kandhal, (2000) conducted a study to evaluate the density gradients in samples compacted by the Asphalt Vibratory Compactor (AVC) and the Superpave Gyratory Compactor and found that vibratory compaction produces specimens with the highest density at the top and with less density at the bottom. Gyratory compaction, on the other hand, results in less density at the top and the bottom of samples and significantly more compaction in the middle of the sample.

Although, the gyratory compaction does not produce specimens most representative of site compacted material, SHRP eventually identified it as the most suitable method for the Superpave mix design and several researchers perceived it as the most appropriate laboratory device to assess the mechanical properties of asphalt mixtures (Butcher, 1998, Tarefder and Zaman, 2002). The particular advantages offered by gyratory compactors are

the facilities both to control the density of the specimen and to assess mixture workability.

While there is a wide array of proposed compaction techniques, two broad methods remain notable: slab compaction and gyratory compaction. In the UK, HMA specimens for laboratory testing need to be compacted in accordance with one of the methods described in BS EN 13108-20:2016 (BSI, 2016d).

Specimens for testing have to be compacted from loose bituminous mixture or obtained by coring or sawing from a trial area in accordance with one of the methods presented in Table 2.2.

Table 2.2. Compaction methods in the UK

Compaction Method	**Standard**
Impact compaction	EN 12697-30
Gyratory compaction	EN 12697-31
Vibratory compactor	EN 12697-32
Roller compaction	EN 12697-33
Cores from trial areas	-

2.7. Laboratory Testing

Permanent deformation has long been recognised as a major problem on flexible roads. A survey carried out by the University of Maryland Superpave team reveals, that the industry rates rutting as the most important distress type that should be correlated to the performance test which could be included in the Superpave volumetric mix design method (Witczak et al., 2002). Hence, there is a great desire for a laboratory test method which could accurately and reliably evaluate the deformation resistance of asphalt mixtures.

Although, the last 20 years of development has led to significant changes and modifications in mix design technology and testing techniques, a good understanding of the fundamental behaviour is still lacking and the tests used in practice are often empirical and not well validated (Brown and Gibb, 1996). Results of several studies clearly demonstrate that there is no "perfect" test method for all types of HMA mixtures placed under varying loading and environmental conditions (Witczak et al., 2002).

The "Desired Laboratory Performance Test" should accurately and precisely measure a mixture response over a wide range of conditions (i.e. stress condition, loading time, temperature, etc.) and reproduce the field loading regime as closely as possible. At the same time the test results must allow determination of a mixture's ability to resist pavement deformation (Witczak et al., 2002).

The stress condition can be reproduced in the laboratory only with great difficulty (Read and Whiteoak, 2003). The stress paths to which an element of material in a pavement is subjected have long been recognised as complex. Loads generated by traffic induce radial, axial and shear stresses (see Figure 1.5) and as the wheel passes over the element, these stresses change with time as shown in Figure 2.22. As the wheel approaches an element in the pavement, initially the major stress component is a horizontal shear stress. When the wheel is directly over the element, the major stress component is the vertical stress and as the wheel travels away from the element, the major stress component becomes a horizontal shear stress with the opposite sign to the initial shear stress.

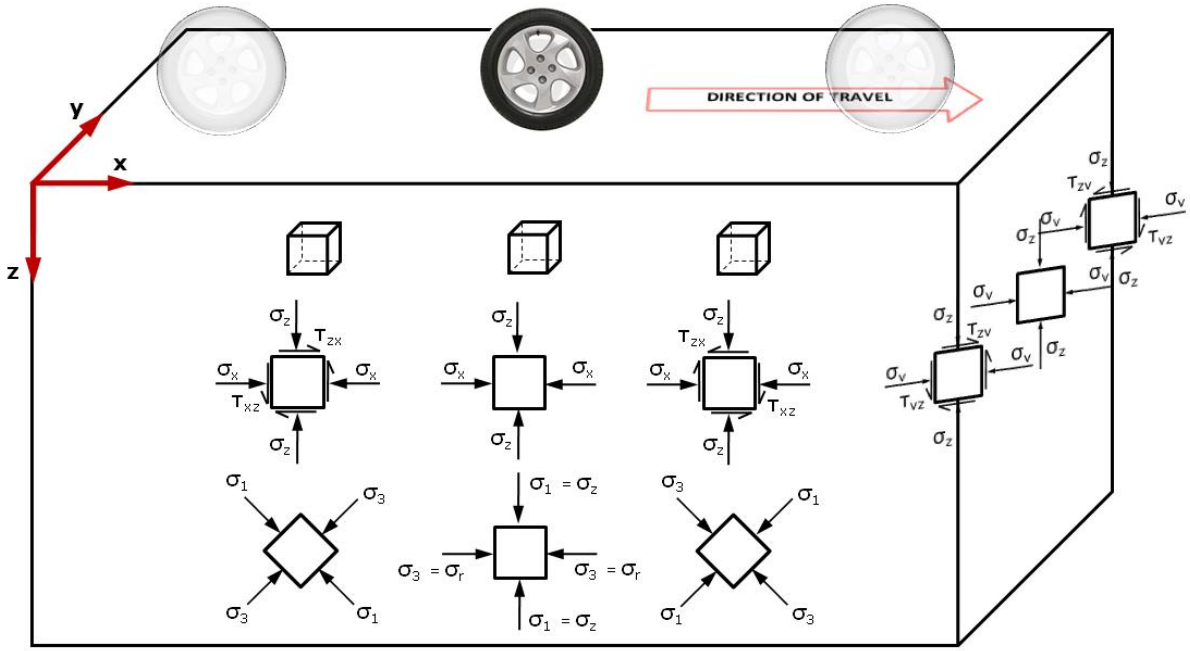


Figure 2.22. Different stresses acting on an element in the pavement

Pell and Brown, (1972) discussed the need to design laboratory materials testing apparatus that could reproduce the stress conditions experienced in a pavement structure under traffic loading. Figure 2.22 illustrates the variations in normal and shear stresses in a pavement element beneath the centre line of a moving wheel load. Particularly hard to reproduce is the reversed shear stress on the element (Figure 1.5), which has been recognised as a major contributor to the rutting. As discussed in Section 1.2, rutting appears to be more closely related to the shear deformation rather than densification. Therefore, if accurate predictions of rutting are to be made, a laboratory test should duplicate the states of stress that are encountered within the entire rutting zone, in particular where the shear stress is greater than the normal stress. Accordingly, the susceptibility of mixes to rut should be measured using apparatus capable of directly applying shear stress (Monismith et al., 1994).

Over the years, various types of test have been developed to provide precise information on permanent deformation in HMA. These tests can be divided into the following three groups:

1) Fundamental:
    - Uniaxial and Triaxial Creep Test
    - Repeated Load Triaxial Test
    - Simple Shear Test (SST)
2) Simulative:
    - Wheel Tracking Test

3) Empirical

- Marshall Stability Test

Since empirical methods, such as the traditional Marshall Stability Test, have proved to have very limited relationship to performance of asphalt (Gibb, 1996, Read and Whiteoak, 2003), only fundamental and simulative tests will be discussed.

2.7.1. Uniaxial and Triaxial Creep Test

The creep test is the simplest experimental tool for investigating the behaviour of bituminous mixes. In 1970 Shell implemented this equipment to define permanent deformation characteristics of different mixes for particular environmental conditions and traffic (Gibb, 1996). A cylindrical specimen is set up between end platens and placed within the loading frame. The specimen is subjected to a constant axial stress at a fixed test temperature and a total permanent strain is measured under unconfined or confined conditions. Detailed information of static creep test procedures can be found in reports by Van de Loo, (1978) or Liu, (1995). A diagram layout of the prototype uniaxial creep equipment is shown in Figure 2.23 (Cooper and Brown, 1989).

Results of the creep test, when expressed as relative deformation (measured change in height divided by the original height) are independent of the shape

of the specimen and of the ratio of height to diameter, provided that the specimen's ends are parallel, flat and well lubricated (Hicks and Esch, 1990). This will minimise lateral end restraint and ensure uniform stress distribution.

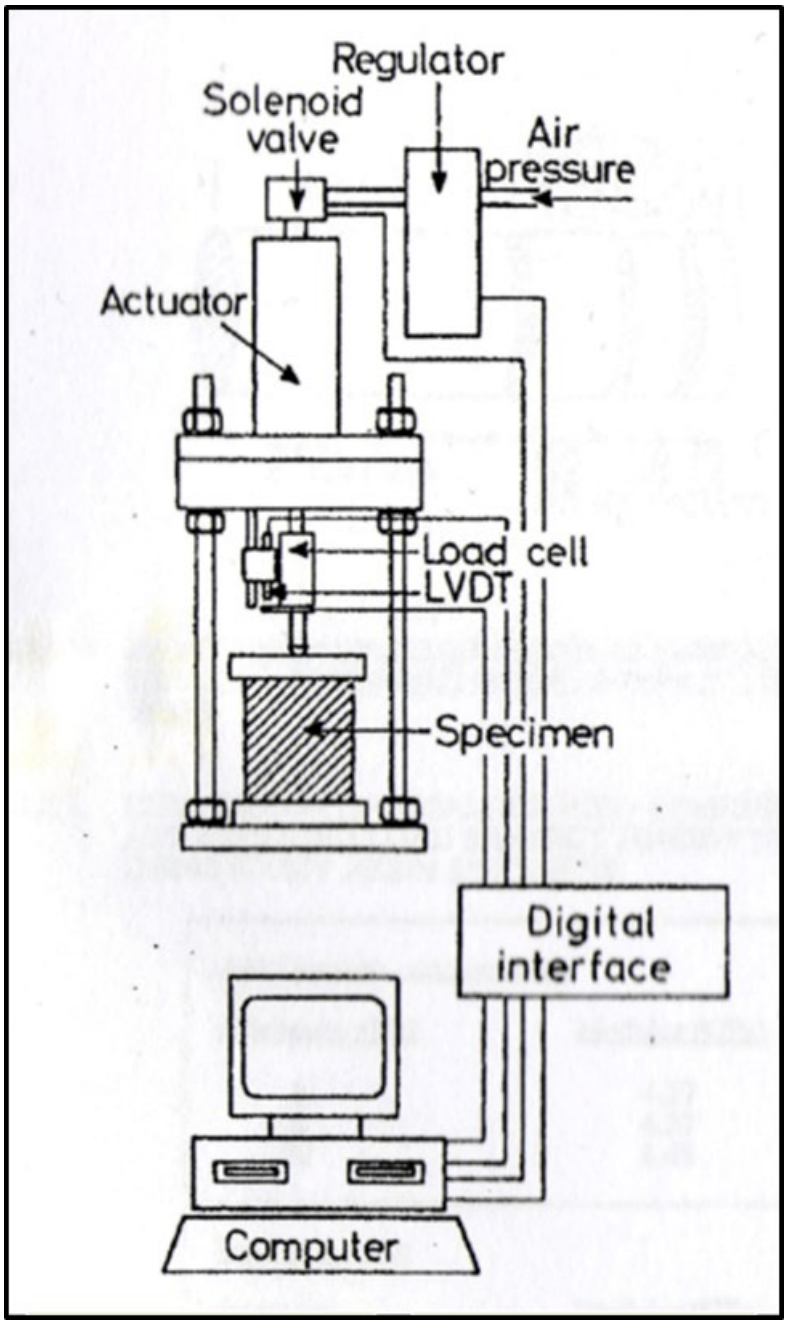


Figure 2.23. Diagram layout of uniaxial creep equipment (Cooper and Brown, 1989)

Strain obtained from this test is measured as a function of the loading time at a fixed test temperature. Figure 2.24 shows a typical creep curve representing development of strain as a function of time. It can be seen that the permanent strain curve can be divided into three phases; the primary phase in which compaction of the mixture leads to rapid strain rate decrease. This is followed by a constant rate of accumulation of strain, steady state creep. In the third phase, tertiary creep, the strain rate increases rapidly leading to creep rupture.

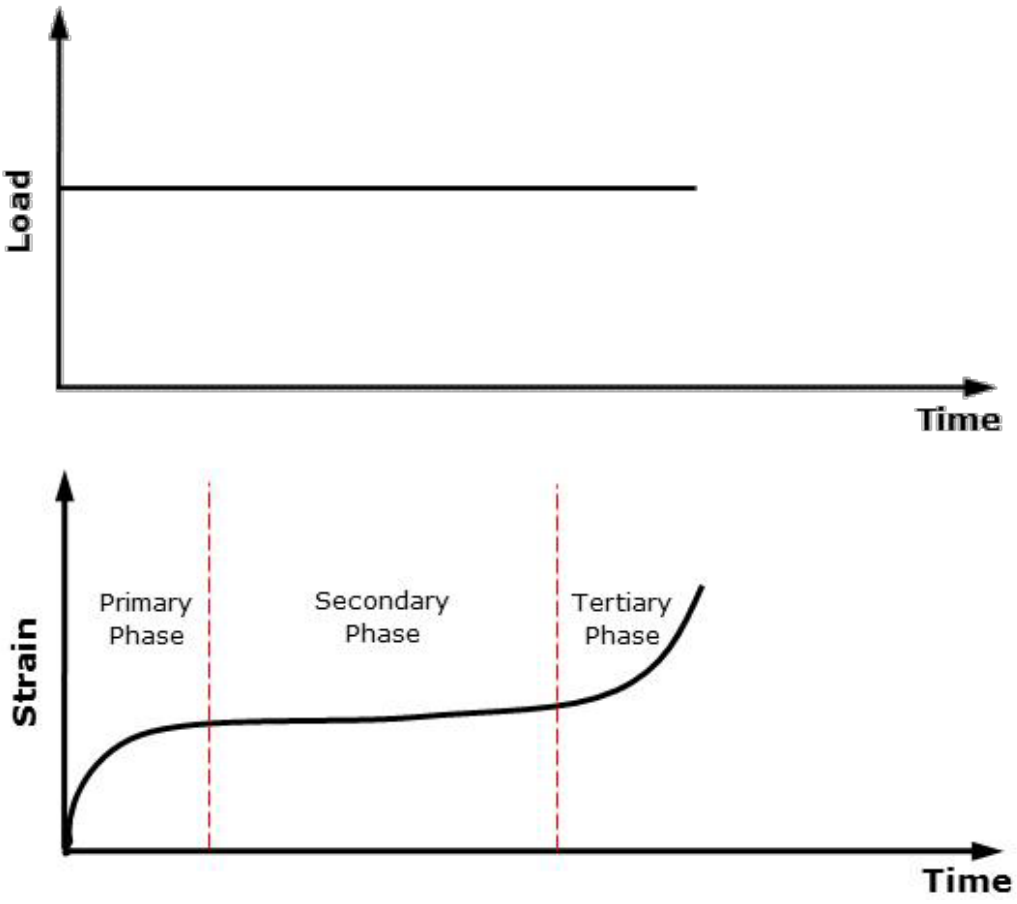


Figure 2.24. A typical creep strain response

Extensive research using the creep test (unconfined or confined) for determining bituminous material properties and assessing rutting susceptibility has been conducted. Uge and Van de Loo, (1974) found that results from the static creep tests at the higher stress levels seem to be inconsistent. They concluded then that the creep test must be performed at relatively low stress levels and low temperatures (within the linear range of material). The need to use a stress level within the liner range has been attributed to the fact that insitu stresses are high, but the loading time is small compared to the loading time in the creep test.

Hills, (1973) clearly demonstrated that the creep test results under-predict rut depth measured in the pavement. Similar conclusions arose from Brown and Snaith is work (Brown and Snaith, 1974). In another publication (Harvey et al., 2001) it was reported that creep testing may over-predict rutting for mixes containing modified binders and procedures may therefore require correction. Similar conclusions were drawn by Tayebali et al., (1992).

Brown and Foo, (1994) conducted a study that evaluated rutting potential of dense graded asphalt mixes. The unconfined and confined creep was measured. They pointed out that the confined test was more representative of insitu performance.

Although, the test is simple, quick and inexpensive, its ability to predict pavement performance is questionable because the test conditions do not closely simulate in-service pavement conditions (Gibb, 1996).

2.7.2. Repeated Load Triaxial Test

The nearest practical test to capture the insitu stress regime is the repeated load triaxial test. This test is able to directly apply principal stresses, as shown in Figure 2.25, but only two stress components can be varied independently out of maximum six for general conditions.

Exactly as in the creep test, the cumulative permanent deformation is presented as a function of a number of load cycles and three distinct zones can be identified (Witczak et al., 2002). Even though, the repeated load test is very similar to the creep test, Monismith et al., (1994) concluded that the repeated load test provides a better measure of rutting characteristics than the creep test.

On the other hand, it should be noted that the repeated load test was found to be more sensitive to mix variables than the creep test. Several studies (Barksdale and Miller, 1977, Monismith and Tayebali, 1988) have indicated that the increase in the bitumen content, when using the repeated loading test, significantly increases the plastic deformation of asphalt mixtures. There

was no significant effect noted on the same mixtures under the static creep conditions.

Pell and Brown, (1972) pointed out that the repeated load triaxial test equipment could only reproduce the insitu normal stress regime (see Figure 2.26) and that the associated variations in shear stress could be very significant, particularly in the asphalt layer. Later Brown and Bell, (1977) concluded that data from triaxial testing tend to overestimate rut depth. This is because the triaxial configuration generates data on the axial permanent strain, which is only equal to the vertical value insitu when the wheel load is immediately above the element (see Figure 2.22). Hence, the principal stresses applied by the triaxial equipment relate to an insitu element that rotates as the wheel passes, a phenomenon known as “principal stress rotation” or “shear reversal”.

Pell and Brown, (1972) concluded that research up to that date had properly focused on apparatus that captured the most important stress parameter related to the failure mode of interest. Hence, for asphalt, tensile and flexure testing was used to study fatigue cracking and triaxial testing was at least on a safe side for permanent deformation. This configuration was also used extensively to study the resilient characteristics of soils, granular materials and asphalt as the secondary effects of shear stress reversal were not considered to be of such importance where small strains were involved. This was later confirmed by Chan and Brown (1994).

Thrower, (1978) reported that triaxial testing should not be relied completely on to define pavement performance. He further suggested that state of stress encountered in upper layers cannot be duplicated in triaxial test. A drawback of this technique is that the shear reversal effect (see Figure 1.5) cannot be reproduced.

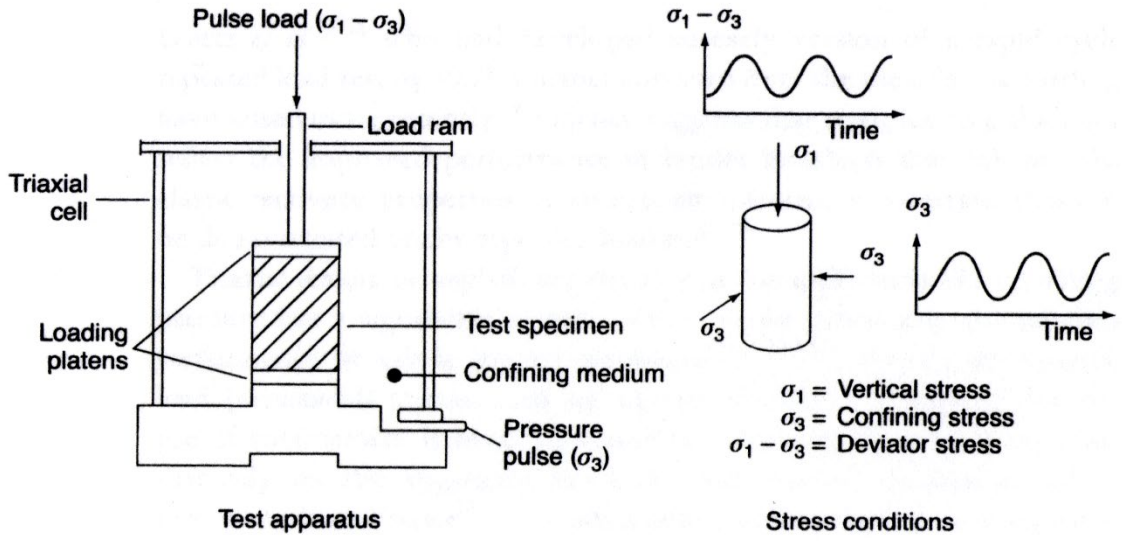


Figure 2.25. Repeated Loading Triaxial Test (Read and Whiteoak, 2003)

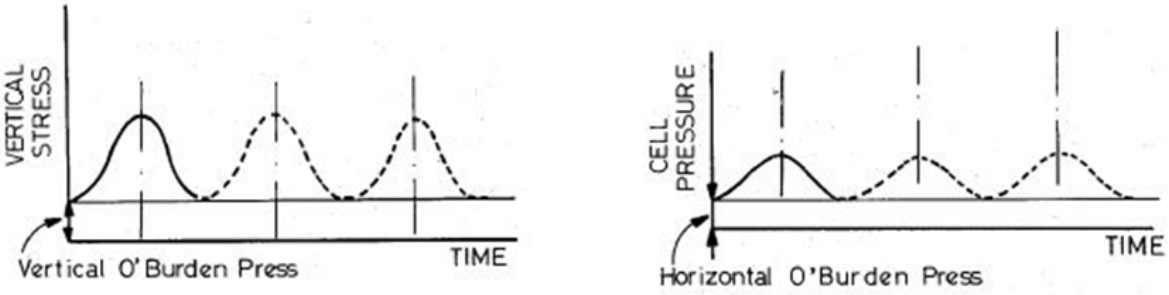


Figure 2.26. Stress regimes under a moving wheel in a triaxial compression test (Pell and Brown, 1972)

2.7.3. Superpave Shear Test (SST)

Since the shear flow was recognised as being the primary cause of rutting, the US SHRP study led to the development of the SST. During their research, the team at UCB concluded that it was necessary to design and build a direct shear apparatus to study the permanent deformation characteristics of asphalt. This was driven by the stress conditions they calculated in the critical zones of the asphalt layer under the edge of the wheel load where the shear to normal stress ratios exceeded those that could be applied in a triaxial test. In order to develop an apparatus that was not unduly complex but which captured the importance of shear stress application under repeated loading, they developed the SST rather than going back to their HCA configuration (Monismith et al., 1994).

The SST was introduced to complement the Superpave volumetric mixture design method and it was envisioned that this simple performance test would play a key role in the quality control and acceptance of HMA mixtures. The equipment is capable of applying direct shear to laboratory specimens (see Figure 2.27) and the data can be correlated with field performance (Harvey et al., 2002).

The SST was designed to execute a variety of performance-related tests on HMA, but a number of serious problems were found and many of these tests were found to be unreliable. Only two procedures were found to be reasonably

accurate, the frequency sweep test and repeated shear at constant height (RSCH) procedure (Christensen Jr et al., 2002). Detailed information of both procedures are described in *AASHTO TP7 (AASHOT, 1994).* In RSCH test, the vertical stress on the specimen is adjusted to ensure that the height and, therefore, the volume remain constant so that all the strain is derived solely from shearing action. The results from this test yield relationships between permanent shear strain and the number of load applications for a particular combination of temperature and applied shear stress.

The SST is the simplest tool that permits controlled rotation of the principal axes of strain and stress which is important in studying permanent deformation. Although, over recent years this test has become quite widely used in US research laboratories for predicting the rutting resistance of asphalt mixtures, the SST test method has a number of drawbacks (Cooper and Brown, 1989, Brown et al., 2005), such as:

1) "The use of a circular specimen and no side platens introduces non-uniform stress conditions".
2) "Application of a shear stress and a vertical normal stress without the ability to measure the lateral stress on the specimen means that the complete stress regime is not known. This makes fundamental interpretation of test results difficult".
3) "The standard SST test is conducted at constant height to eliminate any volume change. However, to achieve this, the normal stress has to be

adjusted during testing, which means that the shear to normal stress ratio varies during a test".

4) The SST test method is regarded as too complex and expensive to use for routine design.

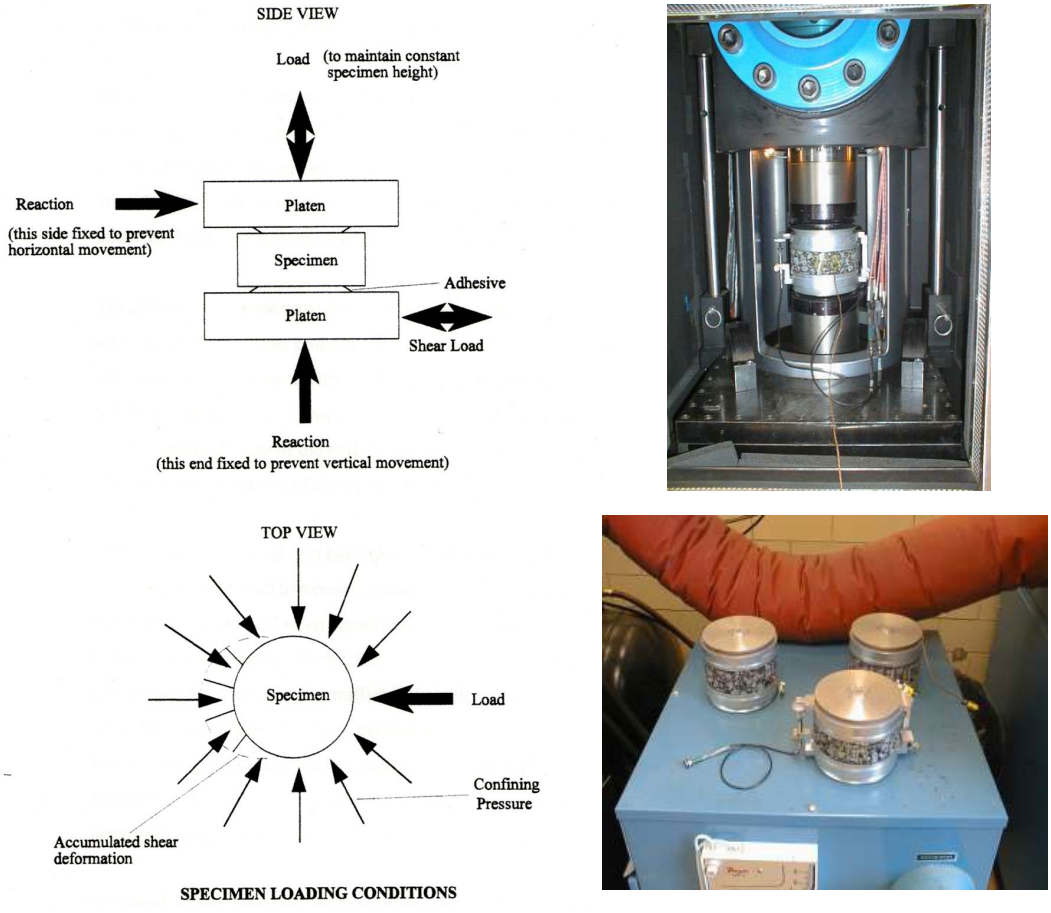


Figure 2.27. The Superpave Shear Test (SST) device (Harvey et al., 2002, Sousa, 1986)

Therefore, the shortcomings of this test configuration are similar to those identified for granular materials testing but its use for asphalt over the past decade has demonstrated that it is effective as a research tool, as part of a design method for rutting and for the design of asphalt mixtures intended for

heavily trafficked situations (Deacon et al., 2002, Harvey et al., 2002, Monismith et al., 2000). In its use under constant height conditions, by definition, no data are collected about volume change, though this could in principle be done with the equipment.

2.7.4. Wheel Tracking Test

The wheel tracker is an empirical laboratory device designed to assess the liability of bituminous material to deform under conditions which simulate the distresses caused by many years of exposure to traffic within a matter of hours by rolling a wheel across a sample of asphalt concrete under specific temperature and humidity conditions. In general, the procedure is to move a loaded wheel backwards and forwards across a prepared specimen under specified conditions of speed and temperature (in the UK 45°C or 60°C). These devices do not account for seasonal changes in traffic, temperature, or environment. The rate of rutting which develops in the wheel path is monitored continuously and plotted against time. The test specimens can be either slabs manufactured in the laboratory or 200mm diameter cores cut from a pavement. Detailed procedures and requirements for the UK wheel-tracking test are described in BS 598: Part 110: 1998 (BSI, 1998).

The test is usually terminated after 45min, unless the rut depth exceeds 15mm prior to this time. The material resistance is assessed by measuring the

resultant rut depth after a given number of passes or rate of tracking (in millimetres per hour) (Read and Whiteoak, 2003).

It should be highlighted that general properties of mixtures change over time due to oxidation of asphalt. The aging progressively increases viscosity (stiffness) of the bitumen material, making the road more resistant to rutting at higher temperatures. Hence, any form of accelerated loading testing e.g. (HRB, 1954, HRB, 1955, HRB, 1962) is likely to indicate pavement lives much shorter than would have been found in practice (Croney, 1991). As age hardening does not take place during accelerated pavement testing, permanent deformation of asphalt accelerates, leading to earlier failure.

Nevertheless, this test facilitated rapid measurement of pavement response to load and allowed comparisons to be made between calculated pavement responses and actual field performance. Generated data formed the basis for the pavement design methodology used until today (Papagiannakis and Masad, 2008).

Over the last 15 years, several different rut testers have been developed, ranging from extra large-size to small-size devices. Figures 2.28-2.31 show the most prominent laboratory-scale trackers. All of these devices can be reasonably well correlated to the insitu rut performance. However, the complex stress regime makes it difficult to determine fundamental material properties from wheel tracking test results.



Figure 2.28. The Laboratoire Central des Ponts et Chaussées (LCPC) wheel tracker, also known as French Rutting Tester (FRT) (PI, 2010)

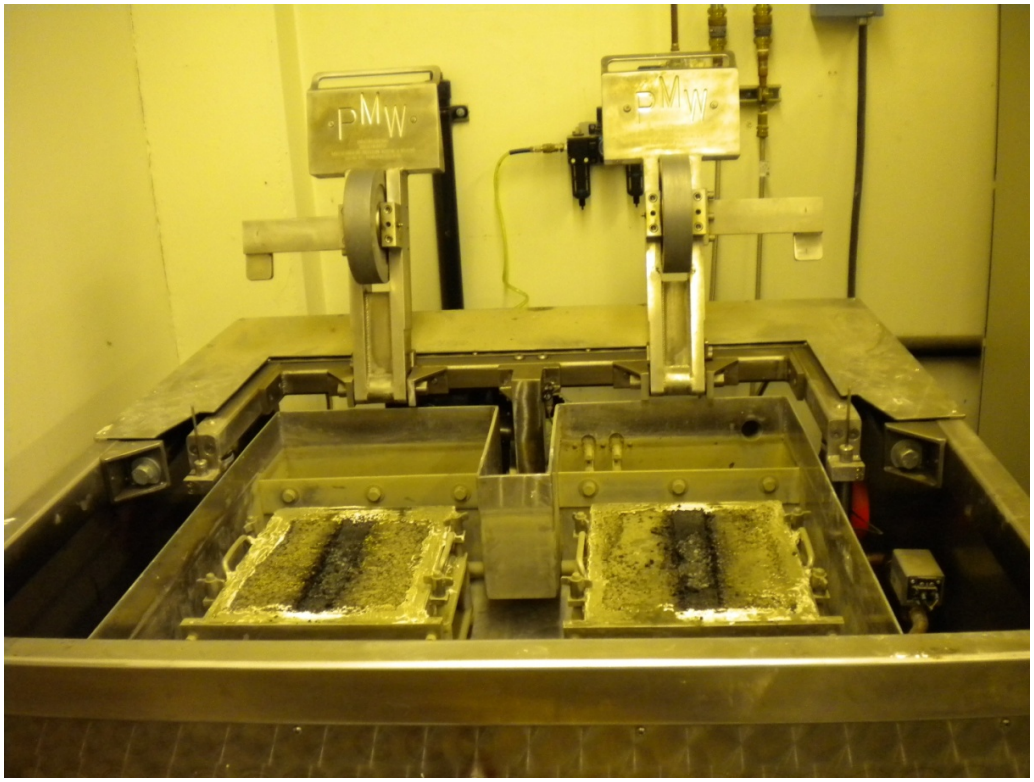


Figure 2.29. Hamburg Wheel Tracking Device (HWTD)



Figure 2.30. The Nottingham Slab Testing Facility

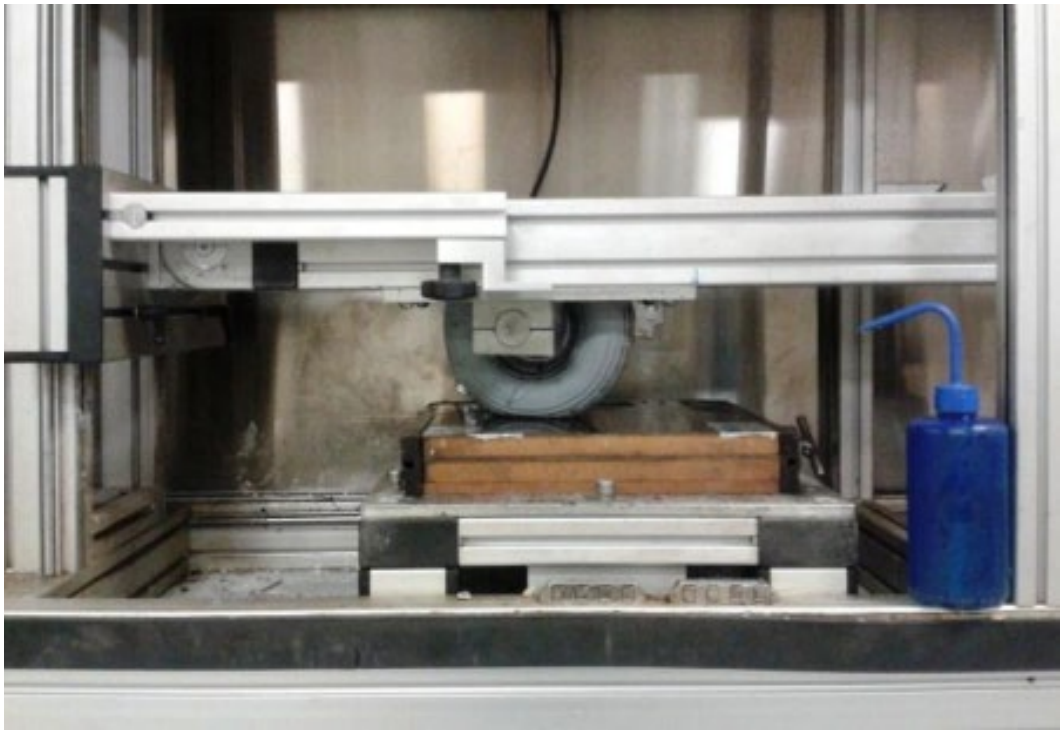


Figure 2.31. TRL Wheel Tracker (Sanders et al., 2015)

2.8. The Hollow Cylinder Apparatus (HCA)

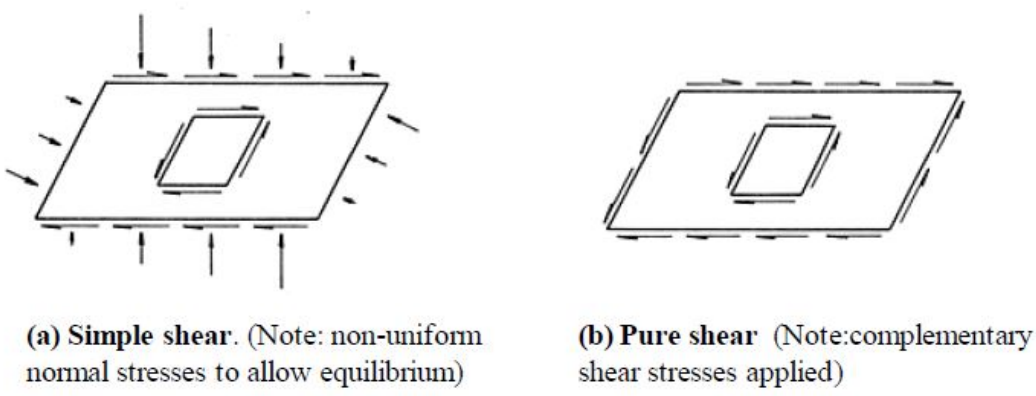
Pell and Brown, (1972) concluded their discussion by stating that the time had come to develop apparatus that could directly apply shear stresses to test specimens as well as normal stresses. The Nottingham pavement research team pursued this philosophy over subsequent years but with an emphasis on unbound materials.

Thin long hollow cylindrical specimens have been used periodically to simulate different stress conditions on various materials for decades (Alavi, 1992). They have been used predominantly in geotechnical investigations and due to its great success in generating a variety of stress paths, a similar approach was followed in asphalt research and a realistically sized HCA for the testing of asphaltic concrete was developed.

2.8.1. Research on Granular Material

The new apparatus developed during this project is based on the results of earlier research on granular materials, which clearly demonstrated that the accumulation of permanent strain under repeated loading is significantly affected by the shear stress regime applied in laboratory tests and that this should model that which occurs in the pavement. A brief review of this earlier work and how it evolved from soil mechanics research is the subject of this section.

Two approaches to direct shear testing of cohesive soils were introduced in Scandinavia during the 1950's as improvements to the old standard square Casagrande shear box. Kjellman's apparatus (Kjellman, 1951) was improved later by Bjerrum and Landva, (1966) and both used cylindrical test specimens with reinforced rubber membranes between the loading platens. The stress conditions in these tests were non-uniform near the edges of the loading platens to retain equilibrium because no arrangement for formal application of the complementary shear stress was provided [Figure 2.32 (a)]. In addition, the circular section also caused non-uniformities. Roscoe, (1953) introduced the Simple Shear Test for sand in an attempt to obtain better stress conditions in the centre of the specimen and by use of load cells built into the loading platens. He used a rectangular specimen which was deformed in shear in the shape of a parallelogram. This latter approach was followed at Nottingham by Ansell and Brown, (1978) and Shaw and Brown, (1986) when developing apparatus for the repeated direct shear testing of sand-sized granular materials. They demonstrated that, while useful data could be obtained, the precise applied stress and resulting strain conditions were impossible to determine, even with their sophisticated measuring techniques and did not provide the pure shear environment of Figure 2.32 (b). For this reason, the Nottingham group adopted the principle of torsional hollow cylinder testing in order to obtain improved stress conditions and facilitate accurate measurement of the resulting deformations for conditions simulative of those under a moving wheel load.



(a) Simple shear. (Note: non-uniform normal stresses to allow equilibrium)

(b) Pure shear (Note:complementary shear stresses applied)

Figure 2.32. Simple shear and pure shear

The principles involved in hollow cylinder testing of soils have been reviewed by Saada, (1988). The hollow cylindrical specimen can be subjected to axial (W) and torsional (M) loads, applied to the ends of the hollow cylindrical specimen that is subjected to lateral confining pressures (po, pi). This configuration allows independent control of the magnitude of the three principal stresses and rotation of the major-minor principal stress axes facilitating more generalised stress path testing (O'Kelly and Naughton, 2003). Figure 2.33 shows the stress conditions within an element of the HCA specimen wall after applying an axial force (W), a torque (M) and inner and outer cell pressures (pi, po).

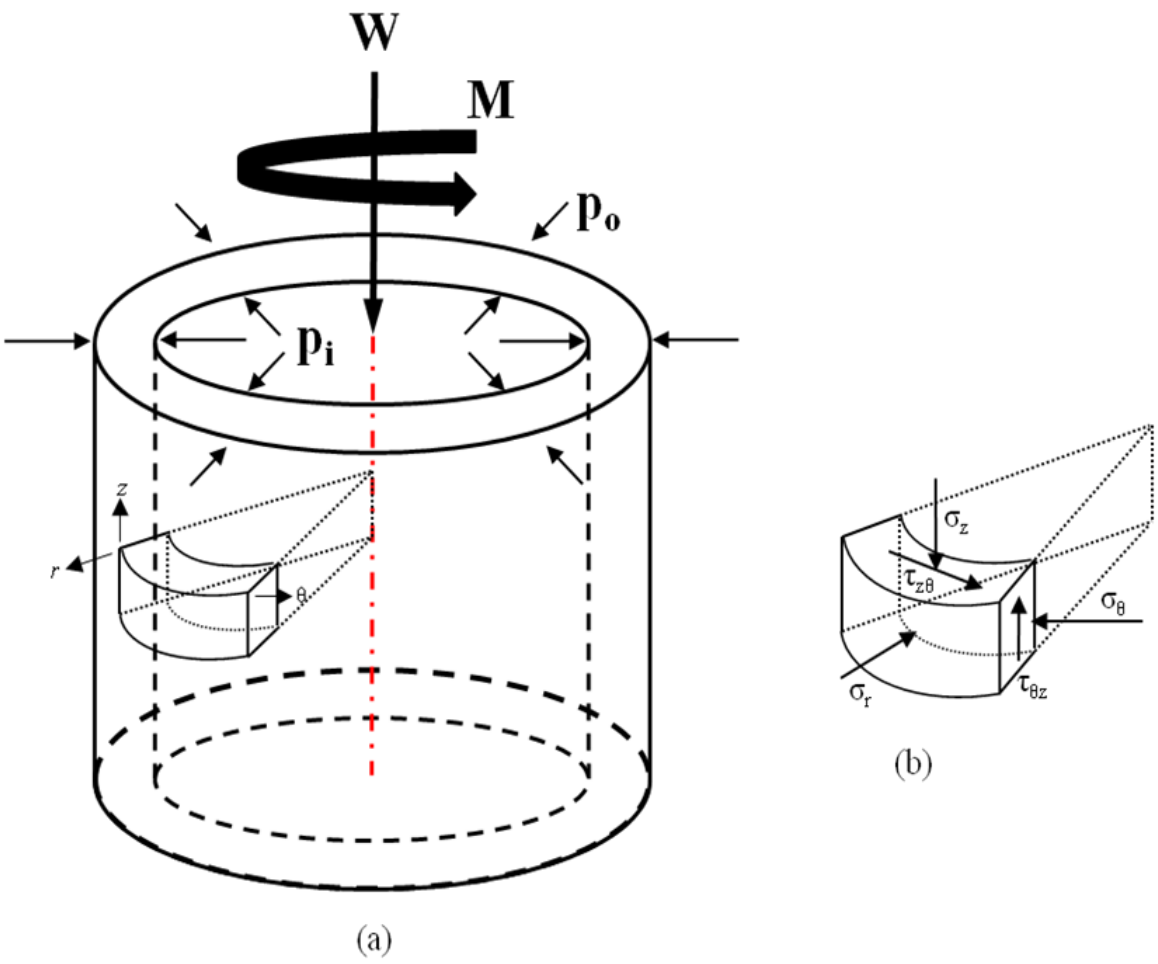


Figure 2.33. Stress regime on an element of the wall of the HCA

The HCA existed in Nottingham for a number of years. The first apparatus was developed in 1985 (Figure 2.34) and since then it has been continuously evolving to meet different research needs and to gather accurate and reliable data on pavement behaviour under repetitive wheel loading.

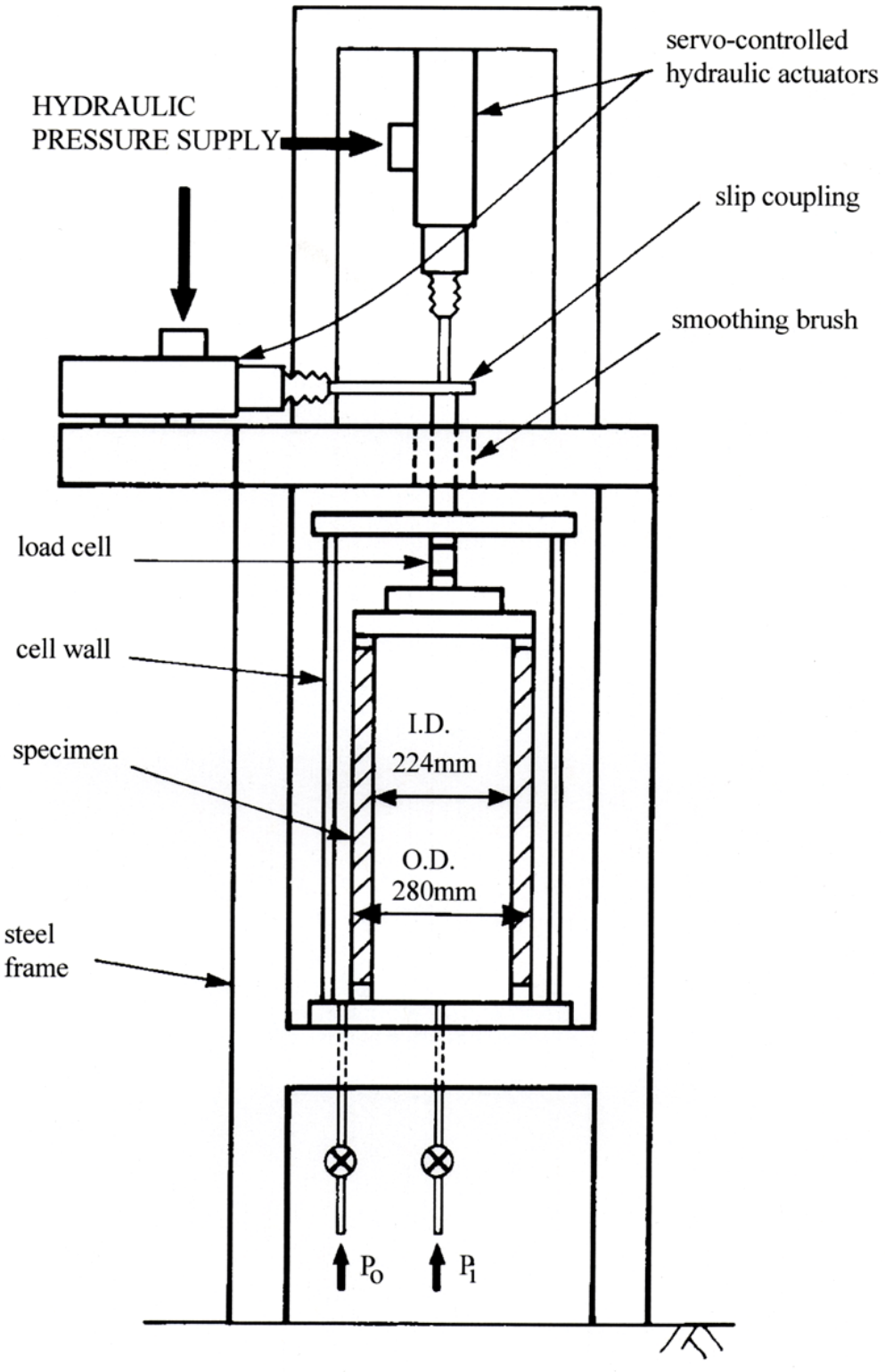


Figure 2.34. The Nottingham Hollow Cylinder Apparatus – Basic Arrangement (Cooper and Brown, 1989)

The HCA used at Nottingham for testing granular materials was described by Brown and Richardson, (2004). It evolved from an earlier version, some results from which were presented by Chan and Brown, (1994). This, in turn, was based on a similar monotonic loading facility developed by Hight et al., (1983). It utilised all the key features of this type of testing with the exception of differential cell pressure; equal internal and external pressure being applied. The apparatus differed from earlier versions in that it was designed to apply repeated loading using servo-hydraulic systems. The dimensions of the specimens for this HCA were 280mm outside diameter, 28mm wall thickness and 500mm height. The aggregate particle size that could be accommodated was limited by the wall thickness with a maximum size of 5mm being used.

Chan and Brown, (1994) demonstrated that the application of a reversed shear stress, as shown in Figure 1.5, compared with the same magnitude applied in one direction had a marked effect on volume change. Significant compaction occurred under reversed shear, but dilation was measured when it was unidirectional. This compaction effect had been previously noted by Brown and Ansell, (1980) using Simple Shear Testing. Chan and Brown also demonstrated, experimentally, that a similar value of vertical permanent strain developed in a pavement at a particular location under a moving wheel load as in the HCA, when the stress conditions were of the same magnitude. This provided some validation for use of this new apparatus. Brown and Chan, (1996) also demonstrated the importance of shear stress reversal in wheel tracking tests on well graded crushed rock as bidirectional wheel tracking

caused larger ruts than unidirectional and significantly higher than repeated loading on a stationary plate. This point was also addressed by (Brown, 2007) in a more recent paper underlining the significance of principal stress rotation for modelling pavement materials.

Richardson, (1999) employed an HCA for investigating the influence of principal stress rotation on granular material behaviour with respect to initial material anisotropy. He concluded that the subsequent volumetric behaviour was strongly influenced by changes in void ratio during pre-stressing, while the shear strength behaviour was influenced by the direction of induced major principal strain. It has been shown as well that the initial development of strain within the first few cycles had a significant influence on the subsequent rate of permanent strain accumulation.

2.8.2. Application to asphalt

Although the hollow cylinder apparatus is still very rarely used in hot mixture asphalt testing, its development and use has been growing. This type of apparatus was first introduced for asphalt by Sousa, (1986) at the University of California Berkeley (UCB) and, subsequently, used by Alavi and Monismith, (1994) to evaluate viscoelastic properties of asphalt mixtures under axial and shear dynamic loading. Alavi and Monismith, (1994) additionally investigated the effects of combined axial and shear dynamic loading on the permanent deformation characteristic of asphalt. During the preliminary stage of these

experiments, they observed that application of excessive stress may affect the proper ranking of permanent deformation properties. Therefore, they recommended that stress magnitudes are selected such, that the specimen would at least undergo a sufficient number of load application before failure. Alavi and Monismith, (1994) showed that axial stress has a confining effect on the values of permanent shear strain. Shear stress was reported to have a dilatancy effect on the permanent axial strain magnitudes, therefore, this phenomenon should be studied in any permanent deformation investigation of asphalt. Finally they concluded that higher angles of major principal stress rotation resulted in higher permanent shear deformation and more shear dilatancy effect. Crockford, (1993) used an HCA to study the effect of principal-plane rotation on permanent deformation in flexible pavement under compressive and shear loading. Most recently, Rueda et al. (2017) developed a hollow cylinder apparatus (HCT-AM) at Los Andes University (Colombia) to study effect of climatic conditions on the dynamic response of asphalt mixtures.

Based on the previous studies carried out at the University of Nottingham (Chan, 1990, Richardson, 1999, Shaw and Brown, 1986, Thom, 1988) and research in America (Alavi, 1992, Sousa, 1986, Rueda et al., 2017), the HCA appears to have a potential to closely simulate the complex insitu pavement stress regime caused by moving wheel loading. In addition to confining stress and axial deviator stress that can be applied the same way as in a triaxial device, it is also possible both to apply a torque to the cylindrical shape and

also vary the pressure in the centre of the cylinder from the external confining stress. The axial load generates a vertical stress; the torque develops complementary shear stress on horizontal and vertical planes in the wall of the cylinder, whereas variation of internal pressure imposes variation in circumferential stress much greater than variation in radial stress perpendicular to the wall (Thom, 1988). If the considered element is free from end effects, then there are no shear stresses in the radial circumferential plane. The radial stress is a principal stress and the other three stress components define the remaining two principal stresses. As the loads can be applied independently, it is possible to control the magnitudes of the three principal stresses and the inclination of the major principal stress. HCA is particularly advantageous when predicting deformation away from the axis of symmetry of loading. Moreover, the instrumentation can be directly attached to the specimen, enabling accurate strain measurement.

It is desirable to have uniformities in the stress and strain distributions within the specimen. This and the capability of reliable determinations of loads and displacements are vital for any device as only then the resulting stress and strain states within the specimen can be accurately defined. A HCA disadvantage is that some stress non-uniformity is inevitable, particularly when there is a difference between internal and external confining stress. However, Hight at al. (1983) reported that as long as the ratio of diameter to wall thickness and height to diameter were sufficiently large, such uniformities could be ignored.

The dimensions chosen for the HCA specimens used for this study are in favour of these suggestions. It is therefore expected that the levels non-uniformities have been effectively minimised and hence test results could be interpreted reliably in terms of the average stress and strain components.

The HCA has a capability to generate complimentary shear stresses to the test specimen, it allows the study of material anisotropy, and the principal stress rotation effects can be investigated. The apparatus clearly offers valuable capabilities in determining permanent deformation characteristics of asphalt under three-dimensional state of stress with reversal of shear stress; however, its complexity make it to be essentially as a research tool rather than standardised equipment for routine applications.

2.9. Asphalt Layer Rutting Performance Prediction Models

As was proposed by Monismith et al. (1994), the permanent deformation response of asphalt mixes to loading should be characterised by a rate-dependent constitutive relationship, with a stress analysis being performed for the entire rutting zone (i.e. over the entire lane width), to effectively handle complex constitutive relationships and the transverse distribution of traffic. This relationship should take dilatation under shear and plastic properties into account and must reflect at least the effects of loading time, temperature and stress states. Loading history, e.g. loading time, axle load, wheel lateral position, etc. are essential factors in the analysis of long-term irrecoverable displacement in asphalt mixtures.

A number of models representing the permanent deformation behaviour of asphalt mixes have been developed. A number of these procedures include criteria for limiting values of subgrade strain to levels that preclude rutting at the pavement surface. Design limitations on strain or stress are based on the assumption that, if the maximum vertical compressive strain or stress at the surface of the subgrade is less than a critical value, then rutting will be limited to a tolerable level for a specified number of load applications (Sousa et al., 1991). Unfortunately, such methodology does not necessarily preclude rutting which might occur in the asphalt-bound layer. The Shell method (Claessen et al., 1977) was probably the first attempt to incorporate rutting of bituminous layers in pavement design. Existing models can broadly be categorised into structural and functional performance models (Ullidtz,

1987). In all cases, laboratory tests are necessary to determine parameters representative of permanent deformation behaviour (Monismith, 1994).

The **structural performance models** determine the structural soundness or load carrying capacity of the pavement. They are usually mechanistic-empirical, M-E, and are based on layered-strain analysis with elastic or viscoelastic theories. The M-E models can be employed in the decision making processes regarding pavement design, maintenance and rehabilitation strategies by identifying the structural condition with regard to bearing capacity. The **functional performance models** determine the ability of the pavement to provide a comfortable, safe, economical riding surface to the road users. Functional models determine the rate of deterioration in terms of functional parameters (e.g. evenness (International Roughness Index) and rut depth) with the age of the pavement and are applied on existing pavement as part of the pavement management system (Jelagin et al., 2018).

This study only examines structural performance models and the main five models are briefly summarised in this section. Both layer-strain and viscoelastic methods for predicting permanent deformations in pavements are discussed.

2.9.1. Layer-strain Method

The layer-strain method consists of predicting rut depths using permanent-deformation characteristics determined from laboratory tests together with an

analysis procedure for the pavement structure using either linear or nonlinear elastic theory. The general principle of this method was first proposed by Barksdale (1972) and Romain (1972).

The layer-strain method is considered a simplified engineering approach for predicting rut depth which permits the flexibility of using either linear or nonlinear elastic analysis. While nonlinear elastic theory should provide more accurate results (Brown and Bell, 1977), it has not been used very extensively because of its added complexity.

The prominent examples of M-E elastic models are listed below. It should be noted that although the M-E elastic models are based on elastic theory, they account for time-dependent material characteristics using a type of repeated loading test.

Van de Loo (1976): BISAR Elastic layer theory

$$\varepsilon_p = c\sigma N^a \qquad (2.1)$$

where

εp - axial permanent strain (axial creep test)

c - constant

σ - axial stress level (103.5kPa)

N - number of load applications

a - constant

This model formed the basis of the SHELL method and generally, it overestimates rut depth (Monismith et al., 1994).

Brown and Bell (1977): DEFPAV Nonlinear finite element

$$\varepsilon_p = \left(\frac{q}{a}\right)^b (N) \quad (2.2)$$

where

εp - permanent shear strain (axial repeated load test)

q - deviator stress

N - number of load applications

a, b - constant

Brown and Bell (1977) have compared theoretically-predicted rut depths using the layer strain approach with those actually measured in the Nottingham Test Track. Material properties were predicted using the repeated load triaxial test. Comparison between predicted and measured total displacements indicated good agreement (Monismith et al., 1994).

ARA (2004): American Association of Highway and Transportation Officials (AASHTO) Model

$$\frac{\varepsilon_p}{\varepsilon_r} = k_1 \times 10^{k_2} \times T^{k_3} \times N^{k_4} \quad (2.3)$$

where

εp - permanent strain (axial repeated load test)

εr - resilient strain (axial repeated load test)

T - temperature (°F)

N - number of load applications

k1 - depth adjustment coefficient as a function of layer thickness and depth to the ground water table

k2, k3, and k4 material constants

The AASHTO model was developed under the National Cooperative Highway Research Program (NCHRP) and it is included in the Mechanistic - Empirical Pavement Design Guide (MEPGD) to predict the maximum permanent deformation in each layer as a function of time. The regression parameters are obtained from laboratory tests and field calibrated. The resilient strain εr is obtained by analysing the pavement structure using a response model such as multilayer elastic theory. The air voids within an asphalt layer are an important parameter. It is used in the estimation of the rutting related to post compaction that may significantly increase the amount of rut depth. A time hardening approach related to repeated traffic loading is used to combine the permanent deformation contribution from different axle loads. The model is able to divide the surface rutting between pavement layers, which is valuable in pavement design (Jelagin et al., 2018).

2.9.2. Viscoelastic Method

In this approach moving wheel loads can be considered in conjunction with time-dependent material properties to define the states of stress and strain at particular points in the pavement structure. Material properties can be defined

either in terms of models consisting of finite numbers of Maxwell and/or Kelvin elements in various arrangements or in terms of generalised compliance relationships. An important advantage of this approach is that moving wheel loads can be considered directly. This results in the correct time-rate of loading to be applied to each material element and permits estimates to be made of the lateral plastic flow of material from beneath the moving wheel. While nonlinear viscoelastic response characteristics may provide a more realistic estimate of pavement response, the associated mathematical complexities have limited past analyses to linear characterizations (Sousa et al., 1991). In this approach, material properties within a given layer are assumed to be the same throughout the layer regardless of whether the material is in tension or compression.

This approach resulted in several viscoelastic rutting performance models, such as the VESYS and VEROAD models described below. However, being computationally expensive (time-consuming) the nonlinear viscoelastic and viscoelastoplastic models have gained little usage (Collop et al., 1995).

Kenis and Wang (1997): VESYS Probabilistic linear viscoelastic solution

$$\varepsilon_p\,(N) = e\mu N^{-\alpha} \tag{2.4}$$

where

εp (N) - permanent strain per pulse (uniaxial repeated load test)

α - 1 - S

S - slope of the line on log-log plot of permanent strain versus N

e - peak haversine load strain for a load pulse of duration d = 0.1sec

μ - IS/ e

I - intercept

Similar to the AASHTO, the VESYS model assumes that the permanent strain in an asphalt layer is proportional to the resilient elastic strain. The permanent strain model parameters of the layers are estimated by conducting repeated load (incremental static-dynamic) laboratory tests.

Hopman, (1996): VEROAD linear viscoelastic multilayer computer program

The VEROAD (Visco-Elastic Road Analysis Delft) is a three-dimensional linear viscoelastic multilayer program developed at the Delft University of Technology (Hopman, 1996). The viscoelastic nature of bituminous materials is considered through the Burger's model (or Maxwell-Kelvin-Voigt model) and the layered system can be analysed under stationary or moving wheel loads using the layered elastic theory and the elastic-viscoelastic correspondence principle (Jelagin et al., 2018). The permanent deformation parameters for the plastic component calculation were determined from a triaxial creep test. The VEROAD model also considers lateral traffic wander.

2.10. Conclusions

Permanent deformation of asphalt mixture is a complex phenomenon that depends on many factors, including asphalt binder, aggregates, mixture design, loading time and the temperature. Its accumulation may be partly minimised by an appropriate mix design and efficient construction control.

In order to reduce asphalt mix susceptibility to plastic deformations, specifications of various mix parameters, such as binder type and content, aggregate type and gradation, compaction degree (air voids), are essential. Nevertheless, plastic deformations in an asphalt layer will occur due to combination of densification (volumetric reduction) and shear strain, caused by traffic loads.

Rutting resistance is a major performance measure for designing pavements and proper assessment of permanent deformation behaviour is critical to ensure the structural adequacy of flexible pavement. Although the importance of shear stress application under repeated loading is relatively well understood, its influence on permanent deformation accumulation is usually not considered while designing flexible pavement structures.

Aiming at achieving rut resistant asphalt mixes, field conditions have been simulated in the laboratory by a variety of repeated loading tests. These tests are carried out following specified temperatures and stress magnitudes and variable loading times. However, this chapter has set out some of the main

criticisms of the standard test methods that have been used to date for testing asphalt material.

Layer-strain and viscoelastic methodologies are currently used to predict the development of permanent deformation in asphalt layers. The literature sources reviewed for this report suggest that 1) neither the layer-strain procedure or conventional viscoelastic analysis has been able to accurately and reliably model pavement rutting; and 2) although many researchers recognised that shear stress is the main mechanism causing rutting, suitable laboratory test methods and theoretical models are not yet available for properly treating shear-induced permanent deformation (Monismith et al., 1994).

Available analytical models differ greatly in their estimation of the variation of permanent strain with depth beneath the pavement surface. Further improvements are necessary to extend the prediction of rut depth from the centreline of the loading to the entire rutting zone. Currently the laboratory test procedure makes use of some form of axial compression, either creep or repeated loading. If predictions are to be extended away from the centreline of loading, the laboratory procedure must incorporate provision for states of stress which include significant shear components: such stress states exist off centreline and are particularly important near the tire edges. It also implies that new functions relating stress to plastic deformation will be required to take shear stresses into consideration (Sousa et al., 1991).

3

DEVELOPMENT OF THE HOLLOW CYLINDER APPARATUS (HCA)

3.1. Introduction

The previous chapters have set out some of the main criticisms of the standard test methods that have been used to date for testing asphalt material. With the above in mind, the aim of this project was to develop a more accurate apparatus for quantifying the permanent deformation characteristics of asphalt with respect both to shear and volume change characteristics. At the same time, it was also necessary to develop the test procedures which define the parameters contributing to the mixture performance. This will allow simpler, more practical methods, such as the SST and the various other methods in common use, including the uniaxial or triaxial test to be assessed and calibrated. It will also improve understanding of asphalt mechanics and so assist with developments in computational modelling of pavement rutting through better definition of the required constitutive equations.

The following chapter describes the large torsional Hollow Cylinder Apparatus (HCA) and testing procedures used in the research. The initial design and development of the device was carried out by Chief Experimental Officer, Mr Barry Brodrick in collaboration with suppliers in the Nottingham Transportation Engineering Centre (NTEC) at the University of Nottingham. In order to design the loading actuator, it was necessary to estimate the maximum levels of shear and normal stress which would need to be applied, so that a full range of possible insitu stress levels could be accommodated. The results of this study are presented in Section 3.2. Calculations used to determine stresses and strains in HCA testing are outlined in Section 3.3.

3.2. Large Torsional Hollow Cylinder Apparatus (HCA)

As mentioned in previous Chapters, the HCA has existed in Nottingham since 1985 for the purpose of testing granular materials (Brown and Richardson, 2004). The design of the new Nottingham testing facility was broadly based on this previous experience. The principal aim was to build and commission a new torsional HCA capable of applying high loads representing correct field conditions and able to handle physically larger asphalt specimens with wall thickness large enough to accommodate realistic maximum-sized aggregate.

3.2.1. Linear Elastic Analyses

Controlling Parameters

Determining the states of stress and strain in a pavement section under a load is an essential step in predicting pavement surface deformation. As previously mentioned in the Literature Review, Pell and Brown, (1972) highlighted the importance of relating the stresses in laboratory tests to those insitu. Before studying the behaviour of asphalt mixtures, it is necessary to decide upon control parameters for the investigation. Brown and Bell, (1977) discuss that the use of stress invariants is the most appropriate approach for the correct representation of stress states in an asphalt pavement. The use of stress invariants is particularly advantageous for predicting rutting away from the axis of symmetry of loading. Since the rut depth prediction always requires that the vertical insitu permanent strain be determined, some procedure, independent of the directions of principal stresses is required. The applied stresses can be divided into those causing volume change and those causing shear distortion. The stress conditions at a point in a general three-dimensional stress field can be described by the following parameters:

- p, mean normal stress

$$p = (\sigma_1 + \sigma_2 + \sigma_3)/3 \tag{3.1}$$

- and τ_{oct}, octahedral shear stress

$$\tau_{oct} = 1/3\sqrt{[(\sigma_1 - \sigma_2)^2 + (\sigma_2 - \sigma_3)^2 + (\sigma_3 - \sigma_1)^2]} \tag{3.2}$$

These stress invariants are functions of the principal stresses, σ_1, σ_2, and σ_3, but are independent of the orientation of the axis. Corresponding strain invariants can be determined from the laboratory tests, and better estimates of the insitu vertical strain can be obtained.

For simplicity, particularly in triaxial testing, when the insitu stress condition beneath the centre of a single wheel load is considered, then $\sigma_1 = \sigma_z = vertical\ stress$, and $\sigma_2 = \sigma_3 = \sigma_r = horizontal\ stress$. Hence, the normal and shear stress invariants can be defined as:

$$p = \frac{1}{3}(\sigma_z + 2\sigma_r) \tag{3.3}$$

$$q = \frac{3}{\sqrt{2}}(\tau_{oct}) = (\sigma_z - \sigma_r) \tag{3.4}$$

Moreover, previous HCA studies indicated that the stress ratio, η, and the inclination of major principal stress direction, α, defined as follow:

$$\eta = \frac{q}{p} \tag{3.5}$$

$$\alpha = \frac{1}{2}\tan^{-1}\frac{2\tau_{\theta z}}{(\sigma_z - \sigma_\theta)} \tag{3.6}$$

are also important parameters controlling material behaviour (Chan, 1990).

Theoretical Analyses of Pavements

The key to the improved prediction of rutting in asphalt pavement, as discussed in the Literature Review, lies in the ability to test asphalt materials under as closely as possible reproduced insitu stress conditions.

Consequently, in order to establish the actual stress paths for use in the new HCA testing and in order to design the loading actuator, it was necessary to estimate the maximum levels of shear and normal stress which would need to be applied, so that the full range of possible insitu stress levels could be accommodated. To this end, a number of multi-layer linear elastic analyses were undertaken to calculate the stresses within the layers of asphalt pavements. Normal and shear stresses were computed using the Shell developed BISAR 3.0 program (Shell, 1998) at different depths and at different positions in the transverse and longitudinal directions, as shown in Figure 3.1. Although more accurate modelling could have been carried out using visco-elastic analysis, it was considered that correct orders of magnitude for stresses could be determined from simple linear elasticity. Asphaltic mixture responds to loading in both an elastic and viscous manner. The proportion of each depends on the time of loading and on the temperature at which the load is applied. The pavement structure exhibits elastic behaviour under conditions of low temperature or short loading times.

In order to keep the process as simple as possible, an effort has been made to reduce the number of variables involved in the analysis of pavements. Therefore, a two-layered structure was selected representing a typical pavement configuration consisting of a flexible construction (all bituminous layers combined) on a foundation. In the UK, the pavement design thicknesses are based on four foundation stiffness classes (IAN, 2009).

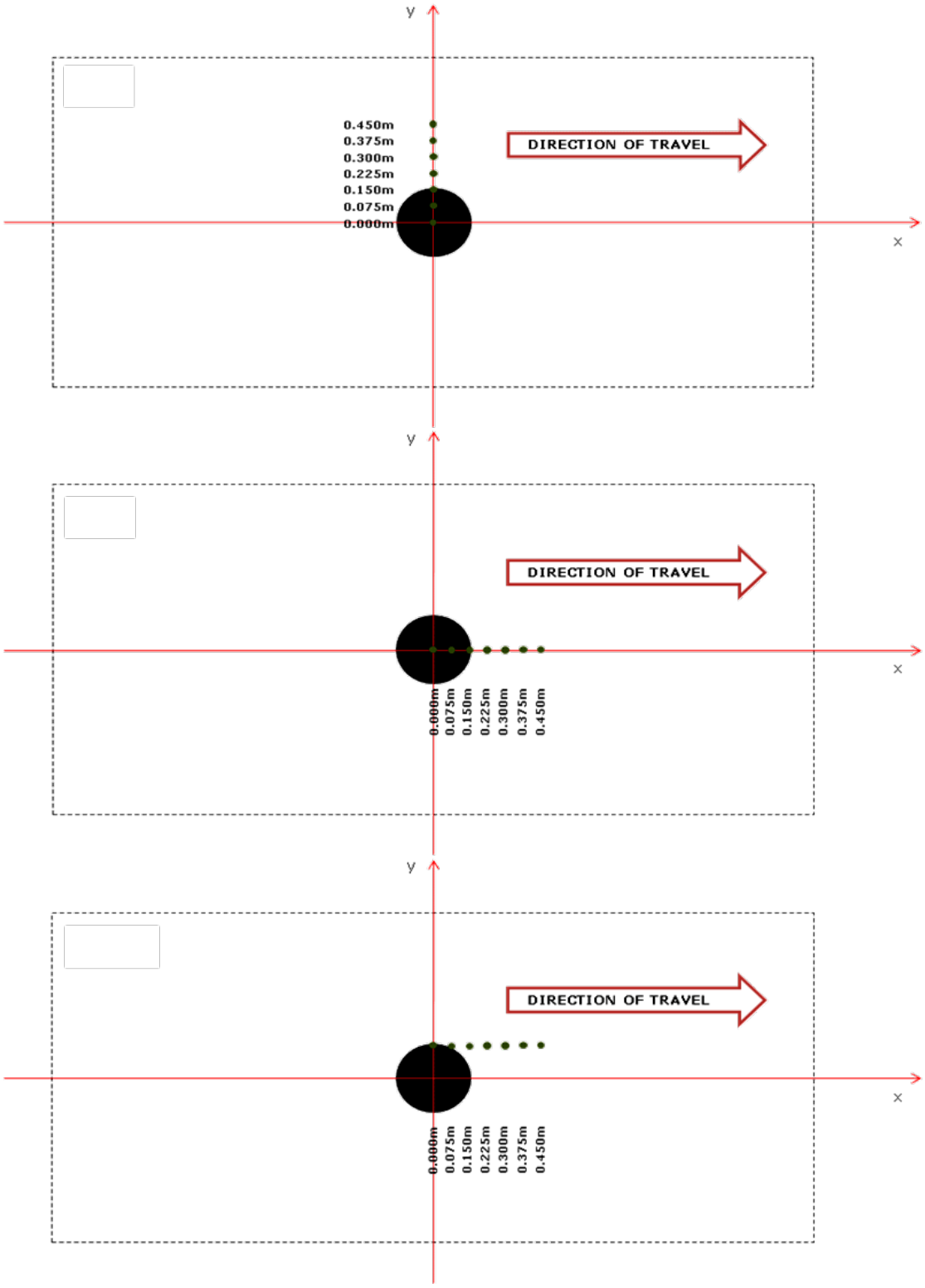


Figure 3.1. Locations of calculated stresses at predefined points using BISAR

Figure 3.2 shows six pavement systems that were investigated with asphalt thickness ranging from 100mm to 400mm, including some with stiffness gradients to model temperature change with depth, overlying a foundation with different support stiffness, relating to the choice of Foundation Class as set out in IAN 73/06 (IAN, 2009). The thickness of the subgrade is infinite. The materials are assumed to be homogeneous and isotropic and are characterised by stiffness modulus (E) and Poisson's ratio (v). Poisson's ratios of 0.35 and 0.30 were assumed for asphalt layer and foundation, respectively.

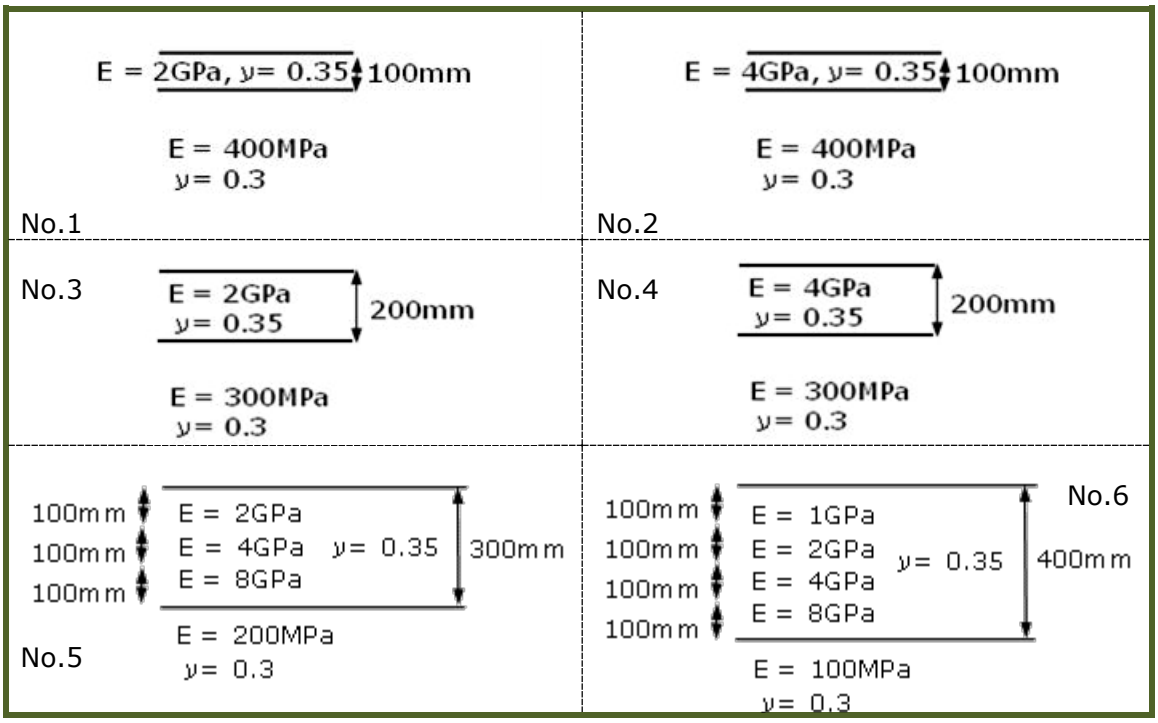


Figure 3.2. Pavement structures analysed

The traffic load is applied over a circular area, with a uniform contact pressure equal to the tire inflation pressure. In most countries, road traffic loading is converted to the legal axle load or standard axle load such as the equivalent 80kN axle load and is used as design input for roads. This can be converted to 40kN per dual wheel loading and typically a 0.565MPa contact pressure per wheel (Nunn, 1997). Therefore, a single, standard vertical wheel load of 40kN with a contact pressure of 565kPa and radius of 151mm is assumed.

As discussed in Section 3.2.1, parameters p, q or η (p/q), and α are suggested to represent stress states in an asphalt pavement. Based on the BISAR results, the p and q stress invariants were calculated and, hence, the stress ratio, η. The orientation of the major principal stress axis was also determined.

As the stress distributions were broadly similar for all the cases, the detailed stress calculations were carried out for only one of the structures, which is Structure No. 3 (Figure 3.2). These computations used only two depths approximately where the maximum shear stress developed, 50mm and 200mm. The results of this investigation are plotted in Figures 3.3 to 3.8.

Figures 3.7 and 3.8 show the stress paths plotted for vertical stress against shear stress and mean normal stress against deviator stress on the centre line of the load and under the edge of the tyre, respectively.

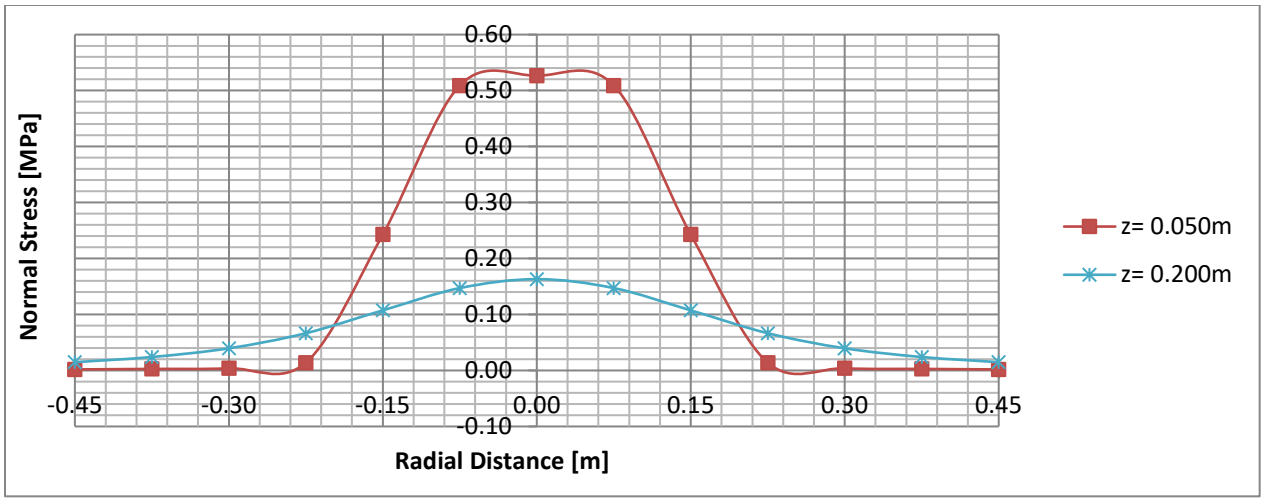
Evidence from previous studies is that rut development arises within the top 50mm to 100mm in the asphalt layers approximately beneath the edge of the load as a result of the repeated application of shear stress from vehicle wheel loading (Lytton et al., 1993, Monismith et al., 1994, White, 2002). BISAR modelling confirmed that the maximum shear stress on the vertical/horizontal plane (τ_{xz}) generally developed under the edge of the load but the actual maximum value of it varied and ranged from 128kPa to 320kPa. The predicted maximum vertical stress occurred close to the surface, within the top 50mm of asphaltic mix and was in range of 224kPa to 566kPa.

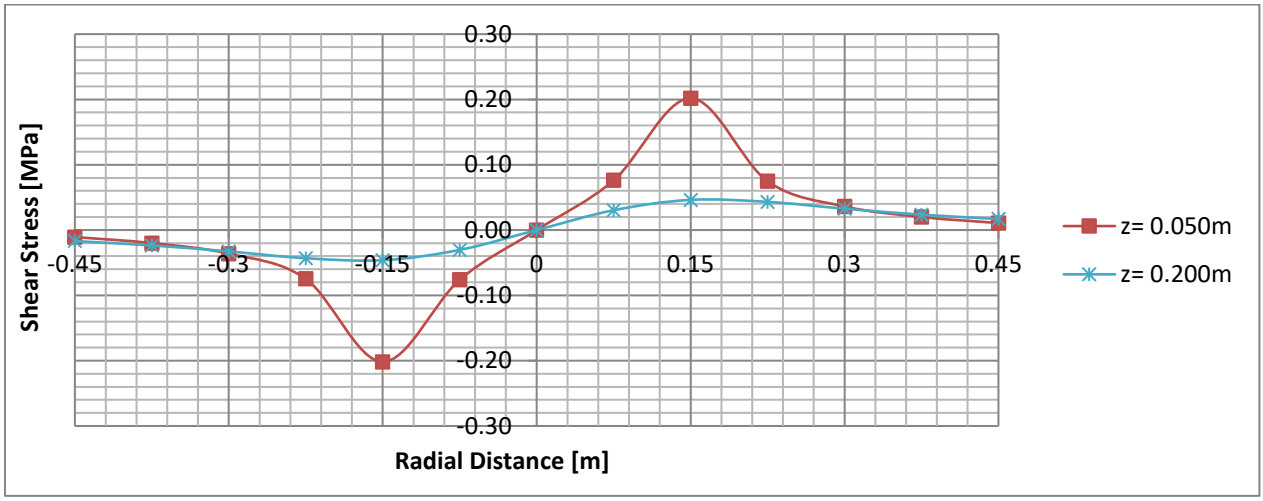
The shear stress parameter (q) varied with radial position but was generally maximum at the bottom of the layer with an approximate range of 350kPa to 1180kPa. The maximum stress ratio, ($\eta = q/p$), however, occurred within the layer and varied between 0.1 and 43.6. The very high values were encountered between 225mm and 300mm from the load centre.

The results of this study suggested that the maximum levels of shear and of normal stress should be 220kPa and 600kPa respectively for loading associated with highway applications and up to 1,300kPa and 3,300kPa for

the larger stresses that would result from aircraft or container terminal traffic.

A runway design using a typical design aircraft such as the Boeing 747 has a wheel load of approximately 225kN per wheel on their main gear and a tyre pressure of 1.39MPa per wheel. The tyre pressure of such a typical design aircraft is roughly double that of a truck tyre pressure.





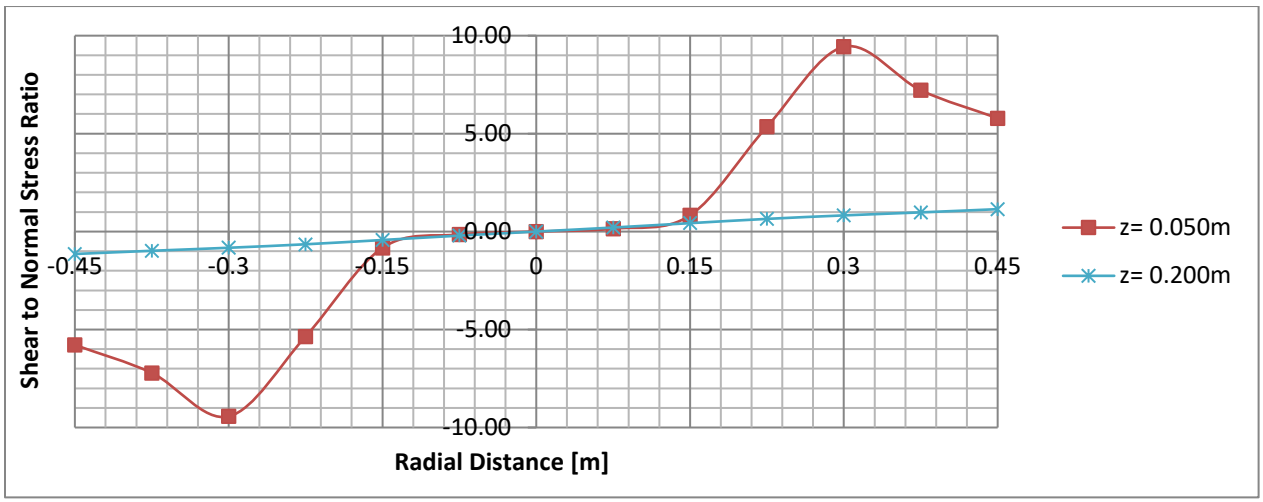


Figure 3.3. Normal and Shear Stresses on centre line of load

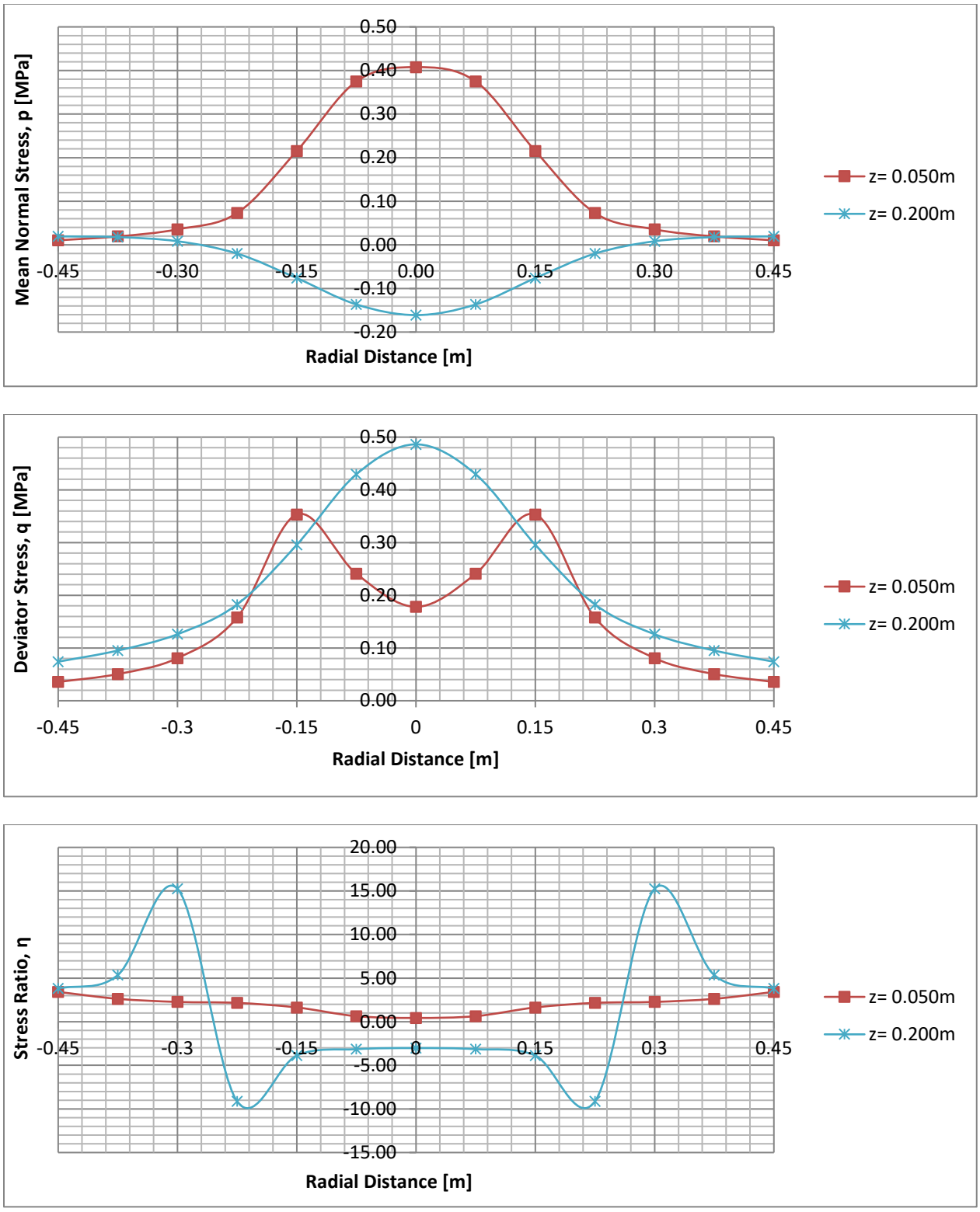


Figure 3.4. Mean Normal and Deviator Stresses on centre line of load

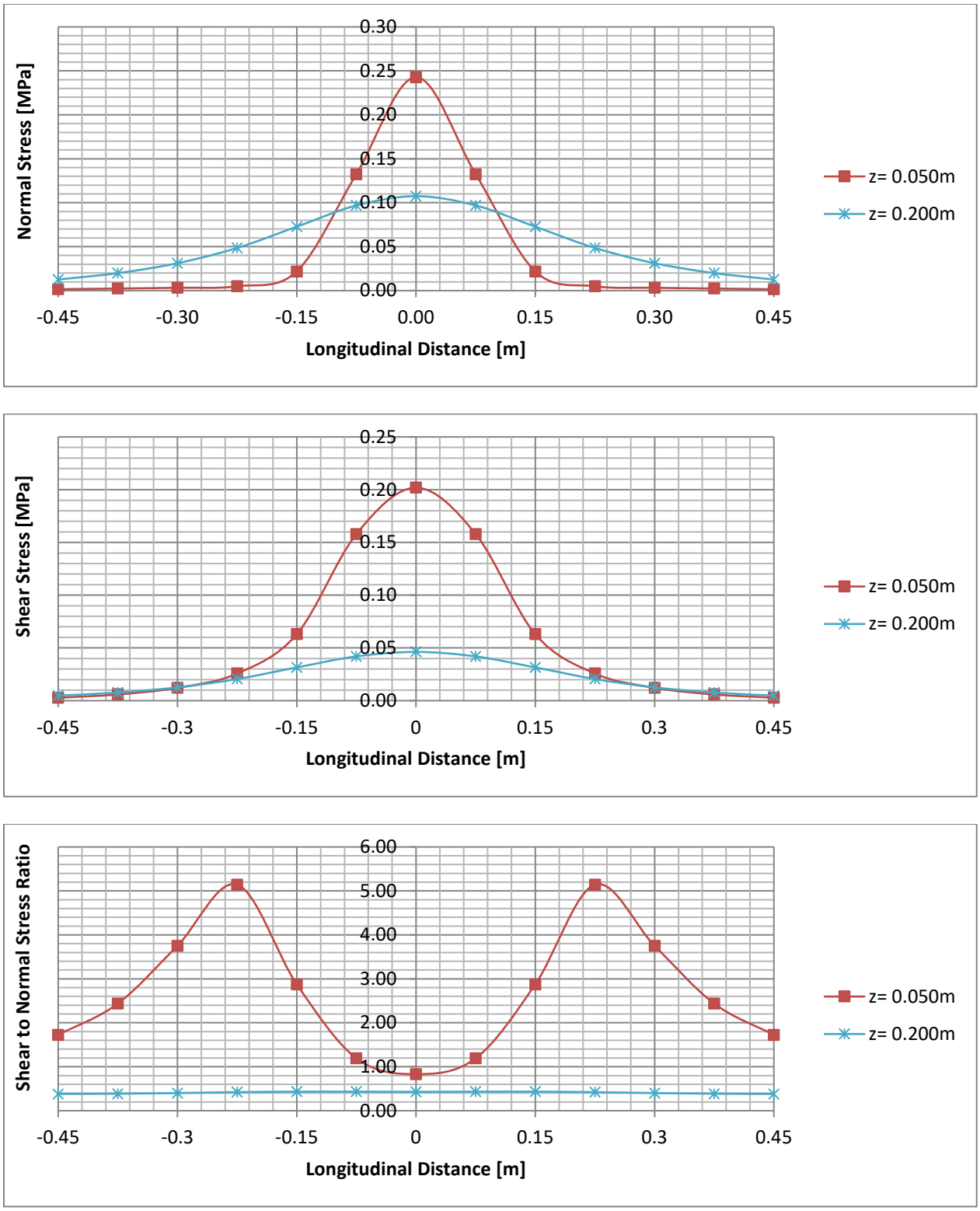


Figure 3.5. Normal and Shear Stresses under edge of load

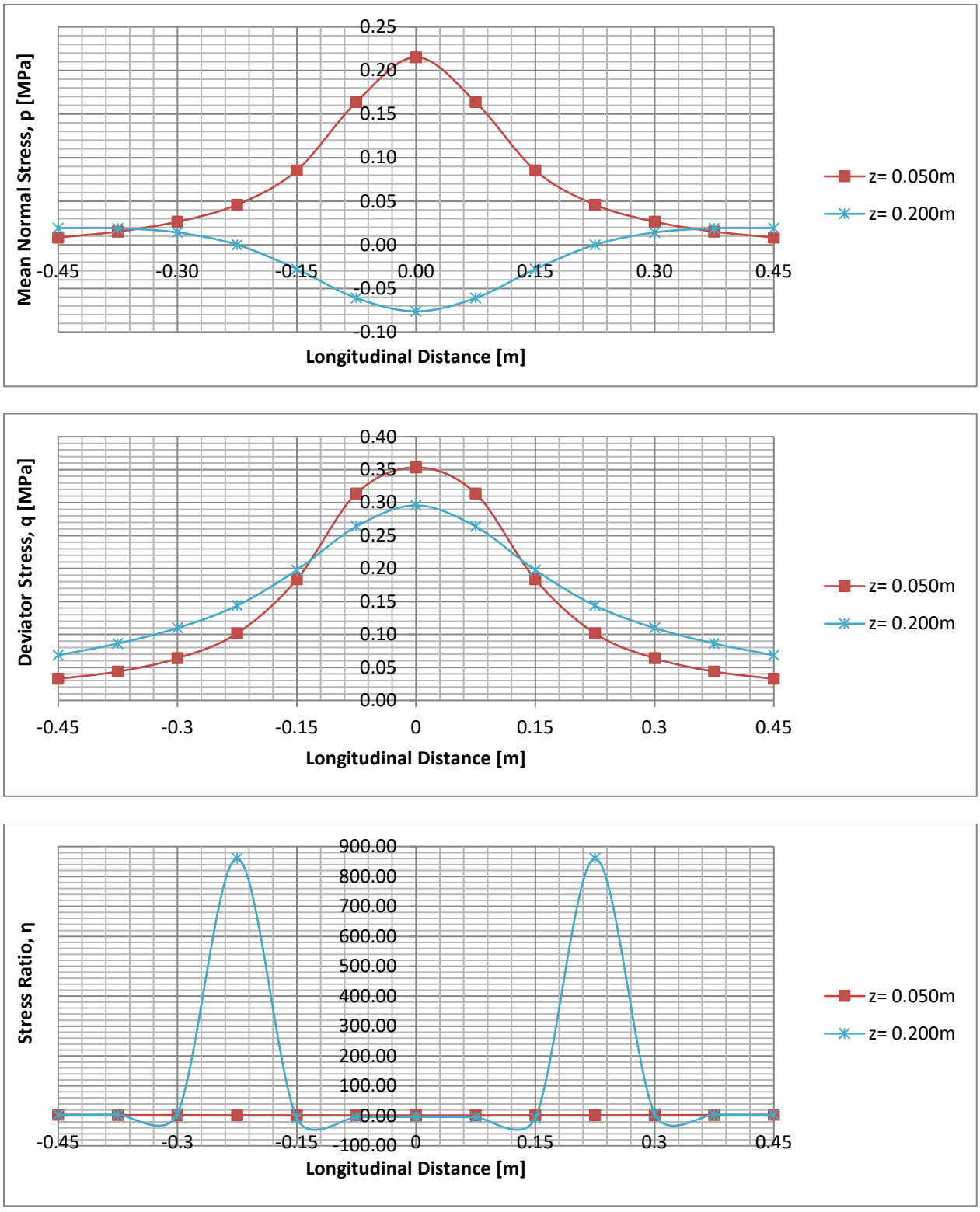
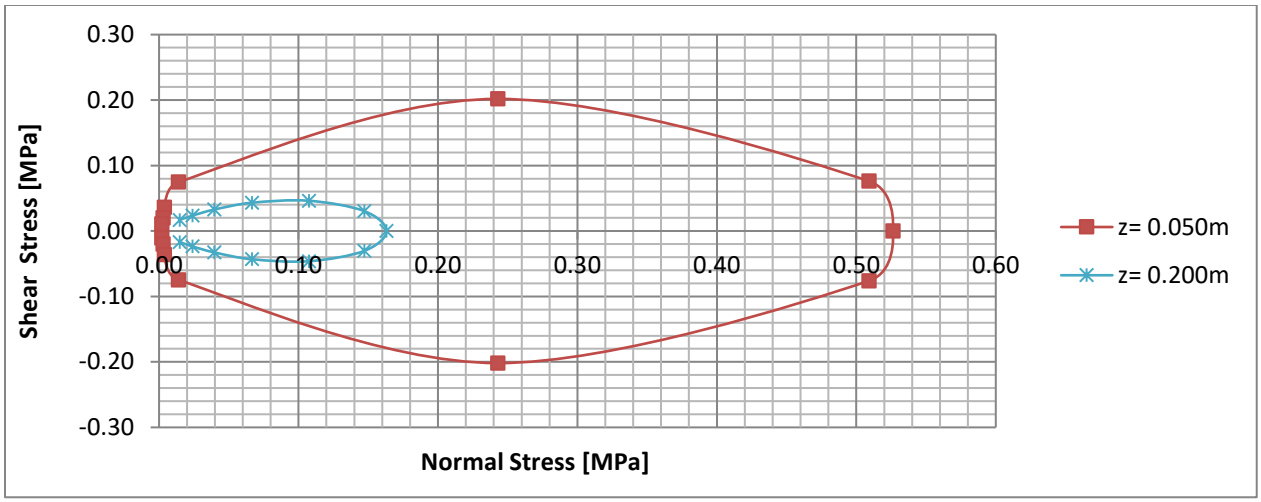


Figure 3.6. Mean Normal and Deviator Stresses on under edge of load



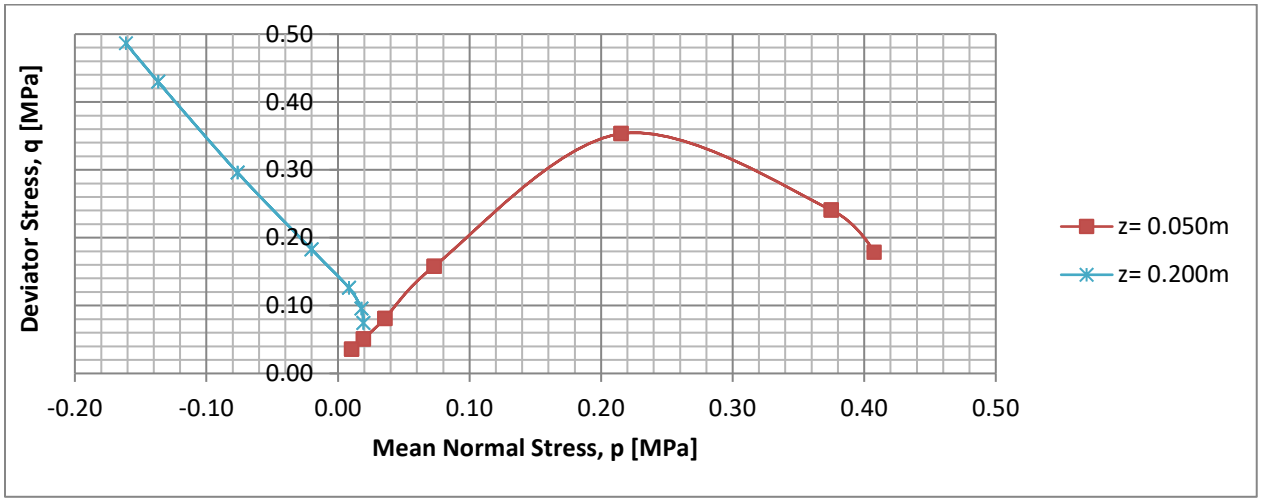


Figure 3.7. Stress Paths on centre line of load

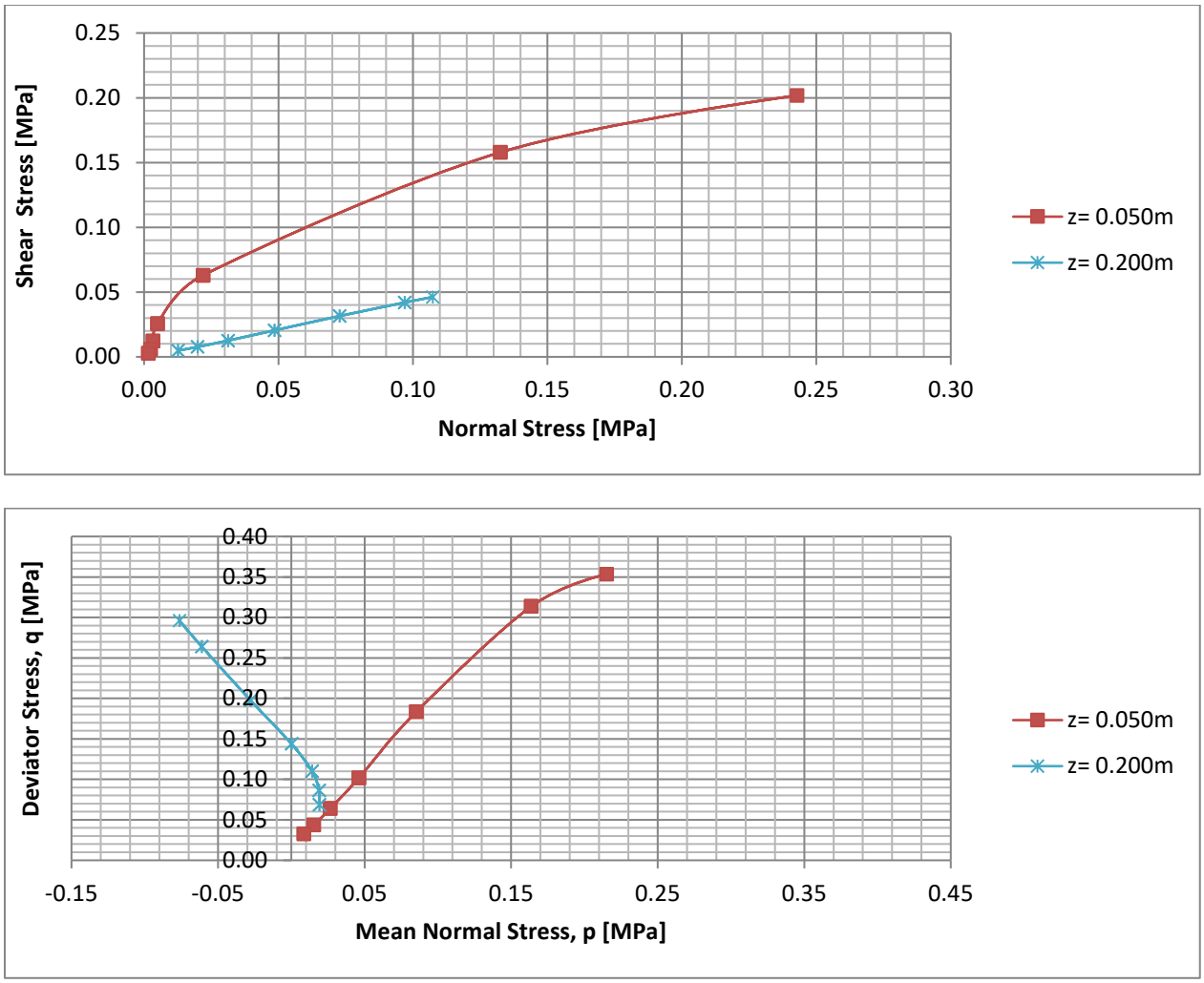


Figure 3.8. Stress Paths under edge of load

3.2.2. HCA Specification

Figures presented above, when considered in the context of the specimen geometry and the mechanism intended for application of the torque to deliver the shear stress, implied the need for a vertical actuator of 28kN - 154kN capacity and shear actuator of 10kN - 59kN. Given the range of actuators available on the market and the need to compromise somewhat on

the size of the facility, a decision was made to select 100kN and 30kN for the vertical and shear actuators, respectively.

To proceed with the HCA design, apart from setting the specimen dimensions and defining the loading ranges from expected levels of vertical and shear stresses, it was also necessary to specify the ranges of loading frequency and temperature that the testing will be run at (see Table 3.1).

Mechanical properties of asphalt are strongly susceptible to loading time and the temperature. It is well known that most of the rutting occurs during the summer time and in order to properly evaluate the phenomenon of rutting in the laboratory it is essential to test specimens within the high temperature range of those encountered in the field (Bouldin and Collins, 1992). In the United Kingdom, the wheel-tracking test is generally carried out at either 45°C or 60°C.

Nicholls and Carswell, (1998a) concluded the resultant deformation is more dependent on loading time than traffic speed (frequency). However, the low deformations due to static load show that dynamic effects are also important. Dynamic response of asphalt mixes in laboratory tests is commonly determined by applying a dynamic load having sinusoidal or haversine waveform with a specific frequency. Walther and Isailovic, (2015) confirmed that different vehicle speeds lead to different strain values in the pavements. As shown in Figure 3.9, a vehicle speed of 90 km/h, which corresponds to a

loading frequency of 10 Hz for a 34cm thick pavement induces the lowest strain value, where loading frequencies of 5Hz and 3Hz, 40 km/h and 20 km/h vehicle speed respectively, show very similar results, and indicate the shortest design life of the considered structure. Moreover, this research concluded that vehicle speeds lower than 40 km/h have significant impact on the service life of asphalt pavements.

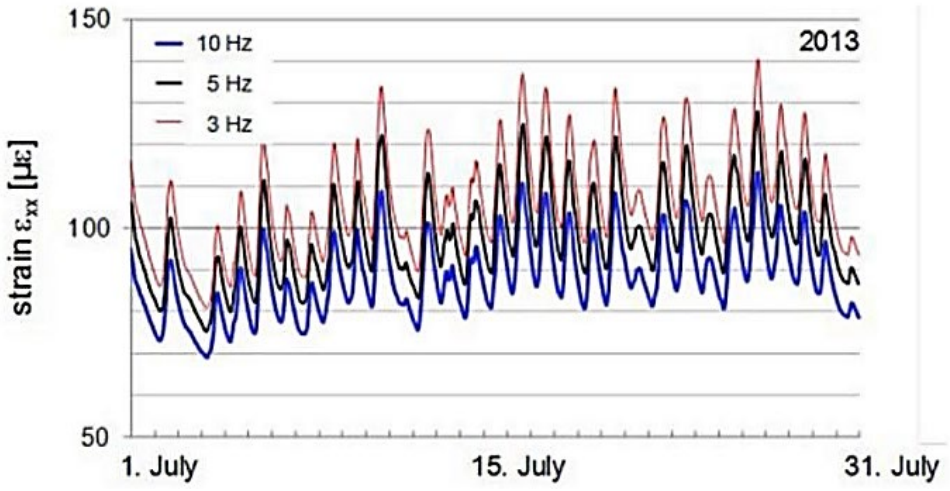


Figure 3.9. Resulting strain evolution at the bottom of an asphalt base course at 34cm depth, taking into account different loading frequencies for duration of one month (Walther and Isailovic, 2015)

In order to investigate the impact of both temperature and time of loading to which the pavement will be subjected on rutting, in addition to the geometric and load parameters defined above, the following additional factors were specified at the design phase of the HCA: applied stress frequencies up to 5Hz, test temperatures from 20 to 45ºC.

A system should be able to apply internal and external pressure to the sample to reproduce the conditions of confinement from the surrounding

material in an asphalt layer. Therefore, confining stresses from 0kPa to 200kPa were selected, applied statically with equal values internally and externally to the cylinder but with the facility to apply differential values in the future.

Table 3.1. Summary of all the factors defined for HCA testing

Specimen Dimensions	H 350mm, OD 350mm, ID 250mm
Vertical Load	Up to 100kN, stroke 0 to 100mm
Torque	Up to 30kN; arc of rotation +/- 15º
Loading Frequency	0 to 5Hz stroke at 5Hz – ≤1.5mm, rotation at 5Hz - 2º
Confining Pressure	0 to 200kPa
Temperature Range	20 to 45ºC

3.2.3. Loading System

A servo hydraulic system was selected as this had the accuracy of control to meet the above specification over the range of loading. Key components of the system are the servo valve on the vertical actuator and the proportional valve on the torque actuator. These allow large actuator loads and strokes to be controlled by small electrical signals.

The operating principal of the closed loop servo control system used for the HCA can be seen in Figure 3.11, which shows a section taken through the vertical loading actuator. This actuator is fitted with a servo valve, and load

and stroke transducers. The transducers measure the mechanical output (load or stroke) of the actuator, in response to an electrical command signal, and convert the output to an electrical signal. This feedback signal is compared to the command signal in a summing junction (comparator) and is arranged to be the opposite polarity to the command signal (known as negative feedback). The resulting difference or error signal is amplified and used as a control signal (drive current) to the servo valve, which controls the oil flow to the actuator in proportion to this current. This flow forces the actuator shaft to move and apply load. Any further change in the command signal generates an error signal which causes the actuator to respond in an attempt to zero the error signal. The larger the error signal the harder the amplifier will drive the servo valve to reduce the error and if the amplifier gain is high enough the actuator will respond rapidly and accurately follow the command signal. In this way the servo valve is able to control high oil pressure (140 bar) and flow (40 litre/min) and direction of flow using just a small electrical signal. Control can be in force (load) or position (stroke). The torque actuator was a different design to the vertical actuator as can be seen in Figure 3.15 and was fitted with a high precision servo-proportional valve but still operated in a closed loop mode with load and position feedback, as shown in Figure 3.10.

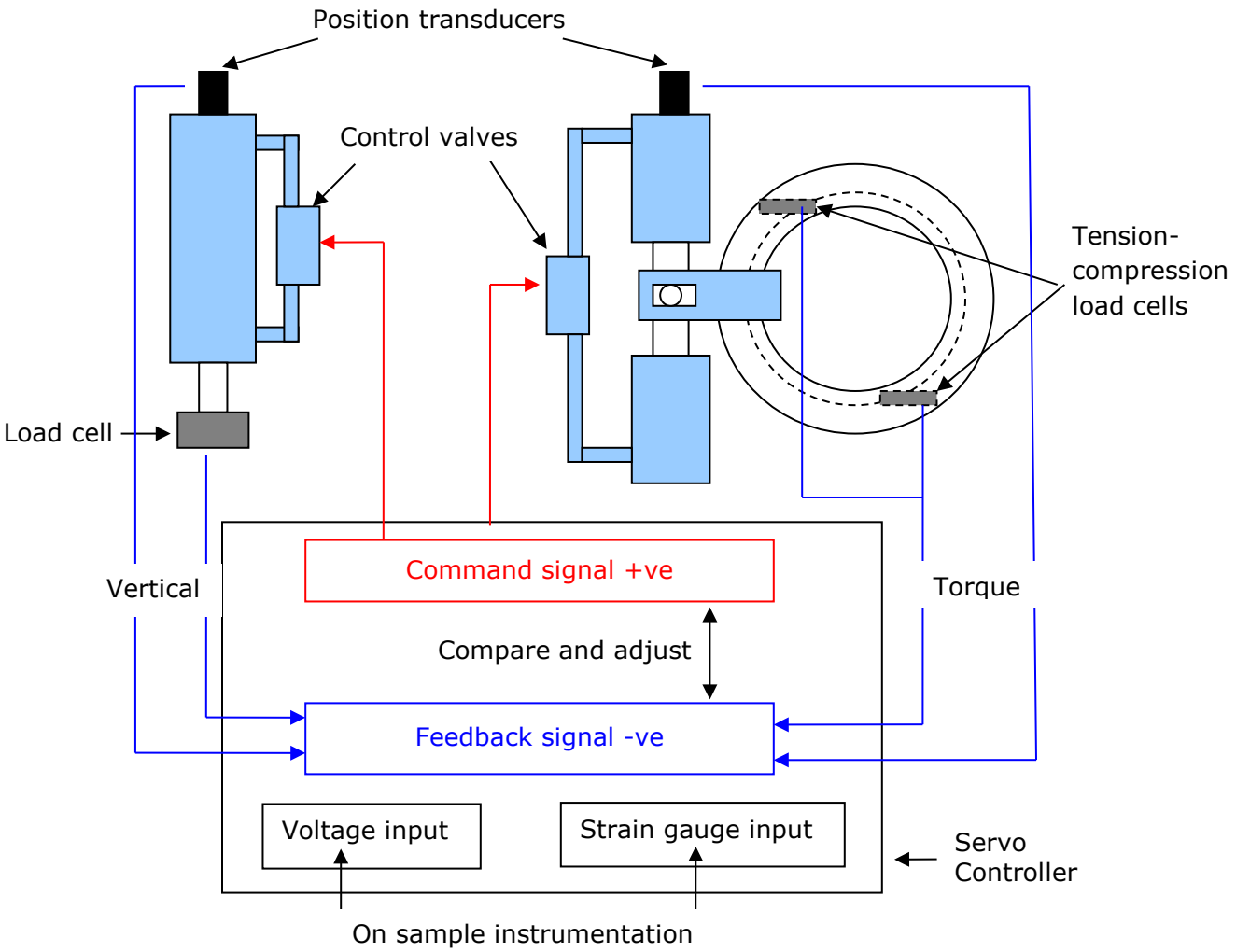


Figure 3.10. Closed loop servo control diagram

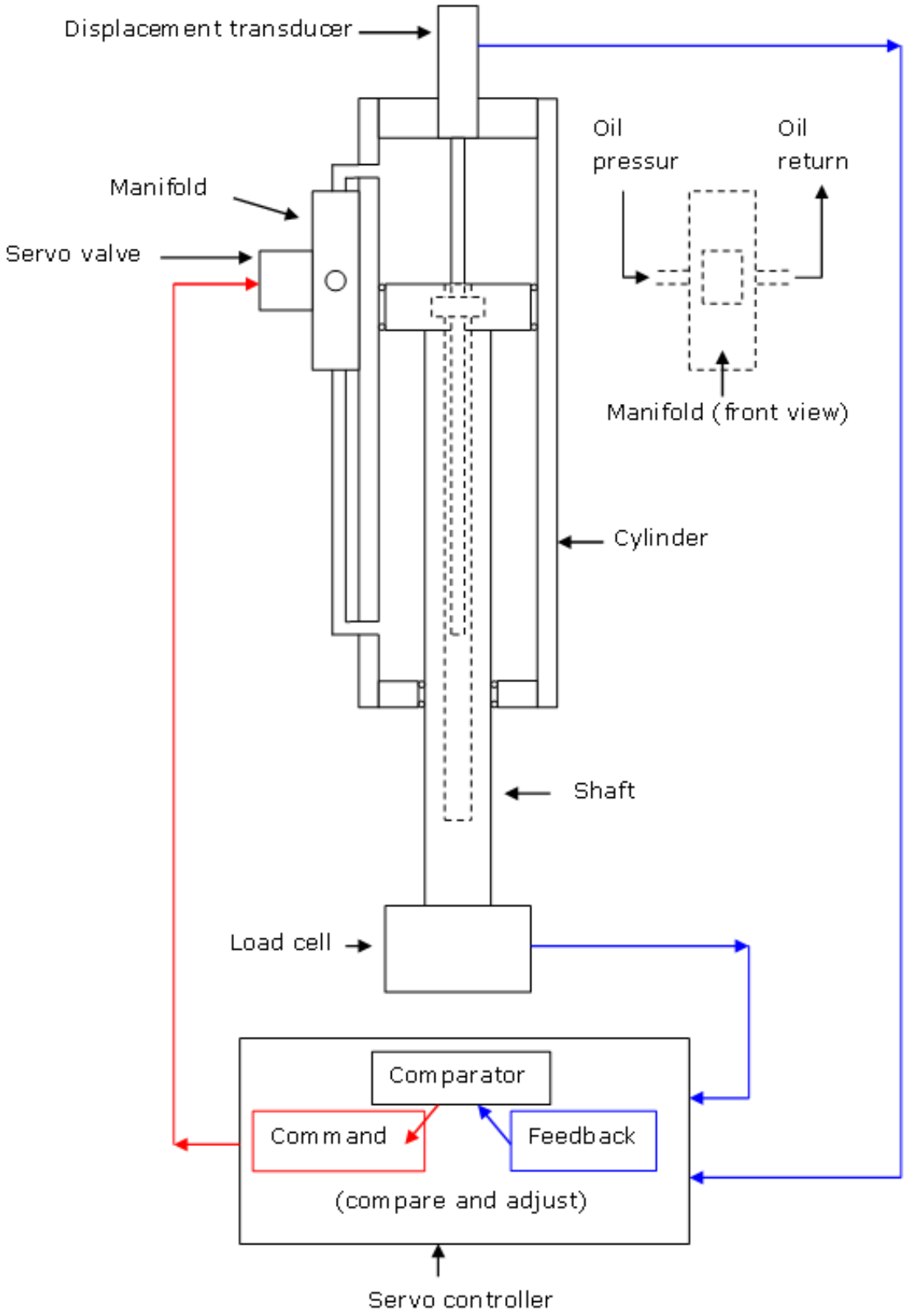


Figure 3.11. Servo hydraulic loading arrangement

Figure 3.12 shows the general configuration of the new torsional HCA and Figure 3.13 is a photograph of it. The large stiff frame was designed to provide an adequate reaction to the applied loads from hydraulic actuators and to accommodate the heavy specimen on a low solid steel base provided to facilitate installation. An intermediate steel crosshead with adjustable height was provided to support the two cylinder torque actuator and an upper solid steel crosshead, also with adjustable height, for location of the vertical actuators. Four round guide columns were used to align the base and crossheads, and these provided stability and strength to resist the vertical and horizontal forces from the two actuators. Two long stroke pistons with extensions were fitted to raise or lower the crossheads prior to clamping them in their correct position after final assembly of the HCA.

The vertical loading components are shown in Figure 3.14. The 100kN actuator with a stroke length of 100mm is fitted above the top crosshead and a position transducer is attached to the top of the shaft to measure its position. Couplings are used to connect the main vertical feedback load cell to the actuator shaft and to an extension shaft below. A collar is used to ensure a direct connection to the extension shaft but allows for ease of separation if necessary.

Vertical load in this instance can be applied in a compressive mode only. Tensile characteristics are limited by the actuator / load cell connection which

has been designed to provide free float characteristics with a maximum tensile force of 10kN to allow raising of the drive mechanism.

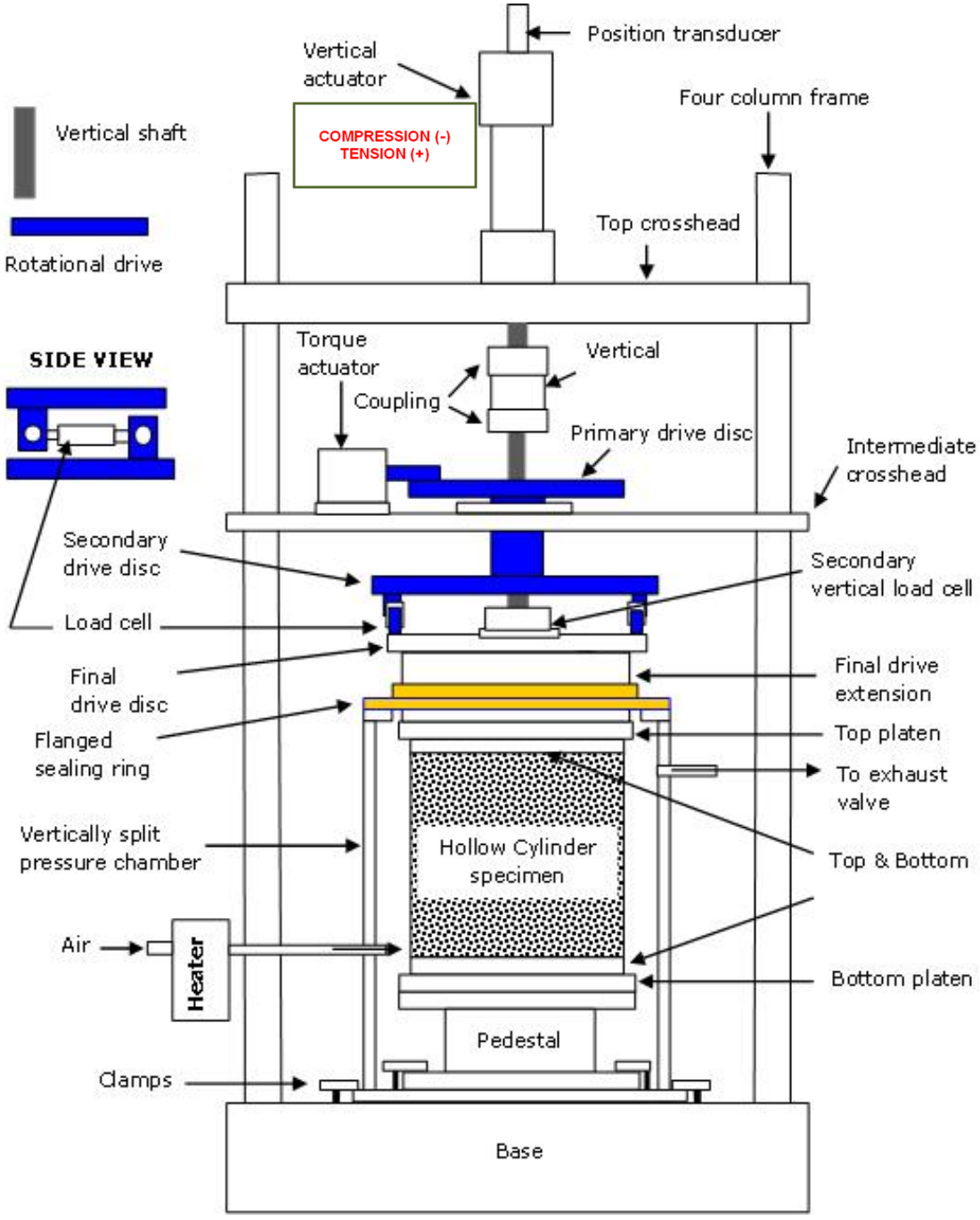


Figure 3.12. Cross section of new Hollow Cylinder Apparatus showing principal components

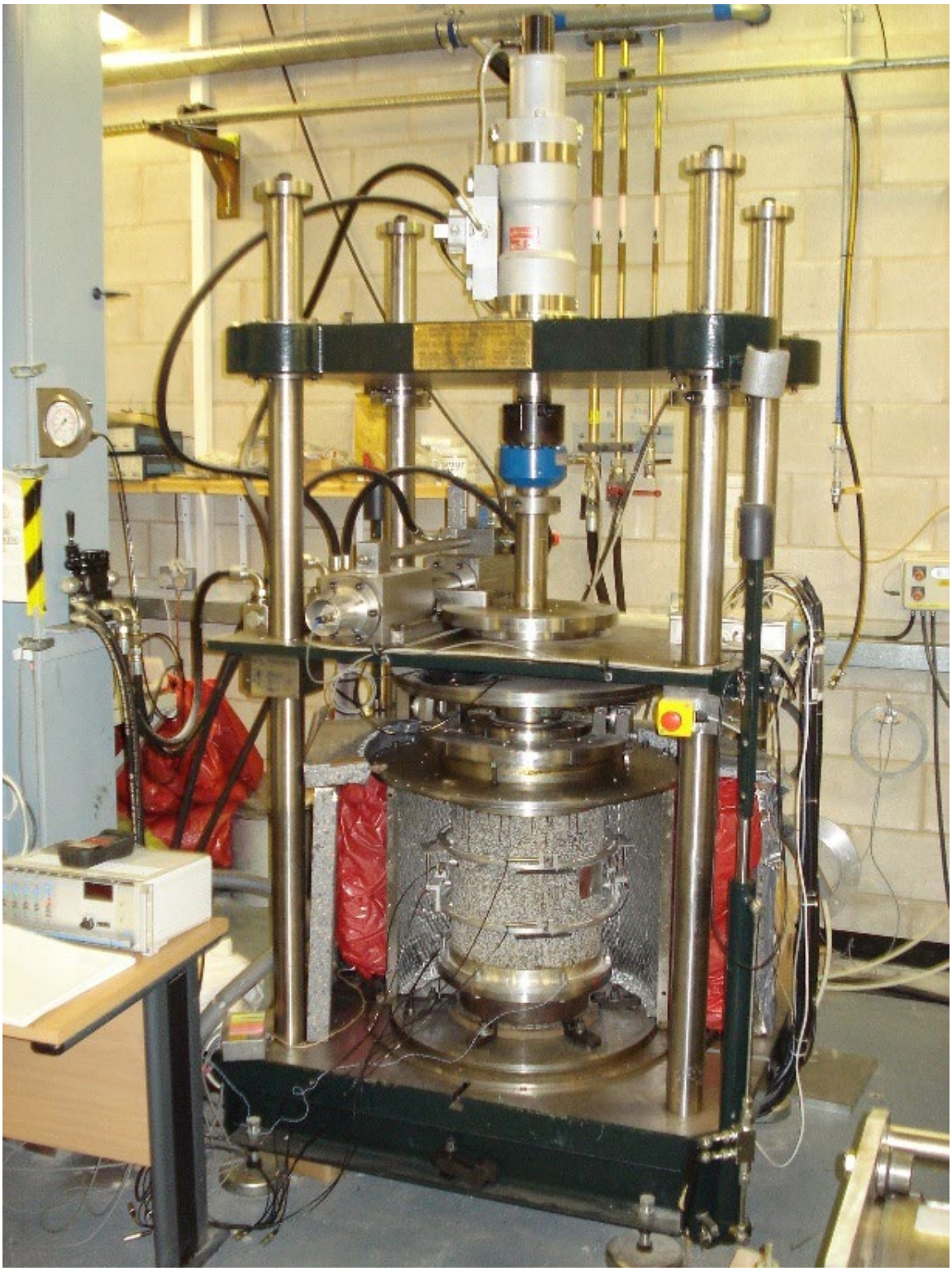


Figure 3.13. HCA with test specimen in position and pressure chamber open

The extension shaft passes through a large clearance hole in the intermediate crosshead and a secondary 100kN load cell is screwed to its end. This load cell is bolted to the inner ring of a large angular contact roller bearing and the outer bearing ring is fitted to the final drive disc, which is part of the torque loading arrangement. The bearing allows vertical load to be applied on a fixed axis and also rotation about the fixed axis without torque being transferred to the vertical loading components.

The secondary load cell provides a check on the upper vertical load cell as the extension shaft has to pass through the torque loading arrangement and some friction may occur.

The side view on Figure 3.15 shows the arrangement for transmitting torque to the top of the specimen using three discs. The 30kN horizontal actuator is fixed to an intermediate crosshead at a 200mm offset from the vertical axis (6kNm torque). +/- 75mm travel is available, which allows +/- 15º of rotation of the final drive plate. The primary drive disc is turned by an arm attached to a central shaft, which is connected to two hydraulic cylinders as shown in the plan view. A pin on the shaft moves the arm and passes through a slot, which accommodates the lateral movement of the arm as the primary drive disc rotates.

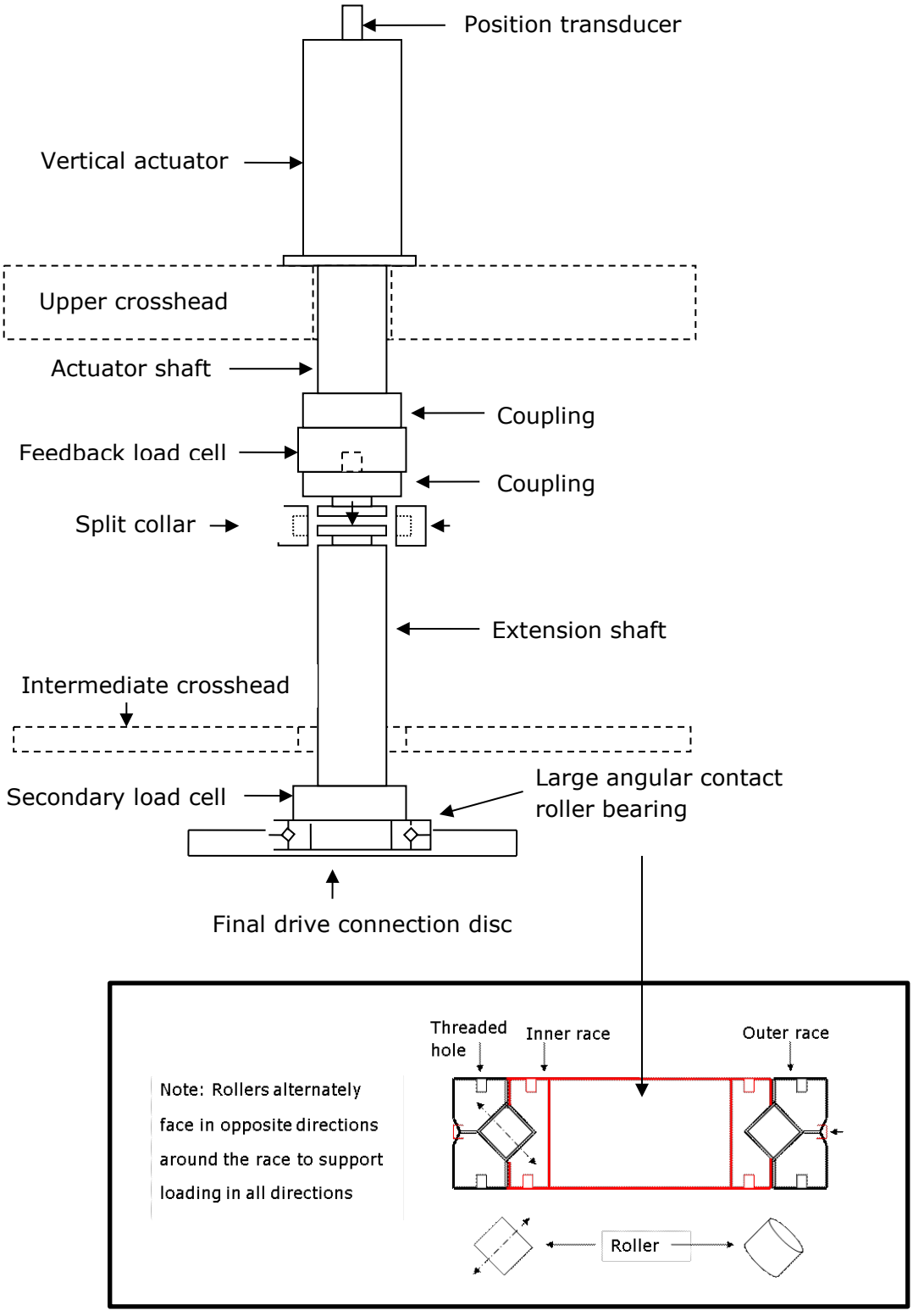


Figure 3.14. Details of vertical load application system

This disc is extended downwards by a short spigot and bolted to the inner ring of a cross roller bearing. The bearing is attached by means of a cover plate to the intermediate crosshead but can still rotate. The secondary drive disc is extended upwards by a longer spigot which connects to the underside of the bearing so that it turns with the primary drive disc.

The torsional load applied during rotation is measured by two tension-compression 25kN load cells linking a secondary drive disc to the final drive disc (Figure 3.15). These are mounted at each end with rose-jointed couplings, allowing the final drive disc to move down about 30mm to follow the permanent deformation of the sample in response to the vertical loading. The load cells and couplings form a link of about 150mm in length and make an angle of 11 degrees to the horizontal for a downward movement of 30mm. This causes a slight reduction in the horizontal force on the final drive for a constant force applied by the torque actuator. The primary drive mechanism and two load cells are shown in Figure 3.16.

The amount of rotation is measured by a position transducer connected to the common actuators' shaft.

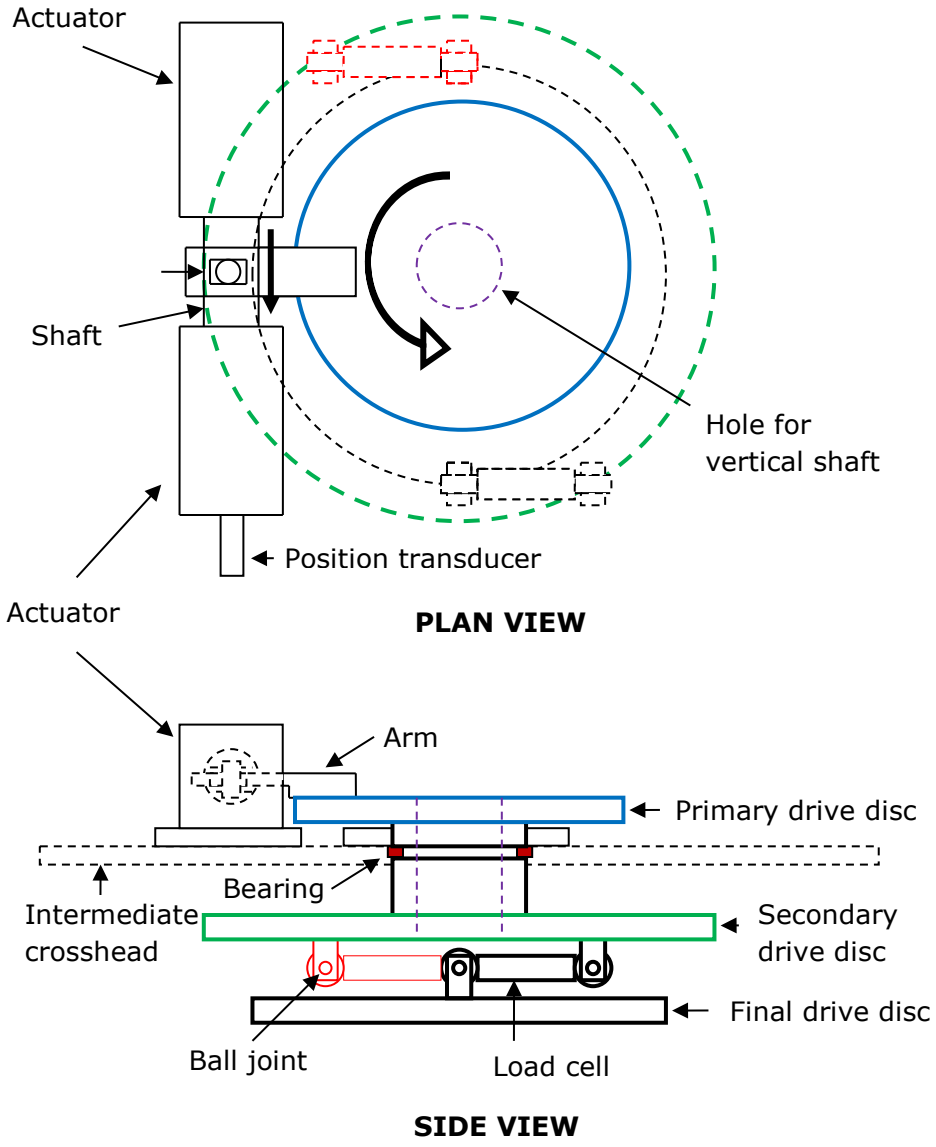
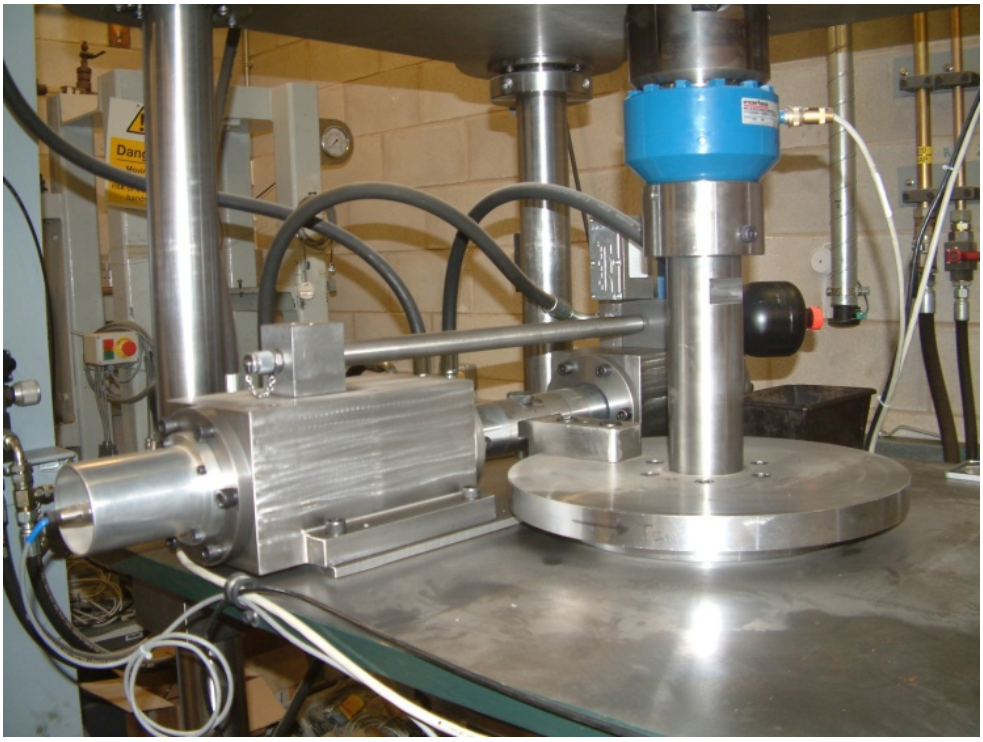
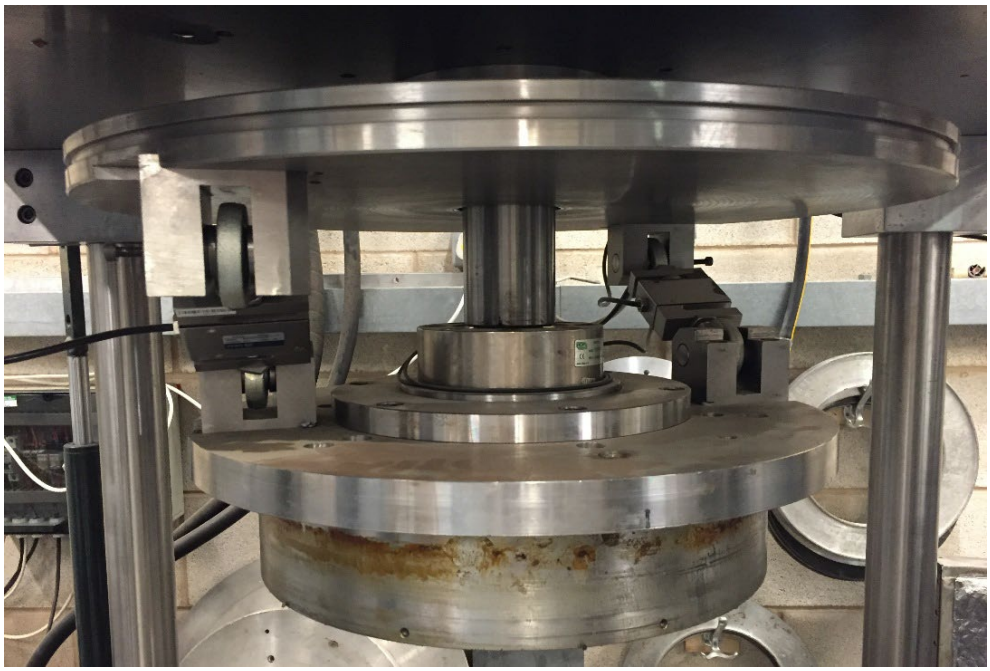


Figure 3.15. Torque application mechanism



(a) Torque primary drive mechanism and actuator



(b) Two load cells and connecting links between the secondary and final disc drives

Figure 3.16. Torque drive mechanism and load cells

Figure 3.13 shows the location of the specimen in a stainless steel pressure chamber, which had to be insulated for temperature control. As shown in Figure 3.17, the cylinder can be split in half and bolted together through vertical flanges either side of the split and bolted to the base through circular flanges welded around the bottom of each half of the cylinder. The top of the chamber and each of the holes within the chamber are individually sealed with 'O' rings.

In order to provide sufficient vertical movement through the chamber top, it was necessary to bolt a cylindrical extension to the final drive disc which is then bolted to the specimen top platen. The bottom specimen platen bolts to a pedestal which is clamped to the base of the pressure chamber which, in turn, is clamped to the base of the loading frame. This method of fixing simplifies the alignment of the specimen and the centralisation of the final drive extension through the pressure chamber cover.

The chamber was used as a temperature controlled container. Air pressure controlled by a regulator was connected to a calibrated pressure gauge and then passed through an air filter combined with an internal heater. The calibration certificates are included in Appendix A. The heated air at the required pressure then passed into the pressure chamber at the bottom so that the specimen was brought up to the test temperature. It was necessary to have a small flow of air through the heater and this was controlled by an exhaust valve attached to an outlet from the pressure chamber. This was

arranged to be near the top of the chamber so that there was movement of the air to ensure even temperature distribution. In addition, the chamber is also intended to simulate conditions of the confinement from the surrounding material in the asphalt layer. Future testing will require internal and external pressure on the specimen to be applied through a regulated pressure supply.

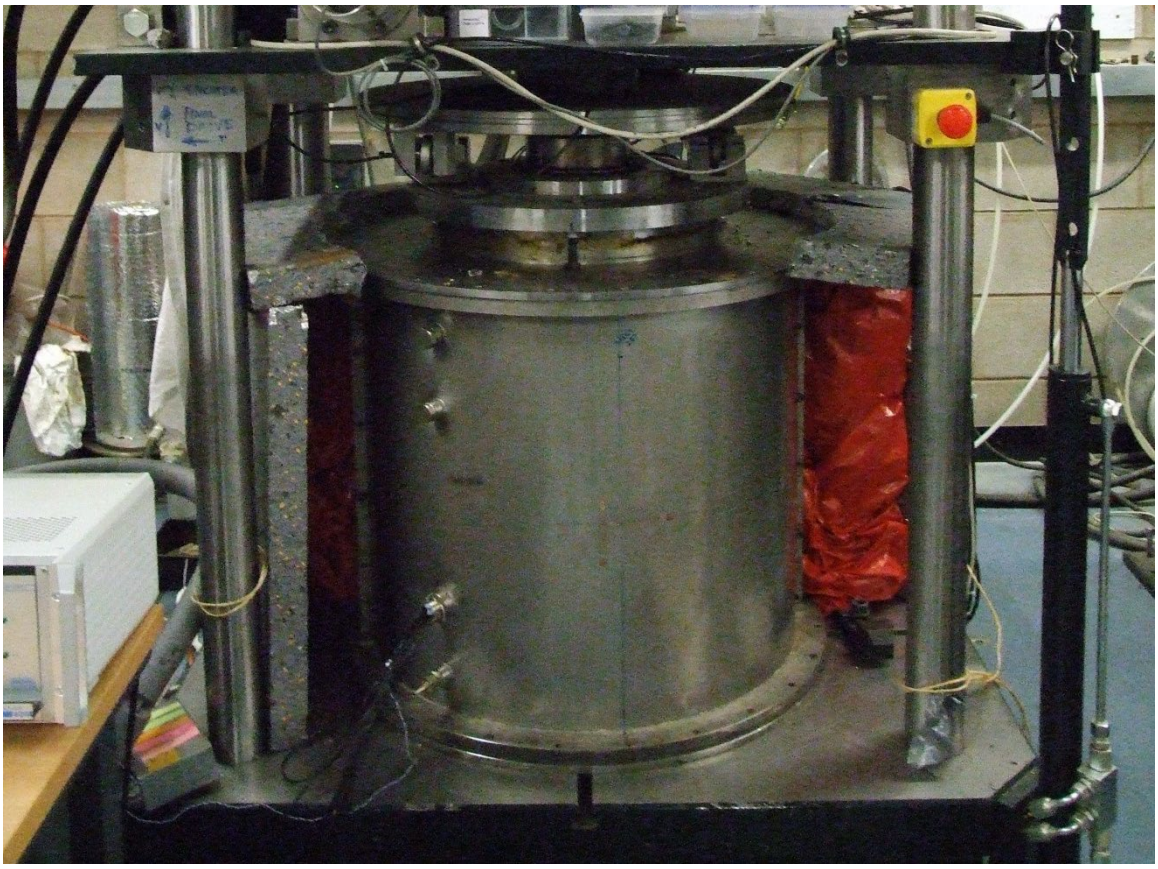


Figure 3.17. HCA with test specimen in position and pressure chamber closed

3.2.4. Specimen Geometry

The dimensions of the HCA specimen were defined by the maximum aggregate size, to account for uniformity of stress and strain distribution across the specimen wall, and by end effects caused by loading platen restraint on the top and bottom surfaces of the specimen. Different studies on HCA's for soils and asphalt have given insights and ideas about suitable dimensions for specimens (Alavi, 1992, Hight et al., 1983).

Chan, (1990) pointed out that in order to minimise stress non-uniformity caused by specimen curvature, it is necessary to increase the external diameter and reduce the wall thickness of the specimen.

Vallerga et al., (1957) indicated that in testing of granular and heterogeneous specimens, in order not to constrain failure mechanisms, it is necessary to define maximum particle size with respect to the specimen thickness. According to him, the ratio of maximum grain size to specimen size of 1 to 3 or 1 to 4 should be adopted.

Saada, (1988) demonstrated the importance of specimen geometry and end boundary conditions. Using the theory of thin elastic cylindrical shells, he revealed that a central zone can be reasonably free from the end effects when dimensions of a hollow cylindrical specimen meet the following criteria:

$$H \geq 5.44\sqrt{R_o - R_i} \quad (3.7)$$

and

$$n = \frac{R_i}{R_o} \geq 0.65 \quad (3.8)$$

where, H is the height, R_o is the external radius, and R_i is the internal radius of the hollow cylindrical specimen.

Based on these studies and needs of this research, the adopted specimen dimensions were as follow:

- Height H = 350mm
- External diameter D_o = 350mm
- Internal diameter D_i = 250mm
- (note: R_i/R_o = 0.71)

Taking 10mm maximum aggregate size as reasonable, this indicated a minimum wall thickness requirement of 50mm to give a ratio of five, which was similar to that used earlier (Brown and Richardson, 2004). The outside diameter of the specimen was fixed at 350mm, again giving similar proportions to the other apparatus. The height of the specimen was selected as 350mm, based on the concept that instrumentation would be arranged around a 150mm long section at mid-height to minimise end effects from the loading platens. These sizes compared with:

- a wall thickness of 25.4mm, an external radius of 114mm and a height of 457mm or 203mm used by Sousa, (1986) and by Alavi and Monismith, (1994) respectively;
- a wall thickness of 25.4mm, an external radius of 63.5mm and a height of 127mm used by Rueda, (2017),

so this new facility is significantly larger than anything used hitherto for asphalt testing of this type.

3.2.5. Deformation Measurement

The instrumentation used to monitor specimen deformations is shown in the schematic of Figure 3.18. The instruments are arranged around the central 150mm of the specimen height to minimise end effects as the test specimens are glued into the end platens and are, therefore, unable to deform radially at each end.

The instrumentation arrangement was designed to make a positive direct contact with the specimen in the central zone. It consists of a set of eight RDP electronics type Linear Variable Differential Transformers (LVDTs) arranged to measure vertical, radial and 45° components with two readings for each.

Pot marked metal studs were glued to the specimen at the required locations to define the measuring points at either end of the gauge lengths. Light

weight fittings to support displacement transducers at various orientations were manufactured, as shown in Figure 3.19.

The two strain collars carrying D5/300AGRA type LVDT's 1, 2, 5 and 6 are located on studs at diametrically opposite points. These serve to determine both the axial and the external radial deformations. The radial measurements are taken both internally and externally (across the open end of the external spring loaded hoops) to define the change in wall thickness.

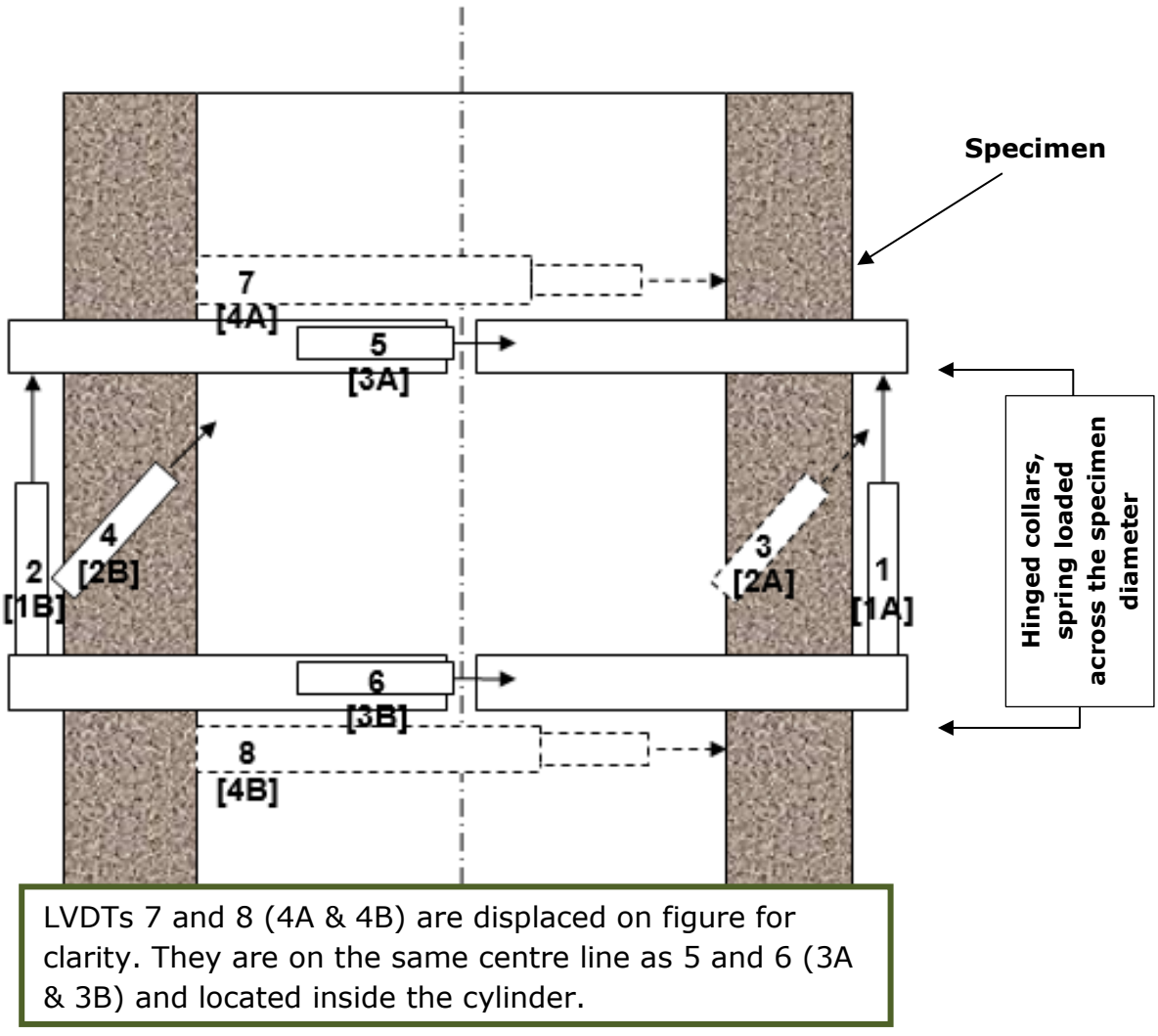


Figure 3.18. Arrangement of deformation measuring instrumentation

The photographs in Figures 3.20 to 3.22 show the LVDT's in position both on the inside and outside of the hollow cylinder. The internal D5/300AGRA type LVDTs were fitted with tubes which were spring loaded directly across the internal diameter and were located into studs glued to the specimen as shown in Figure 3.21. The spring loaded LVDTs 1, 2, 5, 6, 7 & 8 with +/- 7.5mm range were selected, which could cover expected permanent and resilient displacement measured directly on the specimen.

The 45 degree D6/02500URA type LVDTs (3 & 4) are fitted directly onto the specimen as shown on Figure 3.20 and have a displacement range of +/- 2.5mm. They had to fit between the collars as are set at a 100mm gauge length and have a free moving core. They are not spring loaded type to avoid the spring force pushing off the glued studs on the specimen at elevated temperatures.

During testing, the sample must be maintained at constant temperature. A calibrated thermocouple is used to monitor and control the temperature during the conditioning phase. To provide the most accurate indication of the specimen temperature, a thermocouple tip is inserted to the centre of the HC specimen wall as shown in Figure 3.23.

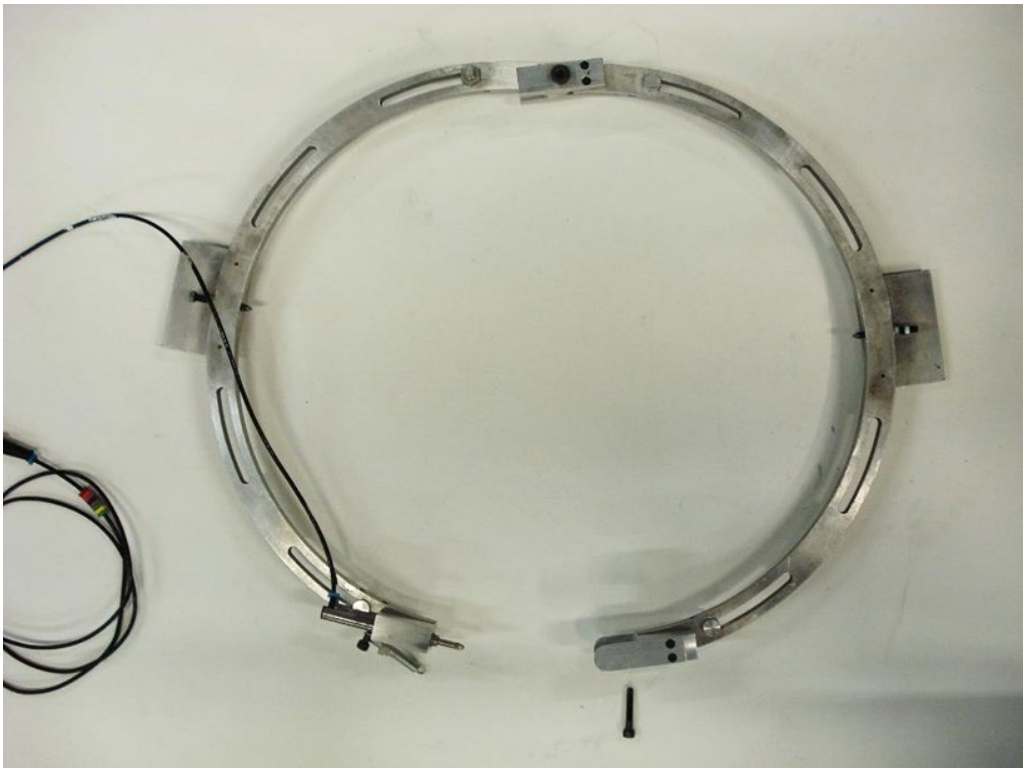


Figure 3.19. Hinged strain collar



Figure 3.20. Vertical and 45° LVDTs

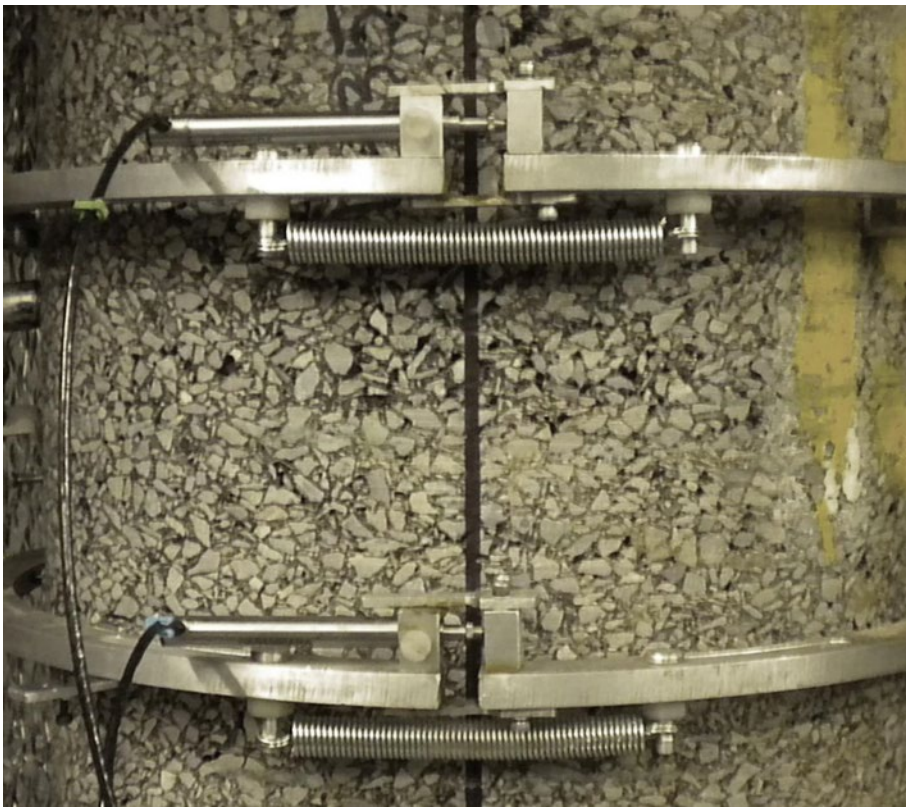


Figure 3.21. Radial LVDTs



Figure 3.22. Internal radial LVDTs

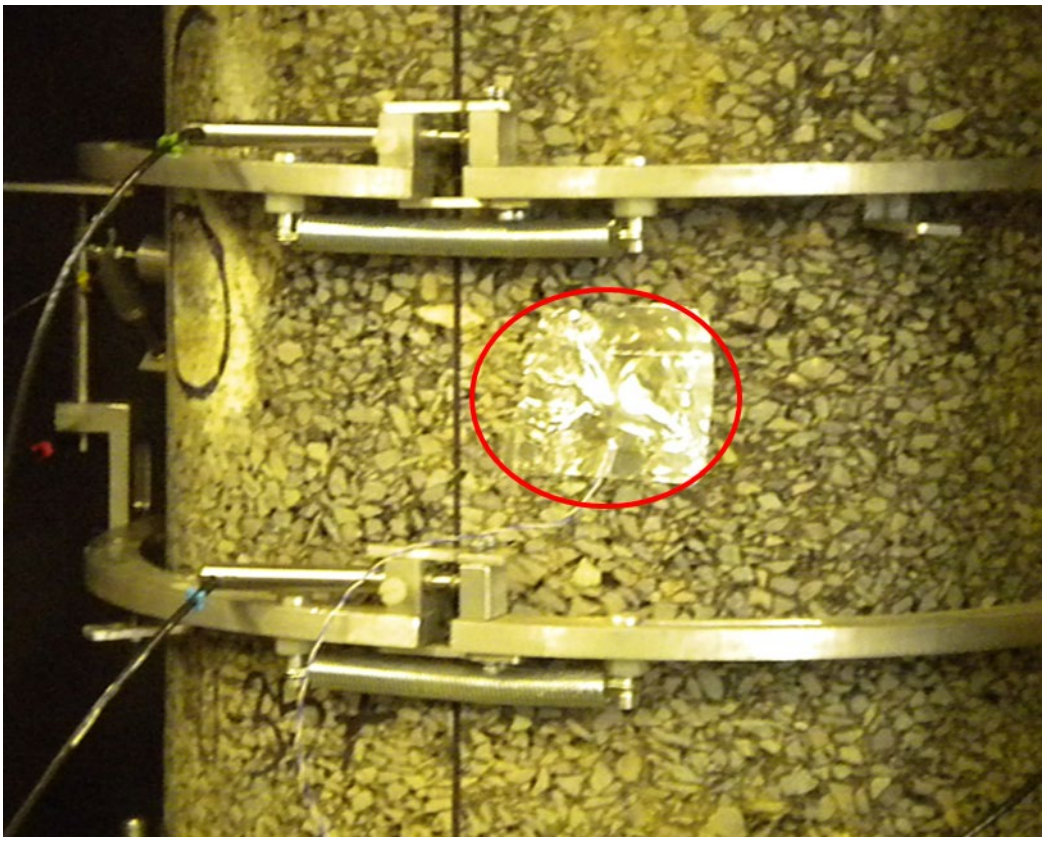


Figure 3.23. Thermocouple attached to the HC specimen

Combining the output from these instruments provides a set of mean values from the sets of replicate data as follows:

ε_z = Vertical strain from LVDT's 1 and 2.

ε_{45} = Strain at 45° from LVDT's 3 and 4.

ε_θ = Tangential strain from LVDT's 3, 6, 7 and 8.

These are then used to compute the principal strains as explained later on in Section 3.3.2. From monitoring the occurrence of strain at an angle of 45° to the vertical, it is possible to construct a Mohr's circle of strain (Figure 3.35).

The shear strain in the z–θ plane can be deduced from the diagram and an average value of shear strain (γ) can be calculated using the following equation:

$$\gamma_{\theta z} = 2\varepsilon_{45} - \varepsilon_z - \varepsilon_\theta \quad (3.9)$$

Where $\gamma_{\theta z}$ is equal to twice $\varepsilon_{\theta z}$ and is comparable with the parameter measured in the SST.

3.2.6. Calibration of the HCA stress and strain measuring system

Instrumentation calibration

All the displacement transducers have a maximum linearity error of +/- 0.1% of full scale and were carefully calibrated before tests with a precise micrometer using the set-up shown in Figure 3.24. Figure 3.25 shows the equipment for checking the calibration of the strain collars.

LVDTs are inductive sensing devices that produce an AC output voltage proportional to the mechanical displacement of a small iron core. These LVDT transducers requiring AC excitation were connected to a signal conditioning unit and an analogue output was adjusted to obtain output such as 1v/mm as shown in Figure 3.26.

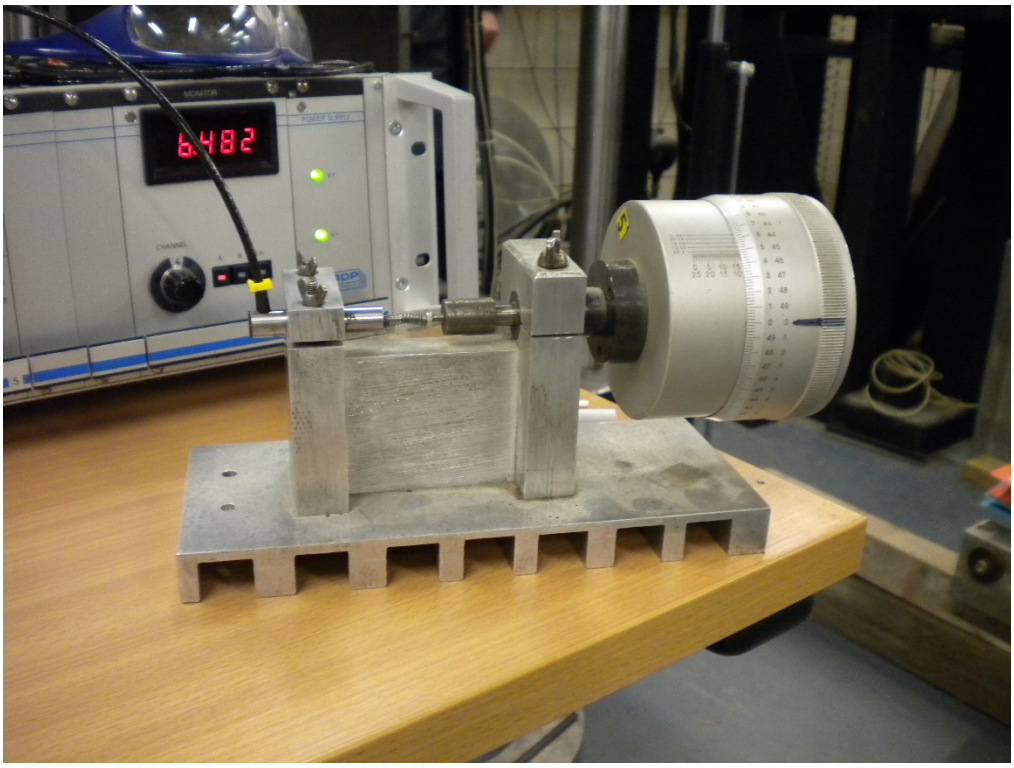


Figure 3.24. LVDT calibration

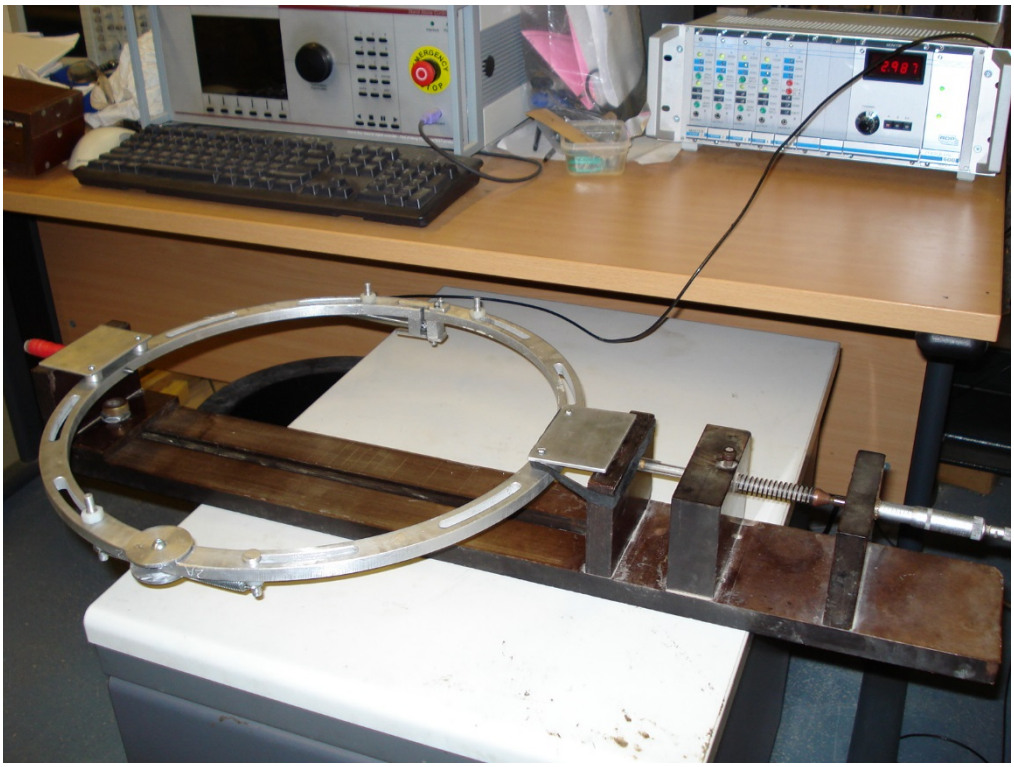


Figure 3.25. Strain collar calibration

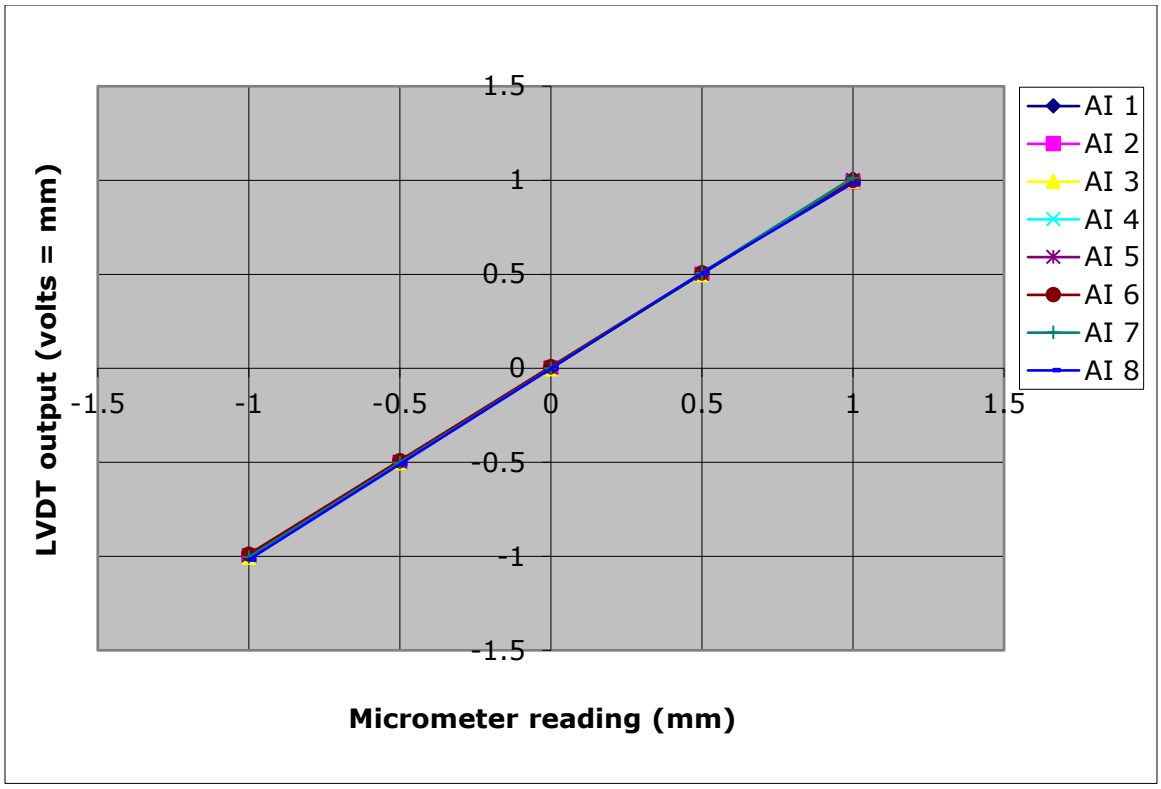


Figure 3.26. HCA on-specimen LVDTs calibration (18/08/2010)

Vertical load cell calibration

The top and secondary vertical load cells (A & B) were supplied with calibration certificates. These calibrations were done by the manufacturer using a National Physical Laboratories certified load cell and provided a sensitivity value in mv/volt which was incorporated in the SmarTEST controller software as part of the calibration procedure. The wizard calibration method was used to configure vertical load cell A input. The manufacturer's calibration data was entered as shown in Figure 3.27. The "Zero TD Offset" was used to get a zero output from the vertical load cell A before the extension and final arrangement was attached. When the final arrangement was attached the load cell read the equivalent force of 0.1kN

due to their weight. This was then cancelled by using the Tare to give a zero reading from the load cell and it was this reading that was used for feedback.

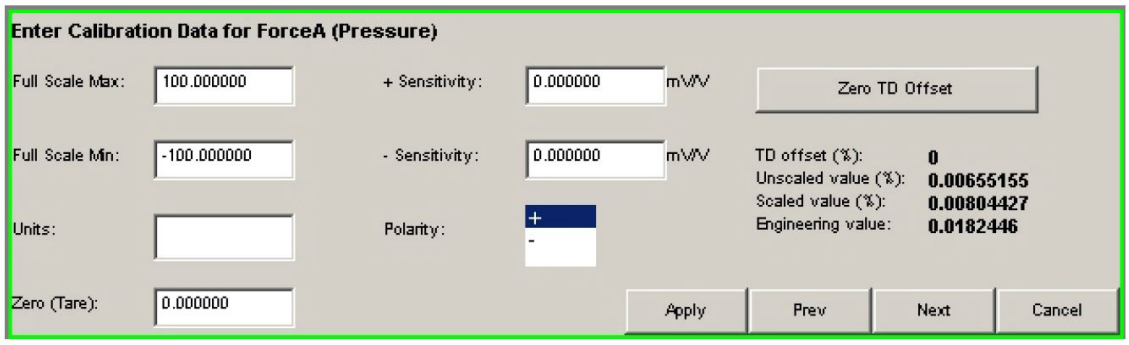


Figure 3.27. Calibration Wizard Window from control software

Torque load cells calibration

Two tension-compression 25kN B3G-C3-2.5T load cells were calibrated by the manufacturer and calibration certificates are included in Appendix A. Their full scale outputs were 3.003 mv/V and the reported combined error was defined to be 0.02% of FS.

With regard to the shear stress, due to the length of the torque load cells, it was necessary to fix them to the final drive disc to operate at an arm length of 200mm from the axis of rotation. The load is then transferred by the disc to operate on the top of the specimen on a 150mm arm. Therefore, when this load was used to calculate the approximate shear stress, the load applied at 200mm was lower by 33 per cent. However, as the HCA requires a torque input in kNm, as long as the torque was calculated using Equation 3.13 (see Section 3.3.2) based on 150mm arm then the correct load was applied

through the two load cells. The formula was therefore used to obtain required torque value by using target shear stress but the load reading was 33 per cent less than the load actually applied to the top of the specimen. Although the load cells are part of the feedback loop, these readings were only needed as a check.

3.2.7. System Control and Data Acquisition

A digital servo control system is used to operate the HCA and it was designed to apply a wide variety of input signals and the control can be either through position (stroke) or force (load). Figure 3.28 shows a schematic diagram of the HCA digital servo control and logging system. An LCD monitor was connected to the portable test controller to allow view of the information on a larger screen, as shown in Figure 3.29.

This standalone controller with LCD front panel can handle up to four digital servo control channels. For the HCA two channels are used and are assigned as Channel 1 for the vertical actuator and Channel 2 for the torque actuator in the control software. Analog I/O modules were added to the test controller to allow all the load cells and deformation instrumentation to be monitored through frequent sampling to defined wave forms.

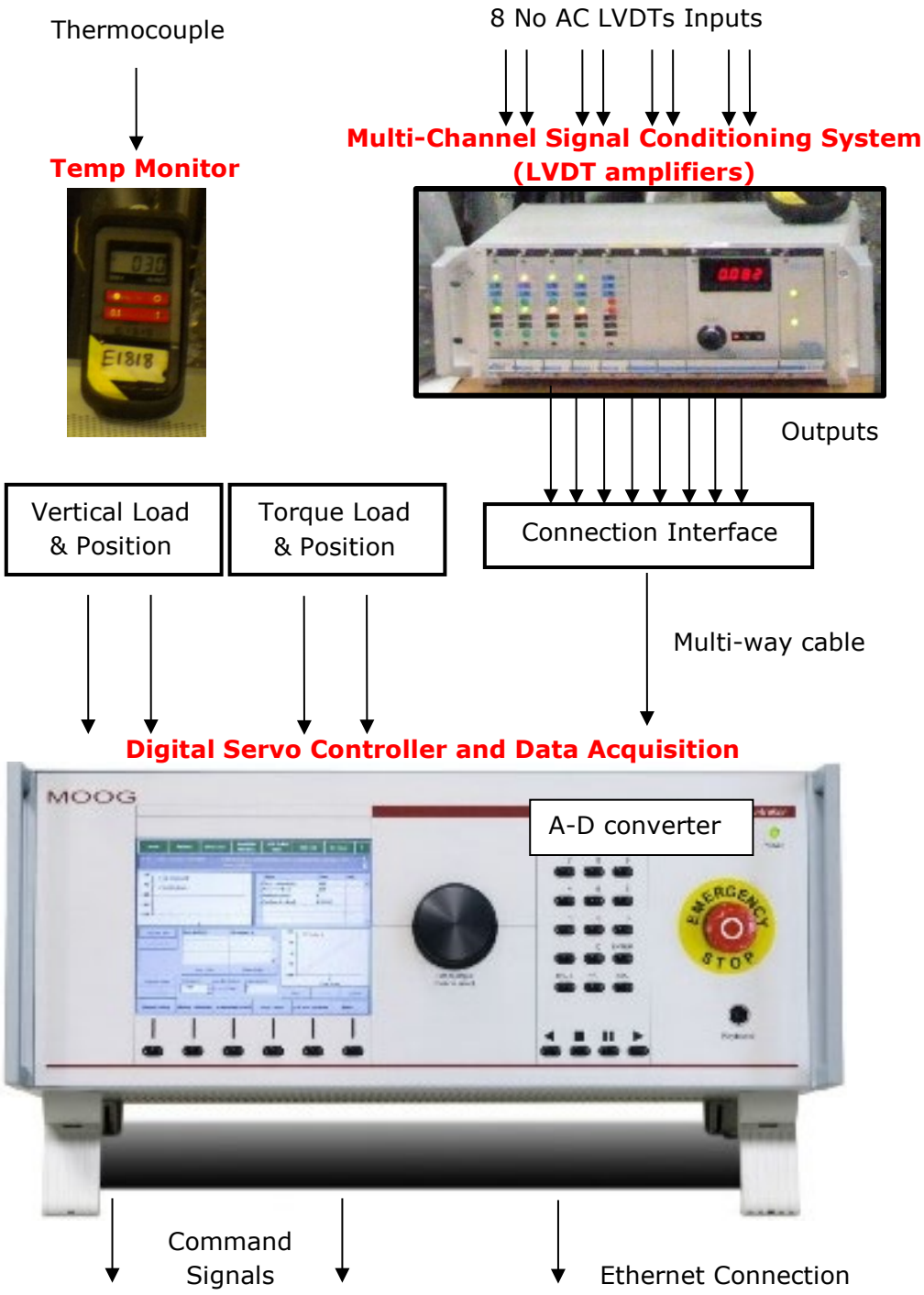


Figure 3.28. Schematic diagram of HCA digital servo control system

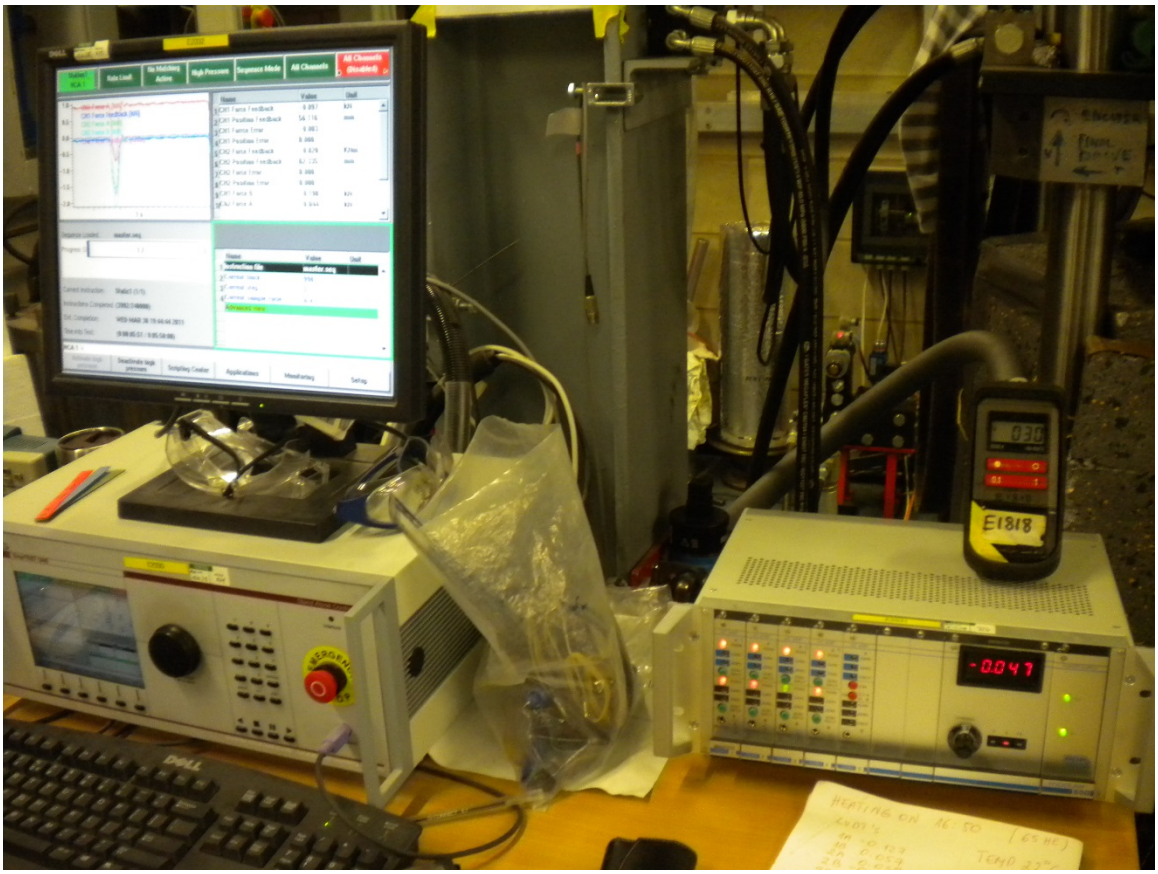


Figure 3.29. HCA digital servo control system

SmartWAVE block-editing software was used to create sequences and download them for local control on the test controller. A sequence is a set of instructions or steps that can be executed by the test controller either locally or remotely. Sequences can run instructions serially or in parallel, which allows the user to run multi-channel, multithreaded instruction sets. Further, the test controller has been optimised to support the local playback of sequences, allowing the user to run multiple independent control channels simultaneously.

A sequence can be composed of any combination of the following instruction types:

- Setpoint - A setpoint instruction assigns a value to a designated property or channel. This set point instruction utilizes step, transition ramp time, and transition type. Typically a sine or ramp is used for the transition;
- Cycle - A cycle instruction, used in a sequence, sets and starts a specific cycle application for a specific duration on a specified property or channel.
- Record - The Record instruction used in a sequence is used to trigger the recording application in the controller. This instruction allows the user to record any property in the test controller at a specific sample rate (DeltaT), for a specified duration. The acquired data is stored locally on the controller at the specified filename and location specified in the instruction.

This provides the possibility of varying the load pulse time and magnitude and also having a variable rest period between load pulses.

As shown in Figure 3.30, for the initial programme of work, the applied load regime was the same as used for the SST, namely 0.1s haversine waves with 0.6s rest periods between each.

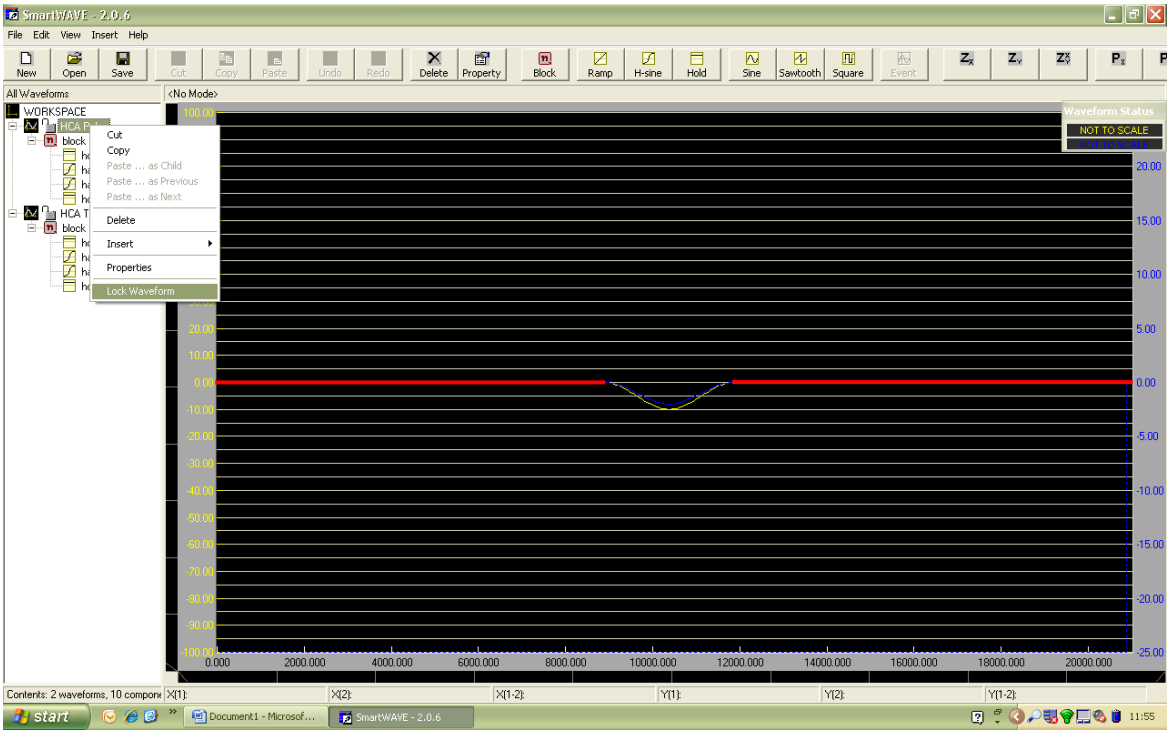


Figure 3.30. The loading waveforms produced by SmartWAVE for HCA testing

To access information stored on the Moog Test Controller, and perform maintenance tasks, such as file management and uploading of data files, use of the web server interface is required. A computer has to be connected to the Test Controller via Ethernet (see Figure 3.31). The raw data are saved in *.fstrm format and the MOOG web interface allows the data output to be converted to the Comma separated files - *.csv. When converting is completed, data files can be saved to a computer.

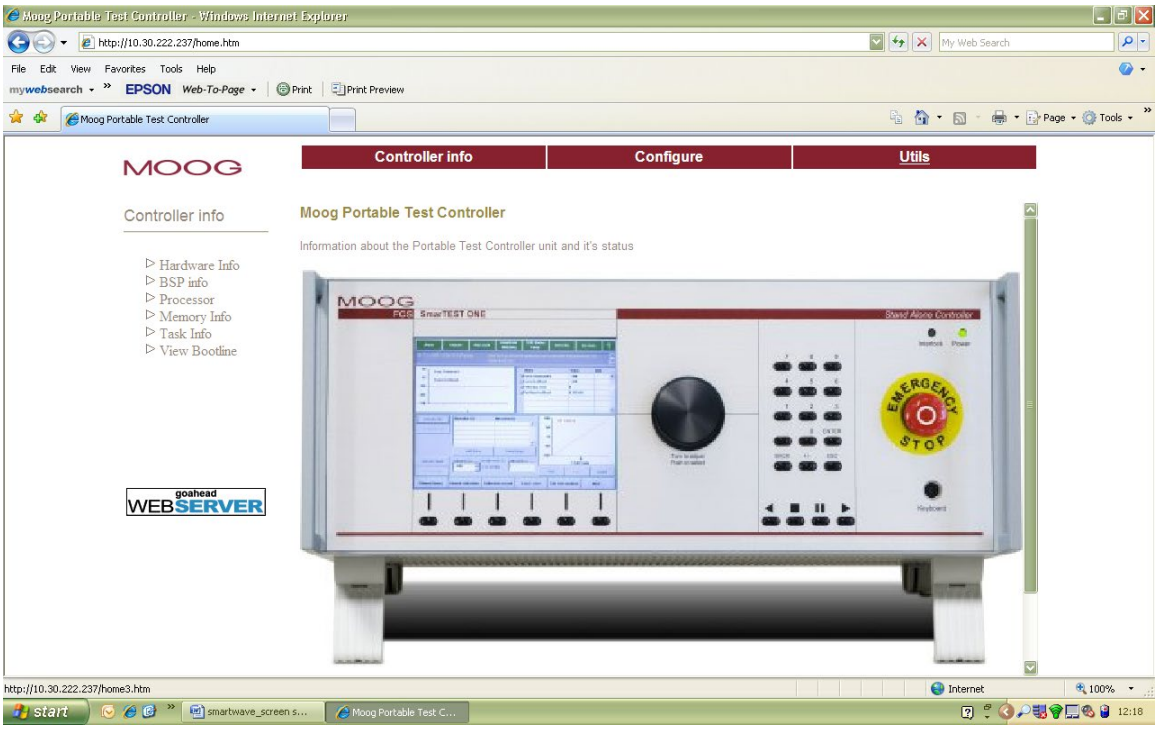


Figure 3.31. Welcome screen of webserver

The specimen temperature is controlled by a heated air system forming part of the confining stress application arrangements as shown in Figures 3.12 and 3.32, and through a thermocouple that was fitted into the wall of the specimen as shown in Figure 3.23.



Figure 3.32. The system used to direct a heated flow of air into the pressure chamber

3.3. Data Analysis of Stress and Strain in HCA

3.3.1. Hollow Cylinder Apparatus Software (HCAS)

To help with the analysis of large data files, development of a filtering software was necessary. NTEC in collaboration with Cooper Research Technology Ltd. developed the HCAS software to take the raw data and analyse on a cycle by cycle basis to give the permanent and resilient strains of the material under test. The data was stored in the CSV Output File chosen by the operator.

For each cycle the software took the following inputs from the recorded data file and calculated the offset and amplitude.

Description	Symbol	Units	Source
Axial Force	W	kN	HCA 1.CH1 Vertical.FCS loop.Force.Feedback
Torque	M_T	kNm	HCA 1.CH2 Torque.FCS Loop.Force.Feedback
Axial LVDT 1	l_1	mm	HCA 1.AI1.Engineering Value
Axial LVDT 2	l_2	mm	HCA 1.AI2.Engineering Value
45° LVDT 1	$l_{45\|1}$	mm	HCA 1.AI3.Engineering Value
45° LVDT 2	$l_{45\|2}$	mm	HCA 1.AI4.Engineering Value
Top Outside Radial LVDT	$l_{o\|T}$	mm	HCA 1.AI5.Engineering Value
Bottom Outside Radial LVDT	$l_{o\|B}$	mm	HCA 1.AI6.Engineering Value
Top Inside Radial LVDT	$l_{i\|T}$	mm	HCA 1.AI7.Engineering Value
Bottom Inside Radial LVDT	$l_{i\|B}$	mm	HCA 1.AI8.Engineering Value
Rotation LVDT	x	mm	HCA 1.CH2 Torque.HardwareConfig.Position. Engineering value
External Pressure	p_o	kPa	N/A – for future use.
Internal Pressure	p_i	kPa	N/A – for future use.

The data was passed through a 20Hz, 2-Pole Butterworth Filter. The peak of the pulse was found by taking the point (positive or negative) which is

furthest from the mean value. The offset was given by taking the average value over 0.3 seconds prior to the pulse and taking the value of the initial offset from this as presented in Figure 3.33. The amplitude was given by subtracting the value at the peak (or trough if negative) of the pulse from the offset.

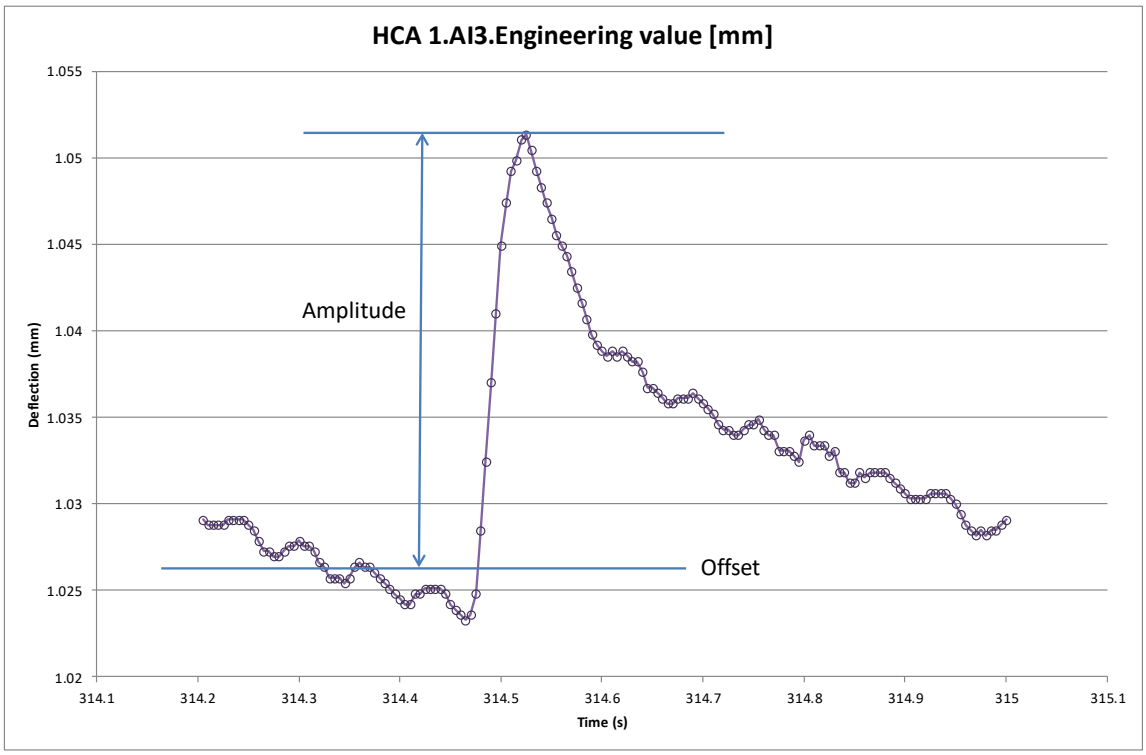


Figure 3.33. Amplitude and offset calculation for one cycle

The resilient and permanent components of strains discussed in the next two sections were calculated for each cycle and sent to the Output File.

3.3.2. Analysis of stress and strain

The stresses existing within an element of the HCA wall have already been shown in Figure 2.33. The axial load (W) generates an axial stress σ_z, while torque (M) contributes to shear stress $\tau_{\theta z}$. Differential values of lateral confining pressures (p_o, p_i) lead to the formation of a radial stress, however when p_o=p_i, then σ_r=σ_θ. In the HCA tests individual stresses and strains vary across the wall and along the height of a specimen due to the effects of wall curvature and end restraint. Therefore, despite careful consideration of specimen dimensions, Hight et al., (1983), Chan and Brown, (1994) and few others suggested assuming that the stresses are uniform and their average values can be defined as follows:

$$\sigma_z = \frac{W}{\pi(r_o^2 - r_i^2)} + \frac{p_o r_o^2 - p_i r_i^2}{r_o^2 - r_i^2} \quad (3.10)$$

$$\sigma_r = \frac{p_o r_o + p_i r_i}{r_o + r_i} \quad (3.11)$$

$$\sigma_\theta = \frac{p_o r_o - p_i r_i}{r_o - r_i} \quad (3.12)$$

$$\tau_{\theta z} = \frac{3M_T}{2\pi(r_o^3 - r_i^3)} \quad (3.13)$$

where W and M_T are the applied axial load and torque;

p_o and p_i are the outer and inner cell pressures;

r_o and r_i outer and inner radius of the specimen;

σ_z, σ_r, σ_θ are average vertical, radial and circumferential stress, respectively;

$\tau_{\theta z}$ is the average shear stress in the θ-z plane.

Similarly, the average strains are defined as follows:

$$\varepsilon_z = \frac{\delta l}{L} \tag{3.14}$$

$$\varepsilon_\theta = \frac{u_o + u_i}{r_o + r_i} \tag{3.15}$$

$$\varepsilon_r = \frac{\delta t}{r_o - r_i} \tag{3.16}$$

$$\gamma = \frac{2\Delta\theta\left(r_o^3 - r_i^3\right)}{3H\left(r_o^2 - r_i^2\right)} \tag{3.17}$$

where δl, u_i, u_o, δt are the changes in height, outer and inner radii and thickness of the specimen wall respectively;

ε_z, ε_θ, ε_r are average vertical, radial and circumferential strains, respectively;

γ is the average shear strain.

3.3.3. Principal stress and strain components

The magnitude and the angle of principal stress rotation can be obtained from the Mohr's circle for stresses as shown in Figure 3.34. This diagram is based on the condition that $\sigma_z > \sigma_\theta$ and $\tau_{\theta z}$ is positive. Since there is no shear stress acting in the radial direction of the hollow cylinder specimen, σ_r and the plane on which it acts must be a principal plane, the θ-z plane.

The principal stresses and the direction of the major principal stress can be defined as follows:

$$\sigma_1 = \frac{\sigma_z+\sigma_\theta}{2} + \sqrt{\left(\frac{\sigma_z-\sigma_\theta}{2}\right)^2 + \tau_{\theta z}^2} \quad (3.18)$$

$$\sigma_2 = \sigma_r \quad (3.19)$$

$$\sigma_3 = \frac{\sigma_z+\sigma_\theta}{2} - \sqrt{\left(\frac{\sigma_z-\sigma_\theta}{2}\right)^2 + \tau_{\theta z}^2} \quad (3.20)$$

$$\alpha_\sigma = \frac{1}{2}\tan^{-1}\left(\frac{2\tau_{z\theta}}{\sigma_z-\sigma_\theta}\right) \quad (3.21)$$

As already mentioned in Section 3.2.1, stress invariants such as the normal and shear stress (p, q) can also be used to describe the stress conditions in a hollow cylinder specimen. They are defined by equations presented in that section (Equations 1.3 and 1.4).

The principal strains in the z-θ plane can be obtained for the Mohr's circle shown in Figure 3.35 and they are defined as follows:

$$\varepsilon_1 = \frac{\varepsilon_z+\varepsilon_\theta}{2} + \frac{1}{2}\sqrt{(\varepsilon_z-\varepsilon_\theta)^2 + \gamma_{z\theta}^2} \quad (3.22)$$

$$\varepsilon_3 = \frac{\varepsilon_z+\varepsilon_\theta}{2} - \frac{1}{2}\sqrt{(\varepsilon_z-\varepsilon_\theta)^2 + \gamma_{z\theta}^2} \quad (3.23)$$

$$\alpha_\varepsilon = \frac{1}{2}\tan^{-1}\left(\frac{\gamma_{z\theta}}{\varepsilon_z-\varepsilon_\theta}\right) \quad (3.24)$$

The strain invariants corresponding to p and τ_{oct} are ε_v (volumetric strain) and ε_s (shear strain) respectively and they are defined as follows:

$$\varepsilon_v = \varepsilon_1 + \varepsilon_2 + \varepsilon_3 = \varepsilon_z + \varepsilon_\theta + \varepsilon_r \quad (3.25)$$

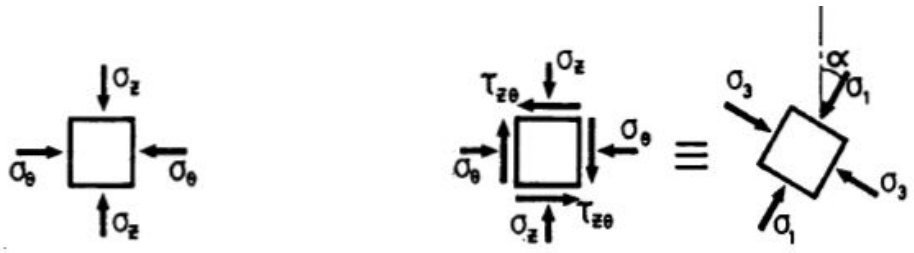
$$\varepsilon_s = \frac{\sqrt{2}}{3}[(\varepsilon_1 - \varepsilon_2)^2 + (\varepsilon_2 - \varepsilon_3)^2 + (\varepsilon_3 - \varepsilon_1)^2]^{1/2} \quad (3.26)$$

Because there is no shear stress acting on the z-r and r-θ planes, it can be assumed that the shear strains ε_{rz} and $\varepsilon_{r\theta}$ are zero. Hence, ε_r becomes the third principal strain and $\varepsilon_r = \varepsilon_2$.

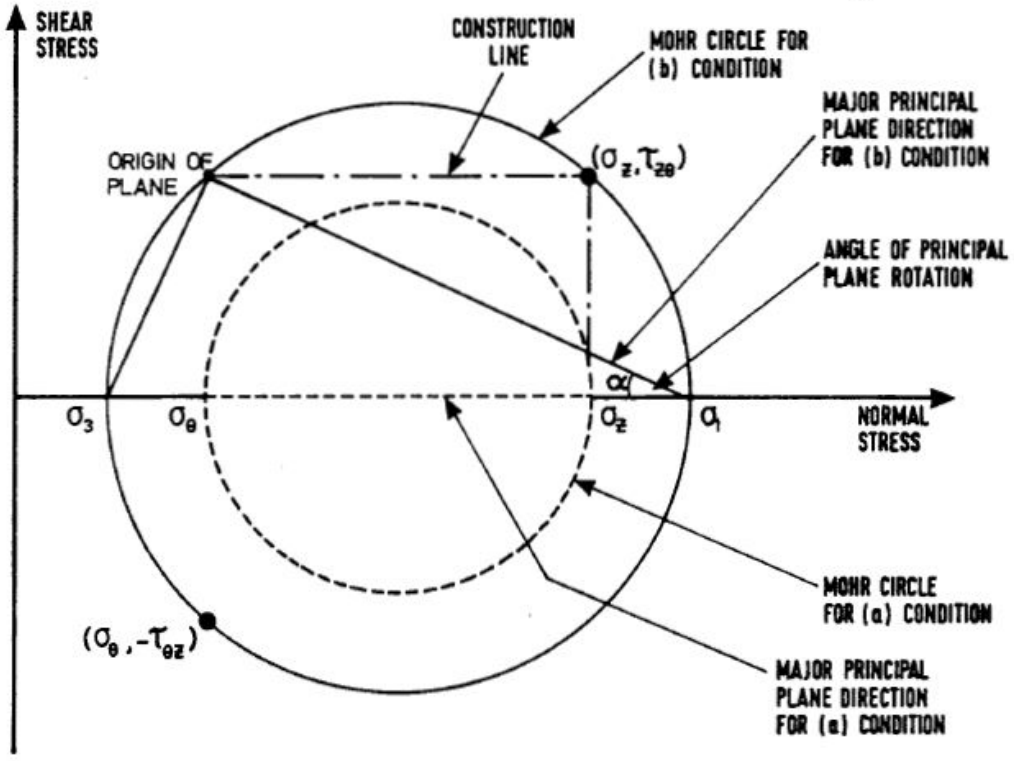
The maximum shear strain in the the z-θ plane is defined as follows:

$$\gamma_{max} = (\varepsilon_1 - \varepsilon_3) \quad (3.27)$$

The strain invariant for q is ε_{max}=0.5γ_{max}

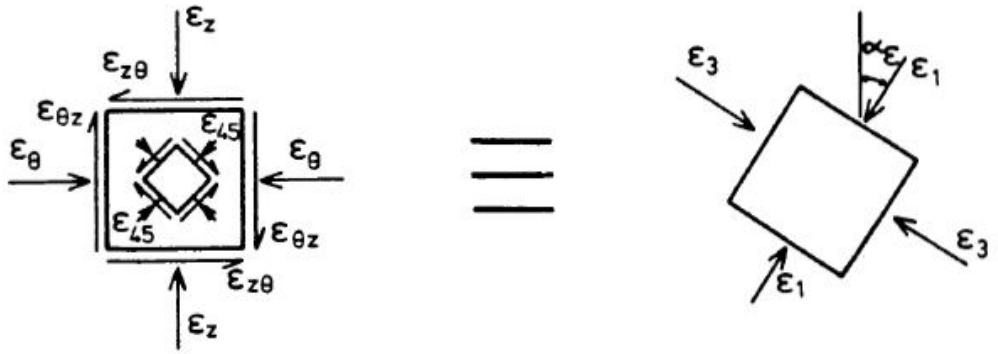


a. Condition with No Shear. b. Condition with Shear.



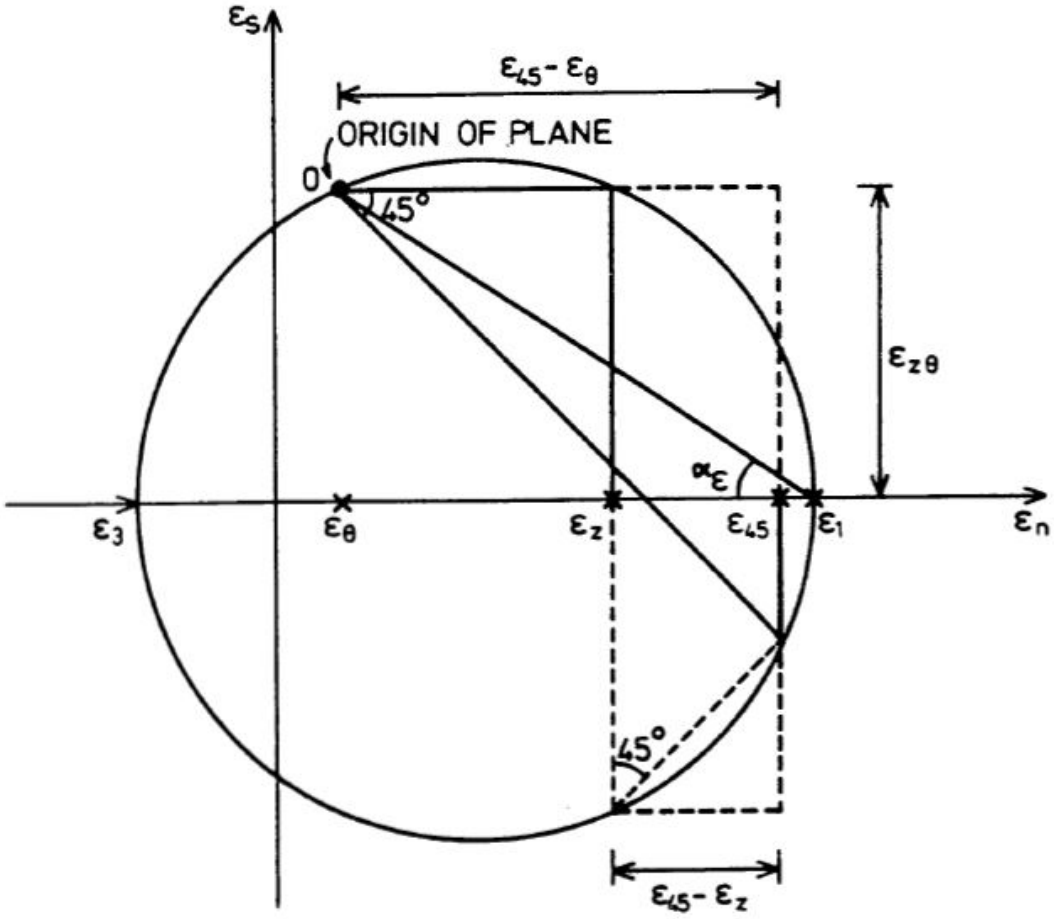
c. Mohr Circle showing Principal Plane Rotation.

Figure 3.34. Principal stresses on the θ-z plane (Chan, 1990)



a. General Strains.

b. Principal Strains and Angle of Rotation.



c. Mohr Circle Construction for Strain.

Figure 3.35. Principal strains on the θ-z plane (Chan, 1990)

4

SPECIMEN PREPARATION AND TESTING SET-UP

4.1. Specimen Preparation

Particularly, when investigating permanent deformation in laboratory tests, it is important and desirable that the method of laying and compaction be as realistic as possible. Compaction plays a major role in the performance of flexible pavements. It has been shown that permanent deformation results are sensitive to differences in method of compaction (Gibb, 1996). It has been also reported by Harvey et al., (2001) and others (Monismith and Tayebali, 1988) that different compaction processes can produce different preferred orientations in aggregate which strongly influence asphalt performance. Therefore, recognition of potential effects of different compaction techniques on properties is essential if a reliable evaluation of mixture performance is to be made. There were several approaches which could be taken, all depending upon equipment availability, number of specimens retrieved, compaction level and coring accuracy.

As discussed in the Literature Review, rolling-wheel compaction has proved to be best suited for preparing laboratory specimens. Among investigated

methods, it appears to simulate insitu compaction quite well (Monismith et al., 1994). During the SHRP an extensive study was conducted of the compaction influences on the permanent deformation response of mixes. Results of the study suggested that some form of rolling wheel compaction was most suitable for laboratory specimen preparation. In addition more recent research (Monismith, 2004) supported the work of the SHRP showing that specimens prepared by rolling wheel compaction are similar in response to field cores.

Therefore, it was considered that taking cores out of a slab compacted by a vibratory roller was the most effective and efficient way of obtaining specimens for this HCA study. The coring procedure involved using two diamond tipped core barrels operated concentrically. During the first year of the project two trials were carried out. Despite care during construction of the first trial sections, thicknesses of the finished slabs were not exactly as specified. Therefore, the first trial indicated that the chosen HCA specimen preparation technique was workable in order to obtain the required quality specimens with regard to dimensions, but several modifications had to be implemented during the second trial in order to achieve the desired thickness of the slab. Overall, the method adopted for sample preparation involved the following four stages:

- Trench Excavation;
- Slab Construction;
- Coring;
- Sawing.

4.1.1. Trench Excavation

In order to provide edge restraint to resist the lateral displacement from imposed loading placed upon the pavement during construction, a 600mm deep trench with dimensions of 2.4 x 6.0m was prepared at Aggregate Industries Hulland Ward site in Derbyshire (Figure 4.3). The width of the trench was designed to accommodate the coring rig, whose dimensions are shown in Figure 4.1.

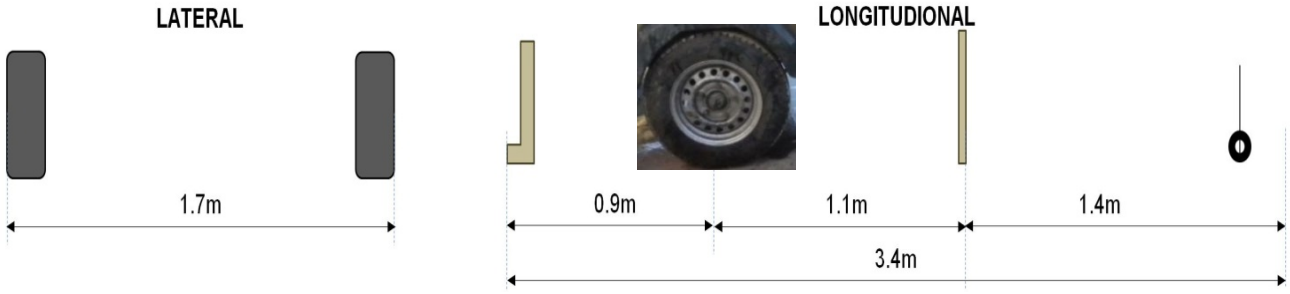


Figure 4.1. Coring rig dimensions: (a) lateral view; (b) longitudinal view

The core layout plan should address space for all of the equipment, enough clearance around the drilling rig to allow for proper equipment layout, and site and equipment access to strategically optimise the slab for safety and productivity. Figure 4.2 presents the core layout plan adopted.

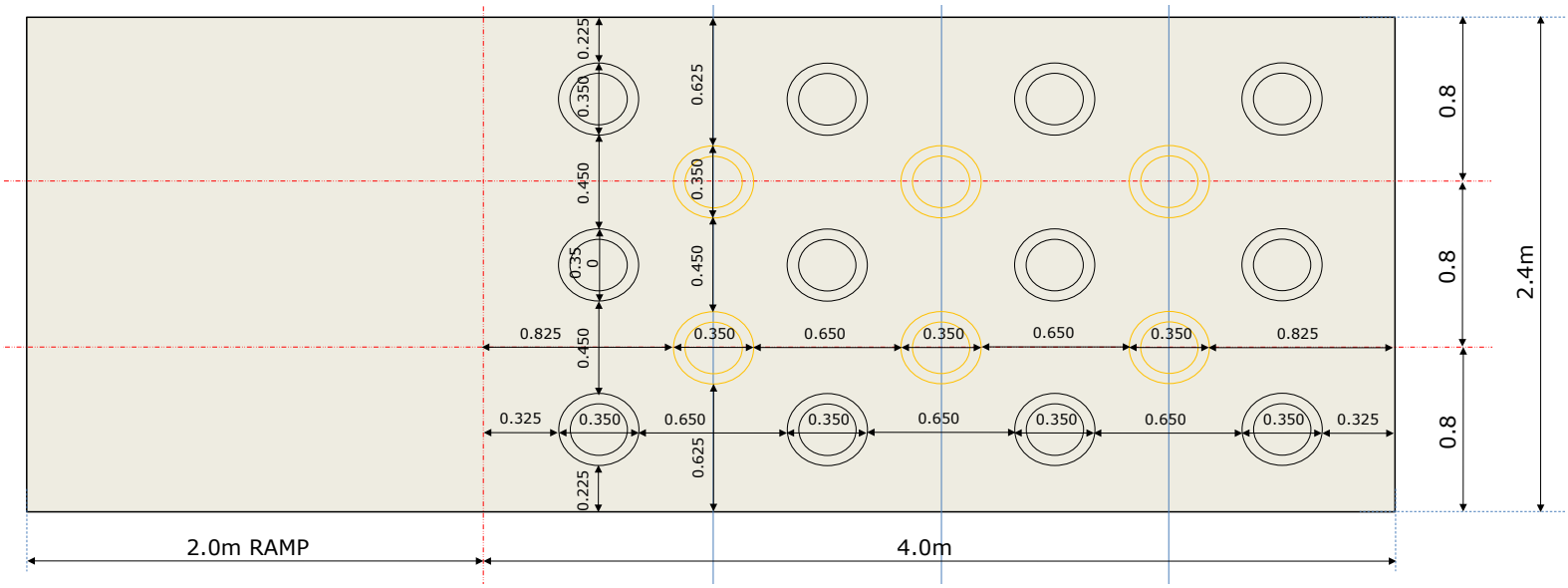


Figure 4.2. Slab dimensions and specimen locations



Figure 4.3. The Aggregate Industries Hulland Ward site – trench excavation

4.1.2. Trial Slab Construction

Before the slab construction could begin, a problem of insufficient surface drainage (Figure 4.4) had to be addressed. The trench was almost entirely filled in with water from recent rain. The subgrade became exceedingly weak and unfit to support the placement and compaction of the asphalt. Thus, in order to bring the level of water down and to provide a stable subgrade, it was necessary to take remedial action. Prior to placing the pavement layers, the water was pumped out and a layer of crushed stone was installed and compacted (Figure 4.5).



Figure 4.4. Prepared trench after rain



Figure 4.5. Installing a layer of crushed stone

As shown in Figure 4.5, in order to achieve adequate layer thickness, reference rods with a levelling string that corresponded to the specified thickness, were installed alongside the trench. The thickness was also marked with paint on the side of the trench.

For the purpose of this research, only a standard continuously graded *AC 10 close surf 100/150* was used. It was supplied by Aggregate Industries and manufactured with a 10mm maximum aggregate size and 5.2% of grade 100/150 bitumen. A specification for this product is presented in Figure 5.15.

Twenty tons of the material was transported from Derby Quarry, which was 22.5km away, by trucks and distributed to the trench by a loader.

In order to achieve a level foundation a 100mm thick *AC 10 close surf 100/150* regulating layer was provided. It was placed on top of a layer of crushed rock, compacted with a double drum roller and covered with a thin layer of sand (Figures 4.6 and 4.7). The layer of sand was provided to stop interlayer bonding between the main test slab and the sub-base.

The actual slab was placed in four, 100mm thick lifts. Mixture rutting is strongly related to volumetric properties, air voids content in particular, therefore the double drum vibratory roller was used to achieve satisfactory compaction. The temperature of the mix just prior to commencing compaction was approximately 153°C. The minimum required specimen length is 400mm and for that reason it was very important to make sure that all layers were installed correctly. Tack coat was applied on half of the slab, as shown in Figure 4.8, in order to compare interlayer bonding of a tack coated surface with an uncoated surface.



Figure 4.6. Installing AC 10 close surf 100/150 regulating layer



Figure 4.7. Sand capping



Figure 4.8. Tack coat

4.1.3. Coring

The coring was performed using a portable rig (Figure 4.9). The constructed slab gave sufficient area for 18 specimens to be cut (Figure 4.2 and 4.11) using two specially fabricated barrels shown in Figure 4.10. In order to achieve hollow specimens with dimensions as per Section 3.2.4, the central part of the cylinder was drilled first followed by the external part, as shown in Figure 4.11. This procedure produced quite accurately dimensioned specimens. The average achieved wall thickness was 50mm measured top and bottom (+/- 1mm). The whole coring process requires about 20-25minutes per specimen. The specimens were transferred carefully to the

laboratory in a refrigerated van during warm weather, to avoid any distortion, and stored in a temperature controlled room at 5ºC.



Figure 4.9. The drilling rig



Figure 4.10. Coring barrels



Figure 4.11. Cutting of test specimens from slab

4.1.4. Sawing

After coring, the standard hollow cylinder specimens were approximately 400mm long. The end planes of the specimen required trimming to the desired testing length of 350mm. Manual handling and trimming of the heavy hollow asphalt specimens in warm conditions (after removal from the cold store), had to be controlled to keep the specimen in its original shape. As well as developing setting-up procedures, this led to the design and manufacture of a rotating jig illustrated in Figures 4.13 - 4.16. Appendix A includes manufacturer details.

The heavy specimen (approximately 42kg) had to be removed from a cold room and transported to the sawing room. Inner and outer thin walled split steel tubes were made as part of the jig to maintain the specimen shape during transportation and trimming. Figure 4.13 shows a specimen with inner and outer steel tubes installed prior to sawing.

It then had to be fitted into the jig (already on the saw) and clamped, so that an initial cut could be taken of about 20mm from one end (Figure 4.14). As shown in Figure 4.15, rotation of the specimen while trimming ensured that the cut surfaces were smooth and at right angles to the vertical axis. The jig was then pushed towards the sawn end and the second cut made (Figure 4.16).

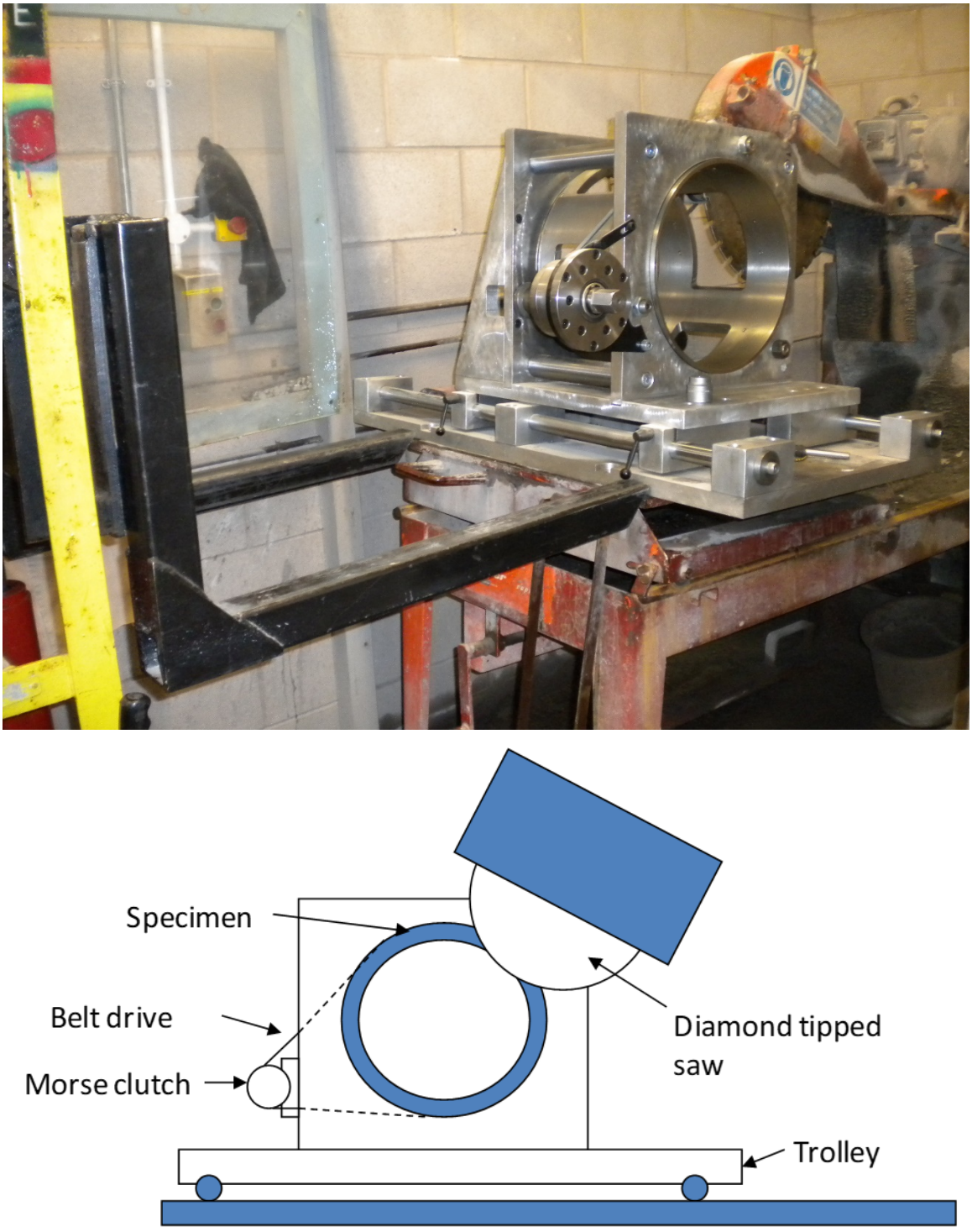
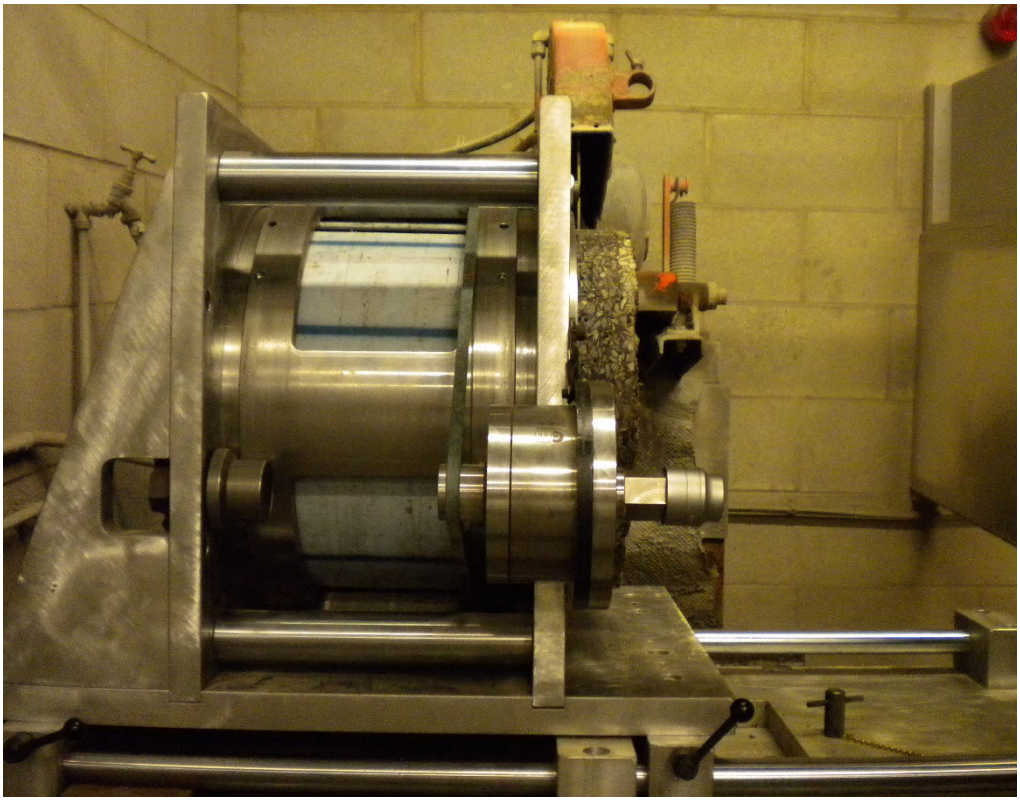


Figure 4.12. Hand rotated trimming jig for HCA specimens



Figure 4.13. HC specimen with inner and outer steel tube



4.14. HC specimen clamped and aligned with a diamond saw blade

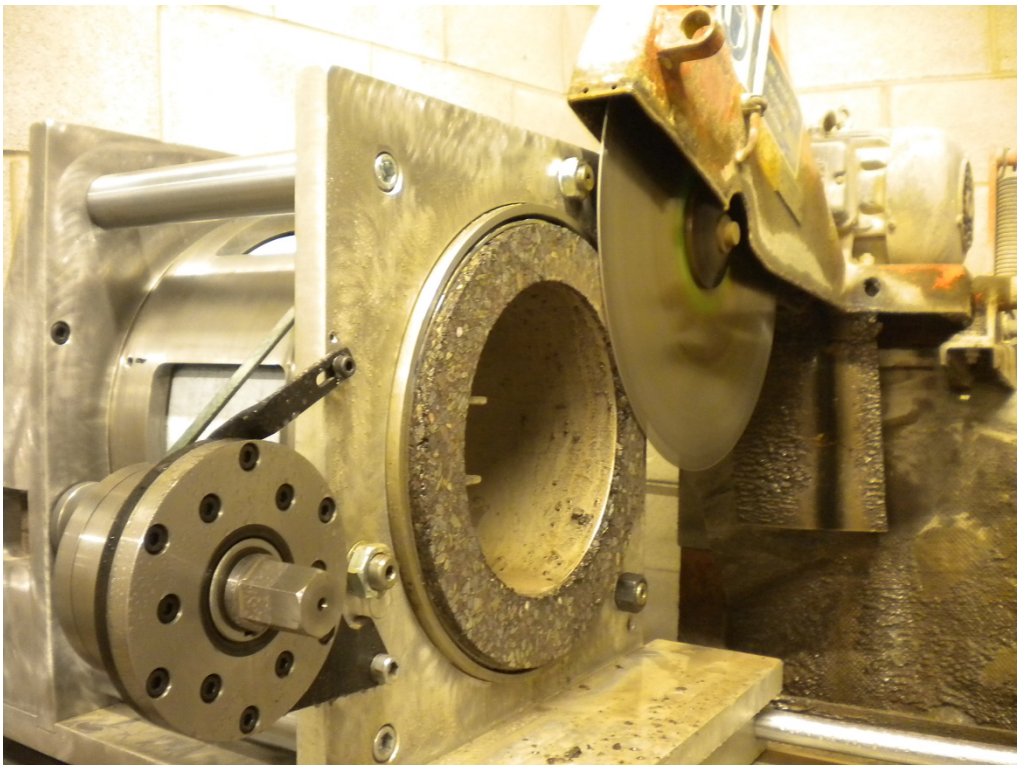


Figure 4.15. Specimen after first saw cut

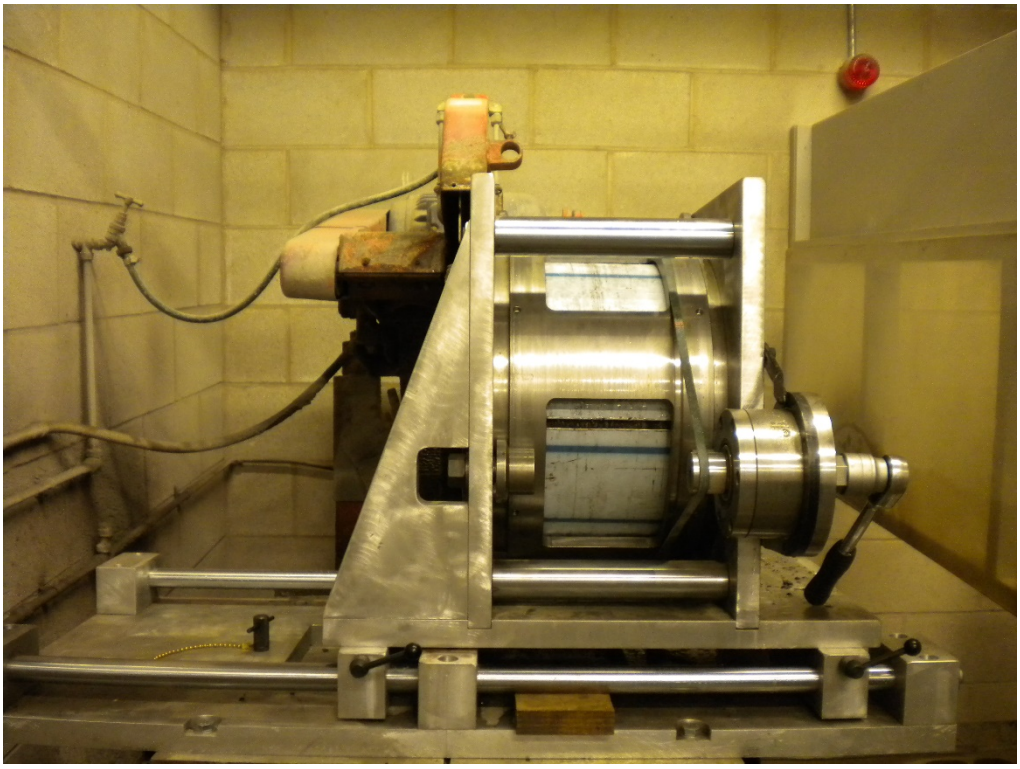


Figure 4.16. Jig set up for second cut

This sawing technique created highly accurate cuts. However, the main difficulties were sliding the jig onto and off the sawing machine using a heavy duty stacker and sliding the specimen into the jig by hand. This procedure was needed to be carried out by two people and required use of lifting facilities.

4.2. Test Set-Up

4.2.1. Determination of Air Void Content

Recognition that the resistance to permanent deformation is strongly dependent upon density of an asphalt mixture and that adequate volumetric composition is essential if desired mechanical properties of an asphalt mixture are to be obtained is discussed in the literature review. Therefore, the air void content of insitu produced specimens was measured in order to monitor volumetric properties.

Due to the shape and large size of the hollow cylindrical specimens, determination of their true air void content was really difficult. Hence, in order to estimate the air void content, additional test specimens 150mm in diameter by 50mm in height were manufactured by coring and trimming 250mm solid cylinders that formed the central part of the HCA specimens. This allowed production of 7 cylindrical specimens per HCA sample. The dimensions were selected to ensure that some of the specimens could be utilised for the SST tests as described in Section 6.2.2 or axial load tests

(Section 6.3.2) in order that these could be conducted on the same material as was used for the HCA experiments. Therefore, some of the specimens were tested in NTEC in accordance with BS EN 12697-6:2012 (BSI, 2012) and BS EN 12697-8:2018 (BSI, 2018). However, the specimens used for the SST tests were shipped to the Pavement Research Centre at University of California, Berkeley, where the air void contents were determined in accordance with the ASTM D1188 parafilm method (ASTM, 2007). The average air void content of these solid cylinders was used to estimate the air void content of the HCA specimens.

The profile of air void contents through each specimen was determined and the values achieved are presented in Section 5.5 of this thesis. It can be seen clearly that air void content varies throughout the slab and this is assumed to reflect the laying procedure on site and inadequate compaction control. However, the overall conclusion from this exercise was that the void content of that volume of each specimen that has most influence on the deformation data was between about 5 and 12%. While this is not ideal, it was considered adequate for initial experiments to proceed.

Due to the extended time devoted to developing and commissioning of the device, only a limited number of HCA tests were performed. Consequently, such variation in the air void content between HC specimens was considered adequate for this project. However, for repeatability of the tests and accuracy of the results, it is important that prepared specimens are uniform

and identical. It is suggested that, in order to overcome the problem in future research, the asphalt laying and compaction method will require improvement. Better quality control on site needs to be adopted.

4.2.2. Glueing

An important aspect of sample preparation is fixing the specimen to the apparatus in a manner that will help minimise the stress concentration effects at and near the glued ends. At the same time, the bond at the interface needs to be strong enough to resist the applied axial load but still not slip during twisting at the top when a torsional stress is applied.

The strength of the glue was checked in advance to ensure that adequate bonding at the interfaces can be achieved. Two tests were performed: an adhesion test on the glue by using two jacks to twist the top of the specimen against a frame and a direct shear test in which the lower end of the specimen was supported and the aluminium base was pushed at right angles to the specimen. Although, it was not possible to determine the strength of the glue because the hollow cylinder specimen broke before the glue interface did (Figure 4.17), Araldite 2011 proved to be strong enough to be used in the future HCA testing.



Figure 4.17. Failed hollow cylinder (an adhesion test on the glue)

Prior to glueing the cores were removed from the controlled temperature room, trimmed and the specimen dimensions (H, D_i, D_o and t) were measured at eight different positions (four at the top and four at the bottom). The values were recorded and average values were used for further stress and strain analysis.

An arrangement for fitting a HCA specimen in alignment with the vertical and torque actuators of the apparatus is depicted in Figure 4.18. The weight of the specimens (42kg) dictated that lifting equipment in the form of a fork lift trolley was needed to manipulate them up to the base of the HCA.

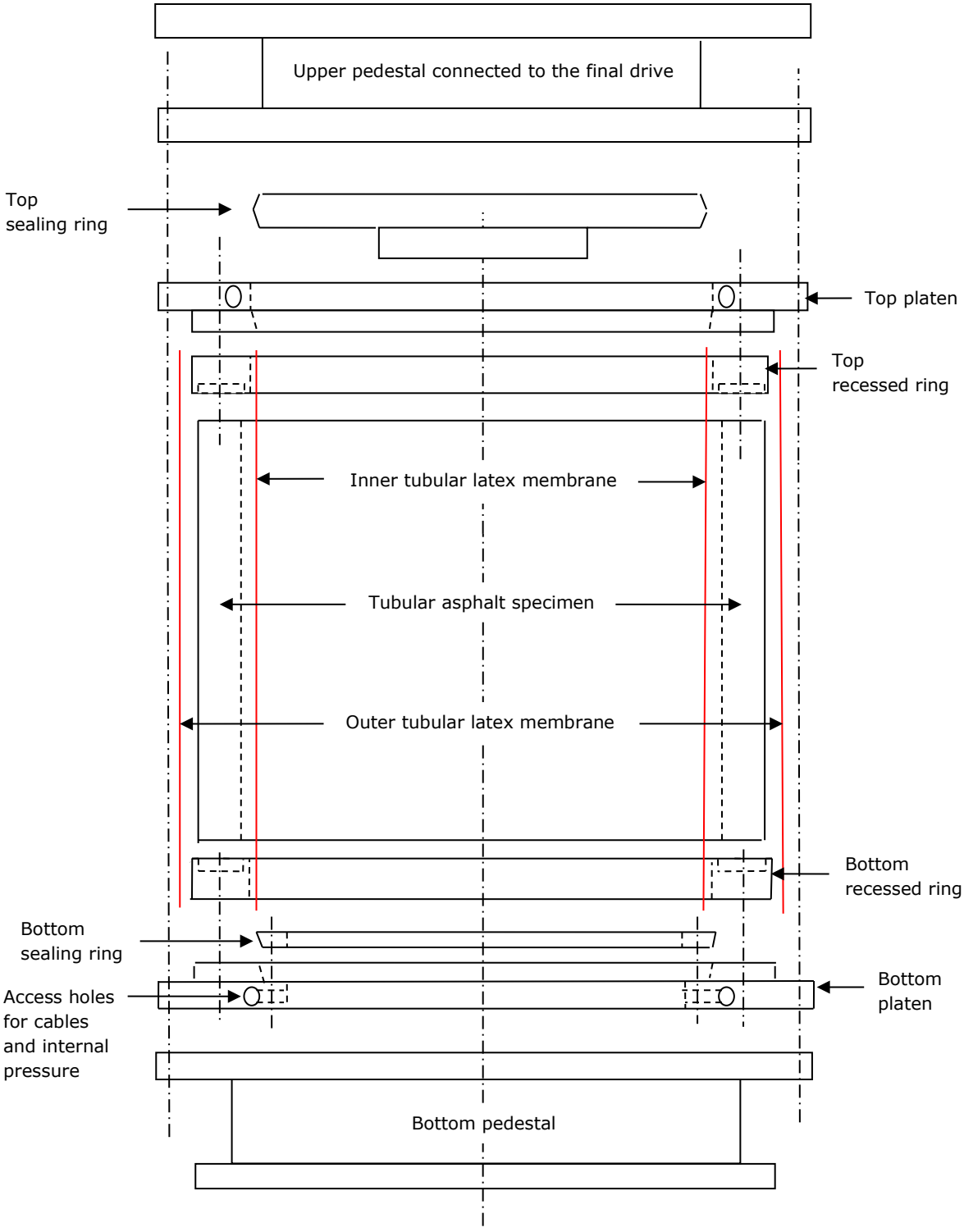


Figure 4.18. The HCA specimen fitting arrangement

Figure 4.19 presents the glueing procedure. The bottom recessed ring was screwed to the bottom platen, which was bolted to the bottom pedestal. Epoxy adhesive was applied to the recess in the bottom ring (a) and the asphalt specimen was lowered into it (b). Consecutively, the top of the specimen was covered with adhesive and the top recessed ring was placed on the adhesive (c). The top platen was screwed to the top ring and the assembly was placed in the HCA as the glue cured to ensure the correct alignment (d). The HCA specimen was left to cure for 24 hours before testing.

The reason for the recessed rings was to have several different sets so that any slight variation in the specimen inner and outer diameters could be accommodated and the end platens could be removed when the tested specimen was placed in an oven to release the recessed rings. Also continual heating and cleaning of the rings will cause them to deteriorate and they can be more readily replaced.

In order to apply confining stress in future testing, provision was made for the fitting of inner and outer rubber membranes as shown in Figure 4.20. The inner membrane is fitted and sealed at the top with a tapered solid disc and at the bottom with a tapered ring. The outer membrane is pulled over the sample and sealed at the top and bottom with ‘O’ rings. Small holes are cut over the instrumentation location studs to allow proper contact with the instrumentation carriers and the membrane is glued to the stud to effect a

seal. It can be seen (Figure 4.18) that holes in the bottom platen can be used to apply an internal confining pressure to the specimen.

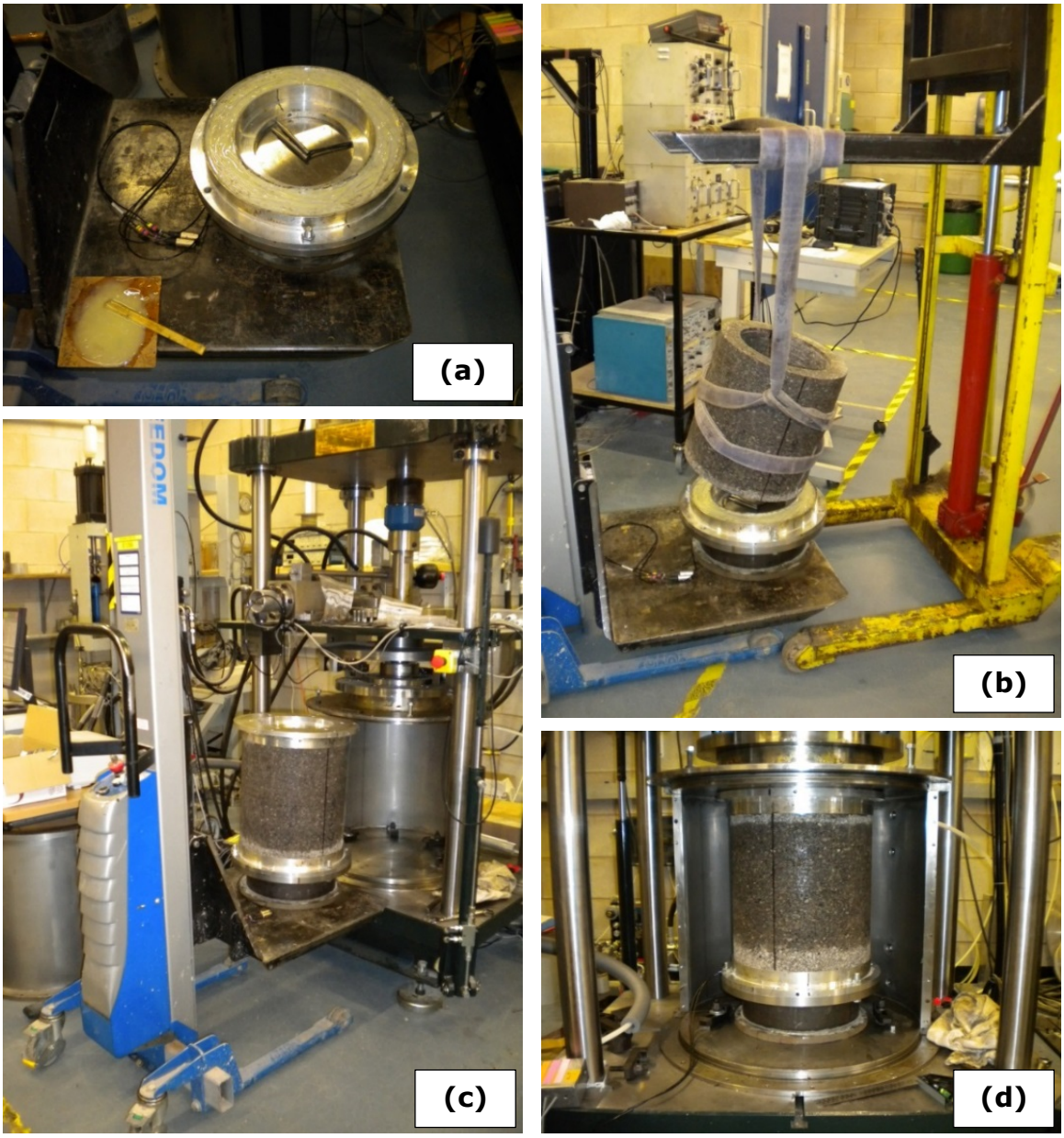


Figure 4.19. HC specimen glueing




Figure 4.20. Inner and outer membranes

4.2.3. Conditioning

Once the glue had set, the specimen was removed and fitted with the on-specimen instrumentation arrangement as shown in the schematic of Figure 3.18 and also Figures 3.20 to 3.22. The assembly was subsequently ready to be transferred back into the apparatus.

The specimen was positioned within a pressure chamber as shown in Figure 4.21. The end platens were then bolted to a pedestal below the specimen and to an extension fitted to the final drive disc. This extension passes through the top cover of the pressure chamber and is of sufficient height to accommodate the vertical deformation of the specimen during testing. Clamps were used to fix the pedestal to the bottom of the chamber and also the chamber to the frame base. This method of fixing facilitated the

alignment of the top platen bolt holes with the final drive extension threaded holes and allowed centralisation of the chamber about the extension. It was possible to apply a high clamping force to resist the torque loading and any vertical tensile forces with these types of clamps which are shown in Figure 4.22. The pressure chamber was then placed around the specimen and the cylinder was bolted together through vertical flanges either side of the split and bolted to the base through circular flanges welded around the bottom of each half of the cylinder. Finally, as shown in Figure 4.23 insulation was fitted around the chamber to reduce heat loss.

A combined air filter and heater connects to the chamber so that heated air passed through the chamber to control the specimen temperature. For unconfined testing a very low pressure was used and exhausted from the chamber with the exhaust valve fully open. The specimen was conditioned for a few hours in order to reach the desired temperature.

The LVDT outputs were monitored throughout the conditioning period and recorded at the test start. During the test specimen deformation was measured and recorded continuously.

A flow chart illustrating the basic principal of the entire process from specimen preparation, through specimen set-up and conditioning period is shown in Figure 4.24. For full testing protocol refer to Appendix B.

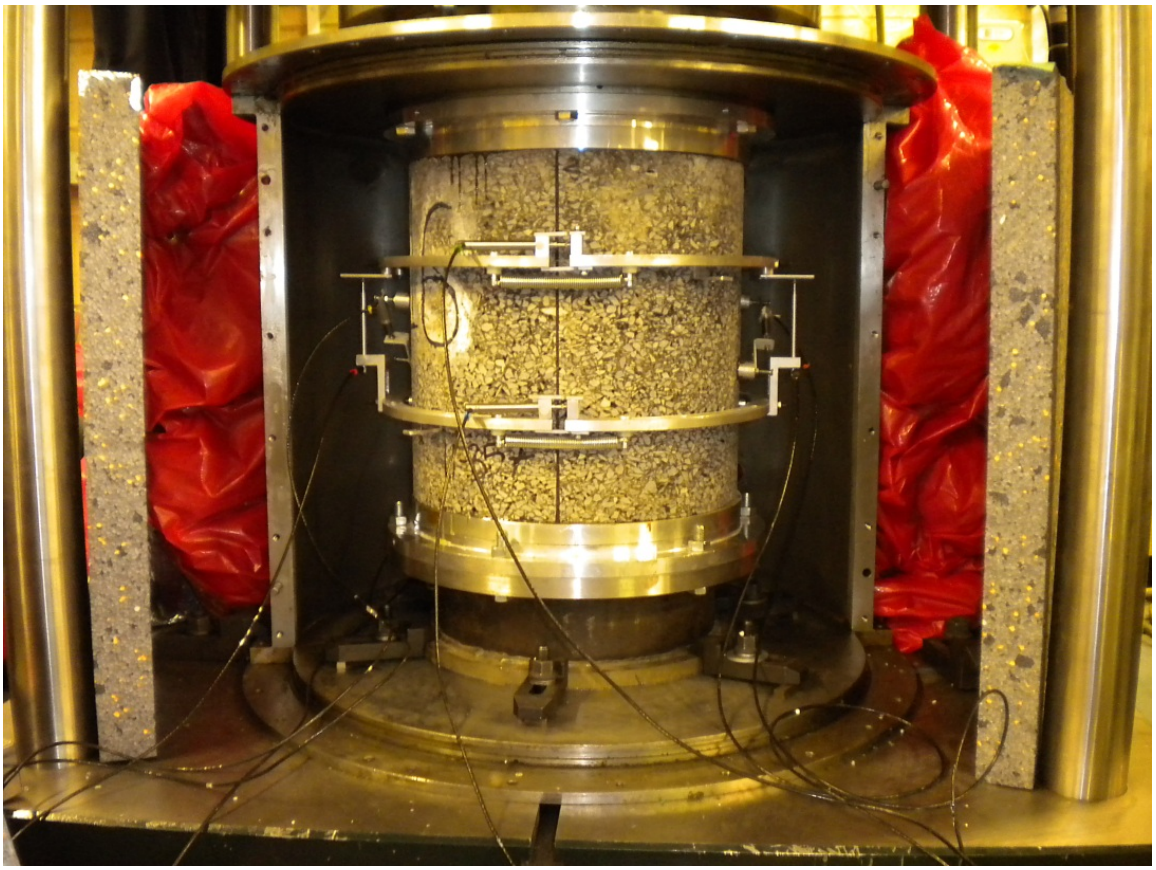


Figure 4.21. HC specimen ready to be tested

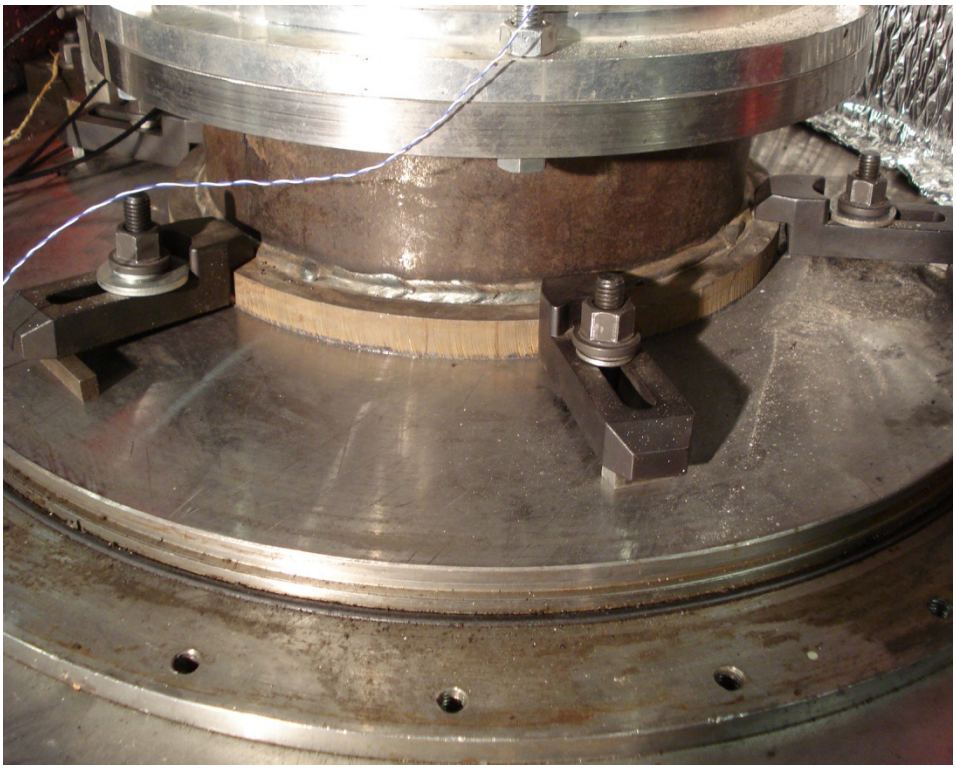


Figure 4.22. Clamps holding the pedestal to the bottom of the pressure chamber

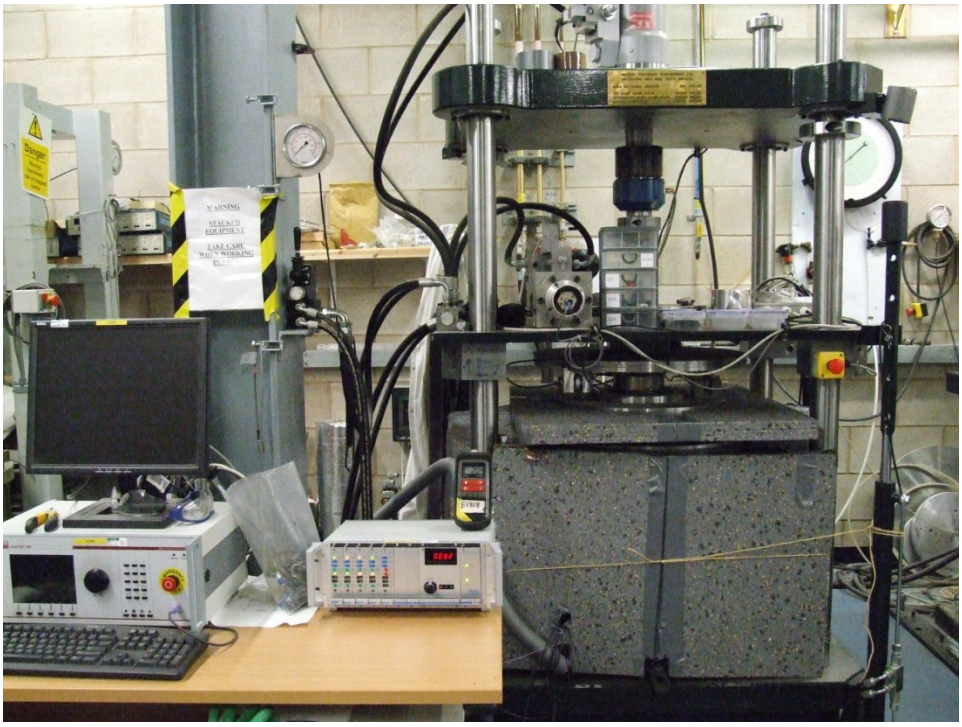


Figure 4.23. Insulation installed around the chamber

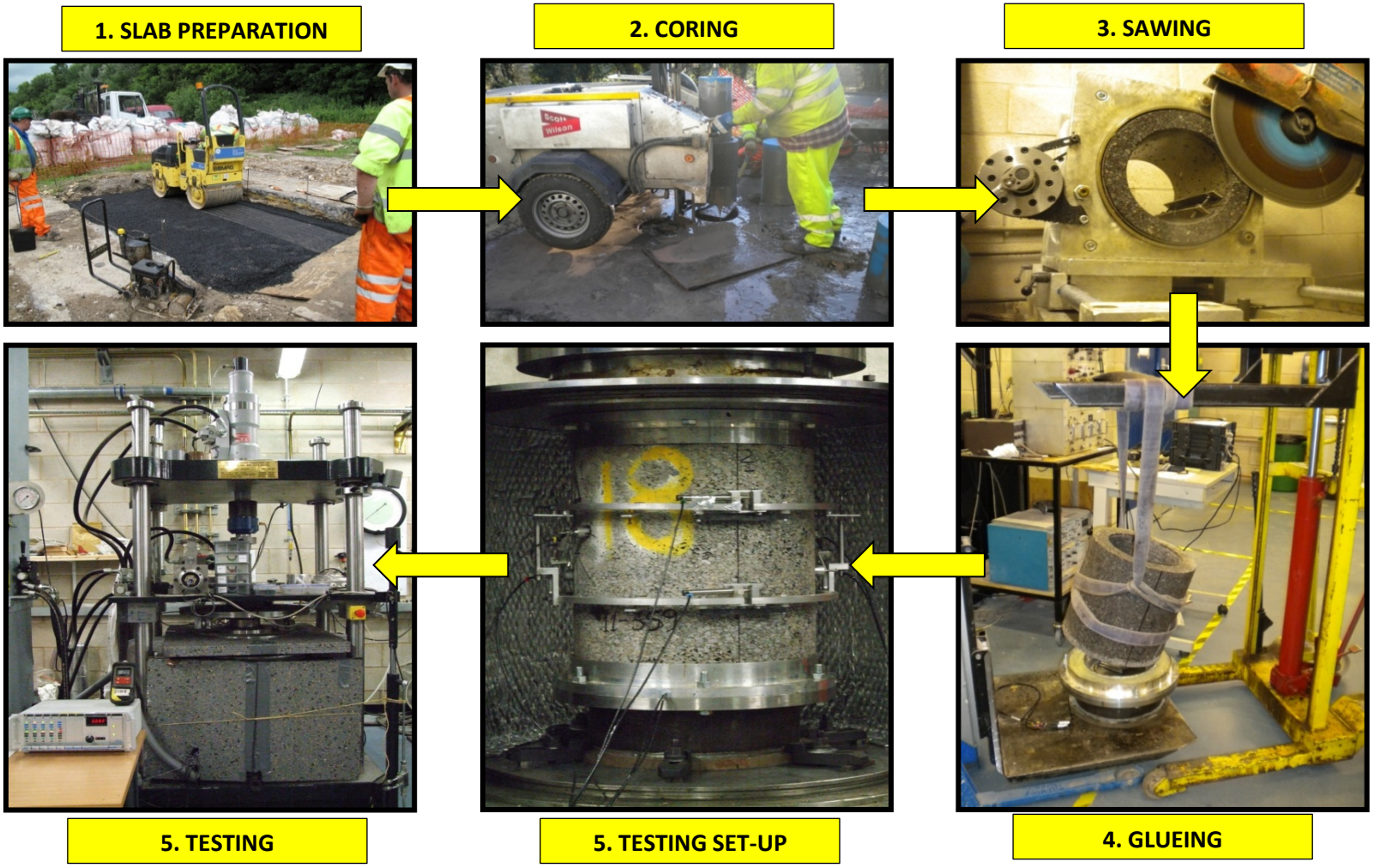


Figure 4.24. Specimen preparation and set-up flow chart

5

TEST PROGRAMME FOR THE HCA TESTS

5.1. Aim of the Investigation

The principal aim of this research was to design, build and commission the new HCA that will allow the generation of high quality experimental data to assist with theoretical modelling of asphalt for pavement performance prediction. A large, innovative torsional HCA has been built and its design and development was described in Chapter 4. This chapter is broadly divided into two main sections. In the first section, the HCA commissioning for the testing of asphalt, in order to apply the complex shear and normal stress paths experienced in a pavement under a moving wheel load is reported. The equipment assessment, conclusions and recommendations that arose from these preliminary tests are also presented. In the latter section, the HCA main testing programme and the findings from this investigation are detailed.

5.2. Commissioning Tests

5.1.1. Introduction

The commissioning of the new HCA progressed over six months. The main objective was to verify that the new HCA was operating properly. This work consisted of careful assessment of all the functions to ensure that when test data is obtained it is as accurate as possible. Testing started with a dummy specimen before progressing to work with asphalt and four such tests are reported in this section. In each case, lessons were learned, and modifications made to the measurement or control systems. Some improvements were also made to the specimen preparation method.

5.1.2. Specimens

In order to ensure that all the systems function correctly, the commissioning work was carried out. Testing started with a polymeric dummy specimen, shown in Figure 5.1, before progressing to work with asphalt. The HCA dummy specimen was manufactured of a polyurethane because this material possesses certain unique properties, such as a high load bearing capacity in both compression and shear. Compression in this case, means that the elastomer will not change in volume under pressure, but may undergo a change of shape under load. However, it will return to its original shape once the load is removed. In addition, the polymer material with a stiffness of 1500MPa was selected to represent well asphalt specimen stiffness.

5.1.3. Test Details

Four hollow cylindrical specimens were used for initial tests aimed at establishing the correct test regime. This included setting up the command signal to the same specification as used in Berkeley for the SST experiments; 0.1s haversine waves with 0.6s rest periods between each. This is illustrated in Figure 5.2.

Table 5.1 identifies the four test specimens that were used for commissioning of the equipment towards the acquisition of reliable test data. At each stage, one or more problems arose and appropriate steps were taken to solve these.

Specimen 5 failed at the interface between the first and second layer (Figure 5.3) but the remaining specimens predominantly failed in tension along 45° planes (Figures 5.4 to 5.6).

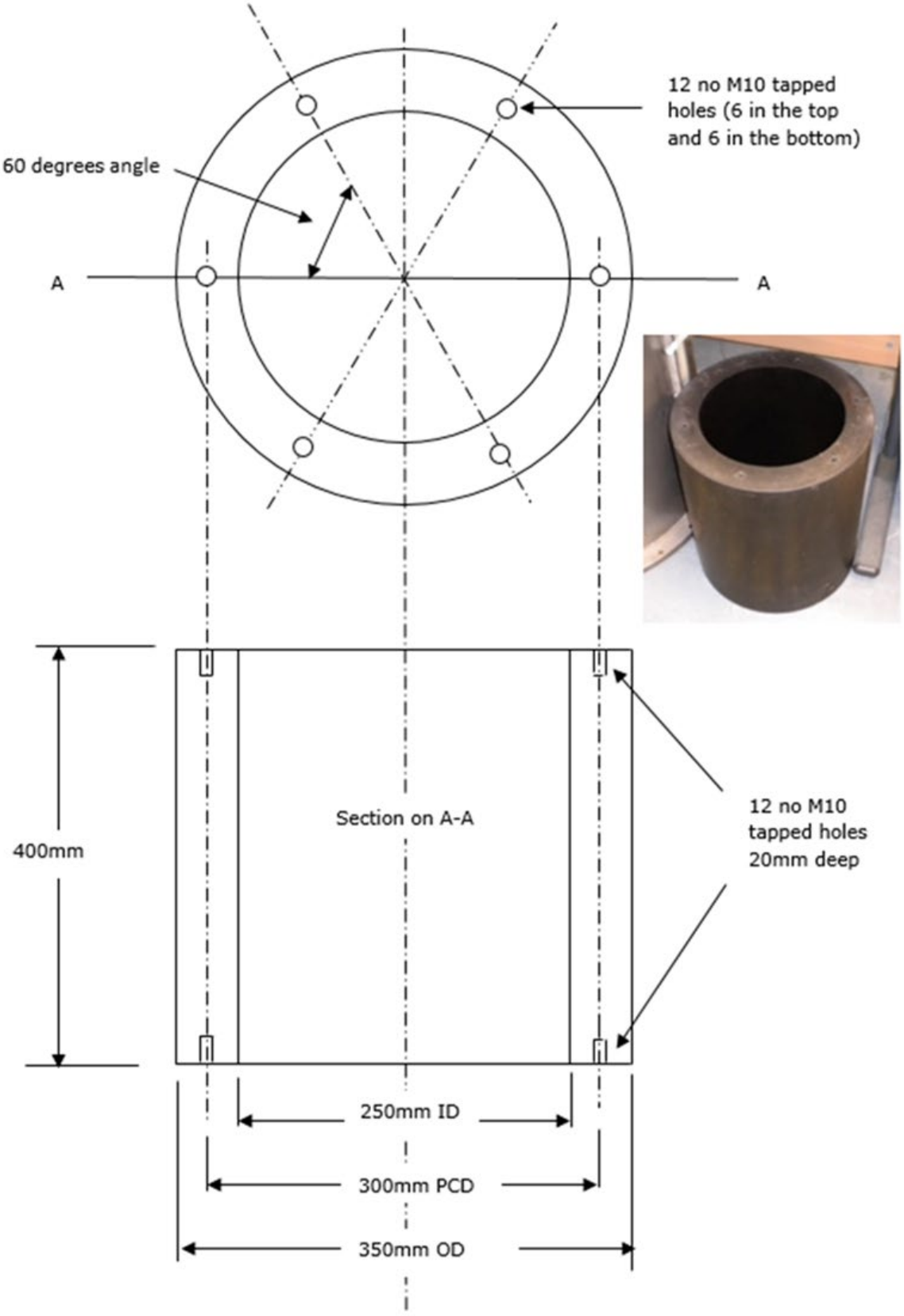
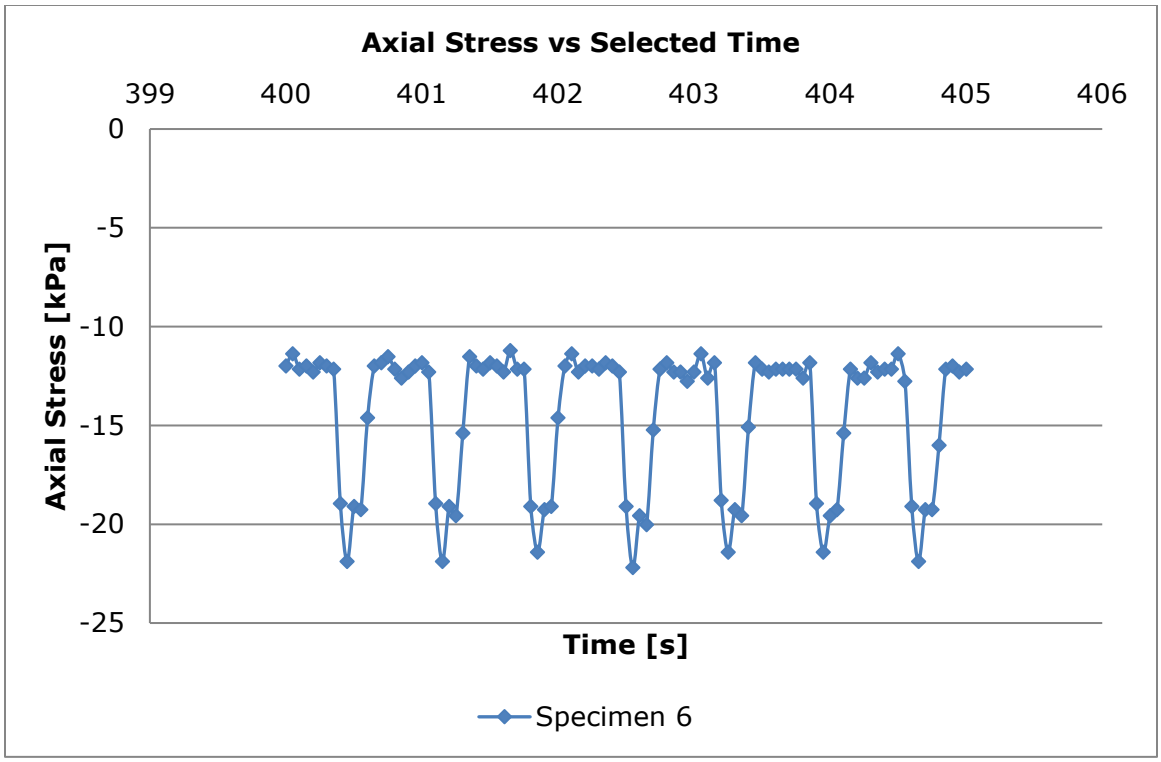


Figure 5.1. Polyurethane cylindrical test specimen

Table 2.1. Test conditions for initial experiments

HC No	Shear stress (kPa)	Normal stress (kPa)	Stress Ratio (target)	Temp (°C) (target)	Cycles No	Failure mode	Comments
5	130	32	2.8 (4.1)	31 (30)	90	Failure at layers interface (Figure 5.3)	Failure could be related to excessive tack coat or >24hr at elevated temp.
6	130	32	4.5 (4.1)	31 (45)	1300	Predominantly shear failure (Figure 5.4)	Further modification of collar supports required. Max. temp achieved was 31ºC.
7	70	28	2.5 (1.4)	37 (55)	8067	None (Figure 5.5)	Strain collars had to be modified. Unable to reach 55ºC.
8	130	32	2.4 (4.1)	30 (30)	212	Specimen became barrel shaped with significant shear failure (Figure 5.6)	The specimen was far too barrel-shaped to perform a reliable measurement. Stresses level and stress ratio to be reconsidered.



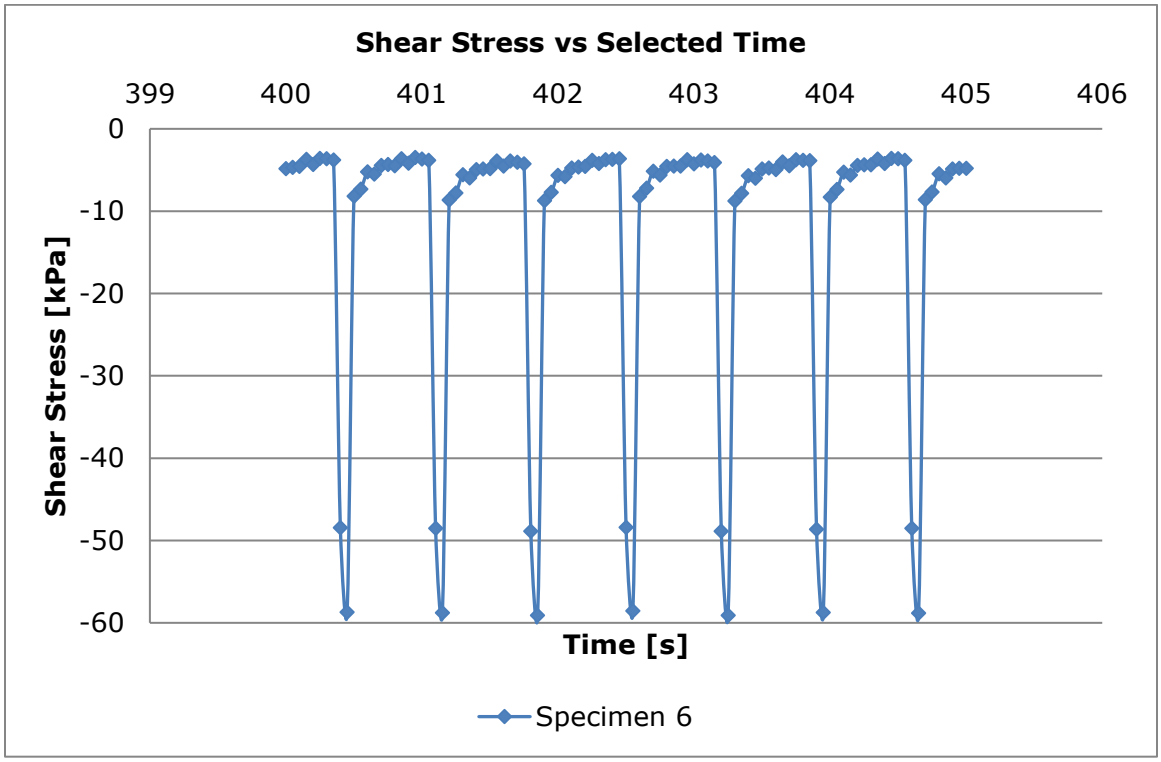


Figure 5.2. Typical applied stress regime



Figure 5.3. Failure of specimen no. 5 through the top interface



Figure 5.4. Specimen no. 6 at the end of the test



Figure 5.5. Specimen no. 7 at the end of the test



Figure 5.6. Specimen no. 8 at the end of the test

5.1.4. Equipment Assessment

Instrumentation

The testing programme was the first opportunity to assess the reliability of the readings from the on-specimen instrumentation. As shown in Figure 3.17, two annular hinged collars were used to support the vertical LVDTs, which were positioned on opposite sides of the specimen. The initial top strain collar is shown in Figure 5.7. The hinge was a flanged cylinder, which was sitting in semi-circular cut-outs machined in each end of the two halves of the collar. The cylinder was held in place by a tension spring which pulled the two halves of the collar together and it was noted that when the collar was fitted to the specimen, the cylinder was difficult to turn. This restrained the opening of the collar as the specimen diameter increased at the start of the test. Also, the springs which held the collar halves together were set below the centre line of the collars and these put a bending moment into the hinged end and open end of each collar, which created friction in the guides. This situation was overcome by joining the collar halves together at the hinged end using a pin arrangement (Figure 3.18), which eliminated the need for the spring.

Figure 5.5 shows the way the vertical LVDTs were clamped to the bottom collar. They relied on the two strain collars remaining level and parallel and improvements were made to this arrangement as the specimen behaviour became clearer during testing. Figure 5.8 shows, on the left, collar supports

glued to the specimen and an extended plate above the vertical LVDT which allowed the LVDT to remain in contact with the upper collar as it moved horizontally relative to the bottom collar during shearing. The supports consisted of a bracket and a screw which enabled the collars to be levelled prior to testing. This arrangement appeared to work satisfactorily. Slight tilting may not be a problem as the errors would be cancelled out by averaging the two LVDTs, as one LVDT output would increase and the other would decrease by the same amount during rotation. Guide plates were fitted above and below the radial LVDTs and the guides kept the open end of the collar in horizontal alignment as shown in Figure 5.9.

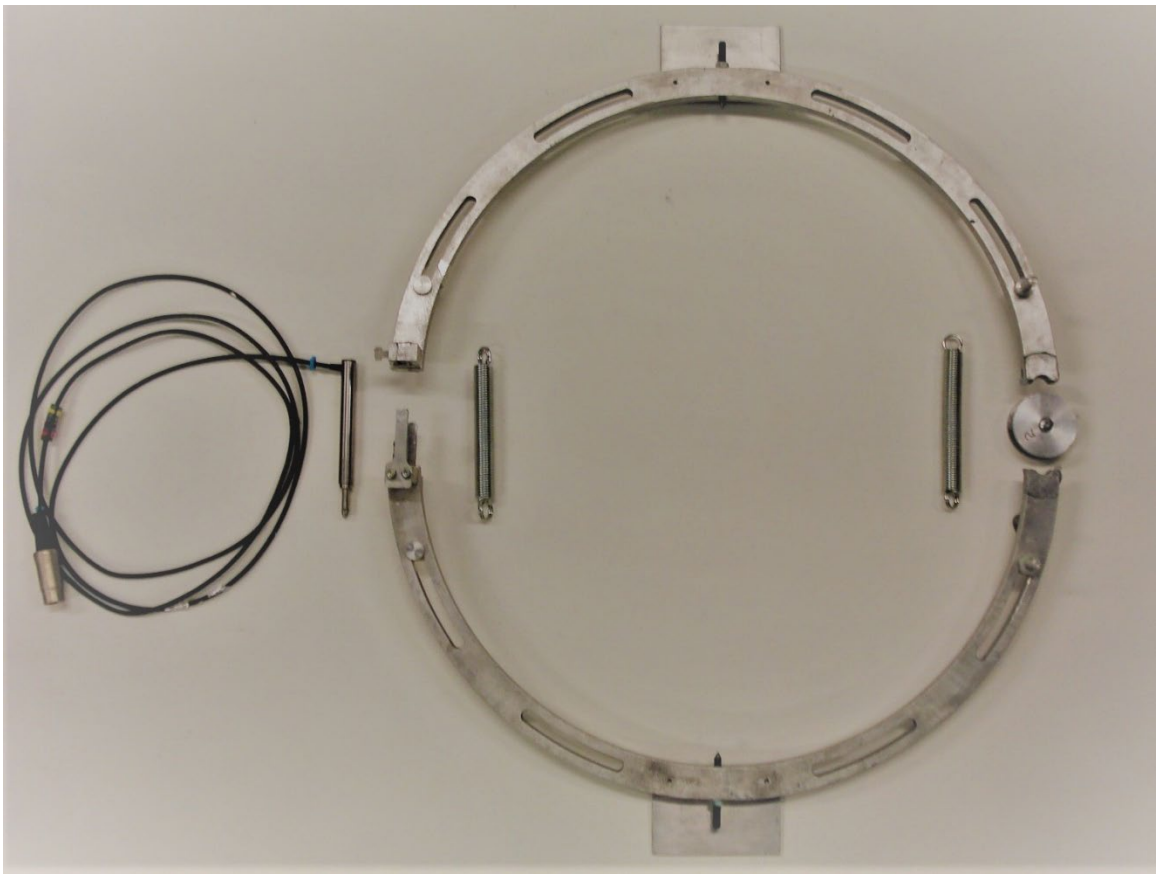


Figure 5.7. Initial top strain collar components



Figure 5.8. Support brackets under the strain collars and the extended plate above the vertical LVDT



Figure 5.9. Guide plates to keep the open end of the collars aligned

Temperature

A major difficulty was encountered in raising the temperature of the specimen to either the 45°C or 55°C values used for the SST test programme at Berkeley. The heated flow of air, which was directed into the pressure chamber, proved unable to raise the temperature much above 30°C to meet the criteria originally specified as described in Section 3.2.2, without extensive insulation because of thermal losses caused by the large mass of metal. The test specimens, although held in position in the HCA, had been at a temperature above 30°C for longer than 20 hours during attempts to achieve at least 45°C. Hence, after the first two tests, a decision was taken to proceed further testing at 30°C.

Control systems

During early stages of the HCA design a coupling was designed as shown in Figures 5.11 and 5.12, with the use of two screws to clamp it to the extension shaft. During the commissioning period the coupling was loaded and unloaded many times and the screws became bent in the clearance slot. This caused friction in the loading system and it was observed that there was some difficulty in achieving the exact stress conditions, as shown in Figure 5.10. This also resulted in the torque for Specimen 7 being applied a few seconds before the vertical load resulting in premature failure. Therefore, it was decided that the vertical extension shaft coupling required a modification. A split collar was made with an internal slot, which pulled the shaft and upper part of the coupling together (see Figures 5.11 and 5.13). It

was then found that the haversine loading carried out without any offset and tension could be applied if required. Figure 5.10 shows that this modification eliminated friction in the loading system and led to the improvement in meeting the specified stress ratios.

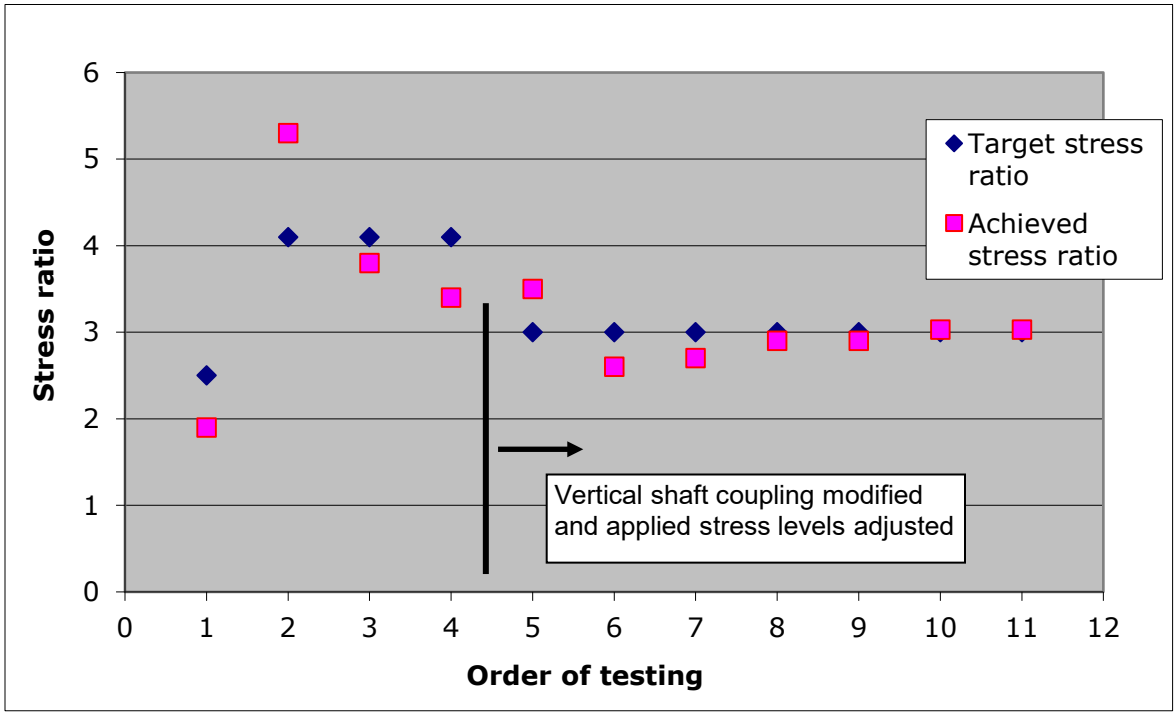


Figure 5.10. HCA haversine testing - improvement in stress ratio control

As it was not possible to see the specimen in the chamber, the tests were continued until the torque actuator neared the end of its stroke. This was equivalent to a rotation of the top of the specimen of between 40mm and 60mm depending on the actuator start point. Consequently, there was considerable distortion of the specimen beyond the point at which it had failed, which was another control issue that needed to be resolved.

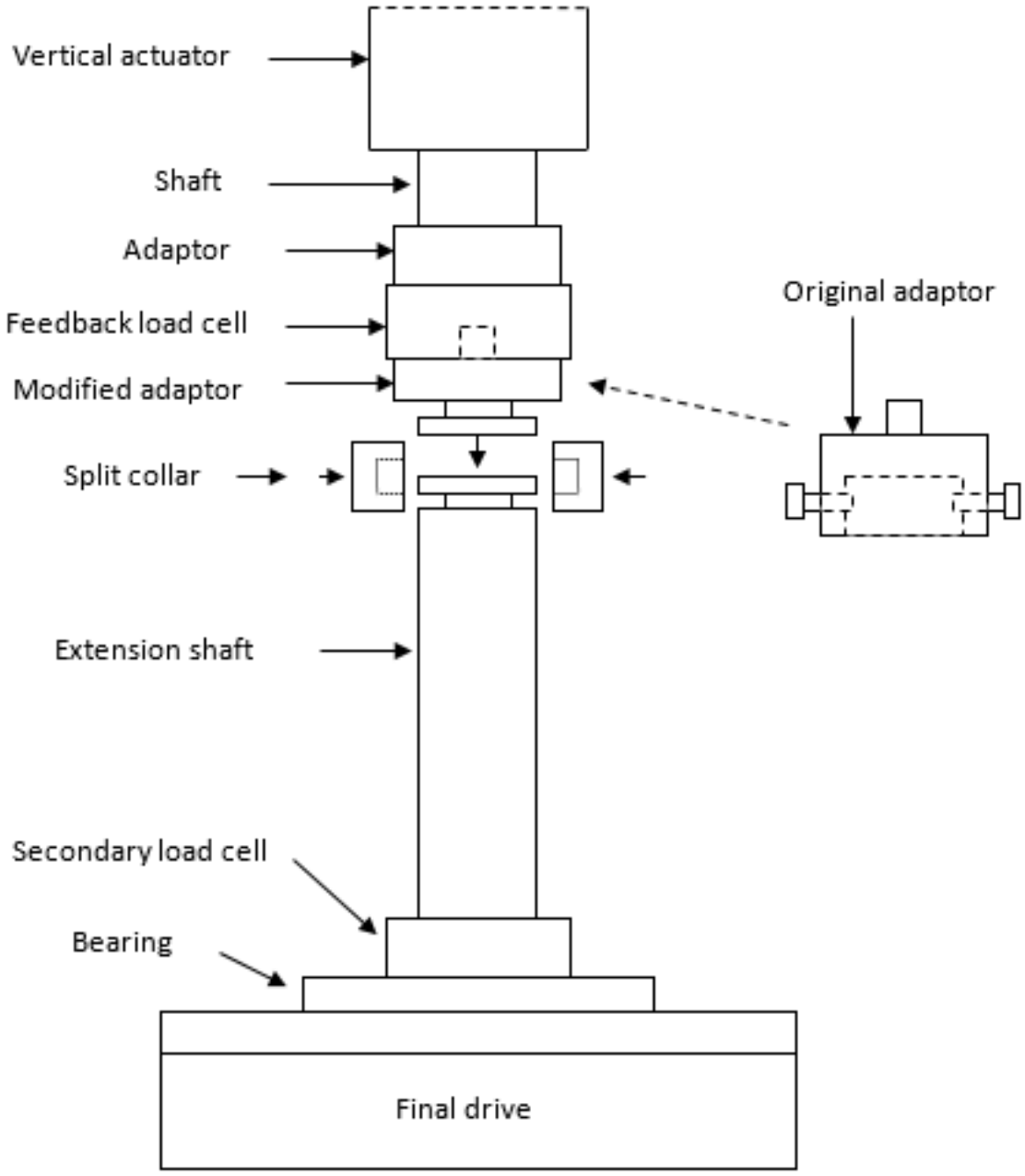


Figure 5.11. Vertical load cell coupling before and after modification



Figure 5.12. Vertical load cell coupling before modification

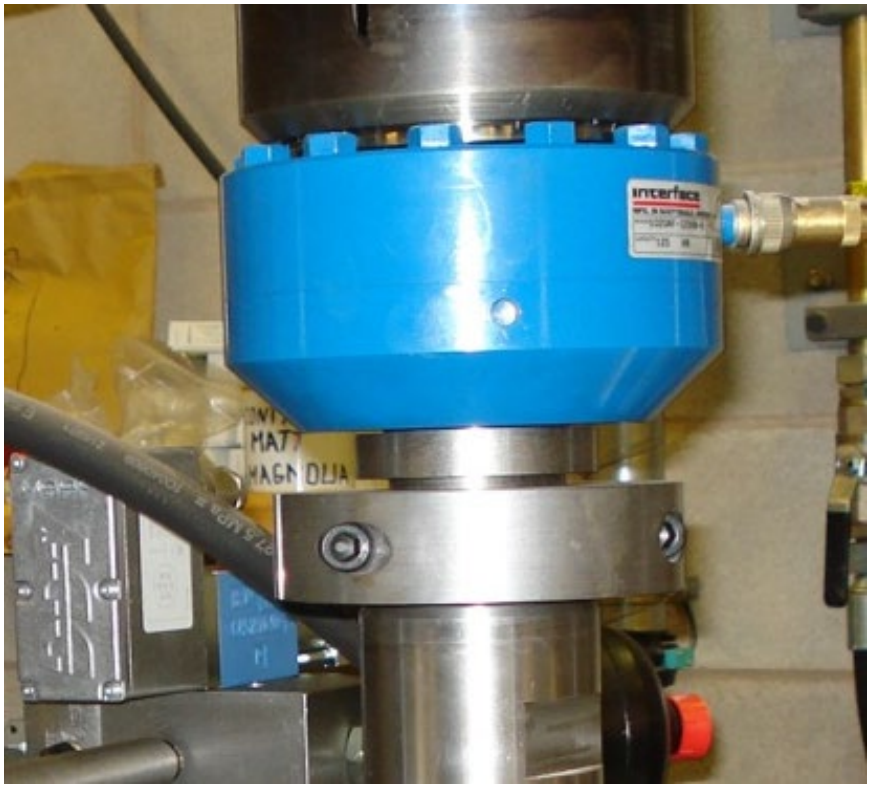


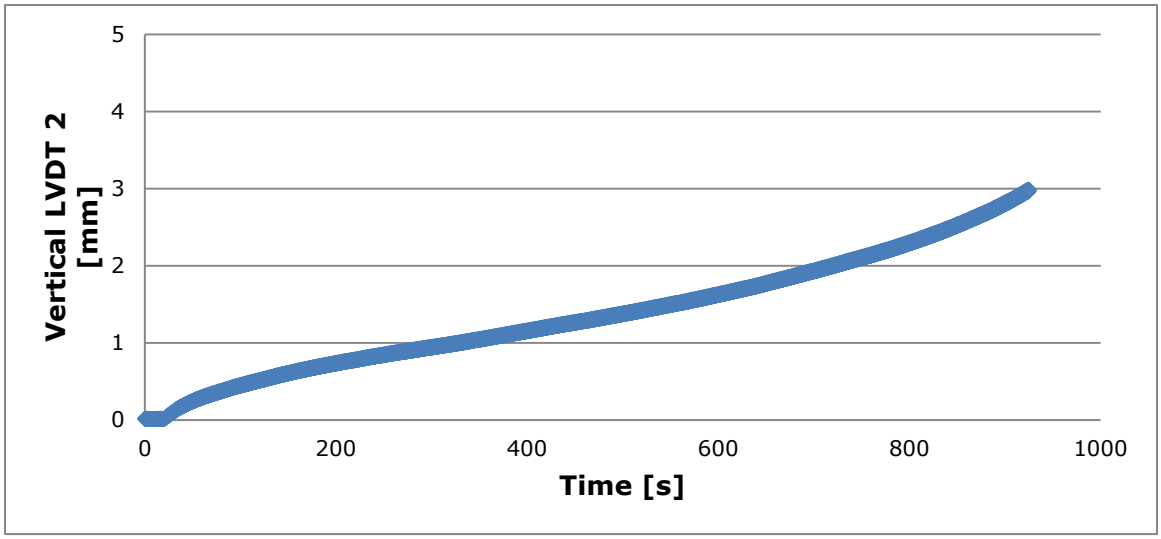
Figure 5.13. Modified vertical load cell coupling

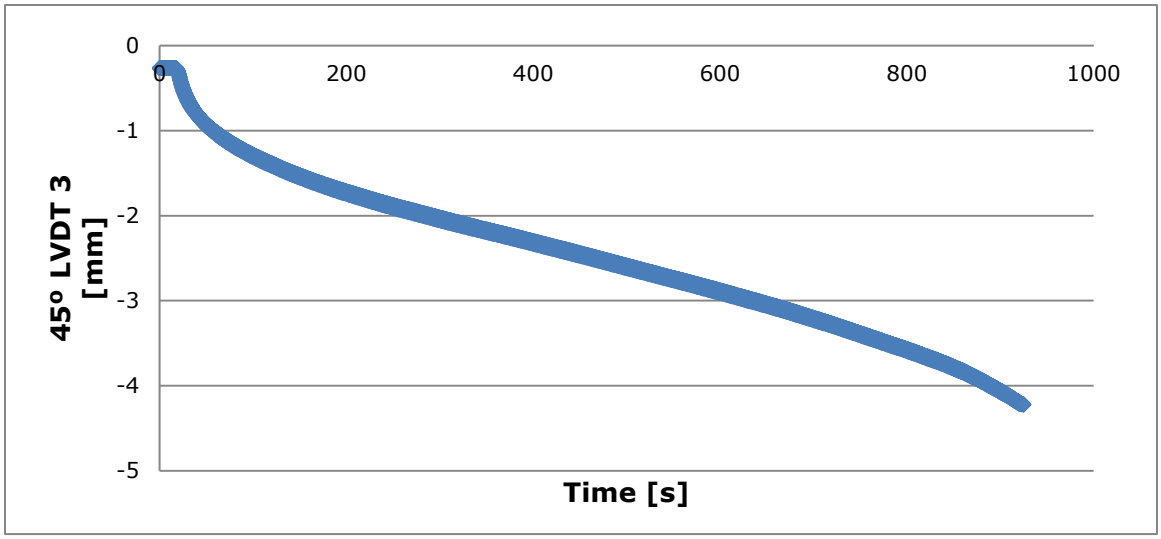
5.1.5. Concluding Remarks

The initial phase of work with this new apparatus involved an extensive period of commissioning in order to ensure that all the systems functioned correctly. The equipment proved to be able to apply more complex stress paths and accurately measure the corresponding deformation in the specimen. The average deformation readings were consistent with the shear stress levels. The typical output from LVDTs is shown in Figure 5.14. In order of confidence in their accuracy the best readings were from the 45° LVDTs closely followed by the vertical LVDTs. The radial LVDTs proved to be satisfactory but could be improved by modifying the collars.

This work resulted in some adjustments to the drive system and also to the instrumentation mounting arrangements.

The temperature control system proved to be unreliable above 30ºC because of substantial heat loss through the metal components. The provision of some additional lagging was necessary to reduce this problem, but modifications will be needed in the future to achieve higher test temperatures. Consequently, HCA tests were to be carried out at 30ºC and it was necessary for further SST tests to be conducted at Berkeley at the same temperature in order to complete the exercise of comparing results from the two experimental facilities.





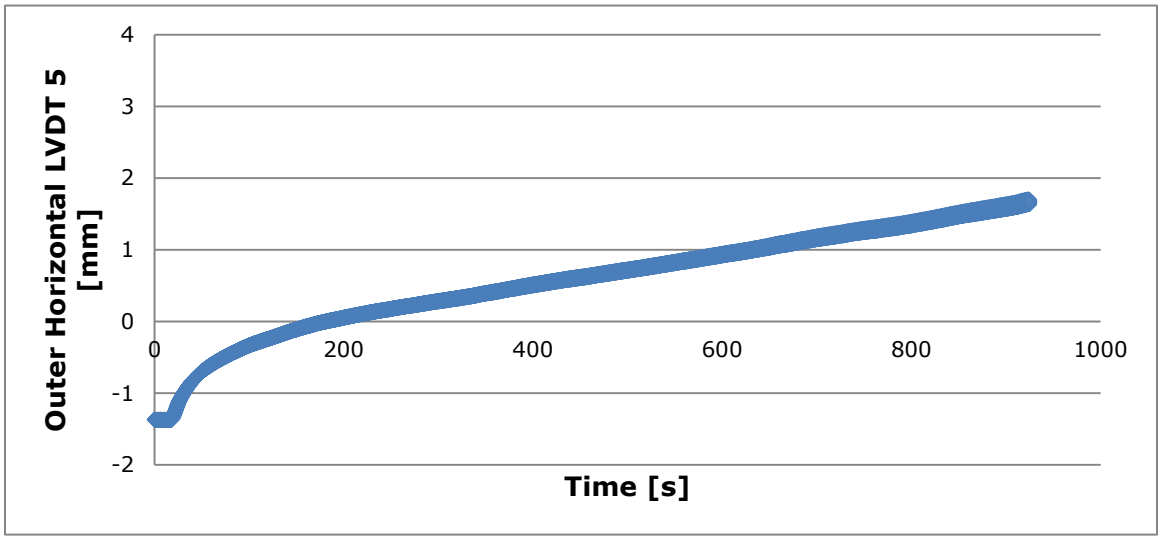


Figure 5.14. Typical output from LVDTs vs time for Specimen no. 6

Overall, it was demonstrated that the specimen preparation method was satisfactory and capable of obtaining the required quality specimens and the apparatus is capable to record consistent stress-strain responses.

Some modifications of the HCA were attempted during this research in order to develop and commission the equipment. However, the problem with the coupling caused a delay to the progress of the project and the time to carry out each test was underestimated. Due to that, improvement of the HCA had to be limited in order to progress the main HCA testing programme. A further study is needed to identify and address any other developments required.

5.3. Main HCA Tests

The main objective of this project was to design and build the new torsional apparatus for the testing of asphalt materials used in road pavement construction, in order to simulate the stress paths experienced under moving wheel loads. As described in previous sections of this report, the objective was met, and the new Nottingham HCA was successfully built and commissioned.

All proposed methods for estimating rutting need a complete mechanistic validation that should include field performance testing. Therefore, at the beginning of the project it was agreed that it will be essential to conduct wheel tracking tests which would allow comparisons of predicted permanent strain profiles with field measurements in order to validate current analytical models. Unfortunately, following a lengthy period of the HCA development and commissioning process, given the limited time available to complete this project, it was decided that the original range of tests needed to be narrowed, focusing mainly on making a comparison between the behaviour of asphalt concrete tested in the HCA and that tested in California with the SST. The initial experiments were designed to allow direct comparisons to be made. 18 HCA specimens produced as per Section 4.1 were used. The tests were performed in accordance with procedures outlined in Chapter 4. The HCA incorporated a number of adjustments to the drive system and also to the instrumentation mounting arrangements to address problems observed during the commissioning period.

5.4. Test Programme

The programme of HCA testing is shown in Table 5.2, from which it is seen that it was based around the use of three stress ratios (1, 2 and 3) each with a set of three applied shear stresses (70, 100 and 130kPa). The stress ratio was defined as shear stress divided by axial normal stress ($\tau_{z\theta}/\sigma_z$ in Figure 2.33). This relates to the stress conditions applied in the SST, which was operated at constant stress ratio rather than in its normal mode of constant height.

The same applied stress regime of 0.1s pulses with 0.6s rest periods was used for both the shear and normal stresses. The shear stress was applied in one direction, again as in the SST. The basic idea was to compare the response of an SST specimen with that of a vertically orientated element in the wall of the HCA, as illustrated in Figure 2.33. Testing was carried out until a rotation of the final drive equivalent to an overall shear strain of approximately 3 percent was reached. The test temperature was 30ºC and two tests were conducted at each stress condition.

Table 5.2. Initial test programme

Test No.	Shear Stress (kPa)	Normal Stress (kPa)	Stress Ratio
1	70	70	1
2	100	100	1
3	130	130	1
4	70	35	2
5	100	50	2
6	130	65	2
7	70	23.3	3
8	100	33.3	3
9	130	43.3	3

*Each test was replicated once

5.5. Test Materials

A standard *AC 10 close surf 100/150* asphalt mixture was selected for initial experiments, with 10mm maximum size continuously graded aggregate containing 5.2 percent of grade 100/150 bitumen as shown in Figure 5.15.

Specification for Product code 2741

AC 10 close surf 100/150

Binder 125 pen Bitumen

Material type: EN 13108 - 1 AC Alias: EN 13108-1 AC: Small Agg

10 sieves aperture/ diameter	Target percent passing	Specified % passing min - max	Control limits % passing min - max
14mm/ 300mm	100	98-100	100-100 ²
10mm/ 300mm	100	92-100	96-100 ¹
6.3mm/ 300mm	65	58-72	61-69 ¹
4mm/ 300mm	-	spacer	spacer
2mm/ 300mm	28	22-34	25-31 ¹
1mm/ 300mm	-	spacer	spacer
500µm/ 300mm	-	spacer	spacer
250µm/ 300mm	12	8-16	spacer
125µm/ 300mm	-	spacer	spacer
63µm/ 300mm	6.0	4.0-8.0	5.0-7.0 ¹
Sample weight for sieving		1000-1600	
Binder content %		4.7-5.7	4.9-5.5
Target Binder %		5.2	
Temperature		140-170	

Remarks:
¹ Mean Deviation from Target specification. ² User defined

Figure 5.15. Material specification

The method described in Section 4.1 was used to produce 18 quite accurately dimensioned specimens. The specimens were prepared and stored in a temperature controlled room at 5ºC. The test procedure used for the HCA tests is described in Section 4.2 of this report.

The profile of air void contents through each specimen was determined as per Section 4.2.1. Figure 5.16 shows how the mean and standard deviation

of void content varied through the test specimens. The data were derived as averages from 18 specimens. The approximate positions of the interfaces between the 100mm lifts that were used for construction of the slabs are shown. There is no obvious influence of these on the void content profiles. The overall mean void content of all the samples from the 18 test specimens was 6.8% with a standard deviation of 1.8%. Figure 5.16 also identifies the zone at the centre of the specimens over which the instrumentation for deformation measurement was located. The mean and standard deviation for this zone were 6.4% and 1.5% respectively, showing marginally less variability than for the overall figures. Figure 5.17 focuses just on the central instrumented zones as these are the most important parts of the test specimens. It presents the mean and standard deviations for all 18 specimens.

The overall conclusion from this exercise was that the void content of that volume of each specimen that has most influence on the deformation data was between about 5 and 12 percent. While this is not ideal, it was considered adequate for initial experiments to proceed.

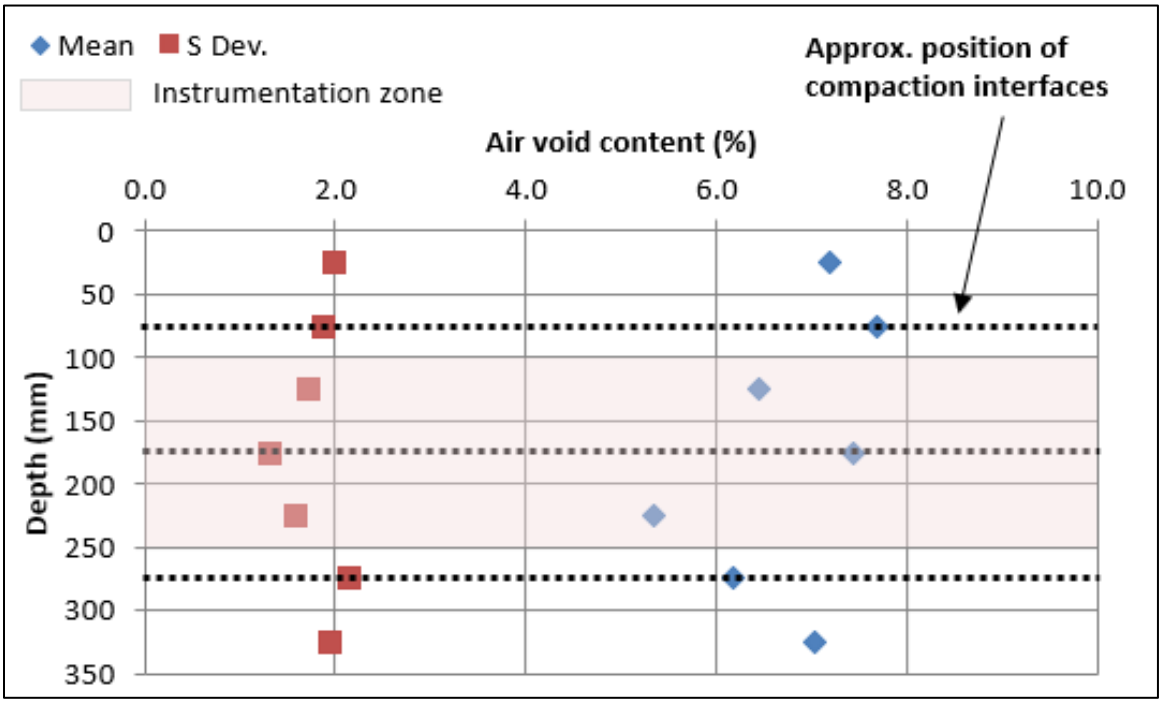


Figure 5.16. Mean and Standard Deviation of air void content profiles through test specimens

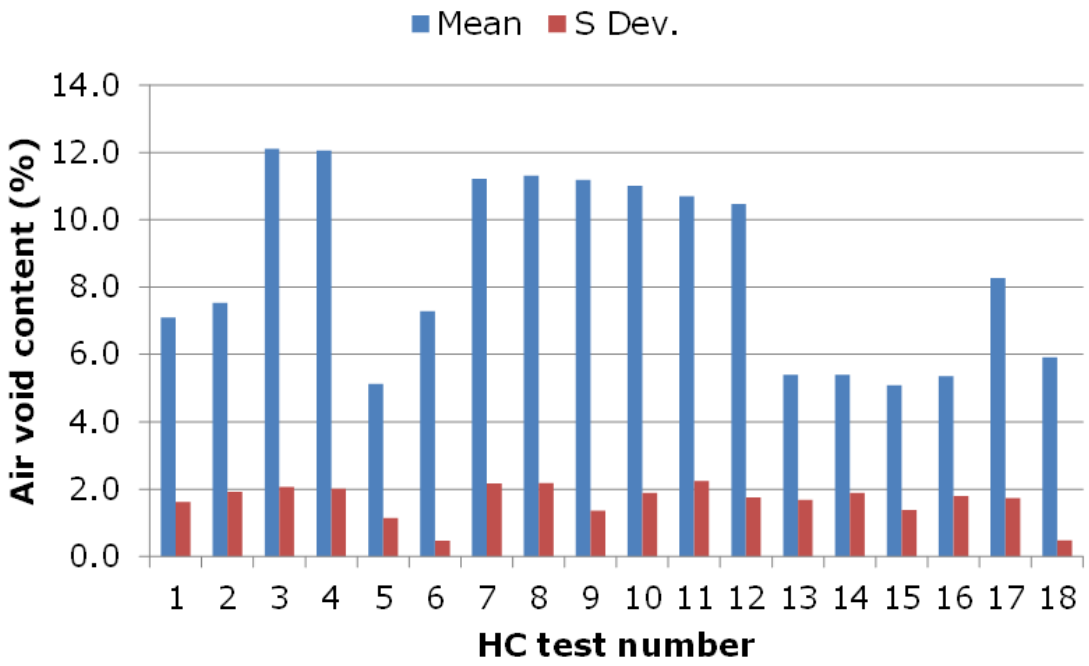


Figure 5.17. Mean and Standard Deviation of air void content profiles through test specimens

5.6. Results of HCA Tests

Typical time histories over three cycles for the axial load and torque are shown in Figure 5.18 for a shear stress of 130kPa and a stress ratio of 1. Figure 5.19 shows output from four of the LVDT's over the same three cycles. It can be seen from this figure that the responses are offset due to permanent deformation that had accumulated by that stage in the test. The transient deformation in response to the applied axial load and torque pulses is clearly visible.

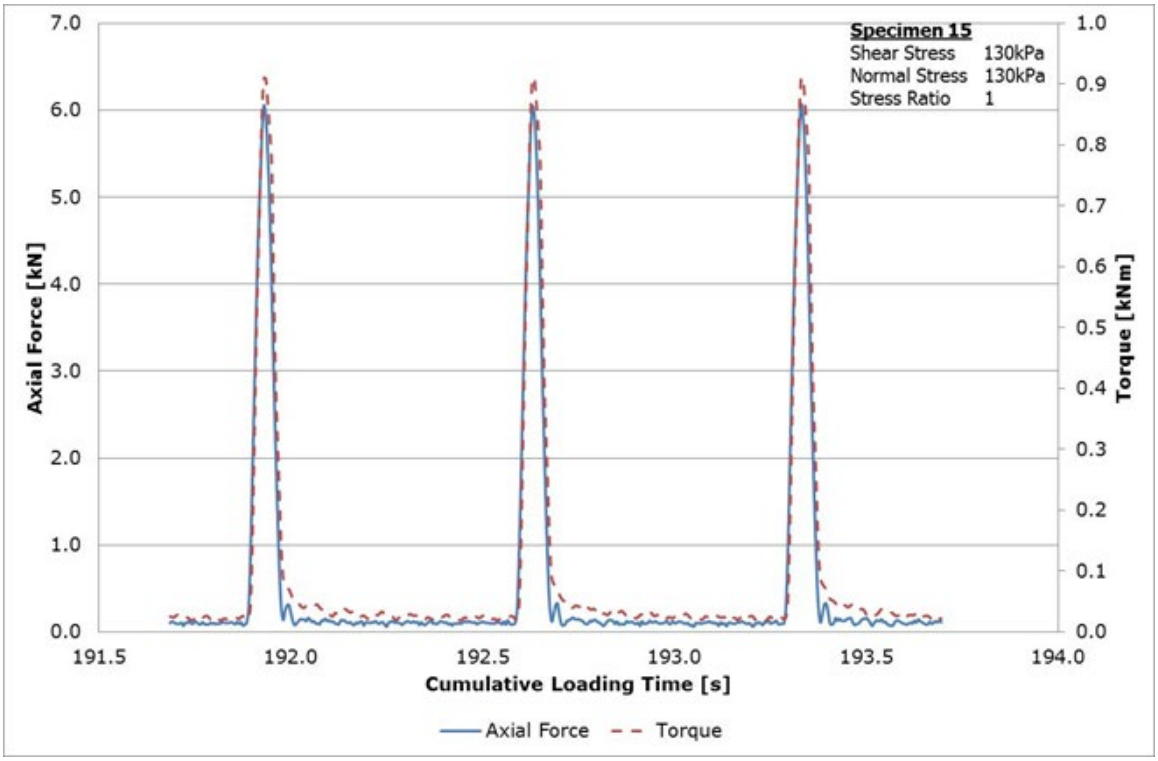


Figure 5.18. Typical wave load for cycles 209 to 211: Test No. 3

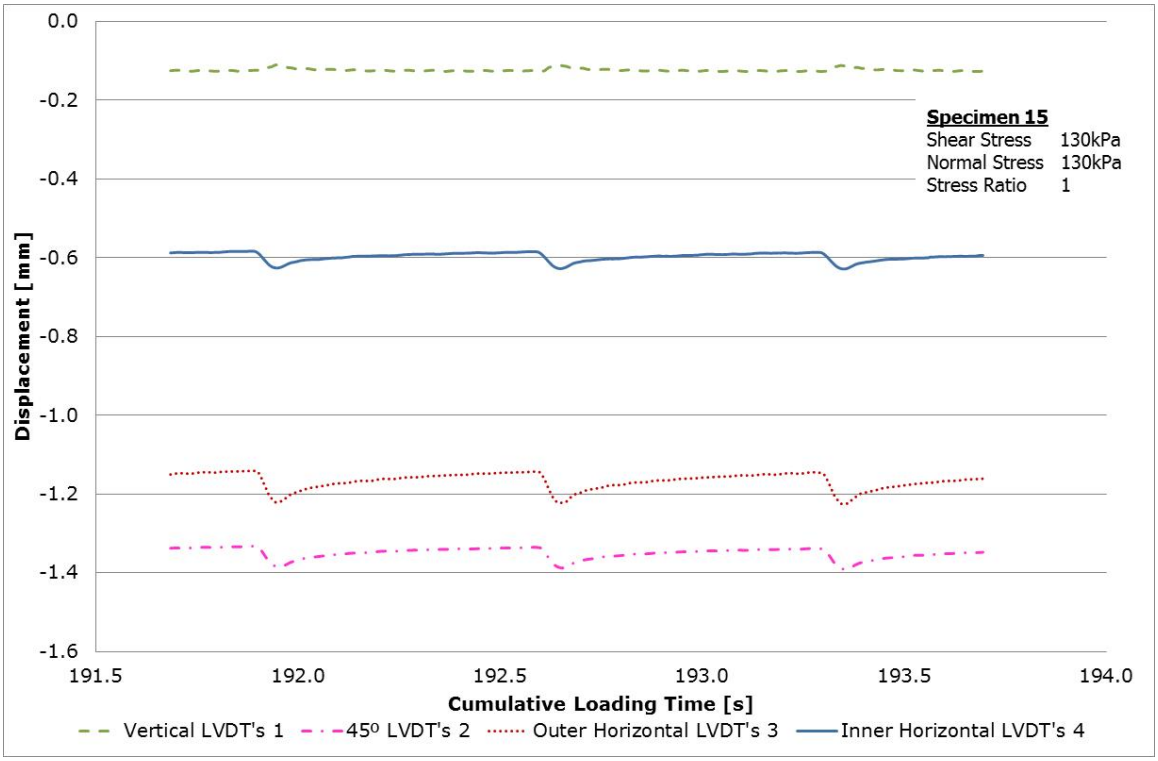


Figure 5.19. Typical response of LVDT's under the load (cycles 209 to 211): Test No. 3

The Literature Review indicated the importance of adopting stress invariants for the correct representation of stress states in an asphalt pavement. The mean normal stress, p, is associated with volume change due to poor compaction, and the octahedral shear stress, q, is associated with shear distortion as a result of high shear stresses in the pavement. Figure 5.20 illustrates stress conditions used in the HCA test programme.

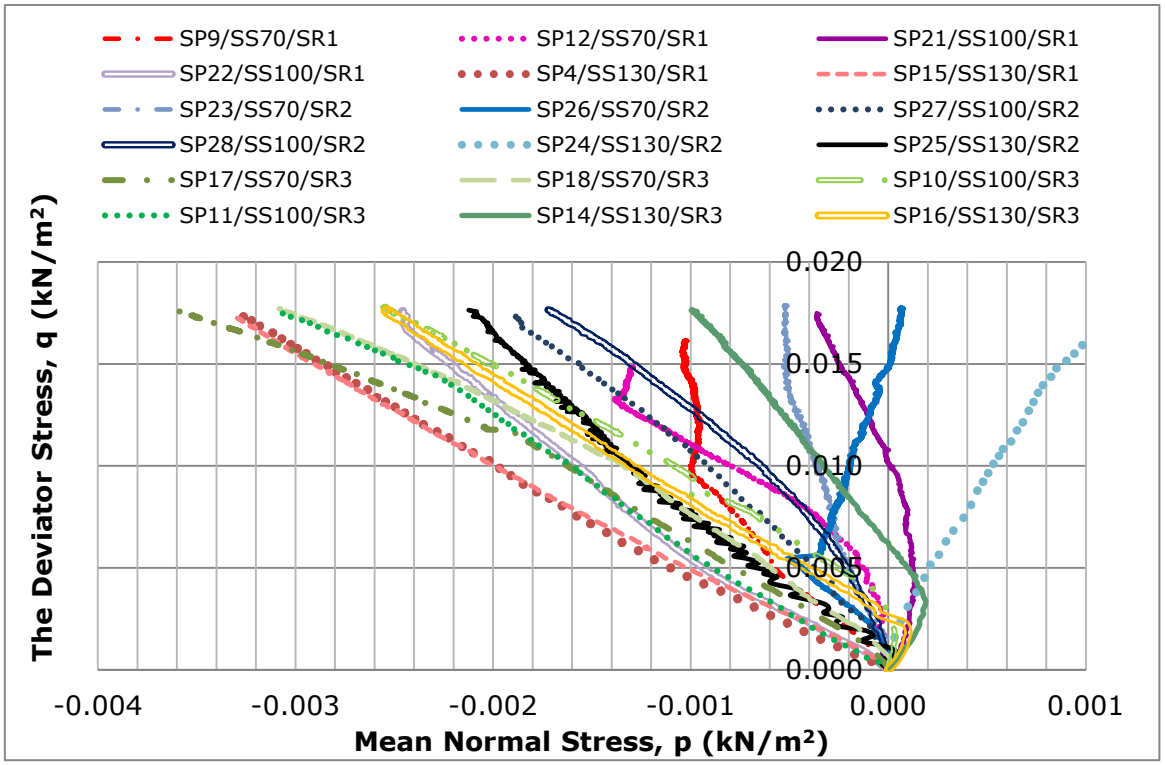


Figure 5.20. The deviator stress vs. mean normal stress
(Key: SP - specimen / SS - shear stress / SR - stress ratio)

Typical data from this investigation are presented in Figures 5.21 to 5.23, where the permanent shear and volumetric strains change as the number of load cycles increases. Each figure illustrates the effects of shear stress level and stress ratio on mixture performance.

Figures 5.21 and 5.22 show the accumulation of permanent shear strain, $\gamma_{z\theta}$ (Eq. 3.9) plotted as a function of the number of load cycles. Each of the curves corresponds to a single test result at a particular value of applied shear stress (e.g. SS130 is an applied shear stress of 130kPa) and a particular stress ratio (e.g. SR1 is a stress ratio of 1). Similar to creep curves

for asphalt mixtures as described in Section 2.7.1, the strain curves have visible two creep regions: a primary where the strain rate decreases and a secondary where the strain rate is almost constant. None of the specimens reaches the tertiary region, where the strain rate increases rapidly as the specimen approaches failure.

It can be seen from Figure 5.21 that the stiffness (resistance to deformation) is sensitive to the applied stress level and an increase in the shear stress magnitude accelerates the rate of permanent deformation substantially. In addition, application of lower normal stress (high stress ratio), results in higher accumulation rate of permanent shear strain. This indicates that axial compressive stress had a confining effect on the accumulation of permanent shear strain. It is also apparent from this figure that the deformation behaviour of the asphalt mixture at particular shear stress levels is similar in shape.

Figure 5.22 indicates that, at low shear stress levels of 70kPa, there is a greater rate of accumulation of permanent strain as the stress ratio is increased from 1 to 3 due to the lower normal stress. However, this is not evident in the tests carried out at shear stress levels of 100kPa and 130kPa. The effect of compressive axial stress on permanent shear strain becomes apparent when the shear stress is relatively low. However, when specimens are subjected to very high shear stress, it appears that increase in permanent shear strain is mainly attributed to shear deformation and the

effect of axial compressive stress on permanent shear strain is negligible. Similar conclusions were drawn by Alavi, (1992) who reported that when shear stress is great enough, the confining effect of axial compressive stress can be overshadowed.

Figure 5.23 shows the permanent volumetric strain, ε_v (Eq. 3.25), plotted as a function of the number of load cycles. Note that negative volumetric strains indicate an increase in volume (i.e. dilation). It can be seen from this figure that all except one of the specimens display permanent dilation. Specimens SP21 and SP14 display a slight volume decrease at first which may be due to initial compaction, followed by an increase in volume with further increase in shear strain. In addition, specimen SP24 and 26 exhibits mainly densification likely as a result of loss of air void content or some other phenomenon that could not be explained based on these results.

Figure 5.23 also shows that generally after an initial period where the rate of permanent volumetric strain decreases (in most of the specimens), the permanent volumetric strain increases approximately in proportion to the number of loading cycles and is not strongly dependent on the stress conditions (i.e. the curves have a similar slope). However, it should be noted that results from more testing are required to confirm this observation.

Lastly, the results suggest that for a stress ratio of SR=1 and SR=2, higher shear stresses tend to cause higher dilatant volumetric strain. However,

Figure 5.23 indicates that for a high stress ratio of SR=3, the dilation phenomenon appears to be independent of the shear stress level.

Figure 5.24 shows the variation of the angle of major principal stress rotation α with stress ratio. It is evident that as stress ratio increases from 1 to 3, the angle of major principal stress rotation α increases, causing higher rate of permanent deformation (Figure 5.22).

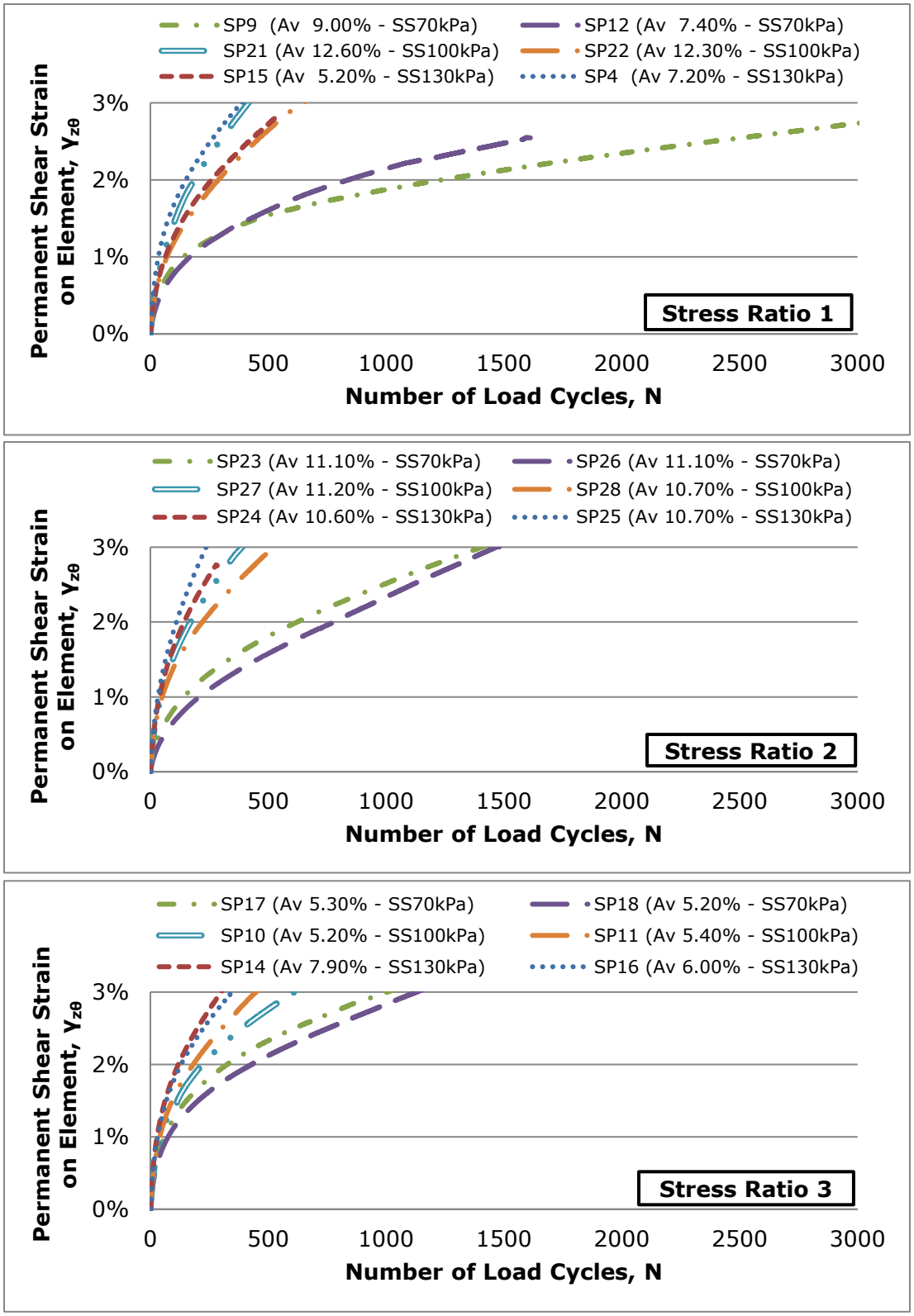


Figure 5.21. Variation of permanent shear strain with number of load cycles for different stress ratios

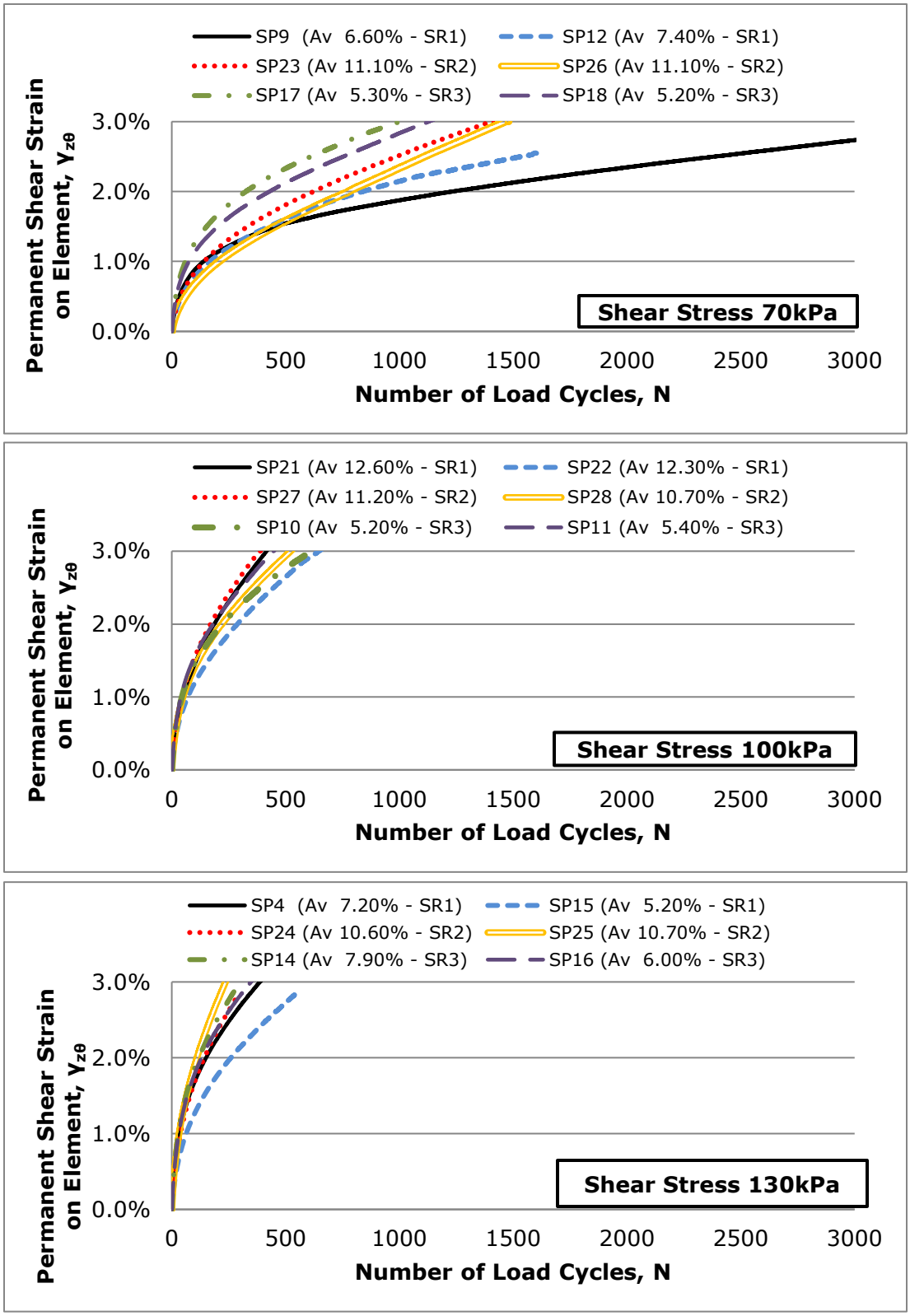


Figure 5.22. Variation of permanent shear strain with number of load cycles for different shear stress levels

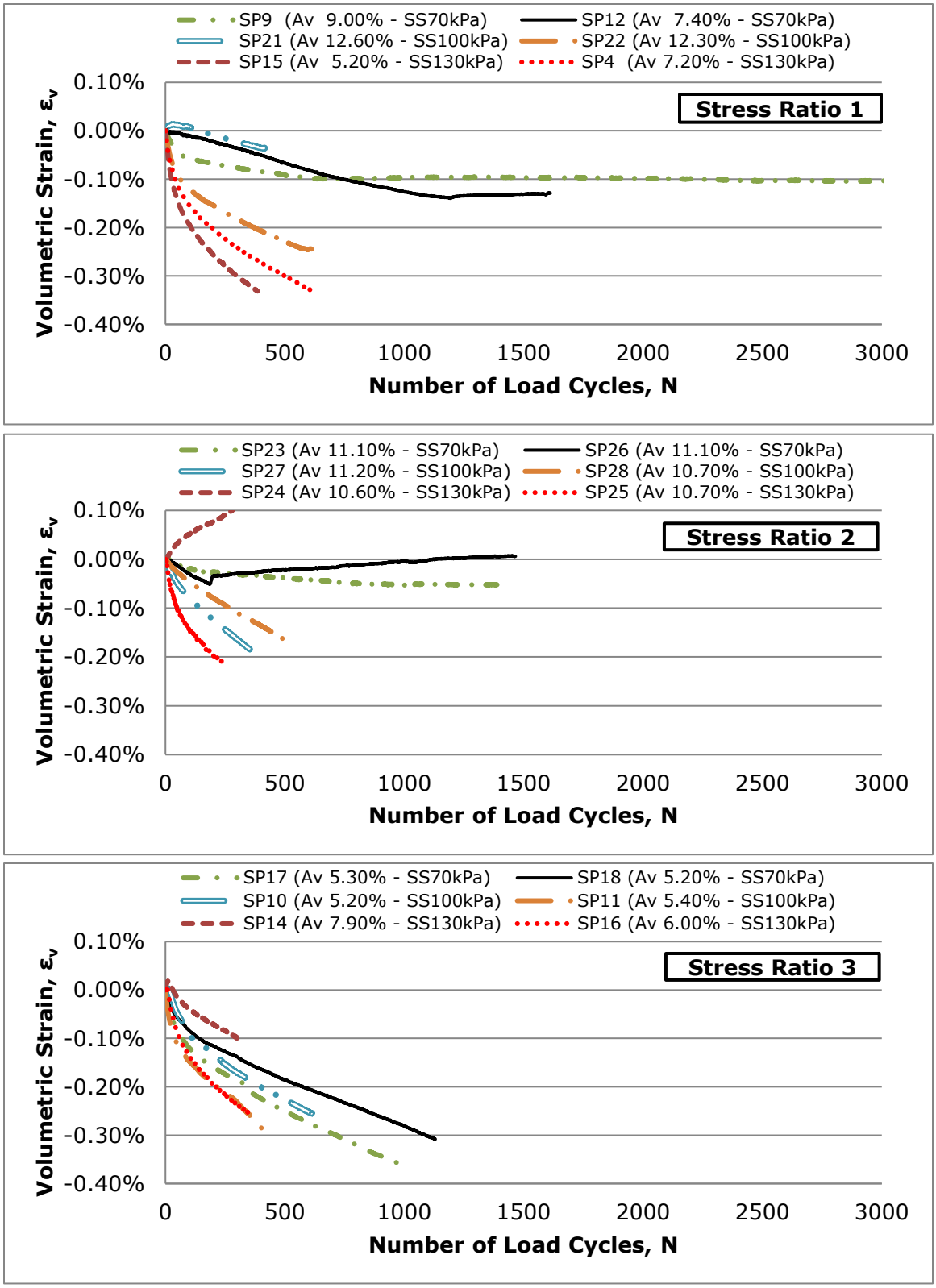


Figure 5.23. Variation of volumetric strain with number of load cycles for different stress ratios

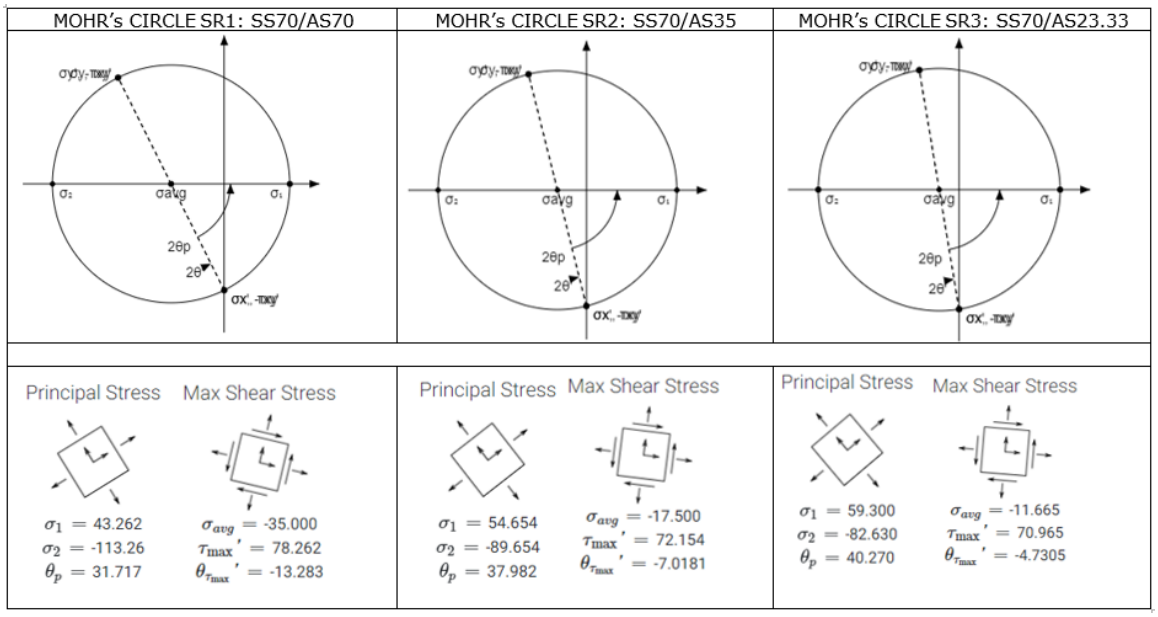


Figure 5.24. HCA Mohr's Circles for shear stress of 70kPa and stress ratio values of SR=1, SR=2 & SR=3

5.7. Summary and Conclusions

The new Nottingham HCA has been successfully developed. It was observed that the equipment properly controls the applied stress signals. The HCA was able to apply more complex stress paths and accurately measure the corresponding deformation in the specimen. The test allowed to test asphalt with realistic sized aggregate (10mm maximum). However, a number of modifications had to be incorporated in order to address issues encountered during the commissioning phase of the work. Further improvement of the equipment might be required but this had to be limited in order to progress the main HCA testing programme.

Overall, it was demonstrated that the specimen preparation method was satisfactory and capable of obtaining the required quality specimens and the apparatus is able to record consistent stress-strain responses.

Due to the extended period of commissioning process, the main HCA test programme had to be narrowed focusing mainly on making a comparison between the behaviour of asphalt concrete tested in the HCA and that tested in California with the SST.

The test programme allowed initial exploration of the relative effects of stress ratio (shear/normal stress) and shear stress level. 18 HCA tests have been performed and the following conclusions can be drawn from this work:

- An increase in the shear stress magnitude accelerates the rate of permanent deformation substantially. This again highlights importance of developing a suitable laboratory test method and theoretical models that could properly treat shear-induced permanent deformation in order to ensure the structural adequacy of flexible pavement.
- Application of lower normal stress (high stress ratio), results in higher accumulation rate of permanent shear. This indicates that axial compressive stress had a confining effect on the accumulation of permanent shear strain. The development of permanent deformation predictive models must therefore incorporate this phenomenon.
- At low shear stress levels of 70kPa, a greater rate of accumulation of permanent strain is observed, as the stress ratio is increased from 1 to 3 due to the lower normal stress. However, tests at higher shear stress level (100kPa and 130kPa) seem to be inconsistent. This shows that the effect of compressive axial stress on permanent shear strain is greater when the shear stress is relatively low. However, when specimens are subjected to very high shear stress, it appears that increase in permanent shear strain is mainly attributed to shear deformation and the effect of axial compressive stress on permanent shear strain is negligible.
- Asphalt was found to dilate under the HCA tests.
- The dilation phenomenon was observed to be shear stress level dependent in conditions where stress ratio is low. However, the tests revealed that when higher stress ratio value (e.g. SR = 3, hence low

axial stress) was used, the rate of development of volumetric strain was independent of the magnitude of shear stress.

- More HCA testing is required to study shear dilatancy effect on permanent axial stress development under the combined loading mode.
- No apparent correlation between air voids content and asphalt mixture performance was found likely due to non-homogeneous characteristics of the slab which led to core specimens with non-consistent void content. Also, too many variables used in the tests made this assessment impossible.

In Chapter 7, these results will be compared with the results of SST and RLAT on the same asphalt mixture.

6

REPEATED LOAD AXIAL TEST AND SUPERPAVE SHEAR TEST

6.1. Introduction

As explained earlier (Chapter 1), one of the objective of this study was to investigate the reliability of the SST test, given the non-uniform stress conditions inherent in its configuration relative to that in the HCA. In addition, comparisons of the new HCA with the simpler compression tests, such as the Nottingham Asphalt Tester (NAT) used routinely for mixture design, is to be carried out in order to understand how reliable this approach is for characterising resistance to permanent deformation under field conditions. Thus, the SST and RLAT tests were performed over a range of stress levels and stress ratios. This chapter presents descriptions of these tests and summarises results obtained from the individual tests. The discussion of these results in the context of the HCA data can be found in Chapter 7.

6.2. Repeated Load Axial Tests (RLAT)

The simple uniaxial creep test is rapidly being replaced by a repeated load version. This is more representative of insitu conditions and on the basis of extensive testing, it has been reported that repeated load tests appear to provide a better measure of rutting characteristics than the creep tests (Brown and Cooper, 1984, Monismith et al., 1994). Moreover, Monismith and Tayebali, (1988) showed that repeated load tests are more sensitive to mix variables than static creep tests. For static creep tests, similar behaviour was observed for different mixtures, while repeated load tests on the same mixtures indicated significant differences in mix response. The RLA testing method has been used for many years for purposes of mix design, quality control, and evaluation of the asphalt mixture resistance to permanent deformation. The test gained wide acceptance, principally due to ease of specimen preparation, simplicity of test procedure and relatively low cost of test equipment. Nevertheless, Gibb and Brown (1993) concluded that the RLAT can rank dense mixtures quite reliably with respect to their rutting resistance in the road.

Based on the literature review the RLAT was selected for further study. With the aim of exploring the possibility of correlating the results from the RLAT with those from the HCA tests in an attempt to verify its accuracy and reliability, the RLAT was carried out on the cores obtained from the central parts of the HCA specimens. The experiments programme adopted axial stress levels that related to the stress conditions applied in the HCA and the SST.

6.2.1. Testing Apparatus

The RLA test developed at the University of Nottingham (Brown, 1995) is an unconfined uniaxial test used now routinely in several countries including the UK to quantify the permanent deformation characteristics of bituminous paving materials using the Nottingham Asphalt Tester (NAT) shown in Figure 6.1. This servo-pneumatic machine uses a low-friction actuator to apply waveforms to produce repeatable stress variations in test specimens that are simulative of those in a road pavement due to moving traffic.

6.2.2. Specimen Preparation

150mm diameter x 50mm specimens were cut for RLAT tests, as described in Section 6.3.2, in order that these should be conducted on the same material as was used for the HCA experiments. The specimens were stored in a temperature controlled room at 5ºC.

Prior to testing, the profile of air void contents of each specimen was determined as per Section 4.2.1 and generally varied between 6.00 and 7.50 percent. Unfortunately, due to lack of remaining specimens, two tests had to be carried out at an average of about 12.50 percent air void content. While this was not ideal because densification has a strong influence on mix behaviour, it was considered adequate for RLAT experiments to proceed. The purpose of this testing was not to compare directly the performance of

mixtures but to compare performance in the RLAT with that in the HCA. Table 6.1 contains a summary of the air void contents used for these tests.

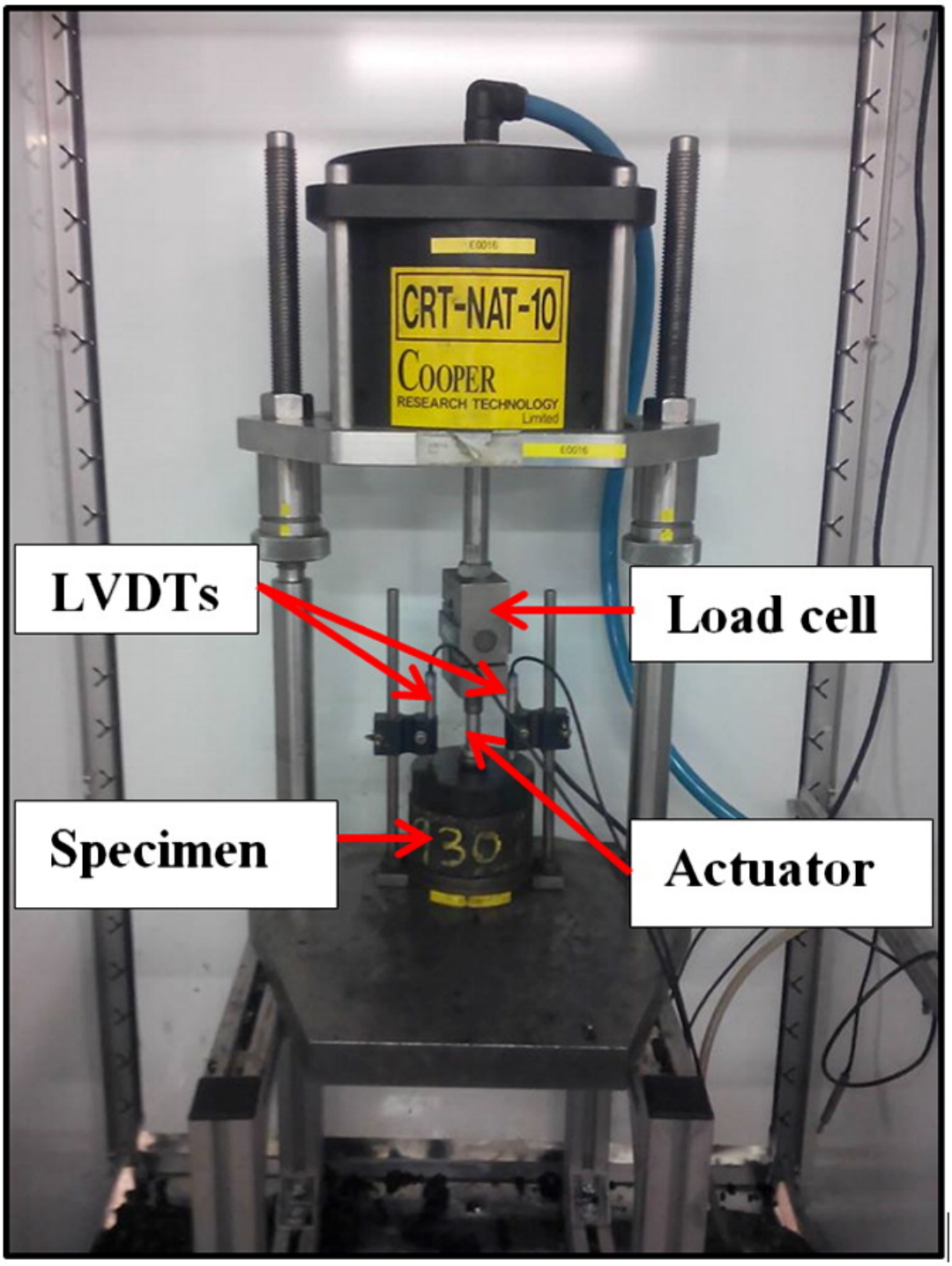


Figure 6.1. Nottingham Asphalt Tester

Table 6.1. Air void contents of RLAT specimens

HC Specimen No	RLAT Core No	Test No	Average void content (%)
9	11-645	1R	6.4
12	11-475		7.5
21	11-1731	2R	12.7
22	11-1738		12.3
15	11-463	3R	6.0
4	11-455		7.2

6.2.3. Test Conditions

The RLA tests were performed at 3 axial stress levels. As in the RLAT the material was only subjected to axial normal stresses, where in the HCA and SST a combination of normal and shear stresses was used, selected axial stress levels for the RLA test programme corresponded to the HCA/SST stress conditions carried out at a stress ratio = 1.

Repeated axial stresses ranging from 70kPa to 130kPa were applied with a time of loading of 1s separated with 1s rest periods, with a loading pulse as shown in Figure 6.2. This shape was applied as this is the standard load pulse used as per DD 226:1996 (BSI, 1996, *Withdrawn*). This is a slightly different wave form to the haversine pulse applied in the HCA and SST, however this was considered of little importance (Terrel et al., 1974). The test was continued for 1,800 load pulses (3,600s). The test temperature was 30ºC and

two tests were conducted at each stress condition. A total of 6 specimens were tested. This testing programme is summarised in Table 6.2.

Table 6.2. RLAT test conditions

Test No	Axial Stress (kPa)	Temperature (ºC)
1R	70	30
2R	100	
3R	130	

*Each test was replicated once

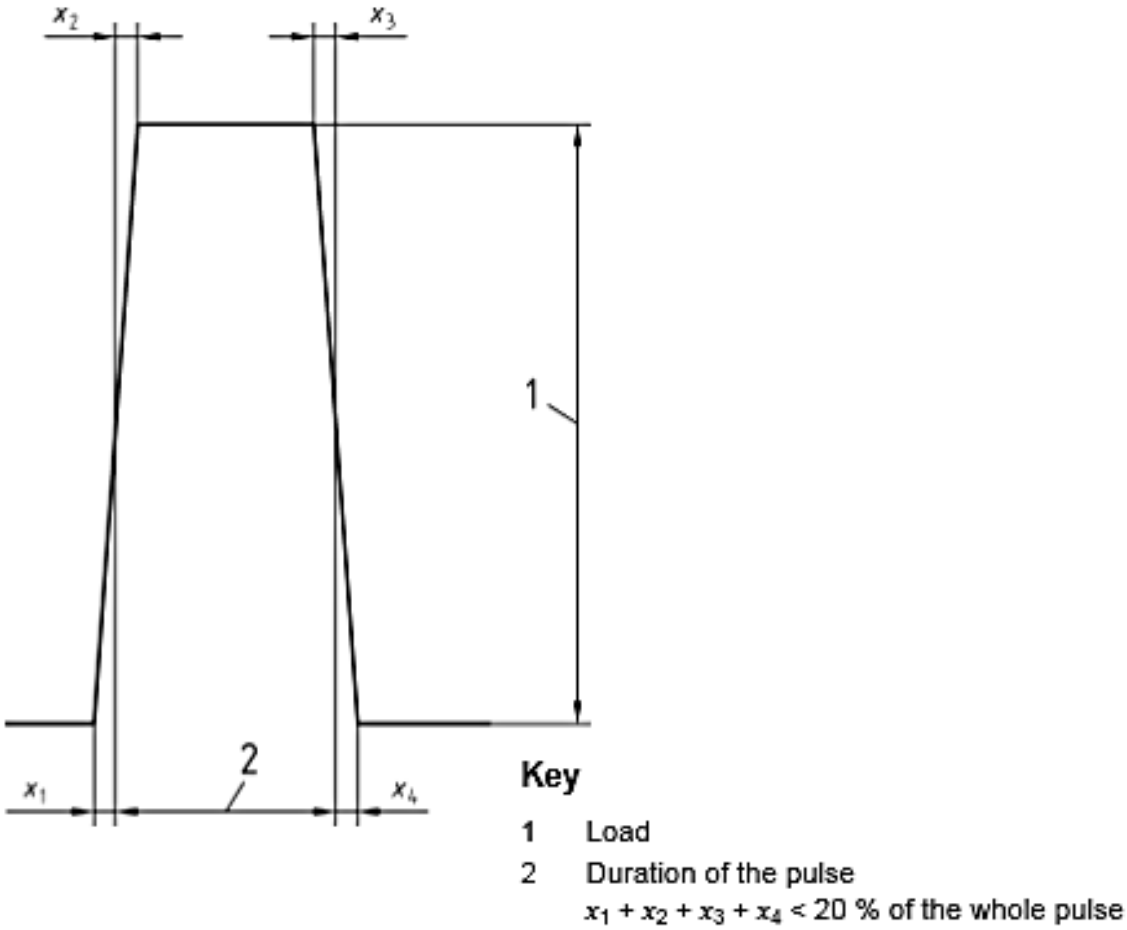


Figure. 6.2. RLAT loading pulse (BSI, 1996, *Withdrawn*)

6.2.4. Test Procedure

The RLAT test was conducted in accordance with DD 226:1996 (BSI, 1996, *Withdrawn*) using the NAT type facilities shown in Figure 6.1. Each specimen was kept in a temperature-controlled cabinet and conditioned at testing temperature until uniform conditions were achieved. After bringing the specimen to the test temperature, the ends of the specimen were coated with a thin layer of silicone grease sprinkled in turn with graphite flakes. The specimen was placed centrally in position on the lower platen and the upper load platen was then placed on the top of the specimen. The two diametrically positioned displacement transducers resting on the upper platen were fitted and the specimen was pre-loaded with a conditioning load equivalent to a stress of 10kPa for 600s. The deformation was measured by the change in distance between the loading platens throughout the test. Both axial stress and strain were logged during the tests by the computer connected to the equipment.

6.2.5. Data Analysis

The axial strain of the test specimen was calculated from the measured deformation at the end of the rest period immediately after application of the load using the Equation 6.3.

The principal stresses acting on the specimen in the RLAT are shown in Figure 6.3. For the RLAT test situation, because of axial symmetry of the

arrangement, two of the principal stresses are the same and equal to the confining stress. Therefore, as the specimen was subjected to compression in the axial direction and no confining pressure was applied in the radial direction, $\sigma_3=\sigma_z$ and $\sigma_1=\sigma_2=\sigma_\theta=0$. The normal stresses are considered as negative while compressive.

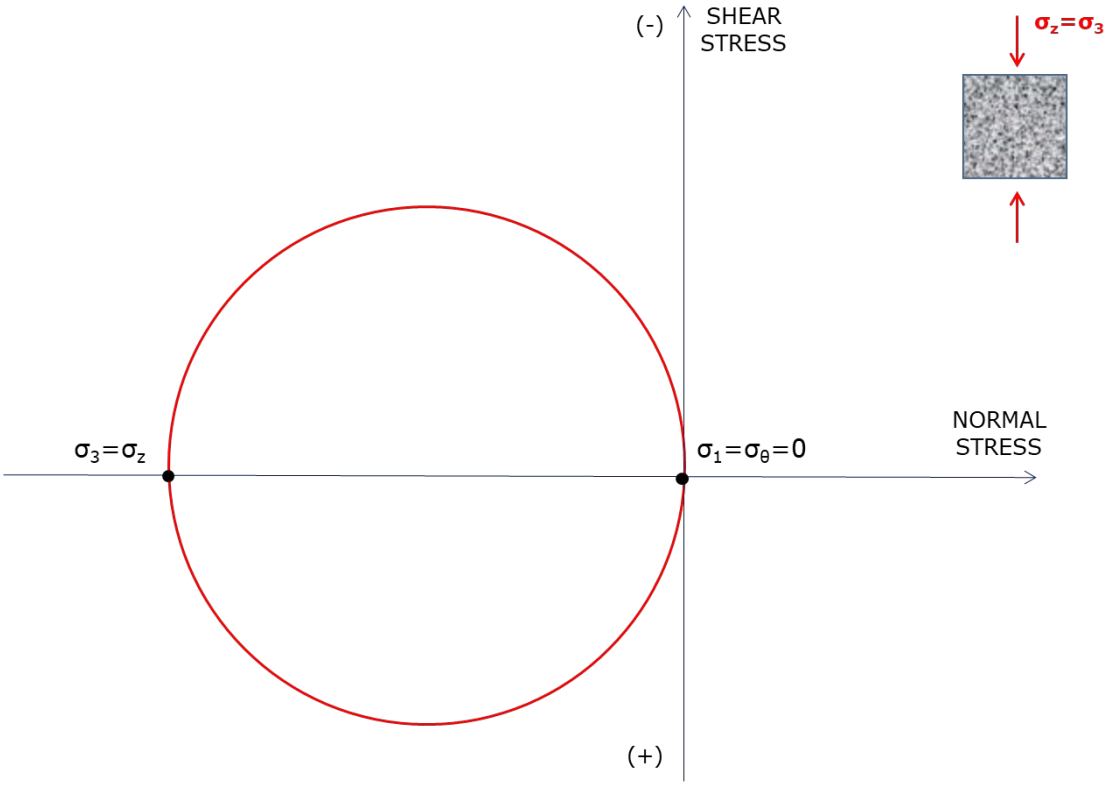


Figure. 6.3. Principal stresses on the θ-z plane in the RLAT

6.2.6. Results of RLAT

Figure 6.4 shows typical results from the RLAT tests, where the cumulative permanent strain is plotted versus the number of loading cycles. It can be seen from the figure that the cumulative permanent strain curves have two regions, as explained in Section 2.7.1. The specimens deform quite rapidly at the beginning of the test (primary region). In the secondary region, permanent strain accumulates in a relatively linear pattern and where the set of curves represent the same axial load, they are relatively parallel. None of the specimens reaches the tertiary region, where the specimen approaches failure.

As expected, permanent strain appears to be dependent on different stress levels and air voids contents. The specimens with higher densities (lower voids) perform better than the less dense mixes and the permanent deformation increased with higher load levels. The indication from the RLAT results is that at very high void contents (above 12%) which would indicate poorly compacted material, the load level effect has less influence on the resistance to permanent deformation than air voids.

After 1,800 cycles of load the magnitude of permanent axial strain obtained under RLAT stress conditions is less than 1.2%.

The Mohr's circle presented in Figure 6.3 shows that the limitations of the RLA test are that it can only simulate the situation when the load is directly above the element. Principal stress rotation (Section 2.8) that occurs in a pavement from a passing wheel load cannot be duplicated in the RLAT and is therefore a limitation of its ability to fully simulate vehicle loading. The state of stress encountered in upper layers cannot be duplicated in RLAT. Also, the radial strain was not measured in these tests, therefore estimation of volume change was not possible.

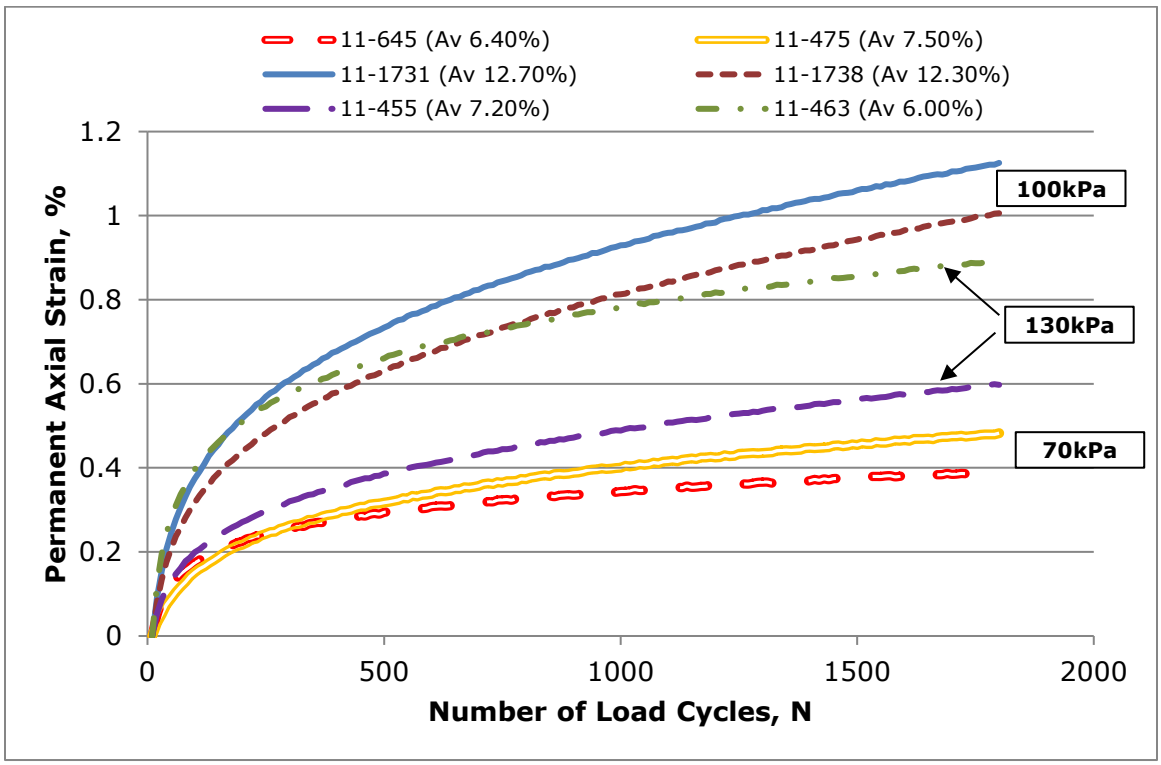


Figure 6.4. Summary of RLAT Tests

6.3. Superpave Shear Test (SST)

As part of the programme of research set out in the original proposal, arrangements were made for testing of asphalt specimens, manufactured in Nottingham to be carried out at UCB in their SST. This equipment was introduced to complement the Superpave volumetric mixture design method and it was envisioned that this simple performance test would play a key role in the quality control and acceptance of HMA mixtures. The equipment is capable of applying direct shear to laboratory specimens and permits controlled rotation of the principal axes of strain and stress which is important in studying permanent deformation. Data gathered using the SST are used as input to the material property, environmental effects and pavement response and distress models to provide prediction of pavement performance.

As discussed in Section 2.7.3, over the past few years this test has become quite widely used in US research laboratories for predicting the rutting resistance of asphalt mixtures, but a number of serious problems were discovered and many of these tests were found to be unreliable. The objective of this work was to carry out tests under selected stress conditions for comparison with results under conditions replicated as close as possible on the same material using the HCA in Nottingham.

6.3.1. Testing Device

The SST is a servo-hydraulic apparatus capable of testing asphalt by applying repeated direct shear to cylindrical test specimens (Figure 6.5) with the facility to control and/or monitor the applied normal stress. As Figure 6.6 presents, it consists of the test module, an environmental control chamber, a test control and data acquisition unit and a hydraulic system. The testing apparatus includes a rigid reaction frame and shear table which is connected to two hydraulic actuators. The environmental control unit chamber maintains constant temperature and air pressure inside the testing chamber. The test control consists of the system hardware and software. The hardware interfaces with the testing apparatus through transducers, and consists of controllers, signal conditioners, and a computer. The software consists of the algorithms required to control the testing apparatus and acquire test data. LVDTs are affixed to specimens to measure axial and shear deformation (Figure 6.7). LVDTs allow the system to operate in a closed loop feedback mode, meaning that LVDT signals are used to control applied testing loads. The hydraulic system contains the hydraulic motor which powers a horizontal and a vertical actuator, which provide the axial and shear loading for different testing conditions. A full description of the test equipment and procedures can be found in AASHTO TP7 (AASHOT, 1994).



Figure 6.5. SST specimen with LVDTs attached

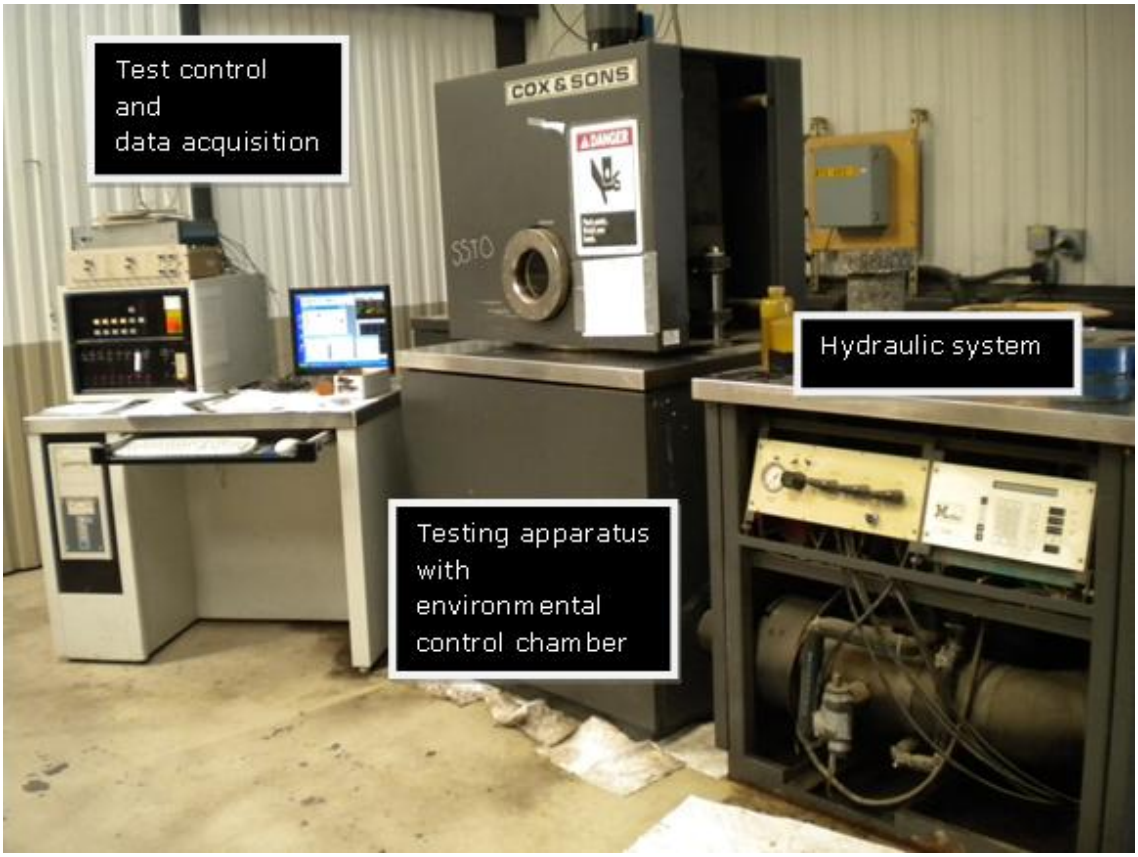


Figure 6.6. General view of the SST in the UC Berkeley Laboratory

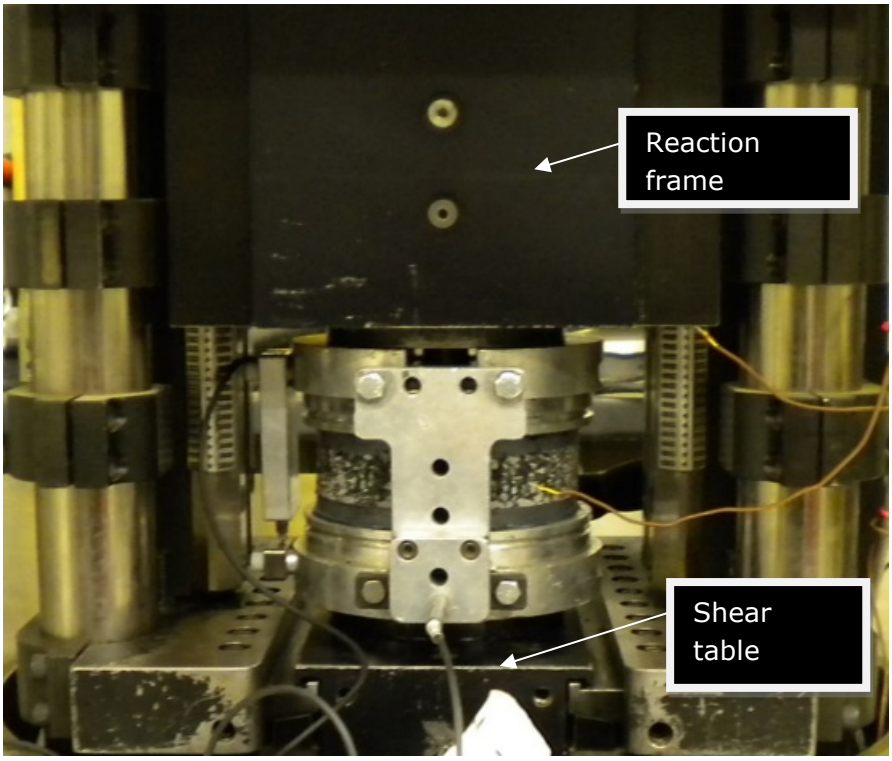


Figure 6.7. SST with test specimen in position

6.3.2. Specimen Preparation

The SST test specimens were manufactured by coring and sawing test specimens 150mm in diameter by 50mm in height from 250mm diameter cores that formed the central part of the HCA specimens produced at NTEC, as shown in Figure 6.8. After shipping all specimens to UCB the air void contents were determined in accordance with the ASTM D1188 parafilm method (ASTM, 2007).

A total of 70 cores were produced from which, 36 with void contents between 4.7 and 12 per cent were selected for testing. Results obtained by this method are presented in Table 6.3. The air voids of the SST test specimens were

matched with the average air void content of the HC specimens measured over the central zone as described in Section 5.5. As discussed before in Sections 4.2.1, 5.5 and 6.2.2, there were clearly differences in void contents, associated with poor workmanship and compaction control on site, but this did not affect the analysis. Furthermore, the SST plots, Figures 6.15 - 6.20, indicate that there was no consistent effect of air void content on performance of the material.

The specimen to be tested was glued to the platens using a gluing device, which compresses the specimen with 32kPa load, ensuring that the platen faces are parallel (Figure 6.9). The specimen was then exposed to the test temperature for approximately two hours prior to testing. After the conditioning period, the specimen was instrumented and placed in the SST to measure both shear and vertical deformation as shown in Figure 6.10.

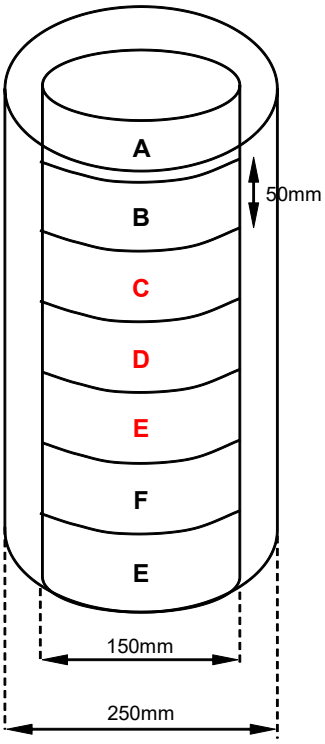


Figure 6.8. SST specimens



Figure 6.9. SST specimen with platens glued to top and bottom



Figure 6.10. SST specimen ready for testing showing LVDT setup

Table 6.3. Summary of SST specimens air void contents

HC Specimen No	Average void content - zone at the centre of HC specimen (%)	SST Core No	Test No	Average void content (%)
Phase 1				
-	-	10-406	1S	4.8
-	-	10-350		7.6
-	-	10-360		5.5
-	-	10-381	2S	5.9
-	-	10-355		6.6
-	-	10-357		7.0
-	-	10-399	3S	5.0
-	-	10-372		7.4
-	-	10-363		6.1
-	-	10-359	4S	7.9
-	-	10-390		6.8
-	-	10-377		5.7
-	-	10-387	5S	4.8
-	-	10-407		6.1
-	-	10-371		7.5
-	-	10-395	6S	5.0
-	-	10-364		4.7
-	-	10-391		6.9
Phase 2				
9	6.60	11-454	7S	6.6
12	7.40	11-452		7.4
21	12.64	11-1734	8S	12.0
22	12.34	11-1741		11.8
15	5.20	11-465	9S	6.5
4	7.20	11-461		7.0
23	11.14	11-1748	10S	9.6
26	11.14	11-1767		10.3
27	11.24	11-1773	11S	10.4
28	10.70	11-1780		10.4
24	10.58	11-1754	12S	9.9
25	10.66	11-1760		9.5
17	5.30	11-447	13S	6.8
18	5.20	11-483		7.3
10	5.20	11-477	14S	5.7
11	5.40	11-481		5.3
14	7.90	11-460	15S	6.6
16	6.00	11-471		6.6

6.3.3. Test Conditions

Initially, the SHRP research proposed six different test protocols for evaluating the shearing characteristics of HMA, including a Volumetric Test, a Uniaxial Test, a Repeated Shear at Constant Stress Ratio (RSCSR), a Repeated Shear at Constant Height (RSCH) and a Frequency Sweep (FS). For the purpose of this study, only three of these tests were carried out: RSCH, RSCSR and FS. The FS data is used to determine the linear viscoelastic properties of the asphalt mixtures that include dynamic shear modulus and shear phase angle. The RSCSR and RSCH tests provide a tool for evaluating rutting performance of the asphalt mixture.

The RSCH test was an optional test for Superpave mixture design (intermediate and complete analysis). AASHTO recently endorsed this test in TP7 and SHRP Superpave mix analysis procedures, for higher trafficked projects, which require a check for tertiary creep behaviour (Cominsky et al., 1994). Tertiary deformation occurs when an asphalt mixture densifies to a very low air void content. In this condition the strain rate increases rapidly as the specimen approaches failure as illustrated in Figure 2.24. The RSCSR test is very similar to the RSCH test, except that the axial load is proportional to the shear load. Similarly, to the RSCH test, this test is regarded as a screening tool to identify mixtures that exhibit tertiary permanent deformation leading to instability and premature rutting. When the strain enters the tertiary creep phase, the mixture fails the screening test, and redesign is required.

Since the RSCH and FS results are beyond the scope of this project, only RSCSR results are presented and discussed below.

6.3.4. RSCSR Tests

In the RSCSR test, repeated synchronised haversine shear and axial load pulses were applied to the specimens. As in the HCA test, the load cycle consisted of a 0.1 second load followed by a 0.6 second rest period. The ratio of shear to axial stress was maintained constant. Tests were carried out until 5 percent shear strain was reached or until failure. The 5 percent shear strain level was selected as previous research found that at this level of shear strain rut depths of about 13mm can be expected (Sousa, 1994). During the test axial and shear loads and deformations were measured. Detailed information on these procedures is described in AASHTO TP7 (AASHOT, 1994).

The initial experimental plan for the SST RSCSR (Phase 1) included testing at two stress ratios (2.5 and 4.1) and two temperatures (45 and 55ºC). However, as concluded in Section 5.1.4 and 5.1.5, the HCA temperature control system proved to be unreliable above 30ºC because of substantial heat loss through the metal components. Hence, it was decided to proceed with the HCA tests at 30°C. Consequently, it was necessary for further SST tests (Phase 2) to be conducted at this temperature in order to complete the exercise of comparing results from the two experimental facilities. Also based on the HCA testing, for the test temperature of 30°C, three stress ratios were

used: 1, 2 and 3. Given the limited time to carry out this work, it was decided to continue all of the Phase 2 tests for 30,000 cycles or 5 percent strain, whichever comes first. Table 6.4 presents details of the RSCSR test plan for Phase 1 and Phase 2.

Table 6.4. RSCSR test conditions

Test No	**Shear Stress, τ (kPa)**	**Stress Ratio**	**Temperature (°C)**
SST RSCSR Phase 1 (each test was replicated twice)			
1S	70	4.1	45
2S	100		
3S	130		
4S	70	2.5	55
5S	100		
6S	130		
SST RSCSR Phase 2 (each test was replicated once)			
7S	70	1	30
8S	100		
9S	130		
10S	70	2	
11S	100		
12S	130		
13S	70	3	
14S	100		
15S	130		

6.3.5. Data Analysis

The axial load generates a vertical stress and the torque develops complementary torsional shear stresses in the vertical and horizontal planes. The stresses acting on a specimen can be given by:

$$\sigma = \frac{W}{A} \tag{6.1}$$

$$\tau = \frac{Q}{A} \tag{6.2}$$

where W and Q are the applied axial and shear load;

A is cross-sectional area of the specimen;

σ is average vertical stress;

τ is the average shear stress.

Similarly, the permanent strains at the end of the test can be calculated using the following equations:

$$\varepsilon_z = \frac{\delta h}{H} \tag{6.3}$$

$$\gamma = \frac{u_{final} - u_{initial}}{H} \tag{6.4}$$

where δh is the change in height of the specimen;

$u_{initial}$ initial shear deformation at the start of the test (nominally zero);

u_{final} final recorded deformation by the shear LVDT at the end of the test;

H is specimen height (platen-to-platen measurement only);

ε is permanent vertical strain;

γ is permanent shear strain.

The principal stresses as well as rotation of principal axes can be calculated from the Mohr's Circle as shown in Figure 6.11. The normal stresses are considered as negative while compressive. The stress condition was characterised by the stress ratio, $\eta = \tau / \sigma$.

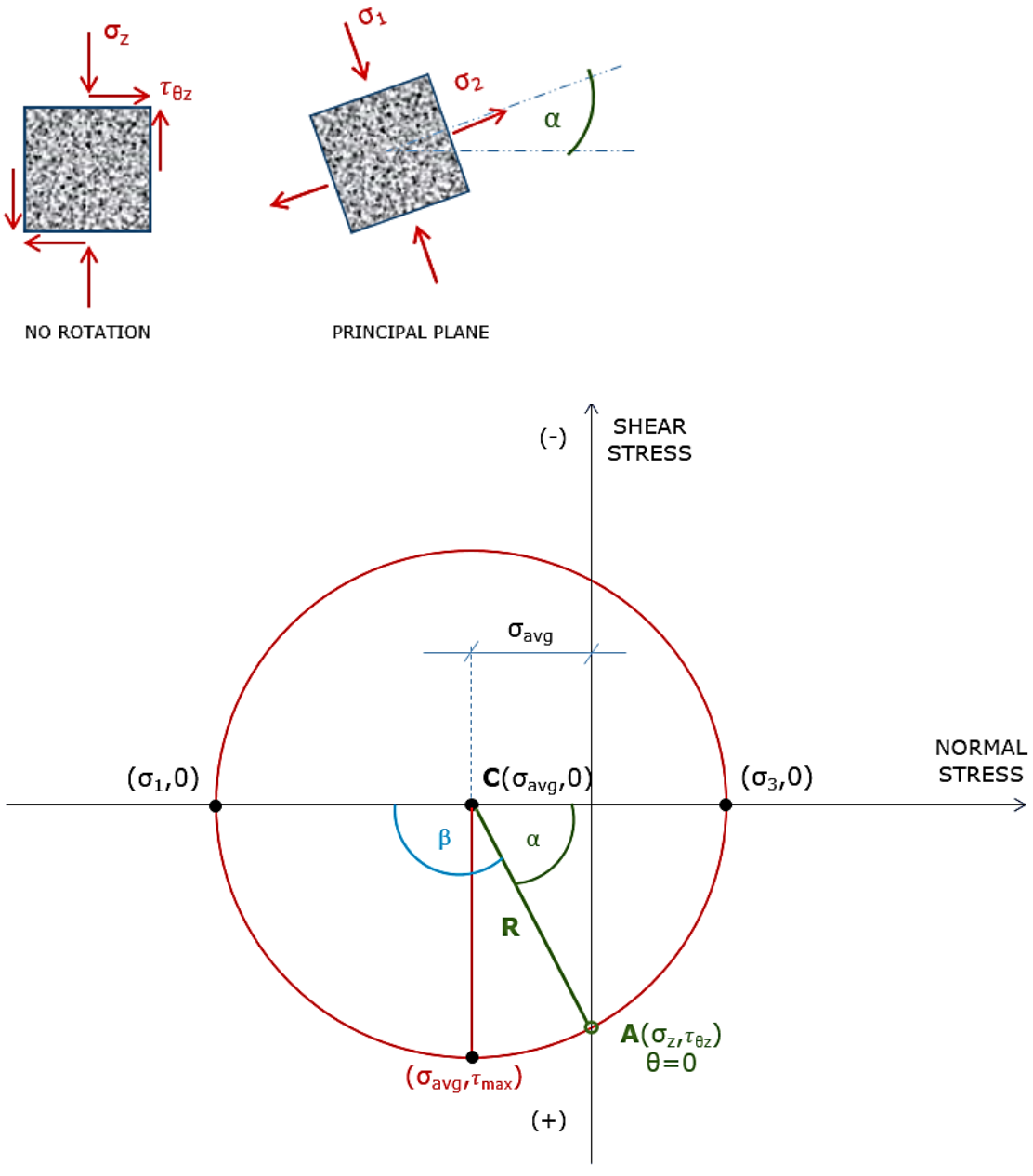


Figure 6.11. Principal stresses on the θ-z plane in the SST

6.3.6. Results of SST RSCSR

Each of the RSCSR tests provided a relationship between the permanent shear strain and the number of load repetitions. The results are grouped by temperature. The initial SST testing results obtained at 45°C and 55°C (Phase 1) are presented in Figures 6.12 and 6.13. In the analysis reported herein, one of the 18 tests is discarded because it gives values orders of magnitude above all others. The results indicate that stress level strongly affects the accumulation of permanent deformation. The tests executed at a shear stress of 130kPa exhibit much higher rate of accumulation of permanent deformation that those carried out at 100kPa and 70kPa.

An examination of the specimens after the SST-RSCSR test conducted at higher shear stress levels such as 130kPa and at a high temperature of 55°C reveals development of many cracks through the specimen (see Figure 6.14). This result is expected in view of the way that shear stress is applied to the test specimen, especially at high temperatures and/or at high loads. However, cracking can influence the measurements and its effects may be considered in the interpretation of the test results once the crack has formed (Monismith et al., 1994).

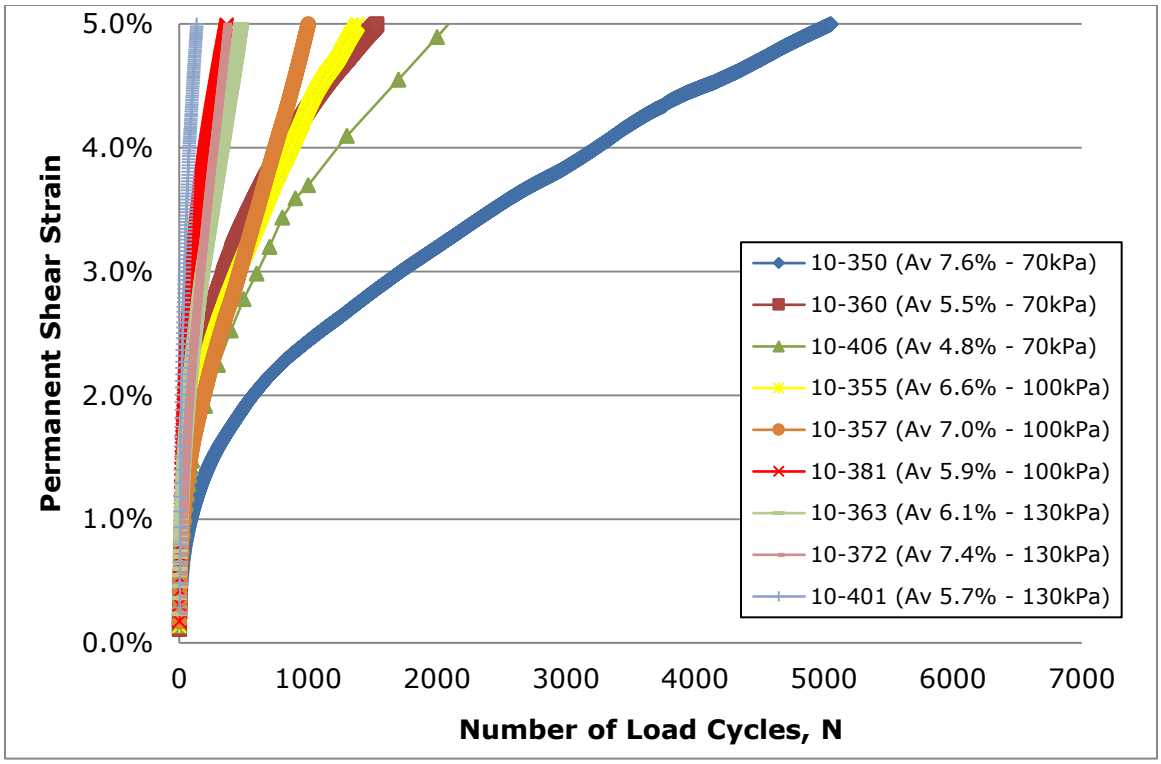


Figure 6.12. SST-RSCSR Tests: Stress Ratio 4.1 / 45ºC (Phase 1)

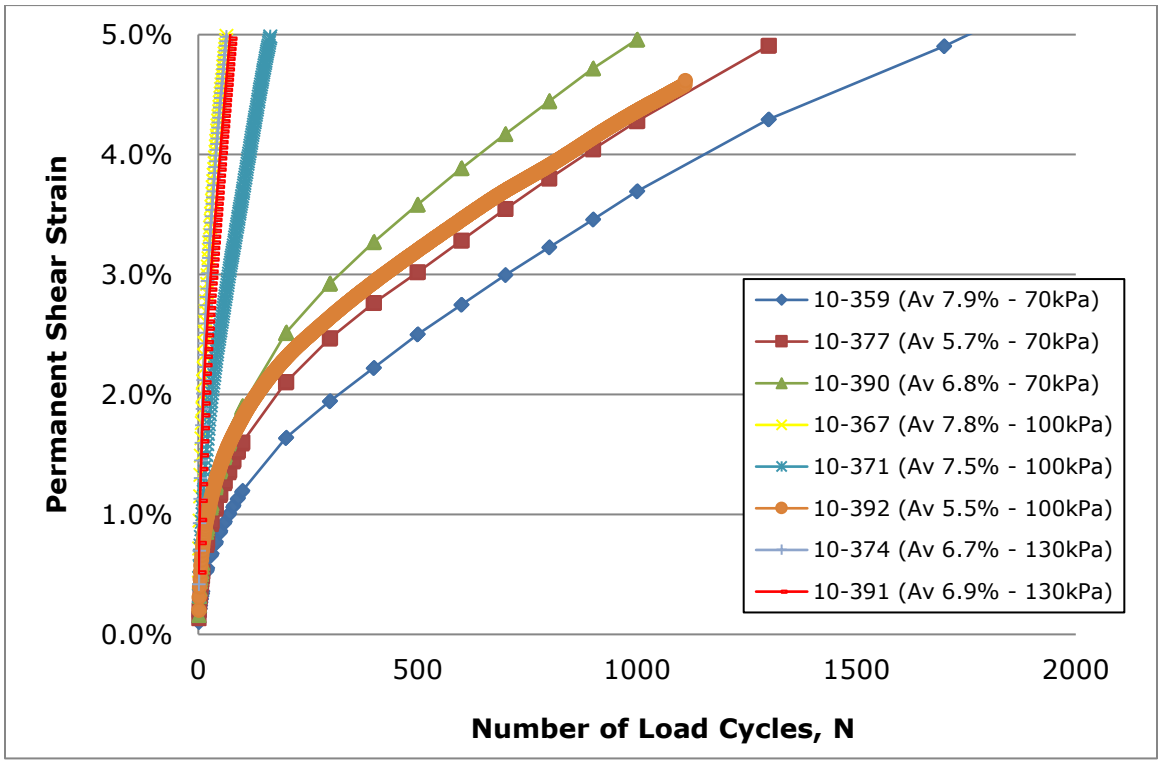


Figure 6.13. SST-RSCSR Tests: Stress Ratio 2.5 / 55ºC (Phase 1)



Figure 6.14. Cracks formed in the SST specimen tested at 130kPa shear stress at 55°C

The SST-RSCSR test plots, Figures 6.12 and 6.13, show also that there was no consistent effect of air void content on performance of the material. As seen in Tables 6.3 and 6.4 there are variations in the air void contents, stress ratios and temperatures, making comparisons of initial SST results almost impossible. This does not, however affect analysis, as the purpose of this testing was not to compare performance of the asphalt mixtures but to compare performance in the SST equipment with that in the HCA test.

The results from Phase 2 SST-RSCSR tests performed at 30°C are summarised in Figures 6.15 - 6.20, where the permanent strain is plotted against stress repetition. Similarly, to creep and RLAT tests, the strain curve can be divided into two regions (Sections 2.7.1 and 6.2.6). The initial high rate of deformation is attributed to the densification of the mixture without significant shear failure. The slope of the secondary region, in which the strain varies linearly with time, is defined as the steady-state strain rate at the prescribed stress, in line with the prescription of Ossa et al., (2006) and Taherkhani, (2006). During this deformation phase, repeated loads densify the mix, developing better aggregate interlock and improving shear stiffness. It can be seen from the figures that the characteristic shape of the curve obtained for most of the samples is similar, particularly over the linear phase.

The data in Figures 6.15 - 6.17 show the effect of stress ratio, SR, on the resistance to permanent deformation. The results for each of the specimens are grouped by shear stress magnitude. The experiments, as in the HCA tests, involved shear stresses of 70, 100 and 130kPa. During the 30,000 load repetitions of the SST test, most of the specimens failed to enter the tertiary stage at which excessive deformation develops. The tertiary region can clearly be seen only in Figure 6.15 where specimens 11-447 and 11-483 reaches failure range. This can occur when the air void content falls below some critical value after which the binder starts acting as a lubricant between the aggregates, pushing particles apart. However, as this behaviour is only observed for high stress ratio value of SR=3 (relatively high shear stress vs.

low axial stress), at this loading condition, a significant increase in permanent shear strain appears to be associated with shear failure of the asphalt mixture. The presence of tertiary rutting also indicates that the mixture is very unstable under high shear stress conditions (Chowdhury and Button, 2002).

For stress ratio values of SR=1 & SR=2, the asphalt mixture exhibits similar response characteristics. However, the highest shear strain resistance is observed for stress ratio value of SR=2. These experiments indicate that, for the combined mode of loading, the magnitude of permanent shear strain can be affected by the axial stress level. It is evident that axial stress is one of the major factors affecting development of permanent deformation. This data highlights the importance of selecting the proper stress state for laboratory evaluation to ensure that it is representative of that which occurs insitu.

The data have been plotted in another way to illustrate the effect of shear stress magnitude, τ, on the SST results. This is shown in Figures 6.18 - 6.20 where results are grouped by stress ratio. For a stress ratio values of SR=1 and SR=2, as was to be expected, an increase in the permanent shear strain is obtained as shear stress level increased.

However, Figure 6.20 indicates that for a high stress ratio value of SR=3, the magnitude of permanent shear strain in specimens tested under these stress conditions, was generally greater than for stress ratio values of SR=1 & SR=2. Similar behaviour is shown in Figure 5.21 for the HCA tests. As discussed

before in Section 5.6, when axial stress is relatively low but at the same time shear stress is great enough, the confining effect of axial compressive stress can be overshadowed. At this state of stress, the mixture became unstable and the load magnitude does not appear to influence the permanent strain with a similar trend. This can be possibly associated with the development of internal damage of the material as a consequence of the high shear strains and gradual loss of aggregate interlock.

As can be seen in Figures 6.17 and 6.20, there is a lack of data points for specimen 11-471 tested at high stress levels. This is due to the rapid specimen failure at those conditions.

For design purposes, it would be sensible to avoid the critical states of stress that intensify rutting. This can be achieved by using materials more resistant to permanent deformation and/or by controlling loading conditions either by varying the pavement structure or the vehicular characteristics (e.g. tire pressures). Francken, (1977) found that for each mixture, there is a state of stress and temperature above which it becomes unstable (i.e. permanent deformation develops at an accelerating rate). He also identified a threshold in the stress field above which a given mixture exhibits premature failure. From these data, he developed a modified deformation law model relating axial permanent deformation under creep loading to state of stress, frequency of loading, and temperature (Francken et al., 1987).

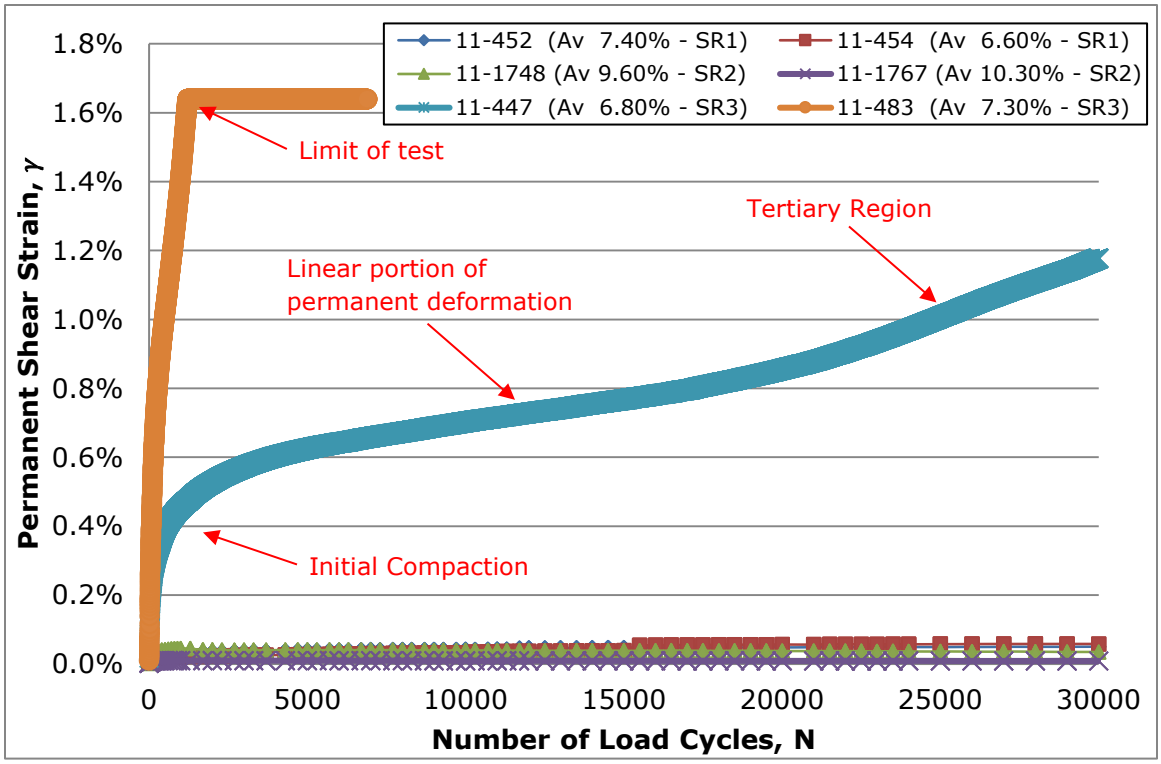


Figure 6.15. The effect of SR on permanent deformation for τ=70kPa

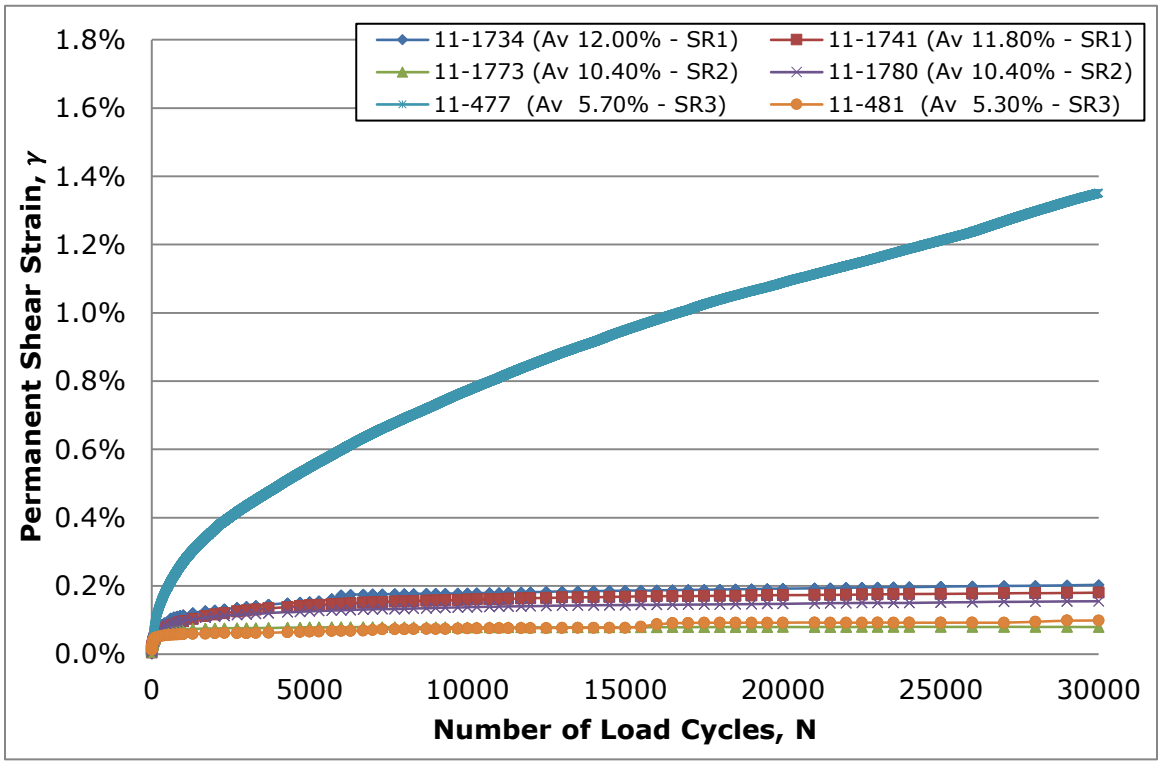


Figure 6.16. The effect of SR on permanent deformation for τ=100kPa

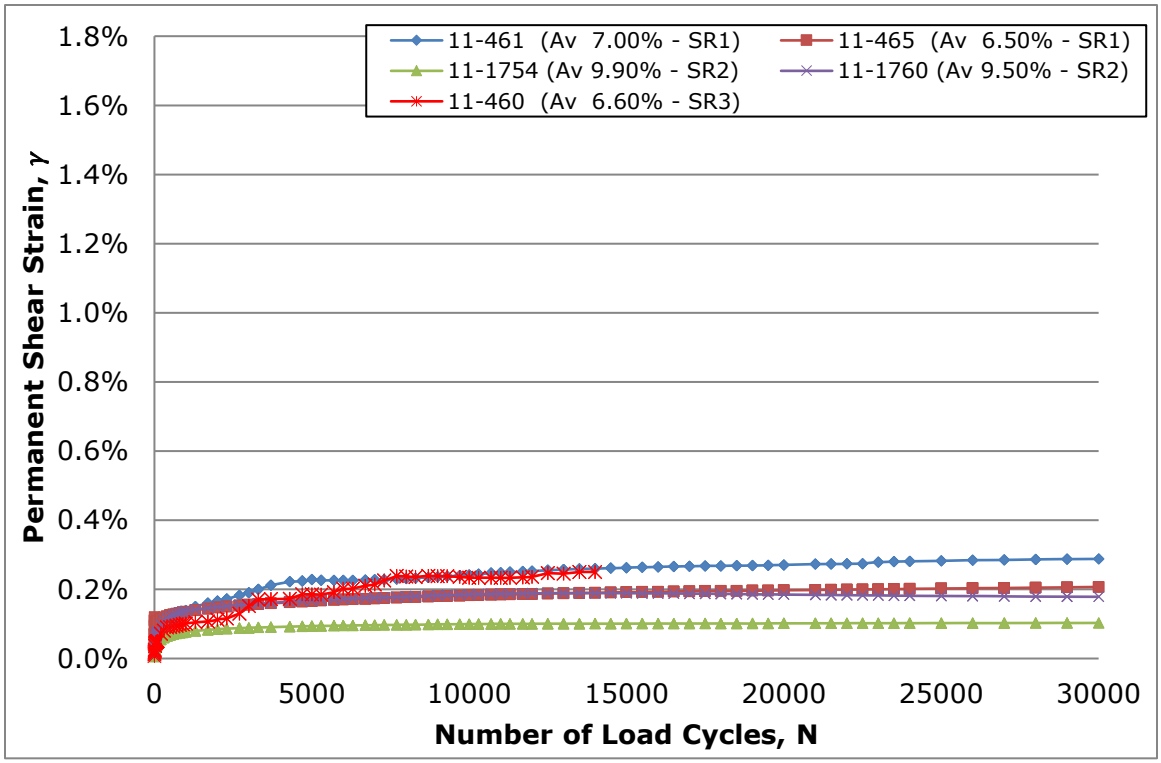


Figure 6.17. The effect of SR on permanent deformation for τ=130kPa

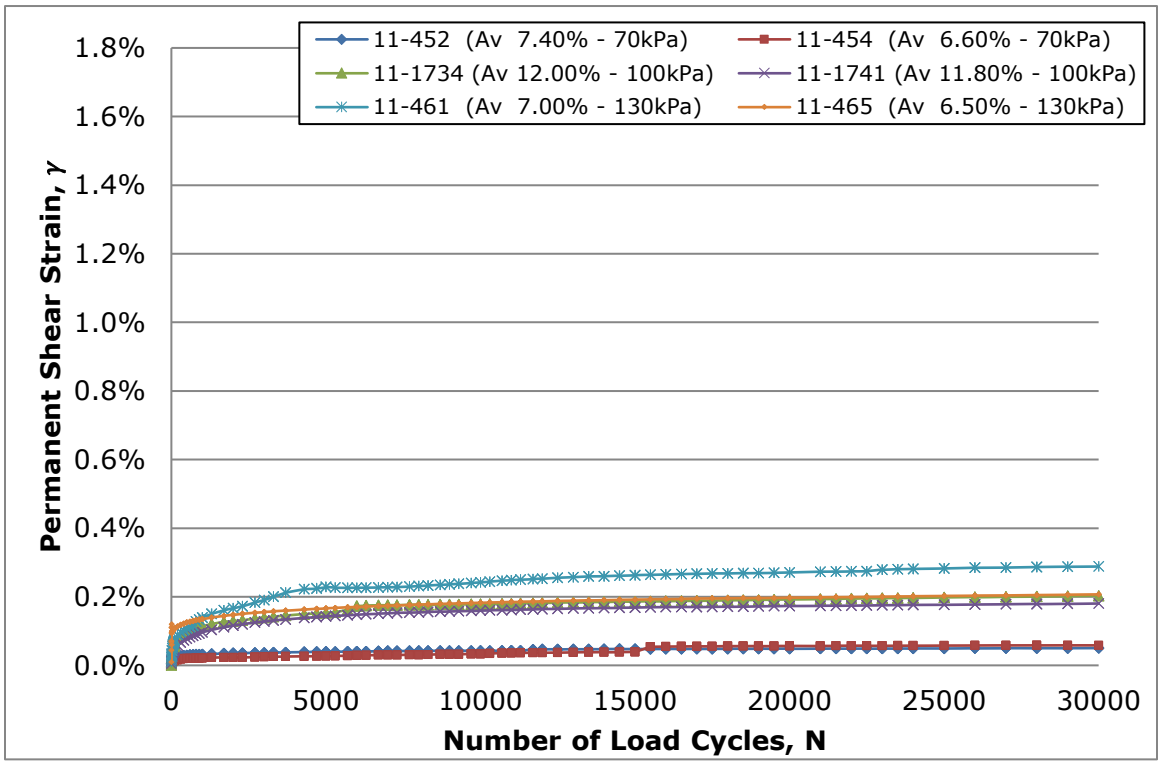


Figure 6.18. The effect of τ on permanent deformation for SR=1

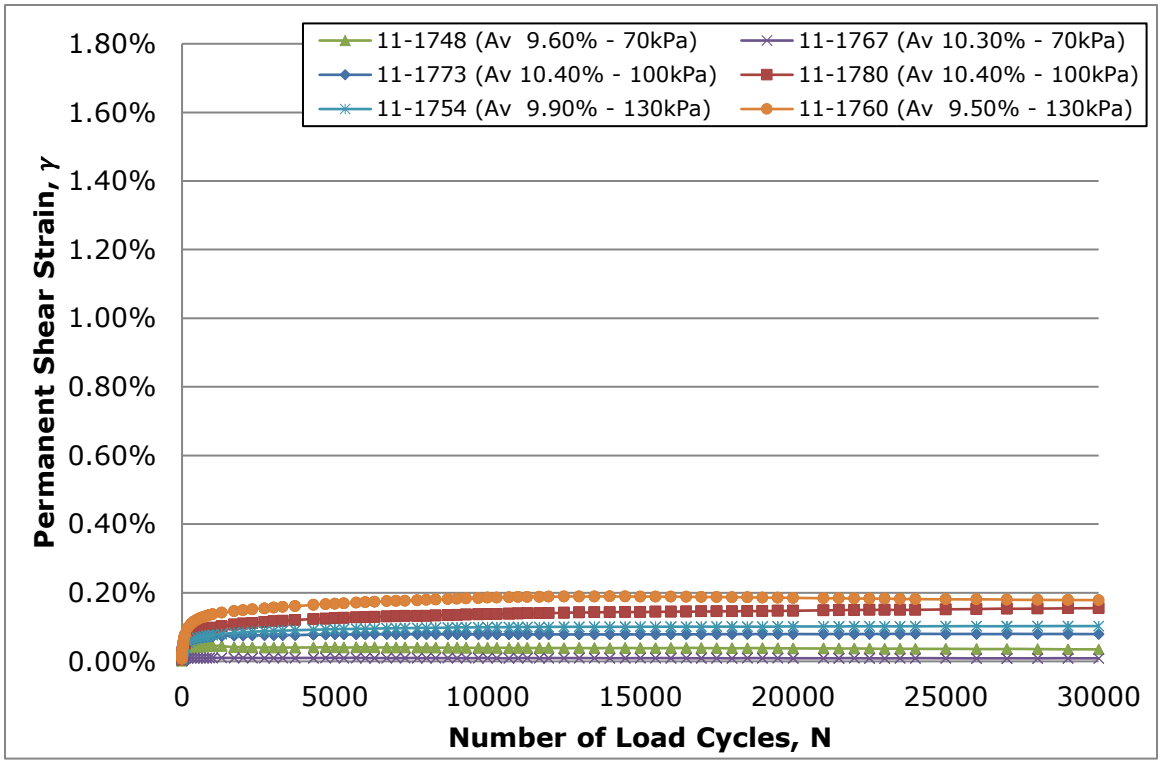


Figure 6.19. The effect of τ on permanent deformation for SR=2

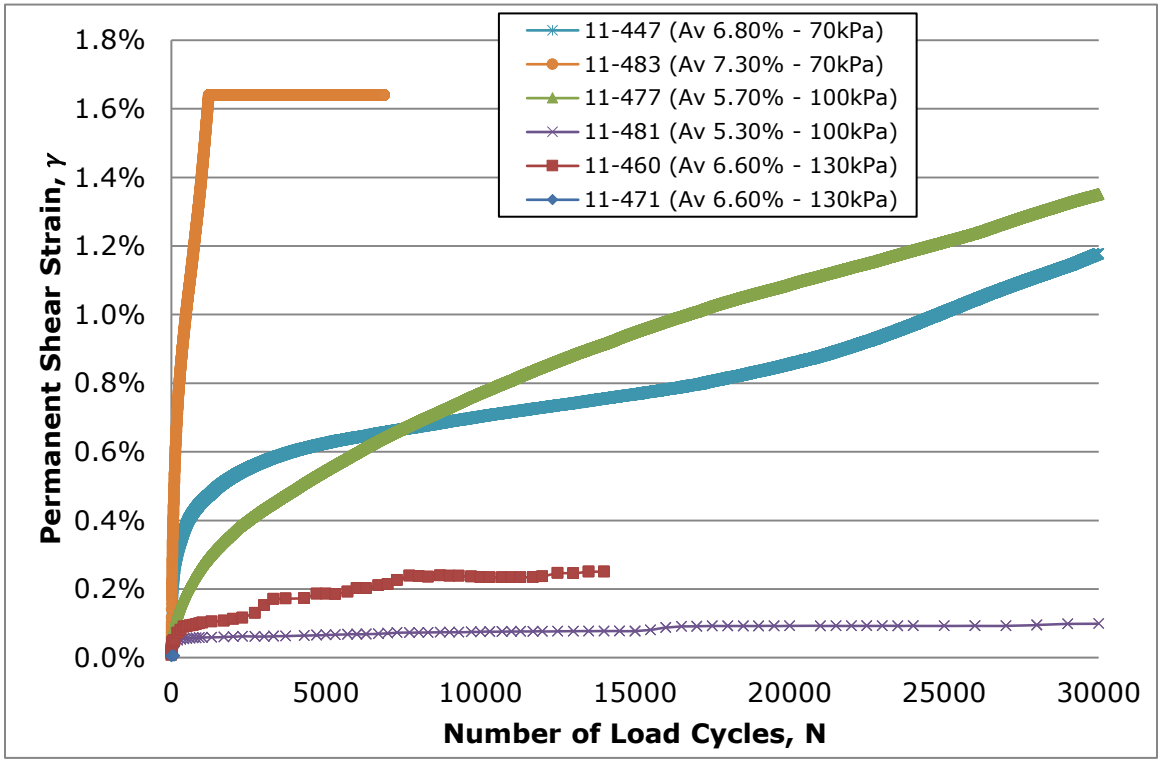


Figure 6.20. The effect of τ on permanent deformation for SR=3

Figures 6.21-6.23 illustrate the variation of axial strain with load repetition. Figures 6.21 and 6.22 show the effect of combined (shear and axial) loading on the values of permanent axial strain and the results are grouped by stress ratio. Comparison of the strain values indicates, that permanent axial strain was dependent on applied shear stress level. Higher axial permanent deformation was recorder for higher shear stresses. This can be a sign of shear dilatancy phenomenon which was also investigated by Alavi, (1992).

The results for high stress ratio of SR=3, are not shown because most of the samples appeared to fail very soon after starting the test.

It can be seen, that at the same shear stress level, the related permanent axial strain rate is lower for higher stress ratio (Figure 6.23). As expected, this shows that permanent axial deformation is dependent on the axial stress magnitude. The decrease in axial stress magnitude resulted in lower permanent axial strain.

Figure 6.21 to 6.23 also indicate that the deformation behaviour of the asphalt mixture at particular stress conditions is similar in shape. After 30,000 load cycles the permanent axial strain obtained in these tests is predominantly very low, with the maximum value below 0.38%.

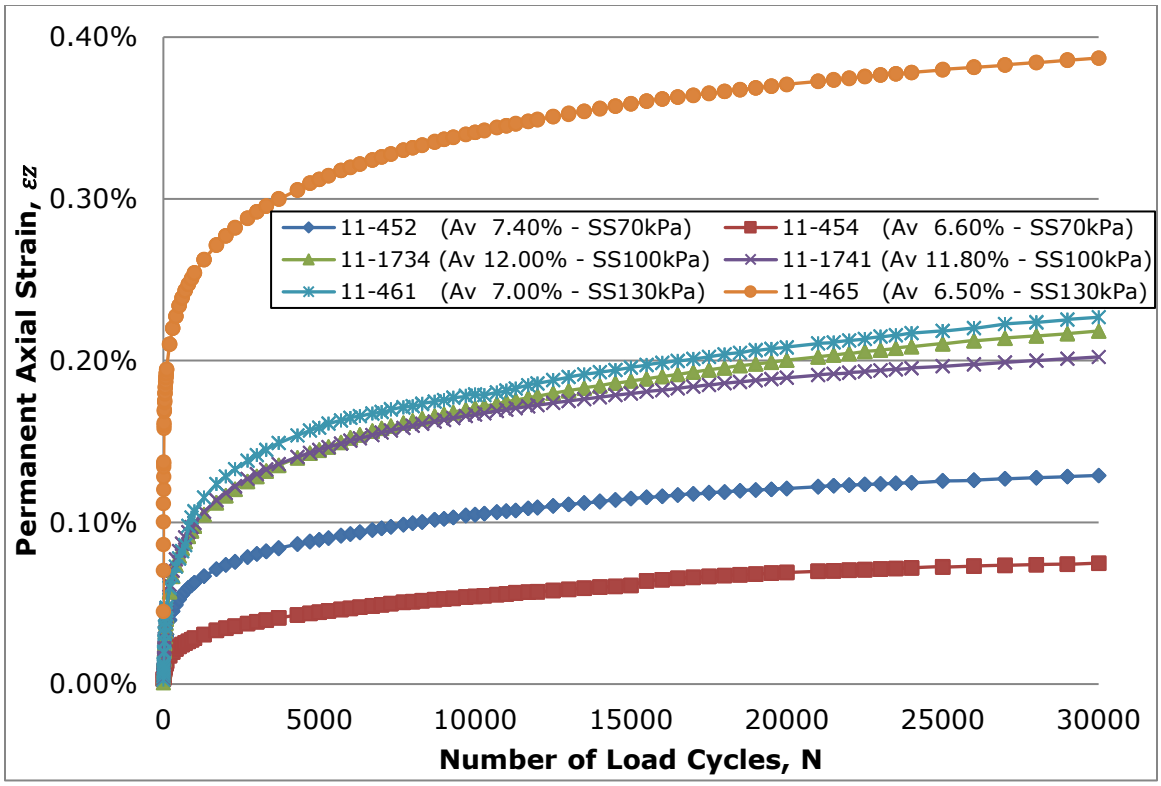


Figure 6.21. The effect of τ on permanent deformation for SR=1

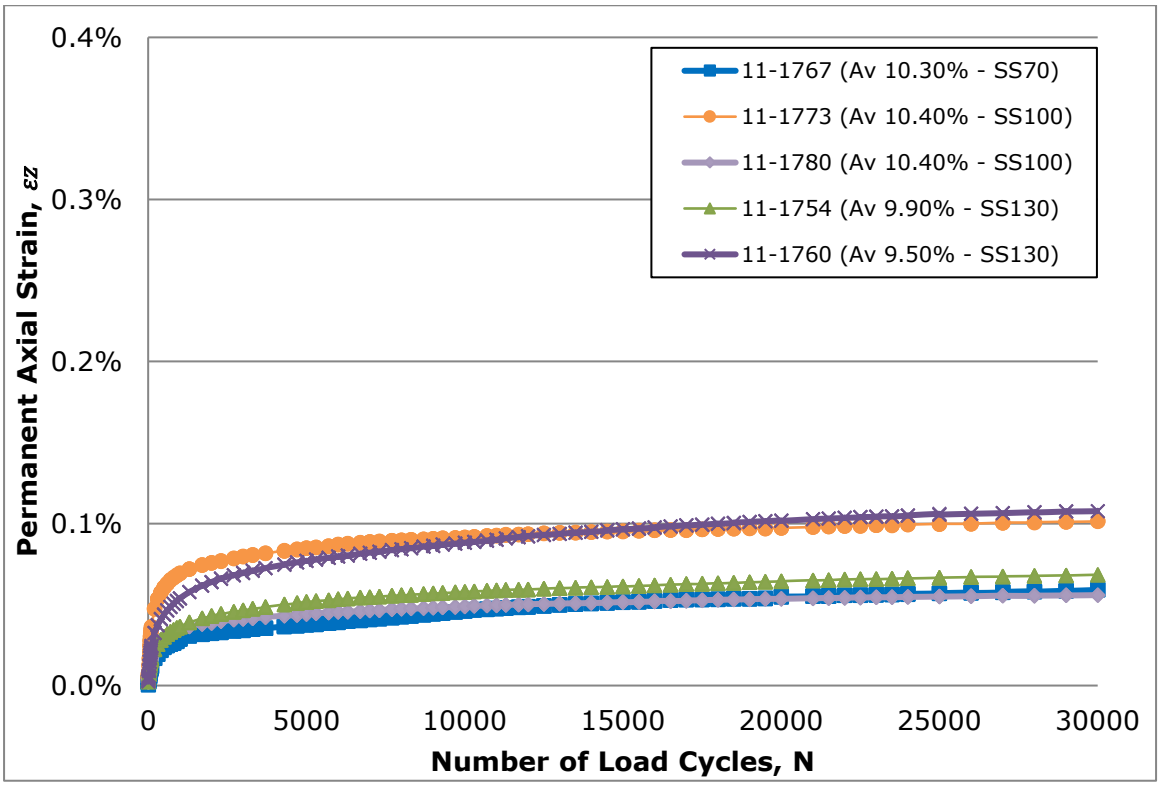


Figure 6.22. The effect of τ on permanent deformation for SR=2

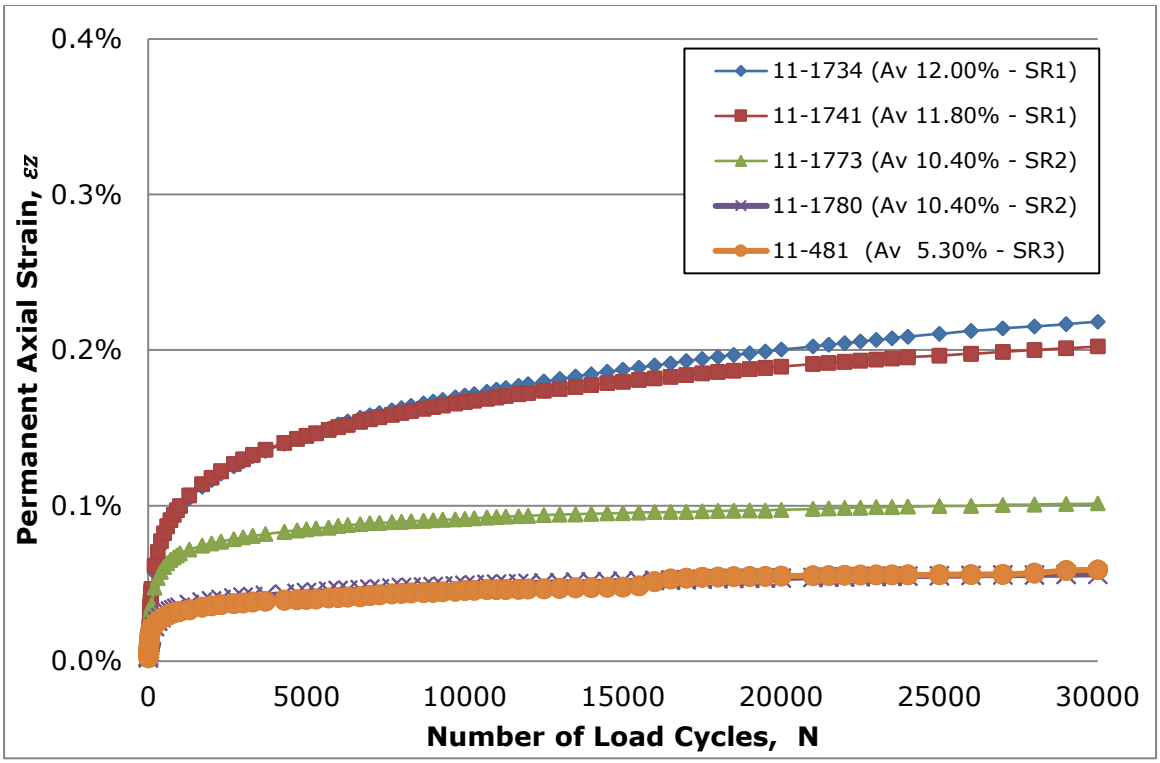


Figure 6.23. The effect of SR on permanent deformation for τ=100kPa

Lastly, the plots also show that the air void content does not significantly affect the asphalt mix performance. These results seem to be in contradiction with results from many studies indicating that the performance of asphalt is strongly dependent on density of a mixture (see Section 2.6.2). The reason for this is not fully understood and it is recommended to investigate the issue in the future HCA research programme.

6.4. Summary

SST and RLAT tests were conducted using conditions similar to the conditions used in the HCA tests. The following summarises important findings of the study:

- For the same state of stress, the shape of strain curve obtained for most of the samples is similar, particularly over the linear phase.
- As expected, permanent deformation increases with load levels which was confirmed by both test methods.
- SST results show that for a stress ratio values of SR=1 and SR=2, as was to be expected, an increase in the permanent shear strain is obtained as shear stress level increased. However, for a high stress ratio value of SR=3, the magnitude of permanent shear strain in specimens tested under these stress conditions, was generally greater than for stress ration values of SR=1 & SR=2. Similar behaviour is shown in Figure 5.21 for the HCA tests. This indicates that when axial stress is relatively low but at the same time shear stress is great enough, the confining effect of axial compressive stress can be overshadowed.
- The SST reveals that at high stress ratio (SR=3), mixture became unstable and the load magnitude does not appear to influence the permanent strain with a similar trend. This can be possibly associated with the development of internal damage of the material as a consequence of the high shear strains and gradual loss of aggregate interlock. Therefore, the results may be unreliable.

- At this state of stress, the load magnitude does not appear to influence the permanent strain in a similar trend. This is not the case in the RLAT, therefore clearly this is associated with effect of combined axial and shear load conditions. This may suggest that the SST test for estimating rutting is more reliable under lower stress conditions and lower stress ratios.
- Comparison of the strain values indicates, that permanent axial strain in SST was dependent on applied shear stress level. Higher axial permanent deformation was recorder for higher shear stresses. This can be a sign of shear dilatancy phenomenon which was also investigated by Alavi, (1992).
- The effect of stress ratio on the axial permanent strain in SST was shown, indicating that the strain rate increases, with lower stress ratio (Figure 6.23). As expected, this shows that permanent axial deformation is dependent on the axial stress magnitude. The decrease in axial stress magnitude resulted in lower permanent axial strain.
- The RLAT plot indicates that the specimens with higher densities (lower voids) perform better than the less dense mixes.
- The effect of air voids is less clear from the SST. The plots show that the air void content does not significantly affect the asphalt mix performance. However, this seems to be in contradiction with results from the RLAT and earlier studies (Chapter 2) that have found that the aggregate structure is important, and the asphalt performance is strongly dependent on density of a mixture. The reason for this is not

fully understood and it is recommended to investigate the issue in the future HCA research programme.

In Chapter 7 the results from these tests are assessed and discussed in the context of the HCA data.

7

DISCUSSION AND COMPARISON WITH HCA

7.1. Introduction

The results of the tests carried out in the three testing machines are presented in Chapters 5 and 6. With the aim of evaluating the use of the HCA as a means of providing precise information on permanent deformation of asphalt mixture response representative on insitu conditions, tests were carried out over a range of shear stresses and stress ratios at 30°C. Chapter 5 contains the HCA test program and presents the results of this testing. Chapter 6 presents experimental work and results from RLAT and SST tests carried out at NTEC and at UCB, respectively. Both of the tests used selected stresses that simulated as closely as possible the HCA conditions, in order to provide a comparison between the results of these routine performance tests and the data obtained from the HCA. Consequently, only discussion of results from all the tests carried out during this project is presented below.

HCA tests provided essential results to validate the more widely used rutting prediction laboratory tests and future pavement modelling. Data derived from

the RLAT and SST are further analysed in this chapter and compared to the HCA measurements. The conclusions will be presented in Chapter 8.

7.2. Permanent Shear Strain

Data for an accumulation of permanent shear deformation with load cycles obtained from the HCA and SST tests in axial and shear repeated loading have already been presented in Figures 5.21-5.22 and 6.15-6.20. Both tests were carried out under as close as possible stress conditions. These data suggest that under most conditions considered, the permanent shear strain increases gradually with the number of load cycles.

It should be noted, however, that in specimens tested in the SST at a high stress ratio of SR=3, the mixture became unstable and the load magnitude does not appear to influence the permanent strain with a similar trend. This can be possibly associated with the development of internal damage of the material as a consequence of the high shear strains and gradual loss of aggregate interlock. Therefore, the results may be unreliable.

A comparison between Figures 5.21 - 5.22 and 6.15 – 6.20 shows that large differences are obtained for the permanent shear strain rates and the shear strain magnitudes obtained from the HCA are found to be much higher. This shows apparent discrepancy between these tests. The following observations are made:

- The results grouped by stress ratio illustrate that the accumulation of permanent shear strain is dependent on the shear stress magnitude. It is clear that higher shear stress increases the permanent shear strain.
- At low shear stress levels of 70kPa, a greater rate of accumulation of permanent strain is observed, as the stress ratio is increased from 1 to 3 due to the lower normal stress. However, this is not evident in the tests carried out at shear stress levels of 100kPa and 130kPa. Similarly, SST results show that for a stress ratio values of SR=1 and SR=2, as was to be expected, an increase in the permanent shear strain is obtained as shear stress level increased. However, for a high stress ratio value of SR=3, the magnitude of permanent shear strain in specimens tested under these stress conditions, was generally greater than for stress ration values of SR=1 & SR=2. This shows that the effect of compressive axial stress on permanent shear strain is greater when the shear stress is relatively low. However, when specimens are subjected to very high shear stress, it appears that increase in permanent shear strain is mainly attributed to shear deformation and the effect of axial compressive stress on permanent shear strain is negligible. Similar conclusions were drawn by Alavi, (1992).

- The SST reveals that at high stress ratio (SR=3), the mixture became unstable and the load magnitude does not appear to influence the permanent strain with a similar trend. This can be possibly associated with the development of internal damage of the material as a consequence of the high shear strains and gradual loss of aggregate

interlock. At this state of stress, the load magnitude does not appear to influence the permanent strain in a similar trend. This is not the case in the RLAT, therefore clearly this is associated with effect of combined axial and shear load conditions. This may suggest that the SST test for estimating rutting is more reliable under lower stress conditions and lower stress ratios.

- Both HCA and SST, showed that the application of lower normal stress (high stress ratio), results in higher accumulation rate of permanent shear strain. This indicates that axial compressive stress had a confining effect on the accumulation of permanent shear strain.
- These experiments indicate that, for the combined mode of loading, the magnitude of permanent shear strain can be affected by the axial stress level. It is evident that axial stress is one of the major factors affecting development of permanent deformation. This data highlights the importance of selecting the proper stress state for laboratory evaluation to ensure that it is representative of that which occurs insitu. Also, any current pavement performance prediction models must be calibrated using realistic strain paths as they occur insitu.
- In view of these results, it seems questionable whether the SST is a suitable tool for investigation rutting characteristics of asphalt mixtures.
- Furthermore, both the HCA and SST results seem not to be influenced by air void content, as demonstrated in Figures 7.1 and 7.2. Despite the void differences between specimens being as much as 6 percent, no consistent effect of densification on the mixture performance was found.

These results are not untypical and are consistent with data reported by Gibb (1996) which also show little or no effect of air voids on performance of materials tested in the RLAT.

Figure 7.3 compares SST and RLAT Mohr's circle. SST tests carried out at a stress ratio value of SR=1 and axial stress levels of 100kPa is plotted versus RLAT carried out at the same axial stress level of 100kPa. In RLAT only a maximum shear stress at 45° to the principal planes can be calculated from the Mohr's circle, and the effect of rotation of principal plane on the permanent shear deformation cannot be investigated. Also, both tests do not have ability to measure the lateral stress on the specimen, therefore the complete stress regime is unknown. This makes fundamental interpretation of test results difficult. Moreover, stress conditions in both tests are very different, making a direct comparison of results very difficult and almost meaningless.

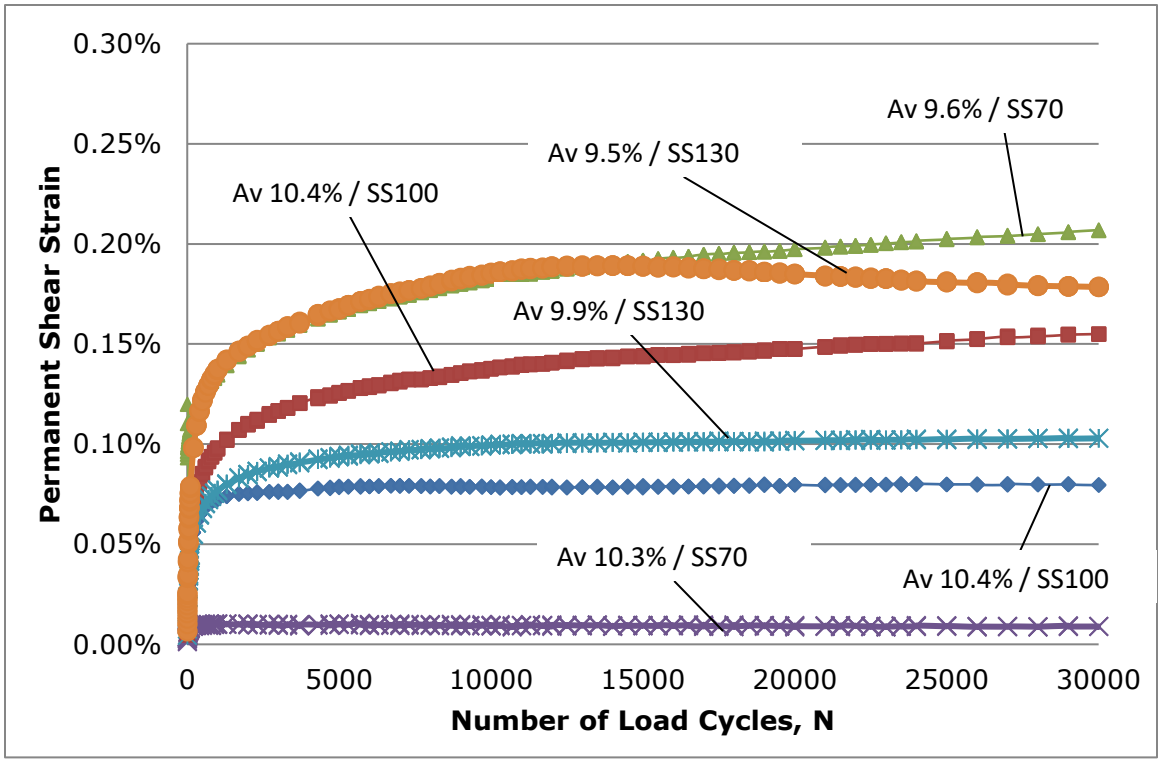


Figure 7.1. Variation in void content and performance: SST SR=2

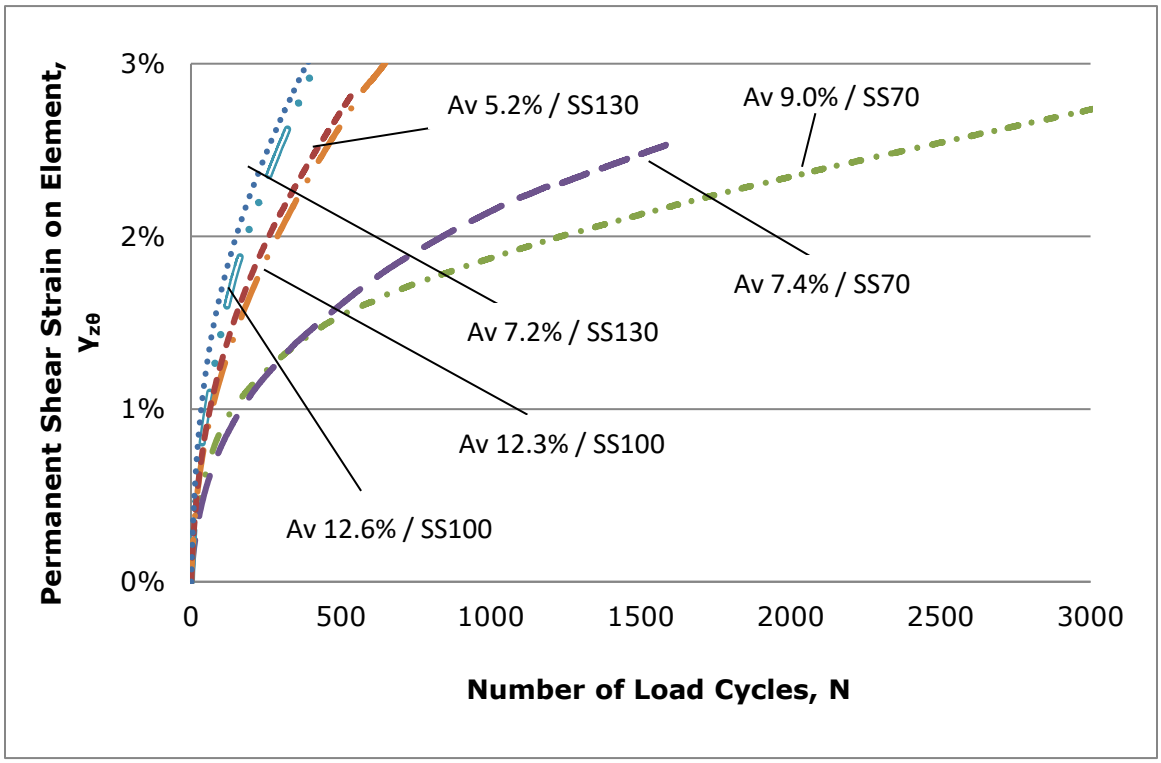


Figure 7.2. Variation in void content and performance: HCA SR=1

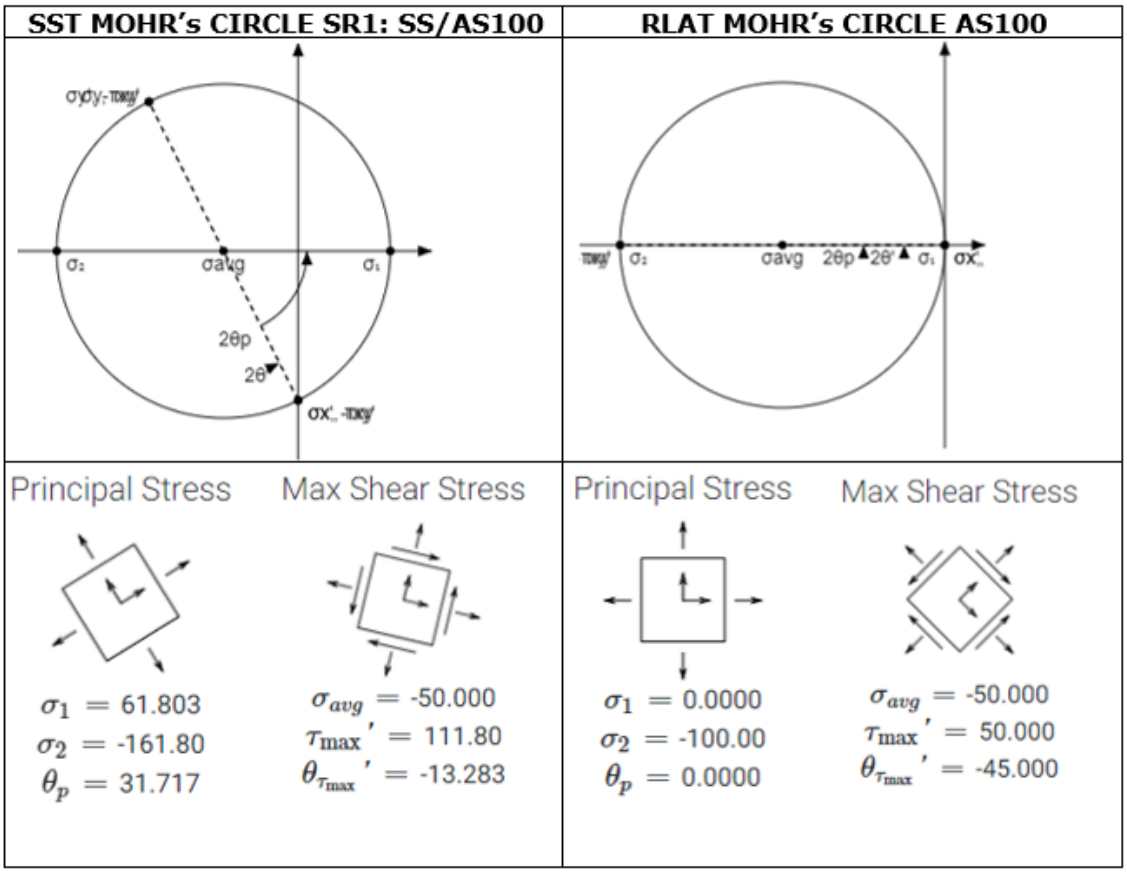


Figure 7.3. SST at SR=1 vs RLAT Mohr's Circle

The results highlight again the importance of the contribution to rutting of shear stresses. Also, as discussed in Section 2, in densely compacted pavements, shear stresses are largely the cause of permanent deformation in the upper asphalt layers. Although many researchers recognised that shear stress is the main mechanism causing rutting, suitable laboratory test methods and theoretical models are not yet available for properly treating shear induced permanent deformation (Monismith et al., 1994). As discussed in Section 2.9, both layer-strain and viscoelastic methods are presently used for predicting permanent deformations in pavements. The layer-strain method

is considered a simplified engineering theory for predicting rut depth which allows use of either linear or nonlinear elastic theory together with the permanent deformation characteristics of asphalt mixtures. Nonlinear viscoelastic models are more realistic than linear viscoelastic models for predicting permanent deformations but, because of mathematical complexities and difficulty in defining an appropriate material model, the linear model is most frequently used. Also, the viscoelastic method has not been shown to be more accurate in estimating permanent deformations observed in pavements in situ (Sousa et al., 1991).

Current analytical models focus on the rut depth under the centre line of loading and do not consider the contribution to rutting of shear stresses at the edges of the tires. Moreover, analytical models differ greatly in their estimation of the variation of permanent strain with depth beneath the pavement surface and theoretical predictions of the distribution of permanent deformation with depth fail to match test track and field measurements.

However, in order to estimate rutting resistance accurately, a model should be developed that directly takes into account the shear stresses developed within the entire zone of permanent deformation, extending outward from the centreline of loading at least to the tire edges. This can be achieved using a finite element technique.

Available analytical models rely on some form of axial compression, either creep or repeated loading tests. Brown and Bell (1977 and 1979) compared theoretically predicted rut depths using the layer-strain approach with those measured in the Nottingham Test Track. Comparisons between predicted and measured total displacements generally indicated reasonable agreement. However, in the cases where upheaval occurred, the prediction was not as good. Material properties were measured using the repeated load triaxial test. Thrower (1978) suggested that the triaxial test is not suitable for investigating materials in the upper layers of asphalt concrete pavements because it cannot duplicate the states of stress that are encountered near the load.

It is required to extend the states of stress under which permanent deformation characteristics of materials are measured in the laboratory to duplicate the states of stress that are encountered within the entire rutting zone, in particular where the shear stresses are relatively greater that normal stresses. Therefore, the new HCA capable of directly applying shear stresses, appears to be more suitable to investigate asphalt rutting properties, which could be then used to modify current rutting prediction equations. More experimental work is required to obtain regression permanent deformation parameters from HCA and field calibrate them.

7.3. Permanent Axial Strain

In order to allow direct comparison of the stress-strain behaviour of the asphalt specimen tested under HCA stress conditions with that tested under RLAT and SST stress conditions, a plot of permanent axial strain accumulating in the HCA against the number of load cycles is shown in Figure 7.4. The results of HCA tests number 9, 12, 21, 22, 15 and 4 are included to be evaluated against the six tests carried out in the RLAT (Figure 6.4). Figure 7.5 illustrates the permanent axial strain results for the SST tests. The results show that permanent axial strain was dependent on different stress levels. An increase in axial stress, resulted in a higher rate of permanent axial deformation in all three tests. However, it can be seen that under the HCA stress conditions, the specimen experienced dilation. Alavi, (1992) also reported that, for the combined mode of loading, the magnitude of permanent axial strain can be affected by shear dilation. Therefore, it is recommended that future HCA research should study shear dilatancy effect on permanent axial stress development in more detail and this phenomenon must be included in new rutting prediction models.

The specimens tested under RLAT and SST conditions, exhibit similar response characteristics, as shown in Figure 7.6. The plot includes SST results from tests carried out at a stress ratio value of SR=1 in order to match normal stresses applied in the RLAT. None of the tests reaches the tertiary phase at which excessive deformation develops. However, the results show that more axial deformation occurs in the RLAT than in the SST. After 30,000 load cycles

the permanent axial strain obtained in the SST is predominantly very low, with the maximum value below 0.4%. This finding implies that the SST provides improved resistance to axial permanent deformation caused by the combined mode of loading. This can be a sign of shear dilatancy phenomenon. Also, the specimen is so confined that in reality there is a quite large horizontal stress generated within the specimen due to the end restraints.

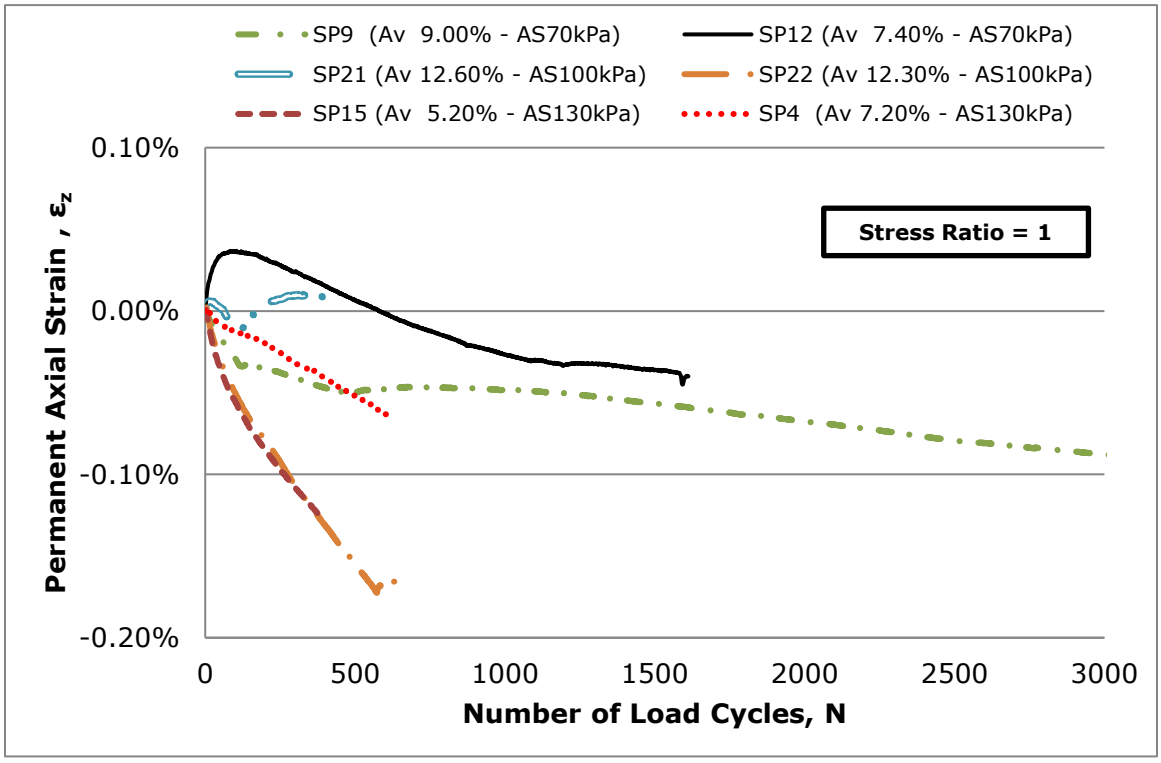


Figure 7.4. Variation of permanent axial strain with load repetition in the HCA

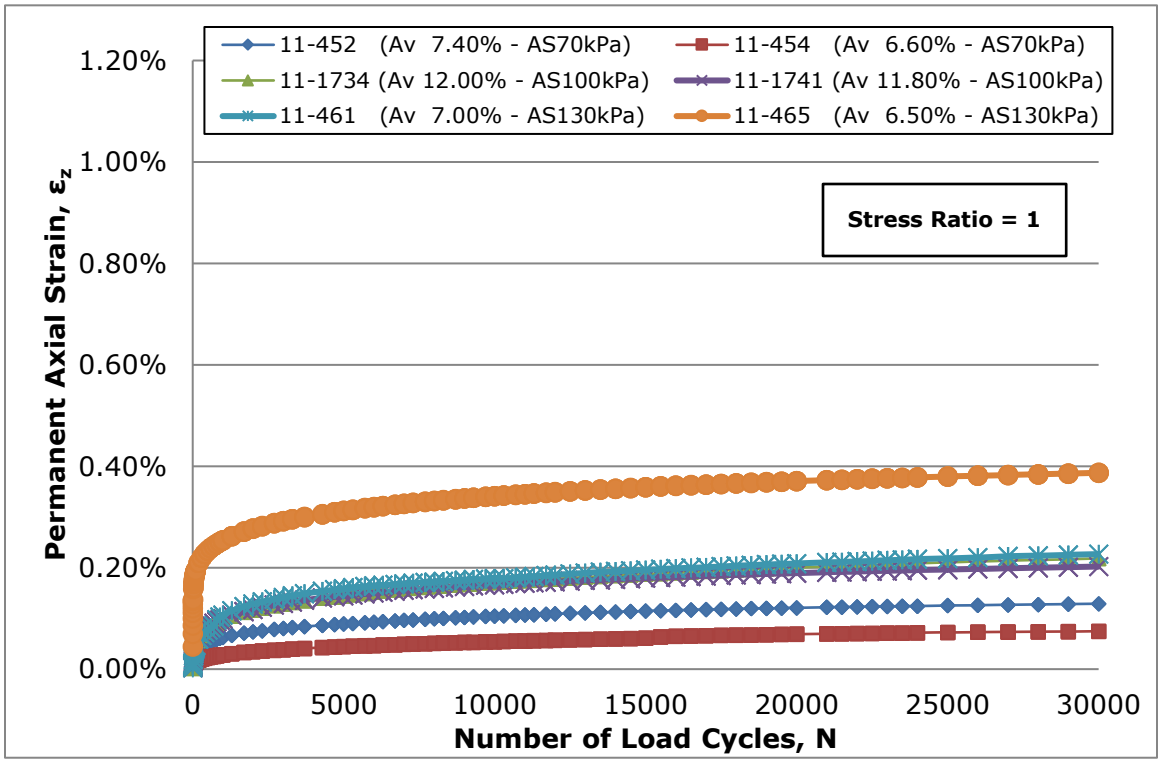


Figure 7.5. Variation of permanent axial strain with load repetition in the SST

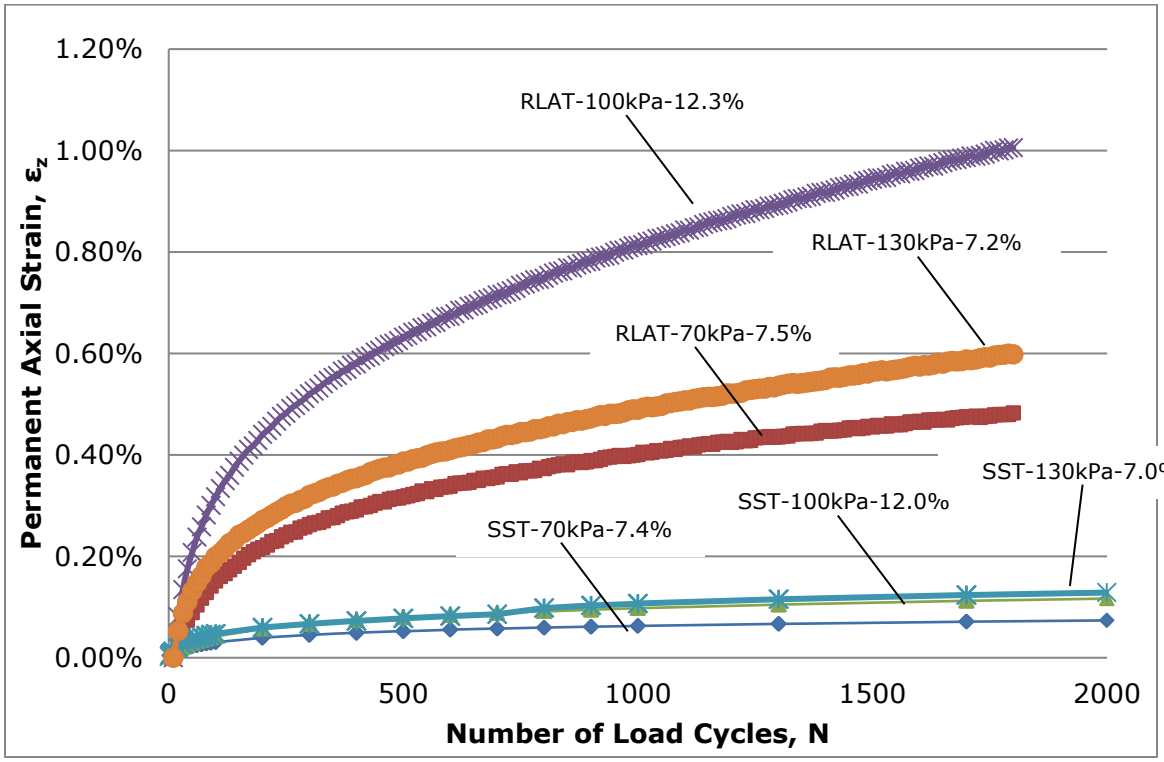


Figure 7.6. Variation of permanent axial strain with load repetition: RLAT vs SST at SR=1 (Key: RLAT/SST-Axial Stress-Air Voids)

7.4. Volume Change Characteristics

It can be seen that the application of a shear stress to the HCA specimen results in dilation (Figure 5.23). Similar conclusions were drawn by Alavi, (1992) and Sousa et al., (1994), who found that mixes may dilate when subjected to shearing deformations. This shows that dilation is an important phenomenon, which should be taken into account in any modelling efforts, if accurate predictions of rutting are to be made. Taherkhani, (2006) reported that ignoring the dilation behaviour of the mixtures causes inaccuracies for prediction of asphaltic mixtures in real pavements.

Analyses of the data from the HCA tests indicate that the permanent axial strain path varies considerably with the magnitude of stresses applied. However, because of the limited number of tests, it is difficult to draw any definite conclusions about their influence. It can also be observed that for low stress conditions, a resulting strain exhibits both compression and dilation. These data highlight the importance of selecting the proper stress state for laboratory evaluation to ensure that it is representative of insitu conditions.

The radial strain was not measured in the SST and RLAT, therefore estimation of volume change was not possible. This did not allow comparison to be made between the HCA and the other two tests.

7.5. Summary

In this chapter, the results of the laboratory investigation have been discussed. This research reveals discrepancies between the RLAT, SST and HCA tests. The literature review stressed the importance of the effect of shear stresses on the accumulation of permanent deformation and the results of this study confirm that better characterisation of the shear properties of asphalt concrete is necessary if accurate predictions of rutting are to be made. It was observed that permanent strain increases with load applications and it is dependent on the applied shear loads.

Additional BISAR modelling, as per Section 3.2.1, confirmed that states of stress in the upper part of the pavement near the tyre edge could best be defined with a test where both the normal and shear stresses could be controlled independently of each other. An axial loading test, such as the RLAT, is not sufficient to duplicate insitu stress conditions in such a manner as to directly measure their influence.

All the above suggests that a laboratory test which measures shear deformations beyond the centre of the loaded area, particularly important near the tire edges, can more accurately simulate insitu loading condition. Also, it is crucial to use an apparatus that can test asphalt mixtures under combined axial and shear loading mode, as both SST and HCA experiments indicated that axial stress plays key role in permanent deformation development when such stress state applied. The data obtained can be used

to develop accurate methodologies for pavement rutting prediction, which are crucial for decision support in pavement design.

The HCA results provide considerable evidence for the dilation phenomenon, which was also observed by other researchers (Alavi, 1992, Monismith et al., 1994). Most of the specimens increase in volume under test, confirming that rut development is essentially controlled by the shear strains that develop in the road. This shows the HCA test maybe a more appropriate tool to investigate asphalt permanent deformation performance than the RLAT and SST.

While one might argue that in the SST it is possible to directly measure the effects of a specific stress state and the device can approximate field situations that are characterised by a pure shear stress, the limitations of the SST became apparent largely through the unknown level of confining stress it applies leading to significantly lower permanent shear strains than in the HCA or in the RLAT.

The effect of air voids is less clear from the HCA and the SST. The plots show that the air void content does not significantly affect the asphalt mix performance. However, this seems to be in contradiction with results from the RLAT and earlier studies (Chapter 2) that have found that the aggregate structure is important, and the asphalt performance is strongly dependent on density of a mixture.

The investigation provides an indication of asphalt mixture behaviour relating to the applied torsional shear stresses. From the results presented, it can be seen that the new HCA equipment has behaved in a consistent manner and the results obtained during this research appear to be generally acceptable. These findings thus provide strong support for the continuing use of the HCA test to predict the response of the material to complex stress conditions such as the one encountered insitu. The flexibility of stress path application afforded by the HCA is such that a wide range of possibilities arise for future research and this is discussed in Chapter 8.

8

SUMMARY, CONCLUSIONS AND RECOMMENDATION FOR FURTHER INVESTIGATION

8.1. Introduction

In order to study the permanent deformation characteristics of asphalt mixtures under loading simulating insitu conditions as closely as possible, the following three objectives were considered during this research:

(1) Design, build and commission a new HCA for testing realistic asphalt mixtures under appropriate stress paths (Chapters 3 to 5);

(2) Generate data on stress/permanent strain relationships to assist in the development of realistic models for the prediction of pavement rutting (Chapters 5);

(3) Compare the results with the SST and the RLAT, simpler permanent deformation tests, used for practical materials design to verify accuracy and reliability (Chapters 6 and 7).

The development of wheel track ruts in asphalt roads is one of the main design criteria for this form of pavement construction, since deep ruts are a

hazard to vehicles. Limitation of the amount of rutting requires detailed knowledge of how asphalt materials respond to the repeated stress applications caused by large numbers of wheel passes. The stress regime in a road is complex and test methods to date have applied simplified stress systems to measure asphalt mechanical properties.

Permanent deformation of asphalt mixture depends on many factors, including asphalt binder, aggregates, mixture design, loading time and the temperature. Its accumulation may be partly minimised by appropriate mix design and efficient construction control.

In order to reduce asphalt mix susceptibility to plastic deformations, specifications of various mix parameters, such as binder type and content, aggregate type and gradation, compaction degree (air voids), are essential. Nevertheless, permanent deformations in an asphalt layer will occur due to a combination of densification (volumetric reduction) and shear strain, caused by traffic loads.

Rutting resistance is a major performance measure for designing pavements and proper assessment of permanent deformation behaviour is critical to ensure the structural adequacy of flexible pavement. Although the importance of shear stress application under repeated loading is relatively well understood, its influence on permanent deformation accumulation is usually not considered while designing flexible pavement structures.

Although many researchers recognise that the shear stress is the main contributor causing rutting, suitable laboratory test methods and theoretical models are not yet available for properly treating shear-induced permanent deformation. Aiming at achieving rut resistant asphalt mixes, field conditions have been simulated in the laboratory by a variety of repeated loading tests. Tests that have been used to date, such as uniaxial, triaxial and wheel tracking, have been designed to evaluate the elastic, viscoelastic, plastic, and strength parameters of asphalt mixtures. These tests are carried out following specified temperatures, stress magnitudes and variable loading times but they only approximate field conditions. The Literature Review set out some of the main criticisms of these standard test methods. It also suggested that another test should be used to investigate properties of materials composing the upper pavement layers because the states of stress encountered in upper layers cannot be easily duplicated in the laboratory.

8.1.1. HCA development and commissioning

The main aim of this project was to develop an apparatus that will improve simulation of insitu conditions resulting in more accurate quantification of the permanent deformation of asphalt with respect to both shear and volume change characteristics. At the same time, it was also necessary to develop the test procedures which define the parameters contributing to the mixture performance.

A number of multi-layer linear elastic analyses were undertaken in order to establish the actual stress paths for use in the new HCA testing and in order to define the necessary applied loads, so that the full range of possible insitu stress levels could be accommodated. BISAR modelling confirmed that the maximum shear stress on the vertical/horizontal plane (τ_{xz}) generally developed under the edge of the load. It was also found that the predicted maximum vertical stress occurred close to the surface, within the top 50mm of an asphaltic mix. The shear invariant (q) varied with radial position but was generally maximum at the bottom of the layer. The maximum stress ratio, ($\eta = q/p$), however, occurred within the layer and varied between 0.1 and 43.6.

Design of the HCA was led by Mr B V Brodrick, a recently retired Chief Experimental Officer with extensive experience of this type of development within the research group. The new HCA has been successfully built. The device can provide both repeated axial (W) and torsional (M) shear loads with regulated internal and external pressures on a hollow cylindrical specimen with 250mm inner radius, 350mm outer radius and 350mm height. The large size of specimen was dictated by the need to test asphalt with realistic sized aggregate. The test asphalt used a 10mm maximum size continuously graded aggregate mixed with grade 100/150 bitumen.

The initial phase of work with this new apparatus involved an extensive period of commissioning in order to ensure that all the systems functioned correctly. This work resulted in some adjustments to the drive system and also to the

instrumentation mounting arrangements. Further improvement of the equipment might still be required but this had to be limited in order to progress the main HCA testing programme.

The temperature control system proved to be unreliable above 30ºC because of substantial heat loss through the metal components. The provision of some additional lagging was necessary to reduce this problem, but modifications will be needed in the future to achieve higher test temperatures as suggested in the next section.

As discussed in Section 2.8, in geotechnics, HCA has been adopted as a practical and reliable device for measuring key performance profiles of clays and granular materials. The use of HCA for testing asphalt with realistic sized aggregate, has not progressed as far as in geotechnical testing. However, due to its great success in generating a variety of stress paths, a similar approach was followed in asphalt research and a realistically sized HCA for the testing of asphaltic concrete was developed. Overall, it was demonstrated that new HCA proved to be a versatile laboratory shear testing equipment that is able to apply more complex stress paths and it is capable of recording consistent stress-strain responses. The HCA is relatively complex, time consuming and, therefore, expensive, making it unattractive as a routine test, but it is very useful as a research tool.

8.1.2. Specimen preparation

To ensure that the test reflects mix response representative of insitu conditions, uniform specimens with engineering properties similar to those in pavements need to be obtained. The specimen preparation method included accurately cutting hollow cylinder specimens from the paved slabs of asphalt using large diameter core cutters. The internal 150mm cores were also used in the research for the SST and RLAT.

8.1.3. Experimental work

A considerable time was devoted to developing and commissioning the new HCA and this took longer than had been planned. Therefore, only a limited test programme was possible. This was based around the concept of comparing results with those from the SST at UCB and the RLAT. The test programme allowed initial exploration of the relative effects of stress ratio (shear/normal stress) and shear stress levels.

It was observed that permanent strain increases with load applications and it is dependent on the applied shear loads, confirming the importance of the effect of shear stresses on the accumulation of permanent deformation. This suggests that a laboratory test which measures primarily shear deformations appears to be the most effective way to define asphalt resistance to rutting. A test where both the normal and shear stresses could be controlled

independently of each other should be used. An axial loading test, such as the RLAT, is not sufficient to duplicate insitu stress conditions in such a manner as to directly measure their influence.

8.2. Conclusions

The main conclusions that emerged from this study are listed below:

- This work highlights the importance of selecting the proper stress state for laboratory evaluation to ensure that it is representative of insitu conditions.
- Better characterisation of the shear deformation of asphalt mixtures is required in order to improve rutting predictions.
- The new test method needs to be able to account for shear stresses at the edges of the tyre loading, not only under the centre line.
- The new HCA equipment was built, and it proved to be a versatile shear testing device, that can follow stress paths involving p, q and α. The flexibility of stress path application afforded by the HCA is such that a wide range of possibilities arise for future research.
- The method of specimen preparation described in thesis was found to be satisfactory and capable of obtaining the required quality specimens (in terms of dimensions). Some improvement needs to be made to compaction procedure in order to achieve more uniform specimens and to get less variable results (see Section 8.3).
- The investigation provides an indication of asphalt mixture behaviour relating to the applied torsional shear stresses. From the results

presented, it can be seen that the new HCA equipment behaved in a consistent manner and the results obtained during this research appeared to be generally acceptable.

- The device shows the potential to correctly reproduce the insitu stress regime and, hence, allow more appropriate relationships to be developed between the applied stresses and the resulting deformations.
- Principal stress rotation that occurs in a pavement from a passing wheel load cannot be duplicated in the RLAT and is therefore a limitation of its ability to fully simulate vehicle loading.
- Increasing load levels resulted in higher rate of permanent deformation of specimens tested in all of the tests.
- Both HCA and SST, showed that the application of lower normal stress (high stress ratio), results in higher accumulation rate of permanent shear strain. This indicates that axial compressive stress had a confining effect on the accumulation of permanent shear strain.
- Analysis of Mohr's circles indicate that development of permanent shear strain is dependent on the angle of major principal stress rotation σ.
- At low shear stress levels of 70kPa, a greater rate of accumulation of permanent strain is observed, as the stress ratio is increased from 1 to 3 due to the lower normal stress. However, this is not evident in the tests carried out at shear stress levels of 100kPa and 130kPa.
- Similarly, SST results show that for a stress ratio values of SR=1 and SR=2, as was to be expected, an increase in the permanent shear strain is obtained as shear stress level increased. However, for a high

stress ratio value of SR=3, the magnitude of permanent shear strain in specimens tested under these stress conditions, was generally greater than for stress ration values of SR=1 & SR=2. This shows that the effect of compressive axial stress on permanent shear strain is greater when the shear stress is relatively low. However, when specimens are subjected to very high shear stress, it appears that increase in permanent shear strain is mainly attributed to shear deformation and the effect of axial compressive stress on permanent shear strain is negligible. Similar conclusions were drawn by Alavi, (1992).

- The SST reveals that at high stress ratio (SR=3), mixture became unstable and the load magnitude does not appear to influence the permanent strain with a similar trend. This can be possibly associated with the development of internal damage of the material as a consequence of the high shear strains and gradual loss of aggregate interlock. At this state of stress, the load magnitude does not appear to influence the permanent strain in a similar trend. This is not the case in the RLAT, therefore clearly this is associated with effect of combined axial and shear load conditions. This may suggest that the SST test for estimating rutting is more reliable under lower stress conditions and lower stress ratios. Therefore, for design purposes, it would be sensible to avoid the critical states of stress that intensify rutting.
- Dilation is one of the most important aspects controlling a mix stability, and it becomes particularly important when evaluation of permanent deformations in high temperatures is undertaken (Monismith et al.,

1994). The HCA results provide considerable evidence for the dilation phenomenon. Analyses of the data from the HCA tests indicate that the permanent axial strain path varies considerably with the magnitude of stresses applied. However, because of the limited number of tests, it is difficult to draw any definite conclusions about their influence. It can also be observed that for low stress conditions, a resulting strain exhibits both compression and dilation.

- The radial strain was not measured in the SST and RLAT, therefore estimation of volume change was not possible.
- The limitations of the SST became apparent largely through the unknown level of confining stress it applies leading to significantly lower permanent shear strains than in the HCA or in the RLAT.
- This research reveals discrepancies between the RLAT, SST and HCA tests and it shows the HCA test is a more appropriate tool to investigate asphalt permanent deformation performance than the RLAT and SST, but it is too complex for routine use.
- No consistent effect of densification on the mixture performance could be determined from the HCA and the SST. The plots show that the air void content does not significantly affect the asphalt mix performance. However, this seems to be in contradiction with results from RLAT and earlier studies (Chapter 2) that have found that the aggregate structure is important, and the asphalt performance is strongly dependent on density of a mixture. The reason for this is not fully understood and it is

recommended to investigate the issue in the future HCA research programme.

8.3. Recommendations for Future Research

The development has been based on earlier experience in soil and granular materials research, which identified the shortcomings of simple shear testing and the advantages of the torsional hollow cylinder format for the accurate application of the complex stress conditions that arise under a moving wheel load in a pavement. The data available to date have only involved rather simple stress paths, in order that comparisons may be made with data from existing equipment such as the SST.

Having made the capital investment to create this major experimental facility, it is now possible to study the mechanical properties of asphalt under the complex stress conditions imposed in a pavement structure by moving wheel loads more accurately than hitherto. The flexibility of the HCA in terms of the stress regimes which can be applied is such that a wide range of possibilities arise for future research. The overall objective for further work should be to use the apparatus as a generator of high quality data on the relationships between applied stress and permanent strain for asphalts of various types, constituents and mixture proportions. These data then should be used both as a reference standard for the simpler tests used in engineering practice and to assist in the development of improved theoretical models for the prediction of rutting.

This work should be then linked to wheel tracking studies using Accelerated Pavement Testing facilities in order to allow for further field validation. A complete mechanistic validation must assure that the profile of permanent strain can be accurately estimated, and the desired accuracy exists between the laboratory and the real field data.

The new HCA for testing asphalt performance was successfully designed, built and commissioned. However, time constraints imposed by the extensive equipment development period meant that the further modifications had to be postponed. Some improvements to the HCA should be made in the future in the light of early experience of its use, notably in respect of increasing the temperature range available.

It is well documented that asphalt performance is dependent on confining pressure (Monismith and Tayebali, 1988) and the HCA chamber is intended to simulate conditions of the confinement from the surrounding material in the asphalt layer. Hence, the author believes that future testing will require internal and external pressure on the specimen to be applied through a regulated pressure supply in order to investigate influence of confinement on permanent deformation.

If results from tests performed on different samples are to be compared, then quality control for the specimen preparation procedure should be improved in

order to minimise the variability in air void content. To produce more homogenous specimens, desired level of compaction should be specified and laying and compaction should be carried out in accordance with the Specification for Highways Works Series 900 (SHW, 2018). Insitu density control should be carried out using nuclear density gauges. It is also recommended to avoid hand placing of asphalt mixtures.

Since other needed material properties can be obtained, an effort should be made to investigate and evaluate the use of the test for obtaining such information. For example, the effect of air voids is less clear from the testing programme adopted. As already discussed in this thesis, the aggregate structure is important, and the asphalt performance is strongly dependent on density of a mixture. Therefore, it is recommended to investigate the issue in the future HCA research programme.

The flexibility of stress path application afforded by the HCA is such that a wide range of possibilities arise for future research. Based on the findings of this study, the following stress variables should be studied:

- Shear stress reversal;
- Stress ratio in terms of both $\tau_{z\theta}/\sigma_z$ and q/p;
- Permanent and resilient strain response as a function of stress invariants p and q and the influence of direction (α) of major principal stress. This will assist the development of improved theoretical modelling.

Further study involving larger number of tests is recommended to determine the variability of the rutting resistance measured by simpler, routine tests such as RLAT or SST and their applicability in mixture design and evaluation.

REFERENCES

AASHOT 1994. AASHTO TP 7 Standard Test Method for Determining the Permanent Shear Strain and Stiffness of Asphalt Mixtures Using the Superpave Shear Tester (SST). Washington, D.C.: The American Association of State Highway and Transportation Officials.

AI 1983. Principles of Construction of Hot-Mix Asphalt Pavements. Manual Series - No. 22. The Asphalt Institute.

AI 1988. Mix Design Methods for Asphalt Concrete and Other Hot-Mix Types. Manual Series No. 2 (MS-2). The Asphalt Institute.

AI 2001. Asphalt Institute. Superpave Mix Design. Superpave Series No. 2 (SP-02). Lexington, KY : Asphalt Institute.

AIREY, G. 1997. Rheological characteristics of polymer modified and aged binder. PhD Dissertation. University of Nottingham, Nottingham.

AKBULUT, H. & ASLANTAS, K. 2005. Finite element analysis of stress distribution on bituminous pavement and failure mechanism. Materials & design, 26, 383-387.

ALAVI, S. H. 1992. Viscoelastic And Permanent Deformation Characteristics Of Asphalt-Aggregate Mixes Tested As Hollow Cylinders And Subjected To Dynamic Axial And Shear Loads.

ALAVI, S. H. & MONISMITH, C. L. 1994. Time And Temperature Dependent Properties Of Asphalt Concrete Mixes Tested As Hollow Cylinders And Subjected To Dynamic Axial And Shear Loads (With Discussion). Journal of the Association of Asphalt Paving Technologists, 63.

ANSELL, P. & BROWN, S. 1978. A cyclic simple shear apparatus for dry granular materials. Geotechnical Testing Journal, 1, 82-92.

ARA., 2004. Guide for the Mechanistic Empirical Design of New and Rehabilitated Pavement Structure. (Report 1-37A), Washington, D. C: Transportation Research Board of the National Academies.

ASTM 2007. ASTM D1188 - 07. Standard Test Method for Bulk Specific Gravity and Density of Compacted Bituminous Mixtures Using Coated Samples. The American Society for Testing and Materials.

BARKSDALE, R. D. 1972. Laboratory evaluation of rutting in base course materials. Proceedings, Third International Conference on the Structural Design of Asphalt Pavements, Vol. I, London, 161-174.

BARKSDALE, R. D. & MILLER, I. 1977. Development of equipment and techniques for evaluating fatigue and rutting characteristics of asphalt concrete mixes.

BJERRUM, L. & LANDVA, A. J. G. 1966. Direct simple-shear tests on a Norwegian quick clay. 16, 1-20.

BONAQUIST, R. F., CHURILLA, C. J. & FREUND, D. M. 1988. Effect of load, tire pressure, and tire type on flexible pavement response. Transportation Research Record.

BONNOT, J. 1986. Asphalt aggregate mixtures. Transportation Research Record.

BOULDIN, M. G. & COLLINS, J. H. 1992. Influence of binder rheology on rut resistance of polymer modified and unmodified hot mix asphalt. Polymer Modified Asphalt Binders. ASTM International.

BROWN, E. & BASSETT, C. 1990. Effects of maximum aggregate size on rutting potential and other properties of asphalt-aggregate mixtures. Transportation Research Record, 1259, 107-119.

BROWN, E. & FOO, K. Y. 1994. Comparison of unconfined-and confined-creep tests for hot mix asphalt. Journal of materials in civil engineering, 6, 307-326.

BROWN, E. R. 1990. Density of asphalt concrete: How much is needed? : National Centre for Asphalt Technology.

BROWN, S. 1975. Improved framework for predicting permanent deformation in asphalt layers. Transportation Research Record.

BROWN, S. 2000. Functions and Properties of Road Layers, London, Thomas Telford Publishing.

BROWN, S. 2007. The effects of shear stress reversal on the accumulation of plastic strain in granular materials under cyclic loading. Design construction of pavements rail tracks: Geotechnical aspects processed materials, 89-108.

BROWN, S. & ANSELL, P. 1980. The influence of repeated shear reversal on the compaction granular mate - rial. International conference on compaction, 25-27.

BROWN, S. & BELL, C. 1977. The validity of design procedures for the permanent deformation of asphalt pavements. Volume I of proceedings of 4th International Conference on Structural Design of Asphalt Pavements, Ann Arbor, Michigan, 22-26.

BROWN, S. & CHAN, F. 1996. Reduced rutting in unbound granular pavement layers through improved grading design. Proceedings of the Institution of Civil Engineers: Transport.

BROWN, S. & COOPER, K. 1984. The mechanical properties of bituminous materials for road bases and base courses. Journal of the Association of Asphalt Paving Technologists, 53, 10-15.

BROWN, S., GIBB, J., READ, J., SCHOLZ, T. & COOPER, K. 1995. Design and Testing of Bituminous Material. Volume 2: Research Report, Submitted to

DOT/EPSRC LINK Programme on Transport Infrastructure and Operations.

BROWN, S., HAKIM, B., THOM, N., COLLOP, A., GRAFFI, C. & ARMITAGE, 2005. Independent Review of the Recommended Mechanistic-Empirical Design Guide and Software: Reliability and Design of Composite (Rehabilitated) Pavements.

BROWN, S. & PELL, P. 1974. Repeated loading of bituminous materials. CAPSA 74. National Institute for Road Research, Republic of South Africa, Durban.

BROWN, S. & RICHARDSON, I. 2004. A hollow cylinder apparatus to study the cyclic loading behaviour of dry granular material. Advances in geotechnical engineering: The Skempton conference: Proceedings of a three day conference on advances in geotechnical engineering, organised by the Institution of Civil Engineers and held at the Royal Geographical Society, London. Thomas Telford Publishing, 369-380.

BROWN, S. & SNAITH, M. 1974. The permanent deformation characteristics of a dense bitumen macadam subjected to repeated loading. Association of Asphalt Paving Technologists Proc.

BROWN, S. F. & Bell, C. A. 1977. The validity of design procedures for the permanent deformation of asphalt pavements. Proceedings, Fourth International Conference on the Structural Design of Asphalt Pavements, Vol. I, Ann Arbor, 467-482.

BROWN, S. F. & BRUNTON, J. M. 1985. An introduction to the analytical design of bituminous pavements, University of Nottingham, Department of Civil Engineering.

BROWN, S. F. & GIBB, J. M. 1996. Validation Experiments for Permanent Deformation Testing of Bituminous Mixtures. Journal of the Association of Asphalt Paving Technologists, 65.

BSI 1996. DD 226:1996. Method for determining resistance to permanent deformation of bituminous mixtures subject to unconfined dynamic loading. London: British Standard Institution. (Withdrawn)

BSI 1998. BS 598: Part 110: 1998. Sampling and examination of bituminous mixtures for roads and other paved areas. Methods of test for the determination of wheel-tracking rate and depth. London: British Standard Institution.

BSI 2012. BS EN 12697-6: 2012. Bituminous mixtures. Test methods for hot mix asphalt. Determination of bulk density of bituminous specimens. London: British Standard Institution.

BSI 2018. BS EN 12697-8: 2018. Bituminous mixtures. Test methods for hot mix asphalt. Determination of void characteristics of bituminous specimens. London: British Standard Institution.

BSI 2016a. BS EN 13108-1: 2016. Bituminous mixtures - Material specifications - Part 1: Asphalt Concrete. London: British Standard Institution.

BSI 2016b. BS EN 13108-4: 2016. Bituminous mixtures. Material specifications. Hot Rolled Asphalt. London: British Standard Institution.

BSI 2016c. BS EN 13108-5: 2016. Bituminous mixtures - Material specifications - Part 5: Stone Mastic Asphalt. . London: British Standard Institution.

BSI 2016d. BS EN 13108-20: 2016. British Standard. Bituminous mixtures - Material specifications - Part 20: Type Testing. London: British Standards Institution.

BSI 2016e. PD 6691:2015+A1:2016. British Standard. Guidance on the use of BS EN 13108, Bituminous mixtures - Material specifications.

BURMISTER, D. M., PALMER, L., BARBER, E. & MIDDLEBROOKS, T. 1944. The theory of stress and displacements in layered systems and applications to the design of airport runways. Highway Research Board Proceedings.

BUTCHER, M. 1998. Determining gyratory compaction characteristics using servopac gyratory compactor. Transportation Research Record: Journal of the Transportation Research Board, 89-97.

CHAN, F. & BROWN, S. 1994. Significance of principal stress rotation in pavements. Proceedings Of The International Conference On Soil Mechanics And Foundation Engineering-International Society For Soil Mechanics And Foundation Engineering. AA BALKEMA, 1823-1823.

CHAN, F. W. K. 1990. Permanent deformation resistance of granular layers in pavements. University of Nottingham.

CHATTI, K., KIM, H., YUN, K., MAHONEY, J. & MONISMITH, C. 1996. Field investigation into effects of vehicle speed and tire pressure on asphalt concrete pavement strains. Transportation Research Record: Journal of the Transportation Research Board, 66-71.

CHEN, J.-S., CHANG, M. & LIN, K. 2005. Influence of coarse aggregate shape on the strength of asphalt concrete mixtures. Journal of the Eastern Asia Society for Transportation Studies, 6, 1062-1075.

CHRISTENSEN JR, D., BONAQUIST, R. & HANDOJO, T. 2002. Field Shear Test for Hot Mix Asphalt. NCHRP Research Results Digest.

CLAESSEN, A.I.M., J.M. EDWARDS, P. SOMMER, AND P. UGE. 1977. Asphalt Pavement Design - The Shell Method, Proceedings, Fourth International Conference on tire Structural Design of Asphalt Pavements, Vol. I, Ann Arbor, 39-74.

COMINSKY, R. J., HUBER, G. A., KENNEDY, T. W. & ANDERSON, M. 1994. The superpave mix design manual for new construction and overlays, Washington, DC, Strategic Highway Research Program.

COLLOP, A. C., CEBON, D., AND HARDY, M. S. A., 1995. Viscoelastic approach to rutting in flexible pavements. Journal of Transportation Engineering, ASCE, 121 (1). pp. 82-93.

COOLEY, L. A. & KANDHAL, P. S. 2000. Evaluation of density gradients in loaded wheel tester samples. Journal of testing and evaluation, 28, 473-484.

COOPER, K. & BROWN, S. 1989. Development of a simple apparatus for the measurement of the mechanical properties of asphalt mixes. Proc. Eurobitume Symposium, 494-498.

CROCKFORD, W. W. 1993. Role of principal-plane rotation in flexible pavement deformation. Journal of Transportation Engineering, 119, 124-141.

CRONEY, D. & CRONEY, P. 1991. The design and performance of road pavements.

DEACON, J., HARVEY, J., GUADA, I., POPESCU, L. & MONISMITH, C. 2002. Analytically based approach to rutting prediction. Transportation Research Record: Journal of the Transportation Research Board, 9-18.

DFT 2006. Transport Statistics Great Britain.

DFT 2018. Road Transport Forecasts 2018: Moving Britain Ahead. England: Department for Transport.

DRAKOS, C. 2012. www.ce.ufl.edu/~rroqu/Class%20Notes%20TTE4811/Topic%202%20-%20Flexible%20Pavement%20Distress.pdf. University of Florida.

DSS 2009. Abaqus Analysis User's Manual. USA: Dassault Systèmes Simulia.

DUNCAN, J. M., MONISMITH, C. L. & WILSON, E. L. 1968. Finite element analyses of pavements. Highway Research Record.

EISENMANN, J. & HILMER, A. 1987. Influence Of Wheel Load And Inflation Pressure On The Rutting Effect At Asphalt-Pavements-Experiments And Theoretical Investigations. Sixth International Conference, Structural Design Of Asphalt Pavements, Volume I, Proceedings, University Of Michigan, July 13-17, Michigan.

EUG 2005. Everseries User’s Guide. Pavement analysis computer software and case studies. Olympia, Washington: Washington State Department of Transportation.

FLETCHER, T., CHANDAN, C., MASAD, E., SIVAKUMAR, K & EVALUATION 2002. Measurement of aggregate texture and its influence on hot mix asphalt (HMA) permanent deformation. 30, 524-531.

FLOWERS, D., GEE, J. & MEADORS, A. 1989. Asphalt Overlays of Concrete Pavements: Case Studies in Arkansas. Transportation Research Record.

FRANCKEN, L. 1977. Permanent deformation law of bituminous road mixes in repeated triaxial compression. Volume I of proceedings of 4th

International Conference on Structural Design of Asphalt Pavements, Ann Arbor, Michigan, 22-26.

FRANCKEN, L. & CLAUWAERT, C. 1987. Charcterization and structural assessment of bound materials for flexible road structures." Proceedings of the 6th international conference on structural design of asphalt pavements, Vol. 1, Ann Arbor.

GARG, N. & HAYHOE, G. F. 2001. Asphalt concrete strain responses at high loads and low speeds at the national airport pavement test facility (NAPTF). Proceedings of the 2001 ASCE Airfield Pavement Specialty Conference.

GIBB, J. M. 1996. Evaluation of resistance to permanent deformation in the design of bituminous paving mixtures. University of Nottingham.

GOODRICH, J. L. 1991. Asphaltic binder rheology, asphalt concrete rheology and asphalt concrete mix properties (with discussion). Journal of the Association of Asphalt Paving Technologists, 60.

HARVEY, J., GUADA, I., MONISMITH, C., BEJARANO, M. & LONG, F. 2002. Repeated simple shear test for mix design: a summary of recent field and accelerated pavement test experience in California. Ninth International Conference on Asphalt Pavements.

HARVEY, J., WEISSMAN, S., LONG, F. & MONISMITH. 2001. Tests To Evaluate The Stiffness And Permanent Deformation Characteristics Of Asphalt/Binder-Aggregate Mixes, And Their Use In Mix Design And Analysis 70.

HENSLEY, M. & LEAHY, R. B. 1989. Asphalt concrete mixtures as related to pavement rutting: case studies. Transportation Research Record.

HICKS, R. 1991. Moisture damage in asphalt concrete, Transportation Research Board.

HICKS, R. & ESCH, D. 1990. State-of-the-art on Rutting in Asphalt Concrete.

HICKS, R. & MONISMITH, C. 1971. Factor influencing the resilient response of granular materials. Highway Research Board.

HIGHT, D., GENS, A. & SYMES, M. 1983. The development of a new hollow cylinder apparatus for investigating the effects of principal stress rotation in soils. Geotechnique, 33, 355-383.

HOFSTRA, A. & KLOMP, A. 1972. Permanent deformation of flexible pavements under simulated road traffic conditions. Presented at the Third International Conference on the Structural Design of Asphalt Pavements, Grosvenor House, Park Lane, London, England, Sept. 11-15.

HOPMAN, P. 1996. VEROAD: A viscoelastic multilayer computer program. Transportation Research Record: Journal of the Transportation Research Board, 72-80.

HRB 1954. The WASHO Road Test Part 1: Design, Construction, and Testing Procedures. Highway Research Board Special Report 18. Washington, D.C.: Highway Research Board, National Research Council.

HRB 1955. Special Report 22: The WASHO Road Test, Part 2: Test Data. . Washington, DC: Highway Research Board, National Research Council.

HRB 1962. THE AASHO ROAD TEST: REPORT 7 - SUMMARY REPORT. Highway Research Board Special Report 61-G. Washington, DC: Highway Research Board, National Research Council

HUBER, G. & HEIMAN, G. 1987. Effect of asphalt concrete parameters on rutting performance: a field investigation. Association of Asphalt Paving Technologists Proc.

HUBER, G. A. 1999. Methods to achieve rut-resistant durable pavements, Transportation Research Board.

HUDSON, S. W. & SEEDS, S. B. 1988. Evaluation of increased pavement loading and tire pressures. Transportation Research Record.

HUNTER, R. N. 1994. Bituminous mixtures in road construction, Thomas Telford.

HUNTER, R. N. 2000. Asphalts in road construction, Thomas Telford.

IAN 2009. Design Manual for Roads and Bridges: Volume 7: Part 2. IAN 73/06 Rev 1. Design of Pavement Foundations. Standards for Highways.

DENIS JELAGIN, D., ABUBEKER AHMED, A., LU, X. & SAID, S. 2018. Asphalt layer rutting performance prediction tools. VTI rapport 968A.

KENIS, W. & WANG, W. 1997. Calibrating mechanistic flexible pavement rutting models from full scale accelerated tests. 8th Int. conference on asphalt pavements, Seattle.

KENNEDY, T. W., ROBERTS, F. L. & LEE, K. W. 1983. Evaluation of moisture effects on asphalt concrete mixtures.

KHAN, Z. A., WAHAB, H. I. A.-A., ASI, I. & RAMADHAN, R. 1998. Comparative study of asphalt concrete laboratory compaction methods to simulate field compaction. Construction and Building Materials, 12, 373-384.

KIM, Y. R., KIM, N. & KHOSLA, N. P. 1992. Effects of aggregate type and gradation on fatigue and permanent deformation of asphalt concrete. Effects of aggregates and mineral fillers on asphalt mixture performance. ASTM International.

KING, G.N., KING, H.W., HARDERS, O., CHAVENOT, P., AND PLANCHE, J.P. 1992. Influence of Asphalt Grade and Polymer Concentration on The High Temperature Performance of Polymer Modified Asphalt, Proceedings of AAPT, Vol. 61, pp. 29-66.

KING, G., KING, H., PAVLOVICH, R., EPPS, A. L. & KANDHAL, P. 1999. Additives in asphalt. Journal of the Association of Asphalt Paving Technologists, 68, 32-69.

KJELLMAN, W. 1951. Testing the shear strength of clay in Sweden. Geotechnique, 2, 225-232.

KRUTZ, N. C. & SEBAALY, P. E. 1993. The Effects of Aggregate Gradation on Permanent Deformation of Asphalt Concrete. Journal of the Association of Asphalt Paving Technologists, 62.

LEAHY, R. B., MONISMITH, C. L. & LUNDY, J. R. 1995. Performance-based properties of asphalt concrete mixes. Engineering Properties of Asphalt Mixtures and the Relationship to their Performance. ASTM International.

LEE, C., WHITE, T. & WEST, T. 1999. Effect of Fine Aggreagate Angularity on Asphal Mixture Performance.

LEECH, D. & NUNN, M. 1997. Deterioration mechanisms in flexible roads. Performance And Durability Of Bituminous Materials. Proceedings Of The Second European Symposium On Performance And Durability Of Bituminous Materials, Leeds.

LIU, C. 1995. Measure of Creep Characteristics of Asphalt Concrete. DTIC Document.

LYTTON, R. L., UZAN, J., FERNANDO, E. G., ROQUE, R., HILTUNEN, D. & STOFFELS, S. M. 1993. Development and validation of performance prediction models and specifications for asphalt binders and paving mixes, Strategic Highway Research Program Washington, DC.

MACCARRONE, S. & HOLLERAN, G. 1990 Development of rut resistant mixes for Australian conditions. Australian Road Research Board (ARRB) Conference, 15th, 1990, Darwin, Northern Territory.

MAHBOUB, K. & ALLEN, D. L. 1990. Characterization of rutting potential of large-stone asphalt mixes in Kentucky. Transportation Research Record.

MAHBOUB, K. & LITTLE, D. N. 1988. Improved asphalt concrete mixture design procedure.

MASAD, E., AL-ROUSAN, J. B., BUTTON, J., LITTLE, D. & TUTUMLUER, E. 2005. Test methods for characterizing aggregate shape, texture. and angularity. Technical Report NCHRP 4-30A, National Cooperative Highway Research Program, National Research Council.

MERRILL, D. 2005. TRL Report TRL639: Guidance on the development, assessment and maintenance of long-life flexible pavements. Transport Research Laboratories.

MONISMITH, C. & BROWN, S. 1999. Developments in the structural design and rehabilitation of asphalt pavements over three quarters of a century. Journal of the Association of Asphalt Paving Technologists A, 68, 128-251.

MONISMITH, C., EPPS, J. & FINN, F. 1985. Improved Asphalt Mix Design. Association of Asphalt Paving Technologists Proc.

MONISMITH, C., HARVEY, J., GUADA, I., LONG, F., VALLERGA, B., NOKES, W. & JEW, A. 2000. Asphalt Mix Evaluations: Case Study at San Francisco

International Airport. Transportation Research Record: Journal of the Transportation Research Board, 133-140.
MONISMITH, C., HICKS, R., FINN, F., SOUSA, J., HARVEY, J., WEISSMAN, S., DEACON, J., COPLANTZ, J. & PAULSEN, G. 1994. Permanent deformation response of asphalt aggregate mixes. SHRP-A-415.
MONISMITH, C. L. 1988. Behavior of Mixes Containing a Conventional and a Polymer Modified (STYRELF) Asphalt.
MONISMITH, C. L. 2004. Evolution of long-lasting asphalt pavement design methodology: a perspective. Lecture presented in June.
MONISMITH, C. L. & TAYEBALI, A. 1988. Permanent deformation (rutting) considerations in asphalt concrete pavement sections. Association of Asphalt Paving Technologists Technical Sessions, 1988, Williamsburg, Virginia, USA.
MUNIANDY, R., JAKARNI, F., HASSIM, S. & MAHMUD, A. 2007. Development of Criteria for Slab Compaction of Laboratory Roller Compactor (Turamesin). American Journal of applied sciences, 4, 908-911.
NF 2007. NF EN 13108-1. Mélanges bitumineux - Spécifications des matériaux - Partie 1: enrobés bitumineux. Paris: Norme Française.
NICHOLLS, J. C. 1998a. Asphalt surfacings, CRC Press.
NICHOLLS, J. C. 1998b. Road trials of stone mastic asphalt and other thin surfacings. TRL REPORT 314.
NUNN, M. 1994. Evaluation of stone mastic asphalt (SMA): A high stability wearing course material. TRL Project Report.
NUNN, M., BROWN, A,WESTON, D,NICHOLLS, JC 1997. TRL250. Design of long-life flexible pavements for heavy traffic. Transport Research Laboratory.
NUNN, M. & SMITH, T. 1994. Evaluation of Enrobe a Module Eleve (eme): a French High Modulus Roadbase Material. TRL Project Report.
O'KELLY, B. C. & NAUGHTON, P. 2003. Development of the University College Dublin hollow cylinder apparatus. Proceedings 56th Canadian Geotechnical Conference, Winnipeg, Ontario.
ODUROH, P. K., MAHBOUB, K. C. & ANDERSON, R. M. 2000. Flat and elongated aggregates in superpave regime. Journal of Materials in Civil Engineering, 12, 124-130.
OSSA, E., TAHERKHANI, H. & COLLOP, A. 2006. Compressive Deformation Behaviour of Asphalt Mixtures.
PAPAGIANNAKIS, A. T. & MASAD, E. A. 2008. Pavement design and materials, John Wiley & Sons.
PELL, P. & BROWN, S. The characteristics of materials for the design of flexible pavement structures. 1972. Presented at the Third International Conference on the Structural Design of Asphalt Pavements, Grosvenor House, Park Lane, London, England, Sept. 11-15.

PI. 2010. Laboratory Wheel Tracking Devices. www.pavementinteractive.org : Pavement Interactive.

QI, X., SEBAALY, P. E. & EPPS, J. A. 1995. Evaluation of polymer-modified asphalt concrete mixtures. Journal of Materials in Civil Engineering, 7, 117-124.

READ, J. & WHITEOAK, D. 2003. The shell bitumen handbook, Thomas Telford.

RICHARDSON, I. R. 1999. The stress-strain behaviour of dry granular material subjected to repeated loading in a hollow cylinder apparatus. University of Nottingham.

ROBERTS, F., KANDHAL, P., BROWN, E., LEE, D. & KENNEDY, T. 1996. Hot Mix Asphalt Materials, Mixture Design and Construction.

ROMAIN, J. E. 1972. Rut depth prediction in asphalt pavements. Proceedings, Third International Conference on the Structural Design of Asphalt Pavements, Vol. I, London, 205-210.

ROSCOE, K. An apparatus for the application of simple shear to soil samples. Proc. 3rd ICSMFE, 1953. 186-191.

RUEDA, E. J., CARO, S., CAICEDO, B. & MONROY, J 2017. A new approach for the advanced mechanical characterisation of asphalt mixtures using the hollow cylinder methodology. Measurement 103, p.333-342.

SAADA, A. S. 1988. State-of-the-art paper: Hollow cylinder torsional devices: Their advantages and limitations. Advanced triaxial testing of soil and rock. ASTM International.

SANDERS, P. & NUNN, M. 2005. The application of Enrobe a Module Eleve in flexible pavements.

SANDERS, P. D., MCROBBIE S., GOPALDAS J., VINER H. E. 2015. PUBLISHED PROJECT REPORT PPR771. Development of a reference surface for the assessment of pavement skid resistance measurement devices. Transportation Research Laboratory.

SEED, H. B., CHAN, C. & LEE, C. E. 1962. Resilience characteristics of subgrade soils and their relation to fatigue failures in asphalt pavements. International Conference on the Structural Design of Asphalt Pavements. SupplementUniversity of Michigan, Ann Arbor.

SGEP. 2010. www.sglpenergy.com/asphalt. Sem Group Energy Partners.

SHAW, P. & BROWN, S. F. J. G. T. J. 1986. Cyclic simple shear testing of granular materials. 9, 213-220.

SHELL 1998. Bisar 3.0 User Manual.

SHW 2018. Volume 1 - Specification for Highway Works. Series 900 Road Pavements - Bituminous Bound Materials. Manual of Contract Documents for Highway Works. Standards for Highways.

SIGURJONSSON, S. & RUTH, B. E. 1990. Use of gyratory testing machine to evaluate shear resistance of asphalt paving mixture. Transportation Research Record.

SMITH, H. A. 1991. Truck Tire Characteristics and Asphalt Concrete Pavement Rutting. Transportation Research Record.

SOUSA, J. B., DEACON, J. A. & MONISMITH, C. L. 1991. Effect of laboratory compaction method on permanent deformation characteristics of asphalt-aggregate mixtures. Journal of the Association of Asphalt Paving Technologists, 60.

SOUSA, J. B., LYSMER, J., CHEN, S.-S. & MONISMITH, C. 1988. Effects of dynamic loads on performance of asphalt concrete pavements. Transportation Research Record.

SOUSA, J. B., SOLAIMANIAN, M. & WEISSMAN, S. L. 1994. Development and Use of the Repeated Shear Test (Constant Height): An Optional Superpave Mix Design Test.

SOUSA, J. B. 1986. Dynamic properties of pavement materials.

SOUSA, J. B., CRAUS, J. & MONISMITH, C. L. 1991. Summary Report On Permanent Deformation In Asphalt Concrete. SHRP-A-318, Washington DC.

STUART, K. & IZZO, R. 1995. Correlation of Superpave G^*/sin with Rutting Susceptibility from Laboratory Mixture Tests: Author's Closure. Transportation Research Record, 183-183.

TAHERKHANI, H. 2006. Experimental characterisation of the compressive permanent deformation behaviour in asphaltic mixtures. University of Nottingham UK.

TAREFDER, R. A. & ZAMAN, M. 2002. Evaluation of Rutting Potential of Hot Mix Asphalt Using The Asphalt Pavement Analyzer.

TAYEBALI, A. A., GOODRICH, J. L., SOUSA, J. B. & MONISMITH, C. L. 1992. Influence of the rheological properties of modified asphalt binders on the load deformation characteristics of the binder-aggregate mixtures. Polymer modified asphalt binders. ASTM International.

TERREL, R., AWAD, I. & FOSS, L. 1974. Techniques for characterizing bituminous materials using a versatile triaxial testing system. Fatigue and Dynamic Testing of Bituminous Mixtures. ASTM International.

THOM, N. 2008. Principles of pavement engineering.

THOM, N. 1988. Design of Road Foundations, PhD Thesis, University on Nottingham.

THROWER, E. N. 1978. Stress inveriants and mechanical testing of pavement materials. Report 810, Transport and Raod Research Laboratory. Great Britain.

UGE, P. & VAN DE LOO, P. 1974. Permanent deformation of asphalt mixes, Shell Research Laboratories.

VALLERGA, B., SEED, H., MONISMITH, C. & COOPER, R. 1957. Effect of shape, size, and surface roughness of aggregate particles on the strength of granular materials. Road and Paving Materials. ASTM International.

VAN DE LOO, P. J. (1976). Practical approach to the prediction of rutting in asphalt pavements: the Shell method. Transportation Research Record 616, Transportation Research Board, 15-21.

VAN DE LOO, P. The Creep Test: A Key Tool in Asphalt Mix Evaluation and in Prediction of Rutting. Association of Asphalt Paving Technologists Proc, 1978.

WA, N. K. K. & MUTHEN, K. J. S. 1997. Dynamic testing of asphalt.

WALTHER, A. & ISAILOVIC I 2015. Effects of low vehicle speed on the service life time of asphalt pavements. Bituminous Mixtures Pavements.

WEB 2011. www.kozielsko.cba.pl.

WEB. 2012. www.paveemntinteractive.org.

WEDDING, P. A. & GAYNOR, R. D. 1961. THE EFFECTS OF USING CRUSHED GRAVEL AS THE COARSE AND FINE AGGREGATE IN DENSE GRADED BITUMINOUS MIXTURES. Association of Asphalt Paving Technologists Proceedings.

WHITE, T. D. 2002. Contributions of pavement structural layers to rutting of hot mix asphalt pavements, Transportation Research Board.

WILLIAMSON, S. & GAUGHAN, R. 1992. A field evaluation of rutting and cracking in asphalt with modified binders. Proceedings, 16th Arrb Conference, 9-13 November 1992, Perth, Western Australia; Volume 16, Part 2.

WILLWAY, T., BALDACHIN, L., REEVES, S., HARDING, M., et al 2008. Published Project Report PPR184: The effects of climate change on highway pavements and how to minimise them: Technical report. Transportation Research Laboratory.

WITCZAK, M., KALOUSH, K., PELLINEN, T., EL-BASYOUNY, M. & VON QUINTUS, H. 2002. NCHRP REPORT 465 Simple Performance Test for Superpave Mix Design. National Cooperative Highway Research Program Report.

WONG, W., HAN, H., HE, G., QIU, X., WANG, K. & LU, W. 2004. Effects of water on permanent deformation potential of asphalt concrete mixtures. Materials and structures, 37, 532-538.

APPENDIX A

MANUFACTURER:

1) HCA CERTIFICATES

2) CALIBRATION CERTIFICATES

3) HCA CUTTING RIG

MICRON PRECISION ENGINEERING SERVICES LTD

EC DECLARATION OF CONFORMITY

CE REFERENCE NO: 28023/09

Manufacturer's Name: Micron Precision Engineering Services Ltd
25 Wharfedale Road
Euroway Trading Estate
Bradford
West Yorkshire
BD4 6SG
Tel: 01274 653400, Fax: 01274 470607

Contact Name: D.A. Cooper
Position: Managing Director

Designation of Equipment: Hollow Cylinder Test Machine

Reference Number: 28023/09

We declare that the equipment designated above has been manufactured in accordance with:-

The EC Council Directive relating to machinery 98/37/EC, any subsequent amendments thereto and the relevant harmonised standards, in particular BS EN ISO 12100 Parts 1 and 2 and EN60204-1:1998 on safety of machinery.

The EC Council Directive relating to electromagnetic compatibility 89/336/EEC and any subsequent amendments thereto and the relevant harmonised standards.

If alterations are made to this machinery without prior consultations with us, this declaration becomes invalid.

Signed:

Name and Position: D.A. Cooper M - Director.

Date: 27/8/09.

EQUIPMENT DESCRIPTION

The equipment has been designed to provide Vertical and Twisting characteristics to an Asphalt specimen of 350 mm OD x 250 mm ID. The sample test height is 350 mm plus adaptors.

It is also proposed that the sample will subject to the above loadings whilst being held within a container to allow a restraining air pressure of 207 kPa and that the temperature range will be within ambient to 45° C

In order to achieve the above, a dedicated press has been designed and manufactured to work within the above criteria.

The frame has been manufactured from solid EN4B steel plates, interconnected with 4 columns of 3.00" Ø EN24T steel.
The base has been manufactured from 3.00" plate, the Intermediate from 25.0 plate and the top from 4.00" plate.

The plates are fully machined to provide alignment and anchoring for the various components.

The top plate clamps are taper lock type units, two per guide column, and are designed for ultimate security but have not been designed to provide rapid release and re-application for frequent position changing.

The intermediate plate is provided with standard type clamping brackets fitted with two clamp bolts each, clearance slots and confirmation spacers. This allows rapid clamping/unclamping to allow adjustment to suit sample variations if necessary.

The Base unit is mounted on fully adjustable metalastick mountings to provide vibration absorbency (to 10 Hz) and a method of providing levelling for floor discrepancies. Two hydraulic cylinders are mounted at opposing corners to allow jacking and temporary securing of Intermediate and top plates whilst resetting the press.

Hydraulic pressure is supplied from the laboratory ring main, via isolating ball valves, isolating 24 v DC electrical control valve, dual pressure selection and associated pressure reducing valves and a PALL pressure filter.
The hydraulic pressure is then supplied to a manifold, mounted on the press which then allows diversion to both servo actuators and the manual control valve for positioning cylinder operation.
Tank returns are also combined at a manifold before returning to the reservoir via the ring main.

VERTICAL.

The servo actuator is a standard, through shaft, MOOG design unit with shaft extension to suit the top plate thickness.

100 kN vertical load (**applied in this instance in a COMPRESIVE mode only**.)
Tensile characteristics are limited by the actuator / Load Cell connection which has been designed to provide free float characteristics with a maximum tensile force of 10 kN to allow raising of the drive mechanism.

The vertical actuator has a maximum stroke of 100.0 mm.
Constraints within the Design to allow for twisting characteristics **will limit this stroke to approximately 97.0 mm and great care should be exercised, at both limits of travel, to ensure that fouling of the load cells and bearings does not occur**

Design Loading Frequency 0 – 5 Hz.
It is anticipated that the vertical loading stroke ≤ 1.5 mm at maximum frequency and maximum load. Operation outside these limits will require re-assessment of operating pressures and flow capabilities of associated auxiliary control equipment.

Instrumentation includes actuator integral positional feedback and two 100 kN load cells, one load cell is positioned directly on the actuator shaft; the second is positioned between the final drive bearing and the load extension shaft.

Transmission of the vertical compressive forces is via a guided shaft, connected at each end with 100 kN load cells, to a large angular contact roller bearing, mounted on the final drive disc. The bearing housing has been machined to provide zero backlash and is sealed with "O" rings to prevent the entry of dust. The bearing was grease lubricated on assembly. All components are high tolerance, sliding fit assembly and are finally secured by clamping components with limited clearance.

TWISTING

The servo actuator is a high pressure, hydraulically driven unit, specifically designed for this application, due to space, linear operation and overhang limitations.

30kN force at 200.0mm radius from the axial centre. (6kNm)
The force can be applied in either compression or tension modes, assuming that the actuator is in the mid position. It is considered that, due to the change in the applied angle, during compression of the sample during testing, greater reliability will be achieved by reducing possible buckling moments and therefore arranging to test the sample in tension loading.
The design force is available at 170 Bar system pressure. SWP is 210 Bar

150.0mm of actuator (+/- 75.0 mm) travel is available.
This allows +/- 15.0° of rotation of the final drive plate. Full travel is available subject to sample limits.

Design Loading Frequency 0 – 5 hz.
It is anticipated that the twisting loading stroke ≤ 1.5 mm at maximum frequency and maximum load. Operation outside these limits will require re-assessment of operating pressures and flow capabilities of associated auxiliary control equipment.

Instrumentation includes an actuator integral positional feedback and two 25.0 kN load cells. Each of the load cells is positioned at 180° between the secondary and final drive shafts. Load cell No1 is installed at a fixed length with the spherical bearings screwed and locked into the load cell arms. No 2 load cell has a clearance hole on the upper, secondary drive end, with adjustable lock nuts to allow zero force setting.

The twisting forces are separated from the vertical application by supporting the complete rotating mass on a large angular contact roller bearing, mounted on the Intermediate Plate. The bearing housing has been machined to provide zero backlash and is sealed with "O" rings to prevent the entry of dust. The bearing was grease lubricated on assembly.
All components are high tolerance, sliding fit assembly and are finally secured by clamping components with limited clearance.
Transmission of the twisting forces is via the twin load cells to the final drive disc, again fully supported on its own bearing assembly

Containment vessel.

- Care should be taken when positioning the removable front or rear covers to ensure that trapping does not occur. Each assembly weighs in excess of 50 kG.
- The assembly provides precision fitting and sealing utilising "O" rings and "O" Ring chord. It is recommended to smear petroleum grease on the mating surfaces to provide retention and reduce the possibility of trapping the rings.
- Initial installation requires that the master Container cap is positioned around the final drive spacer and M5 tapings are provided to retain the cap when the vessel is open. Care must be taken to ensure that these are in position prior to raising the centre assembly such that the Cap cannot drop off the spacer.
- The container base should be pre-assembled with the rear outer half, including the base "O" ring, and loosely bolted in position. This sub assembly can then be offered into position on the base of the press and adjusted to provide alignment with the container Cap.
- Once the cap assembly is aligned, with the "O" ring in position and locating dowels entered the completed sub assembly can be finally positioned on the Press base and secured with the M16 Clamps.
- The press vertical assembly can now be raised with the cap bolts fully loosened, lifting the cap clear to allow insertion of the test piece and its connection.
- The front cover of the containment can now be positioned, security of vertical "O" ring chords and position of base and cap "O" rings confirmed before final positioning and securing to rear half, base and finally cap.
- Maximum working pressure is 30 p.s.i. (207 kPa)
- **The safety relief valve must always be installed when pressurised.**
- Base and cap M10 SCHS should be tightened to 81 N.m
- Vertical clamp half M8 SCHS should be tightened to 40 N.m

Maintenance requirements.

- Daily use check condition of "O" rings and replace if necessary.
- Check condition of SCHS and replace if necessary.
- Annually replace all fixings and "O" rings.

QUALITY HYDRAULIC POWER LIMITED
Taylor House, Minerva Avenue
Chester West Employment Park
Chester CH1 4QL
England, United Kingdom
Telephone: 01244 393500
Telefax: 01244 393501
Email: info@qhp.co.uk
Internet: http://www.qhp.co.uk

CERTIFICATE OF CONFORMITY

INVESTORS IN PEOPLE

BFPA The British Fluid Power Association

881619

QHP HYDAC International

Quality Hydraulic Power Limited

Delivery Address:

[illegible]
[illegible]
[illegible]
[illegible]

DATE.	OUR REFERENCE NO.	YOUR ORDER NO.	ACCOUNT NO.	DESPATCH DATE.
[illegible]	[illegible]	[illegible]	[illegible]	[illegible]

ITEM	DESCRIPTION	QTY	This Despatch	To Follow
[illegible]	[illegible]	1	1	
[illegible]	[illegible]	1	1	
[illegible]	[illegible]	1	1	

"CERTIFIED THAT THE SUPPLIES/SERVICES DETAILED HEREON HAVE BEEN INSPECTED AND TESTED IN ACCORDANCE WITH THE CONDITIONS AND REQUIREMENTS OF THE CONTRACT OR PURCHASE ORDER AND UNLESS OTHERWISE STATED BELOW CONFORM IN ALL RESPECTS TO THE SPECIFICATION(S), DRAWING(S) RELEVANT THERE TO"

Documents No. [illegible]

Authorised _____ On Behalf Of Q.H.P. Limited.

WHITE - CUSTOMER GREEN - SALES OFFICE COPY
YELLOW - PACKING NOTE PINK - WORK ORDER
WHITE-CERTIFICATE OF CONFORMITY

VAT No. 454 0580 59

NETT CASH MONTHLY ACCOUNT

Lorch

Zertifikat/Certificate/Certificat/Certificato/ Certificado

Produktions-Nr./Production No./N° de Fabrikation
Nr.07/09-01202
von/from/de:
bis/to/á:

Sicherheitsventil:
Savety Valve: Type 2122
Soupape de Sûreté: Id.Nr. : 10330
Valvola di sicurezza :
Válvula de seguridad:

Medium: Druckluft
Fluid Type: Compressed Air
Type de Fluide: Air comprimé
Fluido di processo: Aria compressa
Medio: Aire comprimido

Nenndurchmesser/Nominal diameter: Diamétre nominal/Diametro nominale: Diámetro nominal -- DN	8
Einstelldruck /Setting pressare/ Pression d`adjustement/Pressione di taratura /Presión de ajuste - bar:	2,5
Federbereich/Spring range/ Plage d´elasticité /Range di molla/ Margen de resorte - bar	2,5
Ausflussziffer /Flow coefficient/ Coeficient de decharge/Coefficiente di efflusso/Descarga - aw	0,44
Hub/Valve lift/Haussement /Alzata / Alza - mm ho/do	0,22
Durchflussleistung/Discarge/Decharge/ Portata/Rendimiento - (Nm^3/h):	59

KONFORMITÄTSERKLÄRUNG- Gemäß Druckgeräterichtlinie 97/23/EG
DECLARATION OF CONFORMITY- According to the directive for pressure device 97/23/EG
DÉCLARATION DE CONFORMITÉ- Selon la directive 97/23/EG concernant les appareils á pression
DICHIARAZIONE DI CONFORMITA – Secondo il regolamento CE 97/23/EG per gli apparecchi a pressione
DECLARACION CONFORMIDAD – Según recomenaciones sobre equipos de presión 97/23/EG

Hersteller/Manufacturer/Fabricant/Costruttore/Fabricante
J. LORCH Ges. & Co. GmbH, Echterdinger Str. 57, D-70794 Filderstadt-Bernhausen

Beschreibung des Druckgerätes/Description of the pressure device/Description de l'appareil á pression/Descrizione dellàpparecchi a pressione/Descripción del equipo de presión
Federbelastetes Normal-Sicherheitsventil
Spring-loaded standard safety valve
upape de sûreté ressort normale
Valvola di siccureza normalizzata con molla di compressione
Válvula de seguridad
DN 8 Type 2122

Konformitätsbewertungsverfahren/Procedure for assessment of conformity/Proceédure d'appréciation de conformità/Procedimentodi valutazione della conformità/Procedimento de comprobación de conformidad
Modul B und Modul D/Module B and Module D/Module B et Module D/Modulo B e Modulo D/módulo B y módulo D
EG-Baumusterprüfung + Qualitätssicherung Produktion/EC type test + quality assurance production/Contrôle de modèle type CE + assurance qualité produktion/Omologazione CE + Garanzia di qualità della produzione/Zerzifizierungsgesellschaft/Certification organisation/Socéité de certifikation/Ente di certificatione/Control de modelos de construcción y aseguramiento de calidad en la CE:

Zerzifizierungsgesellschaft/Certification organisation/Socéité de certifikation/Ente di certificazione/Compania de certificación
TÜV-Süddeutschland/Mannheim 0036

Angewandte harmonisierte Normen/Used harmonized standards/Normes harmonisées utilisées/Norme armonizzate applicante/Normas Europeas utilizadas
prEN 4126

Angewandte Normen+Spezifikationen/Used standards+specifications/Normes+spécifications utilisées/Norme/specifiche applicante/Normas/especificasiones utilizadas
Richtlinie 97/23/EG, DIN 3320 Teil 1+3, AD-A2 Merkblatt, VD-TÜV- Merkblatt SV100, VD-TÜV- Merkblatt/Instruction sheet/Notice 100/4, Druckbehälterverordnung/regulation for pressure vessels/ordonnance sur les réservoirs sous pression/CE 97/23/EG, DIN 3320 1+3, Bolletino 100/4, Regolomento per i serbatori a pressione/Hoja de instrucciones 100/4- regulaciones de equipos de presión

Bevollmächtigter des Herstellers/Authorized representative of the manufacturer/Fondé de pouvoir du fabricant/Delegato del costruttore/Persona autorizada por el fabricante

GLTG / SCHÖLLKOPF • LTG QS / EISENBRAUN

Name/Name/Nom/Nome/Nombre:
Funktion/function/fonction/funzione/posición: Qualitätssicherung

7.7.2009
Datum/Date/Date/Data

Unterschrift/Signatur/Signature/Firma/Signatura
- SCHÖLLKOPF - EISENBRAUN
(elektronisch erstellte rechtsgültige Unterschrift)

PETER CASSIDY (LEEDS) LIMITED (EST 1962)

HOLBECK LANE, LEEDS L11 9XA

TEL: 0113 245 5457 FAX: 0113 242 6456
E MAIL: sales@petercassidy.co.uk

SURVEY REPORT

CUSTOMER: Micron Precision Eng Services
LOCATION: Micron Precision Eng Services, Euroway Trad Est, Bradford

ORDER N.O: 4002
DATE OF SURVEY: 25/06/09

PROJECT	LOAD APPLIED	RESULTS TOP PLATE	RESULTS PILLARS	TOP PLATE SECURING CLAMPS PART N.O: B302300
To proof load as instructed by Micron Hydraulics	3tonne	0.05mm deflection	No deflection	No Movement
1 x 4 Pillar Press	6.5tonne	0.1mm deflection	No deflection	No Movement
Loadings applied using centrally positioned calibrated hydraulic pump & Ram	9tonne	0.15mm deflection	No deflection	No Movement
	12tonne	0.2mm deflection	No deflection	No Movement
Pump N.o: AJ4495 Ram N.o: 311467				

NAME OF PERSON MAKING THIS REPORT: Neil Halloways

SIGNITURE OF PERSON AUTENTICATING THIS REPORT:



MICRON PRECISION ENGINEERING SERVICES LTD

PROOF TEST CERTIFICATE

REFERENCE NO: 28023/70

Manufacturer's Name: Micron Precision Engineering Services Ltd
25 Wharfedale Road
Euroway Trading Estate
Bradford
West Yorkshire
BD4 6SG
Tel: 01274 653400, Fax: 01274 470607

Contact Name: D.A. Cooper
Position: Managing Director

Designation of Equipment: Hollow Cylinder containment Vessel

Design Pressure: 206.8kPa
Proof Pressure: 310.2 kPa for 10 minutes.
Release and re-apply for a further 10minutes
Relief valve set at 220kPa
Calibrated pressure gauge no. 28023/70

Date of Proof Test 31 JANUARY 2010
Person carrying out test A. PRESLAND

Signature A. Presland

We declare that the equipment designated above has been manufactured in accordance with:-

The EC Council Directive relating to machinery 98/37/EC, any subsequent amendments thereto and the relevant harmonised standards, in particular BS EN ISO 12100 Parts 1 and 2 and EN60204-1:1998 on safety of machinery.

The EC Council Directive relating to electromagnetic compatibility 89/336/EEC and any subsequent amendments thereto and the relevant harmonised standards.

If alterations are made to this machinery without prior consultations with us, this declaration becomes invalid.

Signed:

Name and Position: D.A. COOPER MANAGING DIRECTOR

Date: 31 JANUARY 2010

H889492

P.O.Box 2 Hanzhong,723007
Shaanxi,China
TEL:86-916-2386120,2386122
FAX:86-916-2316952
E-mail:transducers@zemic.com.cn

ZEMIC

CALIBRATION CERTIFICATE

NOTE:

WE CERTIFY THAT THE PRODUCT DESCRIBED BELOW CONFORMS TO ALL APPLICABLE SPECIFICATIONS.CALLBRATION IS TRACEABLE TO THE NATIONAL INSTITUTE OF STANDARDS AND TECHNOLOGY. CALIBRATION IS PERFORMED AT HANZHONG,SHAANXI.WHERE THE LOCAL ACCELERATION OF GRAVITY IS 9.7934m/s^2.

General Data

Model: B3G-C3-2.5t-6B
Serial Number: H889492
Material: STAINLESS STEEL

Capacity: 2.5 t
Excitation: 10 VDC(NOM). 15 VDC(MAX)
Insul Res: >5000MΩ(50 VDC)

Calibration Data

Full Scale Output: 3.003 mv/v
Non-Repeatability: ±0.01 % of FS
Input Resistance: 430±60 Ohms
Temp.Sens.Zero: <0.02 %FS/10℃
Temp.Sens.Output: <0.02 %FS/10℃
Non-linearity: 0.02 % of FS
Cable Length: 6 m
Safe Overload(150%): 3.75 t
Uitimate Overload(300%): 7.5 t

Combined Error: 0.02 % of FS
Zero Balance: <1.0% of FS
Output Resistance: 350±3.5 Ohms
Comp.Temp.Range: -10 ℃ _ 40 ℃
Operating Temp.: -35 ℃ _ 65 ℃
Hysteresis: 0.02 % of FS

Class: C3

SUPPLIED BY
VARIOHM EUROSENSOR

A B C.F 29 09 REF: 121755.

ELECTRICAL CONNECTIONS

RED —— +EXC
BLACK —— -EXC
GREEN —— +SIGNAL
WHITE —— -SIGNAL
BARE —— SHIELD

CAUTION:Cutting cable will affect the Full Scale Output calibration.

QA Manager--Zhushe Zhai

Specifications are subject to change without notice.

DATE:5- 6-2009

All units are produced in a Quality System that meets the requirements of ISO-9001,and the certificate number is 00808Q10508R4M

Q538962A

P.O.Box 2 Hanzhong,723007
Shaanxi,China
TEL:86-916-2386120,2386122
FAX:86-916-2316952
E-mail:transducers@zemic.com.cn

ZEMIC

CALIBRATION CERTIFICATE

NOTE:

WE CERTIFY THAT THE PRODUCT DESCRIBED BELOW CONFORMS TO ALL APPLICABLE SPECIFICATIONS.CALLBRATION IS TRACEABLE TO THE NATIONAL INSTITUTE OF STANDARDS AND TECHNOLOGY. CALIBRATION IS PERFORMED AT HANZHONG,SHAANXI.WHERE THE LOCAL ACCELERATION OF GRAVITY IS 9.7934m/s^2.

General Data

Model: B3G-C3-2.5t-6B
Serial Number: Q538962A
Material: STAINLESS STEEL
Capacity: 2.5 t
Excitation: 10 VDC(NOM). 15 VDC(MAX)
Insul Res: >5000MΩ(50 VDC)

Calibration Data

Full Scale Output: 3.003 mv/v
Non-Repeatability: ±0.01 % of FS
Input Resistance: 430±60 Ohms
Temp.Sens.Zero: <0.02 %FS/10℃
Temp.Sens.Output: <0.02 %FS/10℃
Non-linearity: 0.02 % of FS
Cable Length: 6 m
Safe Overload(150%): 3.75 t
Uitimate Overload(300%): 7.5 t
Combined Error: 0.02 % of FS
Zero Balance: <1.0% of FS
Output Resistance: 350±3.5 Ohms
Comp.Temp.Range: -10 ℃ _ 40 ℃
Operating Temp.: -35 ℃ _ 65 ℃
Hysteresis: 0.02 % of FS

Class: C3

ELECTRICAL CONNECTIONS

RED —— +EXC
BLACK —— -EXC
GREEN —— +SIGNAL
WHITE —— -SIGNAL
BARE —— SHIELD

SUPPLIED BY
VARIOHM EUROSENSOR

A(E)C.F 29 09 REF:12175S.

CAUTION:Cutting cable will affect the Full Scale Output calibration.

QA Manager--Zhushe Zhai

Specifications are subject to change without notice.

DATE:5- 6-2009

All units are produced in a Quality System that meets the requirements of ISO-9001,and the certificate number is 00808Q10508R4M

HCA Cutting Equipment.

THIS EQUIPMENT SHOULD ONLY BE OPERATED AND ADJUSTED BY TRAINED AND QUALIFIED PERSONNELL.
FAILURE TO OPERATE CORRECTLY CAN CAUSE SEVERE DAMAGE AND POSSIBLE FATALITY.
THE EQUIPMENT WEIGHS 100 Kg AND THE SAMPLE WEIGHS 50 Kg. ALWAYS USE THE APPROVED LIFTING EQUIPMENT.

The equipment has been designed to allow the Asphalt sample to be cut cleanly, flat and square at each end and to ensure close tolerance parallelism of cut over an accurate overall length.
Due to the instability of the samples, these are stored and maintained at low temperatures as normal ambient temperatures can cause distortion of the sample over relatively short periods.
The samples also weigh approximately 45 kG's and have to be removed from storage and handled to allow cutting.
In order to minimise relaxation of the sample, inner and outer rings are provided to restrain the sample inside the cutter wheel. The outer ring also allows the use of M10 grub screws to clamp around the outer ring and transmit the rotational forces to allow cutting, without marking the sample.

Operation.

- Visually check condition and security of all components prior to operation.
- **The weight of the cutter is in excess of 100 kG and lifting equipment must always be used to position the equipment on the saw base.**
- Using the lifting equipment provided, raise the cutter assembly and position on the cleared moving saw base.
- Place 4 off M12 x 70 hex head bolts through the provided holes in the cutter base and sliding saw table. When aligned place the provided Tommy bar 12.00 Ø locating dowels into the locating holes and fully tighten the M12 clamping bolts. The dowels ensure that the sample is square to the blade.
- Place the 3.0mm thick plain outer sleeve over the sample and the thinner shouldered sleeve within the sample bore, and, using the approved lifting system raise the prepared sample and offer into the bore of the steel main drive ring.
- Slide the sample and sleeve into the required position to allow cutting of the sample at each end. Progressively and equally tighten the radially mounted M10 grub screws until the outer sleeve is secured around the centrally held sample.
- The main drive ring can be rotated by hand to allow the above tightening, however, it can only be turned in a L/H rotation, viewed on the right hand face and the
- The 3 off expanding shouldered bolts inside the inner sleeve can now be adjusted, by hand, to secure the inner sleeve in the required position and support the sample internally.
- The complete sliding assembly should now be aligned such that the right hand end of the sample can be cut to provide a straight edge against the saw blade but cut clear of the framework and outer and inner sleeves. The locks should be clamped to hold this position.

- The special drop in runner stop pin should be placed in the provided hole in the Right hand guide rail, the saw started and the sample, cutter and saw sliding base be allowed to move into the blade until the stop is reached. At this point the saw blade should have fully cut through the sample wall thickness.
- The supplied 32 A/F socket should now be fixed to the clutch drive spigot and rotated at a suitable speed to rotate the sample under the saw to achieve the desired cut.
- When the cut is finished, approximately 3/4 minutes. The saw table should be withdrawn to the start position and the saw blade stopped.
- Release the locking clamps and slide the table across to achieve the desired cut length, lock in this position and repeat the cutting operation with the saw blade.
- Withdraw the saw table, stop the blade and release the grub screws to release the sample.
- Slide the cut sample from the drive ring, support and remove the sample.
- Dismount the equipment as required, clean, wipe dry and lubricate with light oil before storing.

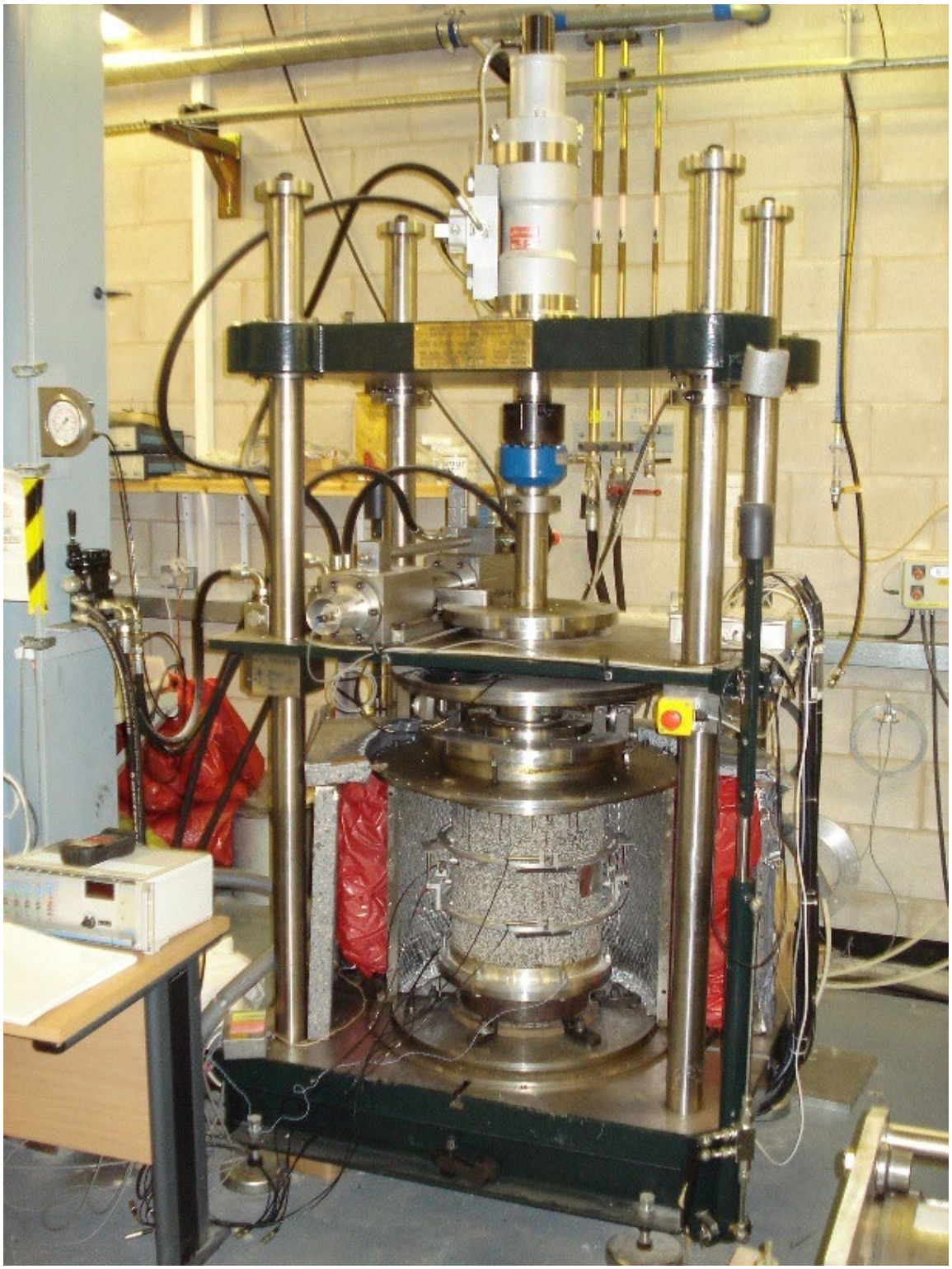
Maintenance.

- Check security and condition of equipment prior to each use.
- Check freedom of rotation of bearings, drive ring and correct locking operation of drive clutch. Lubricate all steel components with light oil / storage spray.

APPENDIX B

HCA TEST PROTOCOL

HCA TESTING PROTOCOL



1 APPARATUS

The new HCA has been successfully built. The device can provide both repeated axial (W) and torsional (M) shear loads with regulated internal and external pressures on a hollow cylindrical specimen with 250mm inner radius, 350mm outer radius and 350mm height. The large size of specimen can be used to test asphalt with realistic sized aggregate. Figure 3.12 shows the general configuration of the new torsional HCA and Figure 3.13 is a photograph of it.

The vertical loading components are shown in Figure 3.14. The 100kN actuator with a stroke length of 100mm is fitted above the top crosshead and a position transducer is attached to the top of the shaft to measure its position. Couplings are used to connect the main vertical feedback load cell to the actuator shaft and to an extension shaft below. A collar is used to ensure a direct connection to the extension shaft but allows for ease of separation if necessary. The extension shaft passes through a large clearance hole in the intermediate crosshead and a secondary 100kN load cell is screwed to its end. This load cell is bolted to the inner ring of a large angular contact roller bearing and the outer bearing ring is fitted to the final drive disc, which is part of the torque loading arrangement. The bearing allows vertical load to be applied on a fixed axis and also rotation about the fixed axis without torque being transferred to the vertical loading components.

The secondary load cell provides a check on the upper vertical load cell as the extension shaft has to pass through the torque loading arrangement and some friction may occur.

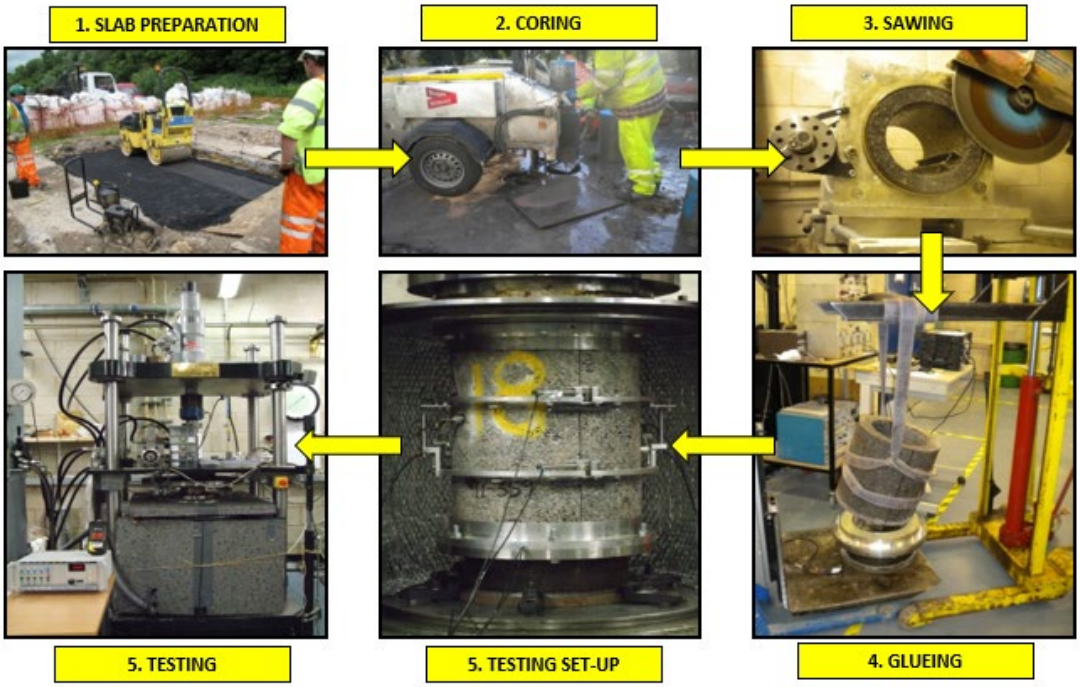
The side view on Figure 3.15 shows the arrangement for transmitting torque to the top of the specimen using three discs. The 30kN horizontal actuator is fixed to an intermediate crosshead at a 200mm offset from the vertical axis (6kNm torque). +/- 75mm travel is available, which allows +/- 15º of rotation of the

final drive plate. The primary drive disc is turned by an arm attached to a central shaft, which is connected to two hydraulic cylinders as shown in the plan view. A pin on the shaft moves the arm and passes through a slot, which accommodates the lateral movement of the arm as the primary drive disc rotates.

Specimen Dimensions	H 350mm, OD 350mm, ID 250mm
Vertical Load	Up to 100kN, stroke 0 to 100mm
Torque	Up to 30kN; arc of rotation +/- 15º
Loading Frequency	0 to 5Hz stroke at 5Hz – ≤1.5mm, rotation at 5Hz - 2º
Confining Pressure	0 to 200kPa
Temperature Range	20 to 45ºC

For full description of the equipment refer to Section 3.

2 Preparation of specimens



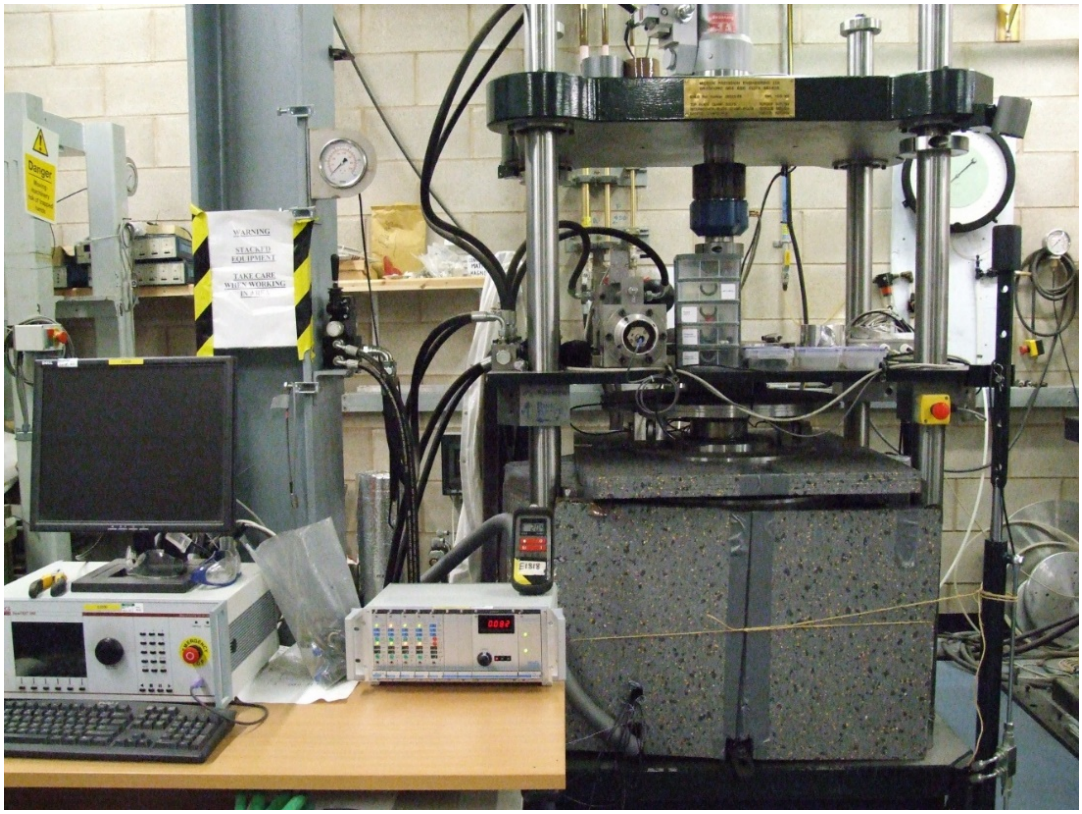
Specimen preparation is discussed in Section 4, and Section 5 describes test set-up procedure.

The following procedures shall apply to undisturbed, cored hollow cylinders:

- Specimens shall be prepared by coring cylinders from a slab. As discussed in Section 4. In order to achieve hollow specimens with dimensions as per Section 3.2.4, the central part of the cylinder should be drilled first followed by the external part, as shown in Figure 4.11. The average achieved wall thickness should be 50mm measured top and bottom (+/- 1mm).
- Transfer specimens carefully to the laboratory in a refrigerated van during warm weather, to avoid any distortion, and then store in a temperature-controlled room at 5ºC.
- Cut and trim the specimen to the required dimensions as per Section 4.1.4. Take care to avoid deforming the specimen during the cutting and trimming process.
- The soil specimen end surfaces shall be plane and perpendicular to the longitudinal axis.
- Examine undisturbed samples prior to testing. If significant disturbance is apparent in the specimen this should be recorded in the test report. Highly disturbed samples will not provide meaningful results and should not be tested.
- Measure the specimen height, diameter, wall thickness and mass immediately prior to gluing. Record average values to used for further stress and strain analysis.
- Determine air voids.
- Glue the specimen as per Section 4.2.2.
- An arrangement for fitting a HCA specimen in alignment with the vertical and torque actuators of the apparatus is depicted in Figure 4.18.

- 6.2.9 Once the glue set, remove the specimen and fit with the on-specimen instrumentation arrangement as shown in the schematic of Figure 3.18 and also Figures 3.20 to 3.22.
- Fit a thermocouple to the wall of the specimen.
- Transfer the assembly back into the apparatus.
- Position the specimen within a pressure chamber as shown in Figure 4.21. The end platens were then bolted to a pedestal below the specimen and to an extension fitted to the final drive disc. This extension passes through the top cover of the pressure chamber and is of sufficient height to accommodate the vertical deformation of the specimen during testing. Clamps were used to fix the pedestal to the bottom of the chamber and also the chamber to the frame base. This method of fixing facilitated the alignment of the top platen bolt holes with the final drive extension threaded holes and allowed centralisation of the chamber about the extension.
- Place the pressure chamber around the specimen and bolt the cylinder together through vertical flanges either side of the split and bolt to the base through circular flanges welded around the bottom of each half of the cylinder.
- Fit insulation around the chamber to reduce heat loss as shown in Figure 4.23.
- A combined air filter and heater connects to the chamber so that heated air passed through the chamber to control the specimen temperature. For unconfined testing use a very low pressure and exhaust it from the chamber with the exhaust valve fully open.
- Condition the specimen till a desire temperature is reached.

- Lower the final drive extension using CH1 set-point until a slight compressive load is observed on the vertical load cell (about-0.3kN) and change to vertical (CH1) force control. Check that the load is still at about -0.3kN and adjust with CH1 set point if necessary. Torque CH2 should be in position control.
- Monitor the LVDT outputs throughout the conditioning period and recorded at the test start. During the test measure specimen deformation and record continuously.
- Specimen ready to be tested is show below:



3 TEST PROCEDURE

- Create sequences in SmartWAVE block-editing software and download them for local control on the test controller.
- Switch on the HCA and the hydraulics.
- Switch on the Moog Test Controller and connect laptop to it vie ethernet cable.
- Note the CH1 vertical force feedback reading, CH1 control mode, the CH2 torque force feedback reading and the CH2 control mode.
- The CH1 vertical force will be probably at about -1.0kN (the weight of the vertical load components) and the CH2 torque force should be close to zero.
- CH1 should be in force control. If not, use set-point for CH1 to set to force control mode at -0.1kN compressive. The nuts on the supporting bolts under the final drive can be screwed down and all three bolts removed.
- CH2 should be in position control. If not, use CH2 set-point to apply a slight -ve load so that the torque load cells have no play in their pinned ends.
- Open SmartWAVE programme and export a sequence to Moog Test Controller (master.seq).
- Go to set recording file.
- Start recording.
- Start test.
- Stop test.
- Stop recording.

4 TEST RESULTS

- Upload Download data to a computer by accessing information stored on the Moog Test Controller. Use of the web server interface. Connect a computer to the Test Controller via Ethernet (see Figure 3.31). The raw data are saved in *.fstrm format and the MOOG web interface allows the data output to be converted to the Comma separated files - *.csv. When converting is completed, save data files to a computer.
- To analyse the data files, use NTEC & Cooper Research Technology Ltd. filtering software. See section 3.3.